

**FURTHER DEVELOPMENT AND VALIDATION OF
TECHNOLOGIES TO LOWER OXIDES OF NITROGEN
EMISSIONS FROM HEAVY-DUTY VEHICLES**

LOW NO_x DEMONSTRATION PROGRAM – STAGE 3

ARB CONTRACT 16MSC010

FINAL REPORT

SwRI® Project Number 03.23379

Prepared for:

California Air Resources Board

Prepared by:

Christopher A. Sharp, Institute Engineer - Program Manager

**Southwest Research Institute
6220 Culebra Road
San Antonio, TX 78238**

April 16, 2021



**FURTHER DEVELOPMENT AND VALIDATION OF
TECHNOLOGIES TO LOWER OXIDES OF NITROGEN
EMISSIONS FROM HEAVY-DUTY VEHICLES**

LOW NO_x DEMONSTRATION PROGRAM – STAGE 3

ARB CONTRACT 16MSC010

FINAL REPORT

SwRI® Project Number 03.23379

Prepared for:

California Air Resources Board

April 16, 2021

Prepared by:



**Chris Sharp, Institute Engineer
Diesel Engine and Emissions R&D Dept.
Powertrain Engineering Division**

Approved by:



**Charlie Roberts, Director
Diesel Engine and Emissions R&D Dept
Powertrain Engineering Division**

POWERTRAIN ENGINEERING DIVISION



Benefiting government, industry and the public through innovative science and technology

DISCLAIMER

The statements and conclusions in this Report are those of the contractor and not necessarily those of the California Air Resources Board. The mention of commercial products, their source, or their use in connection with material reported herein is not to be construed as actual or implied endorsement of such products.

ACKNOWLEDGEMENTS

This effort would not have been possible without a significant amount of support, and contributions of time, materials, and funding from a wide variety of participating organizations.

Southwest Research Institute (SwRI) would like to acknowledge the funding contributions of the South Coast Air Quality Management District (SCAQMD), the Port Authority of Los Angeles (POLA), the U.S. Environmental Protection Agency (EPA), the Manufacturers of Emission Controls Association (MECA), the SwRI-led Clean High Efficiency Diesel Engine VII (CHEDE VII) industry consortium, and the Truck and Engine Manufacturer's Association (EMA).

SwRI would also like to acknowledge major in-kind contributions from Cummins Corporation, both in supplying hardware and in providing large amount of engineering support. As the OEM engine partner for this program, Cummins also supplied valuable industry feedback and evaluation on a wide variety of issues throughout this program.

SwRI would further like to acknowledge the in-kind contributions of hardware and engineering support for numerous MECA member companies. This includes the Eaton Corporation for the supply of cylinder deactivation (CDA) valvetrain hardware, and numerous other suppliers who provided AT hardware, engine hardware options, sensors, components, and significant quantities of design and engineering support.

Finally, SwRI would like to acknowledge the support of the members of the Program Advisory Group (PAG). This group of stakeholders provided valuable guidance, feedback, comment, and criticism over the course of the program.

This Report was submitted in fulfillment of CARB contract 16MSC010 titled "Further Development and Validation of Technologies to Lower Oxides of Nitrogen Emissions from Heavy-Duty Vehicles" by Southwest Research Institute under the sponsorship of the California Air Resources Board. Technical laboratory efforts were completed in October of 2020, and all work was completed as of April 06, 2021.

TABLE OF CONTENTS

ABSTRACT xv

EXECUTIVE SUMMARY xvi

1.0 INTRODUCTION AND BACKGROUND 1

2.0 METHODS AND MATERIALS..... 1

 2.1 Test Engine 1

 2.2 Emission Test Cell 4

 2.3 Test Cycles, Test Procedures, and Preconditioning Procedures 5

 2.4 Low NO_x Aftertreatment Hardware 6

 2.4.1. *Aftertreatment Team 1* 7

 2.4.2. *Aftertreatment Team 2* 10

 2.4.4. *Final Aftertreatment Configuration* 17

 2.5 Low NO_x Engine Hardware Options 19

 2.5.1. *Air Gap Insulated (AGI) Exhaust Manifold* 20

 2.5.2. *EGR Cooler Bypass* 22

 2.5.3. *Charge Air Cooler Bypass* 25

 2.5.4. *Turbine Bypass* 26

 2.5.5. *Cylinder Deactivation* 27

 2.5.6. *SuperTurbo* 32

 2.6 Low NO_x Controls 33

 2.6.1. *Overall Strategy and Engine State Machine* 34

 2.6.2. *CDA Controls* 36

 2.6.3. *Aftertreatment Controller and DEF Dosing Controls* 38

 2.6.4. *Overall Aftertreatment System Control Strategy* 45

 2.7 Aging Methodology 49

 2.7.1. *Final Aging (DAAAC)* 50

 2.7.2. *Development Aging (Hydrothermal Only)* 56

 2.7.3. *De-greening (Hydrothermal Only)* 58

3.0 RESULTS AND DISCUSSION 59

 3.1 Baseline Engine Testing 59

 3.2 Modified Base Engine Calibration Updates 62

 3.2.1. *Steady-state Test Point Selection* 62

 3.2.2. *Steady-state Testing for Modified Engine Calibration Development* 64

 3.2.3. *Transient Evaluations for Modified Engine Calibration* 70

3.3	Engine Hardware Evaluations (Stage 3B)	73
3.3.1.	<i>Steady-State Hardware Testing</i>	73
3.3.1.1.	<i>1000-rpm Elevated Idle</i>	74
3.3.1.2.	<i>1000-rpm 2.5 bar BMEP</i>	75
3.3.1.3.	<i>1000-rpm 5 Bar BMEP</i>	77
3.3.1.4.	<i>1000-rpm 10 Bar BMEP</i>	78
3.3.2.	<i>Transient Hardware Testing</i>	80
3.3.2.1.	<i>Transient Evaluation of AGI Exhaust Manifold</i>	80
3.3.2.2.	<i>Transient Evaluation of 50% EGR Cooler Bypass</i>	81
3.3.2.3.	<i>Transient Evaluation of CDA</i>	82
3.3.2.4.	<i>Transient Evaluation of SuperTurbo</i>	83
3.3.3.	<i>Cold FTP Hardware Performance Summary</i>	86
3.4	Aftertreatment Evaluations	87
3.4.1.	<i>Team 2A Results</i>	88
3.4.2.	<i>Team 2B Results</i>	91
3.4.3.	<i>Team 1 Results</i>	98
3.4.4.	<i>System Comparisons – Final System Down-selection</i>	103
3.5	Final Aftertreatment System Performance with Development Aged Parts	105
3.6	DAAAC-Based Final Aging	114
3.7	Emission Performance of Final Aged Parts at Various Test Points	120
3.7.1.	<i>Initial (0-Hour) Performance</i>	120
3.7.2.	<i>Intermediate Emission Test Points (333-hour and 667-hour)</i>	121
3.7.3.	<i>Full-Useful Life Emission Tests</i>	128
3.8	Sulfation and Desulfation Experiments	136
3.9	GHG Phase 2 Fuel Mapping Results	143
3.9.1.	<i>Phase 2 Fuel Mapping Test Results</i>	143
3.9.2.	<i>GEM Vehicle Results</i>	146
3.10	Estimation of Infrequent Regeneration Adjustment Factors (IRAF)	150
3.10.1.	<i>LO-SCR deSO_x</i>	150
3.10.1.	<i>Active zCSF Regenerations</i>	150
3.11	Field Replay Cycle Evaluations	154
3.11.1.	<i>CARB Southern NTE Route (EMA Field Cycle)</i>	154
3.11.2.	<i>Extended Cold-Start Idle</i>	157

3.11.3 Long Idle Periods (hoteling)..... 158

4.0 SUMMARY AND CONCLUSIONS 160

4.1 Demonstration Results 160

4.2 Technology Feasibility..... 162

4.3 Implications for Onboard Diagnostics (OBD)..... 164

5.0 RECOMMENDATIONS 166

6.0 REFERENCES 168

APPENDIX - 169

EMISSION DATA SUMMARIES FOR ALL TEST POINTS..... 169

LIST OF FIGURES

Figure	Page
Figure 1. Final Stage 3 Advanced Aftertreatment System	xvii
Figure 2. Final Stage 3 NO _x Result Compared to Baseline	xvii
Figure 3. 2017 MY Cummins X15 Engine.....	1
Figure 4. Baseline (Stock) Aftertreatment (Inlet Side) for 2017 Cummins X15 Engine	3
Figure 5. Baseline (Stock) Aftertreatment System for Cummins X15 Engine – Outlet Side and Transfer Pipe.....	3
Figure 6. Team 1 Aftertreatment Primary Concept	7
Figure 7. Candidate Aftertreatment System 1 Installation.....	8
Figure 8. Internal Details for Team 1 Downstream “One-Box” System	9
Figure 9. Team 1 Alternate Configuration (SCR-on-Filter)	10
Figure 10. Team 2A Configuration Schematic (DOC Upstream of LO-SCR).....	11
Figure 11. Team 2B Configuration Schematic (No DOC Before LO-SCR)	11
Figure 12. Team 2 Heated Dosing System Hardware Installed at In-Pipe Location (Used for Configuration 2B).....	12
Figure 13. Production Cummins DEF Doser Installed on Team 2 Downstream Unit	13
Figure 14. Configuration 2A Complete System during Installation	14
Figure 15. Configuration 2A - Details	14
Figure 16. Team 2A Alternate Configuration to Resolve Packaging Questions (Not Used)	15
Figure 17. Configuration 2B – Test Cell Installation	16
Figure 18. Final Stage 3 Aftertreatment Configuration.....	17
Figure 19. Stage 3 Final Aftertreatment Configuration (Shown without Insulation)	18
Figure 20. Stage 3 Final Downstream System Showing Removable Zoned-CSF Module	19
Figure 21. “Stage 3B” Engine Hardware Options Examined	20
Figure 22. AGI Exhaust Manifold for Stage 3 Engine	21
Figure 23. Comparison of AGI and Stock Exhaust Manifolds.....	21
Figure 24. AGI Exhaust Manifold Installed on Stage 3 Engine	22
Figure 25. Pressure and Temperature Measurement Locations on Stock and AGI Exhaust Manifolds.....	22
Figure 26. EGR Cooler Bypass Development Setup for Initial Experiments with 100% Bypass	23
Figure 27. EGR Cooler Bypass Development Setup for Initial Experiments with 50% Cooler Bypass – AGI Manifold.....	24
Figure 28. EGR Cooler Bypass Final Setup for Transient Experiments with Control Valve – Stock Manifold	25
Figure 29. Charge-Air-Cooler (CAC) Bypass	26
Figure 30. Turbine Bypass Valve and Installation (AGI Manifold).....	27
Figure 31. Eaton CDA Hardware for One Cylinder (Shown with Engine Brake Integration)....	28
Figure 32. X15 Cylinder Head Shown with CDA Hardware Installed for All Six Cylinders.....	28
Figure 33. Illustration of Different CDA Modes	29

Figure 34. Example of Torsional Vibration Mapping and Analysis for CDA..... 30

Figure 35. Example of Linear Vibration Mapping and Analysis for CDA 30

Figure 36. Final Base CDA Control Map Implemented for Stage 3 Engine 31

Figure 37. SuperTurbo Hardware Components 32

Figure 38. Installation of SuperTurbo on the Stage 3 Engine..... 33

Figure 39. High-Level Control Structure for Stage 3 Low NO_x Demonstration 34

Figure 40. Engine State M/C and Overall Strategy Control Diagrams..... 35

Figure 41. Example of Control Mode Switching during Cold-FTP 36

Figure 42. Aftertreatment Controller in Overall Control Architecture..... 38

Figure 43. DEF Dosing Controls – Overall System Overview..... 39

Figure 44. LO-SCR Dosing Controller Schematic 40

Figure 45. LO-SCR Control Structure 40

Figure 46. Downstream SCR Dosing Controller Schematic 42

Figure 47. Downstream SCR Controller Structure..... 42

Figure 48. Example of Ammonia Storage Profiles during Hot-Start FTP TRansient Cycle..... 44

Figure 49. Example of Ammonia Storage Tracking and DEF Dosing over Hot-FTP Transient Cycle..... 46

Figure 50. Example of Ammonia Storage and DEF Dosing over Hot-FTP Transient Cycle – After DPF Regeneration 47

Figure 51. Example of Ammonia Storage and DEF Dosing over RMC-SET Cycle – Including Preconditioning Portion..... 49

Figure 52. Arrhenius Rate Law Equation for Thermal Catalyst Deactivation 52

Figure 53. Stage 3 Final DAAAC-Based Aging Cycle – Base Cycle without DESO_x..... 53

Figure 54. Stage 3 Final DAAAC-Based Aging Cycle – Full Cycle with LO-SCR DESO_x..... 54

Figure 55. SwRI DAAAC Engine-Based Aging Cell..... 55

Figure 56. Stage 3 AT System Installed in DAAAC Aging Cell 56

Figure 57. SwRI ECTO-Labtm Burner-Based Aging and Test Stand 57

Figure 58. Baseline Tailpipe BSNO_x emissions for 2017 cummins x15 engine..... 59

Figure 59. Baseline Tailpipe BSno_x Summary 60

Figure 60. Comparison of Initial and Final Baseline Tailpipe NO_x and CO₂ Measurements..... 61

Figure 61. Relation of Selected Calibration Test Points to First 400 Seconds of FTP and Various Vocational Test Cycles..... 63

Figure 62. Idle Test Point Results for Baseline and Modified Calibration..... 65

Figure 63. Cold Coolant Test Results for Baseline, Exploratory, and Modified Calibrations at 1000 rpm and 2.5 Bar BMEP 67

Figure 64. Cold Coolant Test Results for Baseline, Exploratory, and Modified Calibrations at 1000 rpm and 5 Bar BMEP 68

Figure 65. Cold Collant Test Results for Baseline, Exploratory, and Modified Calibrations at 1000 rpm and 10 Bar BMEP 69

Figure 66. Cold FTP Results with Baseline and Two Modified Calibrations – Engine Speed, Torque, and Engine-Out NO_x 70

Figure 67. Cold FTP Results with Baseline and Two Modified Calibrations: Engine Speed, Turbine Out and Stock DOC Out Temperatures 71

Figure 68. Engine Hardware Technologies Evaluated in the Stage 3B Task 73

Figure 69. Steady-state HW Evaluation Results at Elevated Idle Speed of 1000 RPM and 25°C Coolant Temperature 75

Figure 70. Steady-state HW Evaluation Results at 1000 RPM, 2.5 bar BMEP with 25°C Coolant Temperature 76

Figure 71. Steady-state HW Evaluation Results at 1000 RPM, 5 bar BMEP with 30°C Coolant Temperature 78

Figure 72. Steady-state HW Evaluation Results at 1000 RPM, 10 bar BMEP with 35°C Coolant Temperature 79

Figure 73. Transient Evaluation Results with Stock and AGI Exhaust Manifolds. 81

Figure 74. Transient Evaluation Results with Modified and 50% EGR Cooler Bypass Calibrations, Both with Stock Exhaust Manifolds. 82

Figure 75. Transient Evaluation Results with CDA and Modified Cold Calibrations. 83

Figure 76. Transient Evaluation Results with SuperTurbo and Modified Cold Calibrations..... 85

Figure 77. Team 2A Schematic 88

Figure 78. Cold-Start FTP Result for Team 2A 89

Figure 79. Team 2A Impact of Updated Calibration – Lower Early Engine-Out NO_x..... 90

Figure 80. Team 2B Configuration 91

Figure 81. Cold-Start LO-SCR Temperature Improvements from 2A to 2B Configuration..... 92

Figure 82. Cumulative NO_x Mass in Early Cold-Start FTP – Comparison of 2A and 2B..... 92

Figure 83. Cold-FTP Results for Iptimized Configuration 2B 93

Figure 84. Hot-Start FTP Results for Configuration 2B 93

Figure 85. LLC Results for Configuration 2B 94

Figure 86. DeSO_x Mapping at 1000 RPM 3.1 Bar BMEP 95

Figure 87. DeSO_x Mapping – Ideal CDA Modes at Various Engine Conditions 96

Figure 88. DeSO_x Mapping – Air-Fuel Ratio at Various CDA-Enabled deSO_x Conditions..... 96

Figure 89. Filter Smoke Number (FSN) at Various CDA-Enabled DeSO_x Conditions 97

Figure 90. Team 1 Aftertreatment Configuration 98

Figure 91. Cold-Start FTP Results for Team 1 System 100

Figure 92. Hot-Start FTP Results for Team 1 System 101

Figure 93. LLC Result for Team 1 System 102

Figure 94. RMC-SET Result for Team 1 System 103

Figure 95. Final Stage 3 Aftertreatment Configuration (Team 2B+1) 105

Figure 96. Cold-FTP Final Result on Final Stage 3 Development Aged Parts after Optimization 108

Figure 97. Hot-FTP Final Result on Final Stage 3 Development Aged Parts after Optimizationi 109

Figure 98. LLC Result without Accessory Load – Final Stage 3 Development Aged Parts..... 110

Figure 99. LLC Result with Accessory Load – Final Stage 3 Development Aged Parts 111

Figure 100. RMC-SET Results for Final Stage 3 System with Development Aged Parts 112

Figure 101. Comparison of Stage 3 Development Aged and Baseline Results..... 113

Figure 102. Example of Single Base Aging Cycle – Including zCSF Regeneration and LO-SCR
DeSO_x Event 114

Figure 103. 40-Hour Segment of Final Aging Cycle Data 115

Figure 104. Example NO_x Sensor Data over 40 Hours of Final Aging – Early Data Sets 116

Figure 105. Example of Aging Data Near the End of 1000-Hour Final Aging..... 119

Figure 106. Example of Filter Ash Loading Visualization via CT-Scan (500 Hours, 35 g/l ash
load)..... 119

Figure 107. LO-SCR conversion Before and After DeSO_x during Aging 120

Figure 108. Comparison of Development Aged Parts and 0-Hour Final Aged (Degreened) Parts
..... 121

Figure 109. Hot-Start FTP Tailpipe NO_x Levels at Various Intermediate Test Points 122

Figure 110. Temperatures During deso_x Event for First 333 Hours of Final Aging 123

Figure 111. Example of Improved LO-SCR Conversion at High Space Velocity after 550°C
deso_x at 667 Hours 124

Figure 112. Emission Impact of 667-hour Calibration Change..... 125

Figure 113. Comparison of RMC-SET Emissions – 667-Hour versus 333-Hour Showing SCR
System Balance..... 127

Figure 114. Emission Summary for Intermediate Test Points on All Cycles 128

Figure 115. Initial 1000-Hour Tests Before and After Short deso_x Experiment 130

Figure 116. Final Summary of Stage 3 Cycle Emission Results 131

Figure 117. Cycle NO_x Conversion Efficiency at Various Test Points 132

Figure 118. Cold-Start ftp Result at 435,000 Miles after Ash Cleaning..... 133

Figure 119. Hot-Start ftp Emission Result at 435,000 Miles after Ash Cleaning 133

Figure 120. RMC-SET Emission Result at 435,000 Miles after Ash Cleaning 134

Figure 121. Low Load Cycle (llc) Emission Result at 435,000 Miles after Ash Cleaning 134

Figure 122. CARB Extended Idle Test Result for Stage 3 Low NO_x Engine at 435,000 Miles
..... 135

Figure 123. Cycle N₂O Emissions 136

Figure 124. DeSO_x at 525°C After Excess Sulfur Storage during First 333-Hour Aging Segment
..... 138

Figure 125. DeSO_x at 550°C after Excess Sulfur Storage During First 333-Hour Aging Segment
..... 139

Figure 126. Downstream DeSO_x Experiment at 650°C 139

Figure 127. DeSO_x at 550°C after repeated 525°C deso_x events during 667-hour aging segment
..... 140

Figure 128. Short DeSO_x Experiment at 550°C Following 1000-Hour Aging Segment and 36-hr
Equivalent Low Temperature Operation 142

Figure 129. Comparison of Steady-State Fuel Maps Between Stage 3 Low NO_x Engine and
Baseline Engine 144

Figure 130. Comparison of Cycle Average Fuel Mapping Results between Stage 3 Low NO_x Engine and Baseline Engine 145

Figure 131. 2027 GEM Vehicle Simulation Results for Tractors 148

Figure 132. 2027 GEM Vehicle Simulation Results for Vocational Vehicles 149

Figure 133. NO_x UAF Calculation for FTP Cycle 152

Figure 134. NO_x UAF Calculation for RMC-SET Cycle..... 153

Figure 135. NO_x UAF Calculation for LLC Cycle 154

Figure 136. Normalized NTE Southern Route Replay Cycle..... 155

Figure 137. Example of Stage 3 Engine Temperature and NO_x Performance over NTE Southern Route Replay Cycle 156

Figure 138. 3B-MAW Results for NTE Southern Route Replay Cycle 157

Figure 139. Stage 3 Low NO_x Result for Cold-Start with Extended Idle Period (30 Minutes) 158

Figure 140. Stage 3 Result for 8-Hour Idle Evaluation – with Part Load Return-to-Service.... 159

Figure 141. Final Tailpipe NO_x Values Achieved for Stage 3 Demonstration (not Including IRAF)..... 160

Figure 142. Cycle NO_x Conversion Efficiency – Comparison of Aging Methods 161

LIST OF TABLES

Table	Page
Table 1. Cummins X15 Engine Parameters.....	1
Table 2: Candidate Aftertreatment System 1 Catalyst Specifications	7
Table 3. Team 2 Catalyst Specifications.....	11
Table 4. Catalyst Specifications for Final Stage 3 Aftertreatment System.....	17
Table 5. Final Aging Cycle Mode Targets.....	53
Table 6. Engine Speeds and Loads for Selected Steady-State Test Points.....	63
Table 7. FTP Results with Baseline and Modified Calibrations.....	72
Table 8. Summary of Key Parameters from Cold FTP HW Evaluations	86
Table 9. Summary of Key Parameters from Cold FTP HW Evaluations	87
Table 10. Comparison of Key Performance Data for Team 1 and Team 2 Systems	104
Table 11. Aging Statistics for Various Test Points during Stage 3 Final Aging	118

LIST OF ACRONYMS

AMT	Automated Manual Transmission
ANR	Ammonia to NO _x Ratio
ASC	Ammonia Slip Catalyst
AT	Aftertreatment
BMEP	Brake Mean Effective Pressure
BSFC	Brake Specific Fuel Consumption
CAN	Controller Area Network
CARB	California Air Resources Board
CHEDE VII	Clean High Efficiency Diesel Engine VII consortium
CITT	Curb Idle Transmission Torque
CNG	Compressed Natural Gas
CO	Carbon Monoxide
CO ₂	Carbon Dioxide
COV	Coefficient of Variation
CSF	Catalyzed Soot Filter
CWF	Carbon Weight Fraction
DAAAC	Diesel Aftertreatment Accelerated Aging Cycles
DEF	Diesel Exhaust Fluid (32% urea by weight)
deSO _x	Desulfation
DOC	Diesel Oxidation Catalyst
DPF	Diesel Particulate Filter
ECM	Electronic Control Module
EGR	Exhaust Gas Recirculation
EO	Engine Out
EU	European Union
FTP	U.S. Heavy Duty Transient Federal Test Procedure
FUL	Full Useful Life
GEM	EPA Greenhouse Gas Emission Model
GHG	Greenhouse Gas
HDIUT	Heavy Duty In-Use Testing
HW	Hardware
IMAP	Intake Manifold Absolute Pressure
IMT	Intake Manifold Temperature
LLC	Low Load Cycle
LO-SCR	Light Off SCR Catalyst
LTT	Long term trim
MAW	Moving Average Window
MB	Mini-burner
MECA	Manufacturers of Emission Controls Association
MT	Manual Transmission
MY	Model Year
NIST	National Institute of Standards and Technology
NO _x	Oxides of Nitrogen
NTE	Not-to-Exceed
NVH	Noise, Vibration, and Harshness

OBD	Onboard Diagnostics
PAG	Program Advisory Group
PGM	Platinum Group Metals
PM	
PNA	Passive NO _x Adsorber
RMC-SET	Ramped Modal Cycle Supplemental Emission Test
RMS	Root Mean Square
SCR	Selective Catalytic Reduction (ammonia-based)
SCRf	SCR on Filter (SCR coated on DPF)
SwRI	Southwest Research Institute
SPN	CAN Suspect Parameter Number
THC	Total Hydrocarbons
TM	Thermal Management
TP	Tailpipe
UAF	Upward Adjustment Factor (for Infrequent Regeneration)
VGT	Variable Geometry Turbine
WBW	Work-Based Window
WHTC	World Harmonized Transient Cycle
zCSF	Zone-coated Catalyzed Soot Filter

ABSTRACT

The Stage 3 Low NO_x Program is a continuation of on-highway Low NO_x demonstration efforts conducted under previous contracts for CARB by SwRI. Previous efforts focused on an initial technology demonstration on a diesel engine and a compressed natural gas (CNG) engine in the Stage 1 program[1][2][3], and in the expansion of that initial effort to develop a new certification low load cycle (LLC) in the Stage 2 program[4]. This Stage 3 effort builds upon those previous efforts to provide a complete technology demonstration effort on an updated test engine that is representative of current mainstream Class 8 truck in technology (baseline engine). The Stage 3 demonstration also examines additional engine hardware technology options in an effort to show a path to mitigating potential GHG increases from implementing Low NO_x technologies. The final Stage 3 engine incorporates cylinder deactivation (CDA) technology, an advanced dual-SCR dual Diesel Exhaust Fluid (DEF) dosing aftertreatment system, advanced controls, and an updated calibration to demonstrate the feasibility of reaching low tailpipe NO_x levels while maintaining a path to meeting future GHG standards. The final Stage 3 engine-aftertreatment system, aged to the equivalent of 435,000 miles, demonstrated tailpipe NO_x levels of 0.023 g/hp-hr, 88% below current tailpipe standards, and LLC emissions 20 times lower than the baseline engine levels, while at the same time having GHG emissions and fuel economy equivalent to the baseline engine. Strategies for further emissions reductions and next steps recommended for enhancing system durability are also discussed.

EXECUTIVE SUMMARY

Despite decades of progress in cleaning the air, California continues to struggle with some of the most difficult air quality issues in the U.S. The California Air Resources Board (CARB) has stated that meeting federally mandated ozone limits in the National Ambient Air Quality Standard (NAAQS) will require significant reductions in ozone forming oxides of nitrogen (NO_x) emissions across a wide range of applications. NO_x emissions contribute heavily to ambient fine particulate matter pollution as well. Heavy-duty vehicles remain one of the most significant contributors to the overall NO_x inventory, and CARB has indicated that reductions as large as 90% from the current standards may be necessary to achieve air quality goals. To this end, CARB initiated the first of a series of Low NO_x demonstration programs with Southwest Research Institute (SwRI) in 2013, in an effort to demonstrate the feasibility of technologies to achieve this level of NO_x reduction. The program discussed in this report, referred to as the Stage 3 program, was initiated in 2018 and builds on the efforts of the previous programs and has laid the groundwork for continuing efforts by US-EPA and others leveraging the Stage 3 engine and controls. The objective of this program was to demonstrate the technical feasibility of reaching Low NO_x levels up to 90% below the current standards, while maintaining a path towards meeting Phase 2 Greenhouse Gas (GHG) standards. The program goal for Low NO_x was 0.02 g/hp-hr over the current regulatory test cycles, with low load and in-use emissions as low as feasible. The goal of maintaining a path towards meeting Phase 2 standards was defined as maintaining carbon dioxide (CO₂) emissions and fuel consumption at a level comparable to the Baseline engine, if not improving them. In both cases, the program intent was to reach these targets with technologies that are feasible for production by the 2027 model year.

The demonstration was conducted by taking a production 2017 model year Class 8 truck diesel engine (Baseline engine) and adding advanced technologies, such as an advanced aftertreatment (AT) system and engine technologies such as cylinder deactivation (CDA). Advanced controls were developed to manage the new combined engine and AT system, and the whole system was optimized to maximize NO_x reduction while at the same time maintaining or even improving fuel consumption. Because engines must meet emission standards to the end of the mandated useful life, currently 435,000 miles for a Class 8 tractor engine, the demonstration AT system was aged over a specially developed protocol that represented 435,000 miles of field equivalent operation. The final aged system was evaluated on a variety of different duty cycles, including the current regulatory transient Federal Test Procedure (FTP) and Ramped Modal Cycle Supplemental Emission Test (RMC-SET) cycle, and the newly developed LLC that captures the difficult to control low-load urban and vocational operations. In addition, a variety of other operations were evaluated to ensure that the demonstrated results could be expected to translate to similar real-world emission reductions. The final AT system incorporated an innovative close-coupled light-off SCR (LO-SCR) catalyst upstream of a main (underfloor) AT system which consisted of a zone-coated catalyzed soot filter (zCSF), which combined the diesel oxidation catalyst (DOC) function onto a diesel particulate filter (DPF) substrate, and a larger SCR catalyst. This SCR system featured dual Diesel Exhaust Fluid (DEF) dosing nozzles, providing a higher degree of flexibility for NO_x emission control than current AT systems. The final AT system configuration is shown in Figure 1.

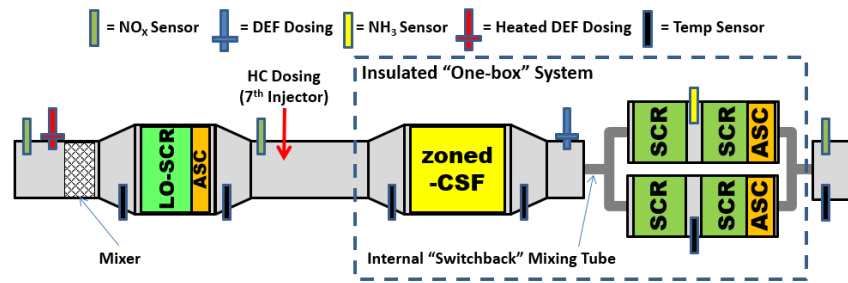


FIGURE 1. FINAL STAGE 3 ADVANCED AFTERTREATMENT SYSTEM

The final demonstrated emission results for this system are shown in Figure 2. The Stage 3 engine achieved an 85% reduction in NO_x on the current regulatory cycles (FTP and RMC-SET) compared to the Baseline at the equivalent of 435,000 miles of aging that accounts for both normal chemical and thermal degradation of the AT system, reaching a tailpipe NO_x level of 0.025 g/hp-hr. On the LLC representing low load urban and vocational operations, the Stage 3 engine reduced NO_x by 95% compared to the Baseline engine, reaching a tailpipe level of 0.052 g/hp-hr. These large reductions were achieved while essentially maintaining CO₂ and fuel consumption at levels equivalent to the Baseline engine. This was accomplished through the combination of advanced AT, controls, and CDA engine technology.

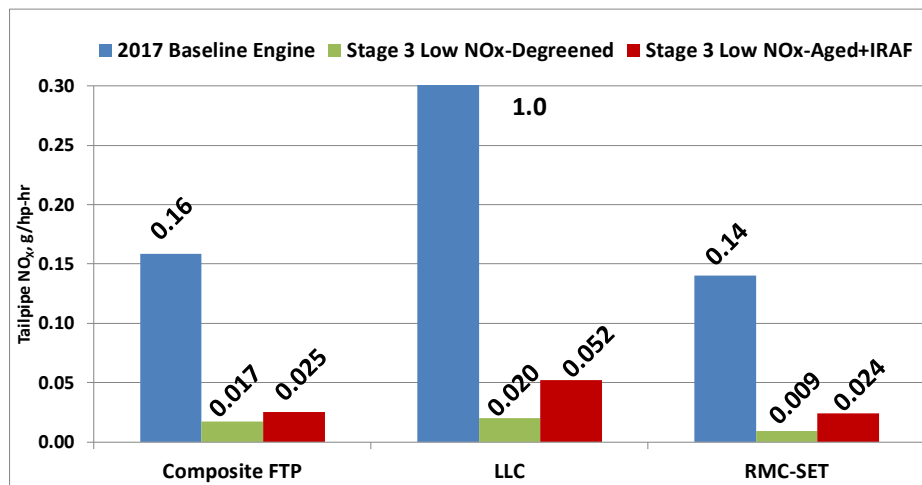


FIGURE 2. FINAL STAGE 3 NO_x RESULT COMPARED TO BASELINE

At the beginning of life, the Stage 3 system demonstrated emissions below the 0.02 g/hp-hr target on the current cycles, but by the end of useful life at 435,000 miles, the demonstration engine was above that target at about 0.025 g/hp-hr. This shift was the result of AT degradation during aging, with the AT system moving from 99.7% NO_x reduction efficiency at the start of life to 99.3% NO_x efficiency at the end of 435,000 miles. Although 0.4% loss of efficiency would appear to be a small change, it was still enough to push the tailpipe NO_x slightly above the program target. In order for production engines to meet a target of 0.02 g/hp-hr, AT system durability will need to be improved by 2027 such that this loss of efficiency is cut in half. There are several potential areas where the Stage 3 AT system durability could potentially be refined and improved.

These include the following: moving from the CSF to a more traditional DOC+DPF architecture, further improved downstream DEF mixing, catalyst sizing, further catalyst reformulation to resist degradation, and further enhancements to the model-based controls (improved long-term trim and aging model incorporation). Further development efforts should focus in these areas, and in fact progress on several such improvements has already been seen in follow-on work by EPA using this Stage 3 Engine and controls.

1.0 INTRODUCTION AND BACKGROUND

This report details the results of a program that represents the continuation of efforts to demonstrate low oxides of nitrogen (NO_x) technologies at Southwest Research Institute (SwRI) on behalf of the California Air Resources Board (CARB) since 2014. The effort detailed herein comprises what is generally referred to as Stage 3 of the Low NO_x Demonstration Program. The Stage 3 program builds on previous efforts conducted under the Stage 1 program (CARB Agreement No. 13-312) and the Stage 2 program (CARB Contract 15MSC010).

In the Stage 1 program, SwRI developed two different technology platforms for demonstration, a diesel platform based on a 2013 Volvo MD13TC Euro VI engine, and a compressed natural gas engine platform based on a Cummins ISX 12G engine. In the final Stage 1b program, the diesel demonstration engine was able to achieve tailpipe NO_x levels of below 0.03 g/hp-hr at the end of useful life, 85 percent below the current heavy-duty standards. However, this was also at the cost of a 1.5 to 2.5 percent penalty in greenhouse gas (GHG) emissions depending on the duty cycle. A significant portion of this GHG penalty was because the base MD13TC engine incorporated waste heat recovery in the form of a turbo-compound system. This system is designed to capture waste exhaust energy and converting it to useful mechanical work, resulted in very low exhaust temperatures that requires a significant amount of heat energy input to enable the advanced aftertreatment (AT) system to function effectively. Overcoming these low temperatures required the use of complex technologies, such as an in-exhaust fuel mini-burner, as well as AT technologies like a passive NO_x adsorber (PNA) which proved to have some challenges maintaining very high NO_x reduction performance over time. The Stage 1 and 1b programs were aimed primarily at current regulatory cycles, the Heavy Duty Transient Federal Test Procedure (FTP) and the higher load Ramped Modal Cycle Supplemental Emission Test (RMC-SET).

In the Stage 2 program, several additional efforts were performed with the aim of expanding high efficiency NO_x control into the low load space. It had been noted that the engines deployed in the wake of the 2010 emission standards performed well under higher load and highway cruise operations, but struggled to maintain NO_x control on lower load duty cycles typical of vocational and urban operations. The Stage 2 program involved several task efforts designed to address this “low load gap” in NO_x emission control. SwRI worked with partners at the National Renewable Energy Laboratory (NREL) to develop a new certification test cycle, designated the Low Load Cycle (LLC), based on real-world vehicles operating on low load duty and vocational cycles. The calibration of the Stage 1 engine was modified and expanded to show the potential for Low NO_x levels under these load conditions. Finally, SwRI examined the accuracy of in-use measurements that could be used to verify emission compliance under low load conditions.

These previous efforts left several open questions regarding further potential improvements to the real capability and durability of Low NO_x emission systems, as well as the potential to develop Low NO_x strategies more consistent with the path to meeting future GHG emission requirements if an engine architecture representing a more mainstream approach was utilized. As a result of these questions, the Stage 3 program described in this report was initiated with the aim of applying the lessons learned from the previous demonstration programs to an up-to-date diesel engine platform that was representative of the mainstream U.S. market. A production MY 2017 Cummins X15 Class 8 truck diesel engine was chosen as the engine platform for this program.

Unlike previous efforts, the Stage 3 demonstration would incorporate a clear target for demonstration of low load emissions controls from the start, with the newly developed LLC added to the list of target cycles. Lessons learned from the previous programs would be applied to improve AT system performance and durability. Technology options, such as the use of close-coupled light-off SCR (LO-SCR) catalysts, which were only examined briefly in Stage 1 would be evaluated in more detail. The newly available Phase 2 GHG procedures would be used to assess the impact of Low NO_x technology changes in vehicle fuel consumption and carbon dioxide (CO₂) emissions.

To maximize the chances to meet program NO_x and GHG targets, a supplemental engine hardware effort, designated Stage 3b, was organized using added third party funding to provide additional engine technology options intended to mitigate potential negative impacts on GHG emissions, and potentially even provide some GHG benefits.

The final result of the Stage 3 (and Stage 3b) program would be a more comprehensive examination of the real potential for Low NO_x emissions in MY 2027 and beyond.

2.0 METHODS AND MATERIALS

2.1 Test Engine

The test engine for this program was a 2017 Cummins X15 Efficiency Series engine. The engine installed in the transient emission test cell at SwRI is shown in Figure 3. The engine selected for this program was calibrated at a nominal 500 hp maximum power rating at 1800 rpm. It was supplied to the program by Cummins, along with the stock AT system. Both the engine and the AT system had previously been de-greened at Cummins prior to being shipped to SwRI and constitutes what is referred to as the Baseline engine. A summary of some basic engine parameters for this test engine is given in Table 1 below.



FIGURE 3. 2017 MY CUMMINS X15 ENGINE

TABLE 1. CUMMINS X15 ENGINE PARAMETERS

Parameter	Value
Configuration	Inline 6 cylinder
Bore x Stroke	137 x 169 mm
Displacement	15.0 L
Rated Power	373 kW (500 hp)
Rated Speed	1800 rpm
Peak Torque	2500 Nm
Peak Torque Speed	1000 rpm
Test Fuel	2-D Cert. Diesel

The engine was an inline 6 cylinder diesel engine that was turbocharged and intercooled, with a single stage turbocharger featuring a variable geometry turbine (VGT). The engine utilized cooled exhaust gas recirculation (EGR) as a primary means of engine-out NO_x control. The engine also featured an intake throttle to help regulate engine air flow and drive EGR under some engine conditions. The engine did feature an asymmetric exhaust manifold design, wherein the front three cylinders were primarily responsible for driving EGR flow through the cooler. The fuel injection system was capable of supporting multiple pilot and post injection events, and was capable of both near and far post injections. For the stock engine, diesel particulate filter (DPF) regeneration was generally performed using post-injection, rather than in-exhaust injection.

Cummins also supplied a significant amount of hardware and engineering support for this program, including calibration access to the engine electronic control module (ECM) using proprietary engineering tools. Cummins also supplied a cylinder head machined and prepared to allow the measurement of cylinder pressure in all 6 cylinders. Significant additional electronic and engineering support for controls development was also provided by Cummins, as detailed later in the section covering Controls.

The stock Cummins AT system was a conventional DOC+DPF+SCR architecture, with the canning arrangement being a modern, “single inline module” design incorporating a compact mixer between the DPF outlet and the SCR inlet. The stock AT system is shown in Figure 4 and Figure 5, depicted from the inlet and outlet sides, respectively. The outlet view also shows the transfer pipe from the engine, which was sized to match a representative truck installation, and verified to be within the temperature drop specifications given by Cummins. The system used a CES ULNOX2 Diesel Exhaust Fluid (DEF) injection system, which utilized a urea cooled injection nozzle. An ammonia slip catalyst was coated on the rear of the SCR catalyst.



FIGURE 4. BASELINE (STOCK) AFTERTREATMENT (INLET SIDE) FOR 2017 CUMMINS X15 ENGINE

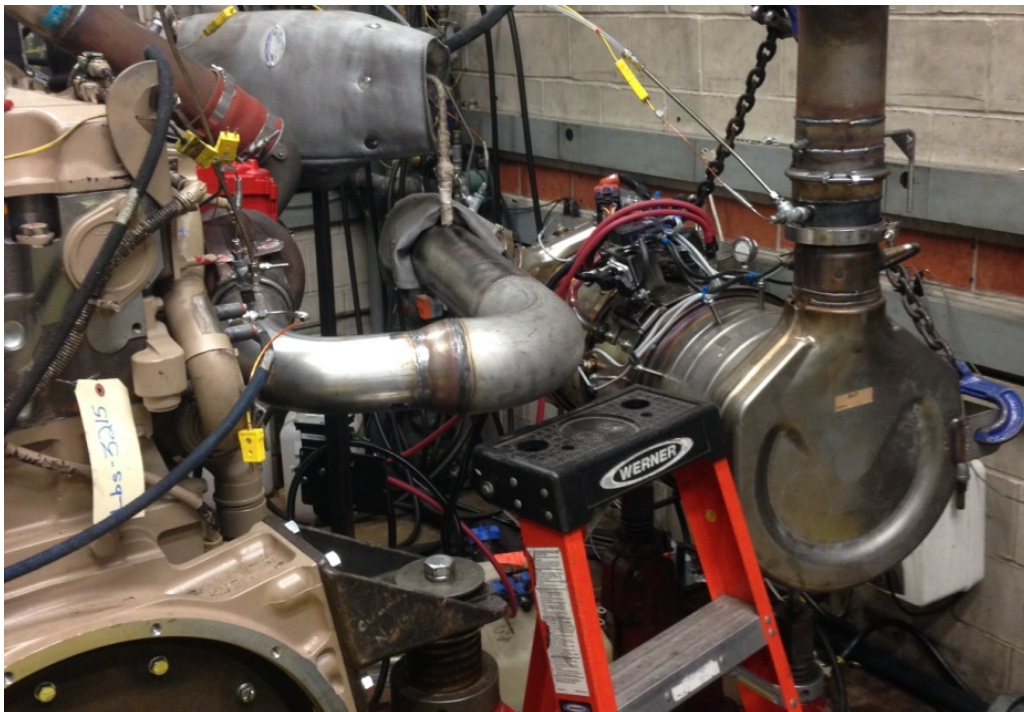


FIGURE 5. BASELINE (STOCK) AFTERTREATMENT SYSTEM FOR CUMMINS X15 ENGINE – OUTLET SIDE AND TRANSFER PIPE

2.2 Emission Test Cell

This program was performed by the Powertrain Division at SwRI in the primary emissions laboratory in Building 87, with the engine installed in Transient Emission Cell 21. This test cell was a transient capable test cell meeting the requirements of 40 CFR Part 1065 for emission certification testing. It features a full-flow constant volume sampling dilution tunnel, and incorporates both Raw and Dilute emission measurements.

Primary tailpipe emission measurements were performed via Dilute Continuous sampling using the constant volume sampling dilution tunnel. A Horiba MEXA 7200D dilute emission bench was used for measurements of THC, CH₄, NMHC, CO, CO₂, and NO_x. Tailpipe particulate matter (PM) measurements were made via SwRI's proprietary secondary dilution system. In addition to the Dilute measurements, an FTIR was also used in the Raw exhaust at the tailpipe to monitor NO, NO₂, NH₃, N₂O, and SO₂, as well as CO₂ and other gases for quality assurance purposes.

Engine-out emissions were also monitored using Raw measurement techniques. A Horiba MEXA 7100DEGR raw emission bench was used for engine-out measurements of THC, CO, CO₂, NO_x, NO, and O₂, as well as intake manifold CO₂ measurement to allow for independent calculation of the EGR rate. Raw exhaust flow measurement was performed via intake air flow measurement using a laminar flow element (LFE) and the chemical balance calculations in 40 CFR Part 1065.650 and 1065.655. During initial baseline tests, engine-out PM was also measured via a Sierra BG3 partial flow dilution system. The partial flow dilution system was used only to establish baseline engine-out PM rates, and again later to verify engine-out PM rates on the Low NO_x engine during development.

During Low NO_x development, an additional FTIR was also utilized at an intermediate point in the system to further monitor NO, NO₂, NH₃, N₂O, SO₂, and CO₂. Both of the FTIR instruments attached to a manifold that allowed measurements at multiple points along the AT system to aid in AT development and calibration, as well as to understand various aspects of AT behavior.

To support combustion and hardware development, an AVL Indimaster high-speed data acquisition system was used to monitor cylinder pressure and fuel injector current on all 6 cylinders. This was crucial for the development and monitoring of systems such as cylinder deactivation, as well as for monitoring combustion stability and performance during calibration development. This system was also used to monitor the timing and triggering the CDA valve actuators during the initial implementation and development stages for that system.

Most of the additional sensors and actuators used for the program were Controller Area Network (CAN)-based, and multiple CAN buses were monitored and recording along with the test cell data. In addition, proprietary control channels were monitored via both ASAP3 for the engine, and CAN for the SwRI integration controller systems. This allowed all data to be recorded and synched onto the SwRI test cell host computer for later ease of use and analysis.

All testing, emission calculations, and test cell quality assurance procedures were conducted in accordance with procedures given on 40 CFR Part 1065, Part 86, and Part 1036. It

should also be noted that, in general, SwRI worked to keep carbon balance for Dilute and Raw emission measurements within the recommended 2% level, although this was not always maintained on some of the tests using some of the prototype Low NO_x AT systems. Even when maintained within the recommended 2% range, this still allowed for variation over time and among systems. In order to enable meaningful comparison of CO₂ emission results over the long performance periods and multiple systems of this program, tailpipe CO₂ emission results were corrected to place them on the same carbon balance basis as the baseline emission results. The approach to this is detailed later under the Results section of the report.

2.3 Test Cycles, Test Procedures, and Preconditioning Procedures

The targets for this program were demonstrated over the relevant on-highway regulatory cycles, including the FTP, RMC-SET, and the newly developed LLC. The CARB Extended Idle test was also run as part of the final demonstration.

For the baseline and final demonstration tests, all tests were run in triplicate. The demonstration test sequence was as follows:

- One cold-start FTP
- 20-min engine-off soak
- Three successive hot-start FTP (with a 20-min engine-off soak between tests)
- 20-min engine-off soak
- One LLC
- One RMC-SET (containing its own preconditioning)

All testing and preconditioning was conducted in accordance with the procedures given in 40 CFR Part 1036 and 40 CFR Part 1065.

Preconditioning for the FTP cycle involved two FTP transient hot-start tests, with a 20-minute soak between the two tests, as outlined in 40 CFR Part 1065. The engine was then placed in overnight cold-soak. Operations prior to the preconditioning FTP tests were not specified, but if a DPF regeneration was needed it was run prior to the start of the preconditioning FTPs. It was found that operations prior to the preconditioning FTPs did not have any impact on the result of the FTP tests. The emission control system was designed and tuned to reach emissions stability with the FTP duty cycle after two FTP preconditioning tests.

Preconditioning for the RMC-SET was conducted as outlined in 40 CFR Part 1065, wherein an RMC-SET cycle is run immediately prior to the start of the RMC-SET test for record. The preconditioning and test cycles were run head-to-tail, with no dwell between the end of the preconditioning cycle and the start of the test for record.

Preconditioning for the LLC involves running at least one hot-start FTP transient cycle. If the test sequence is run as described above, the final FTP hot-start test of the FTP test sequence serves as preconditioning for the LLC, such that no additional engine operation is needed, and the LLC can be run following a 20-minute soak. However, in the event the sequence was interrupted, a preconditioning hot-start FTP transient cycle would be run, followed by a 20-minute engine-off soak and then the LLC test itself.

The CARB extended idle test was run following a hot-start FTP transient preconditioning cycle as described in “California Exhaust Emission Standards and Test Procedures for 2004 and Subsequent Model Heavy-Duty Diesel Engines and Vehicles,” as amended April 2019. Following the preconditioning FTP, the engine was immediately brought to curb idle speed with an appropriate idle load for 30 minutes, after which the engine was brought to an 1100 rpm idle speed with an appropriate idle load for 30 minutes. Idle loads for this test were obtained from Cummins and they were 61 Nm for the 600 rpm curb idle, and 220 Nm for the 1100 rpm idle.

Phase 2 Greenhouse gas fuel mapping tests were also conducted as part of this program, to assess the impact of the Stage 3 Low NO_x configuration on vehicle GHG certification results. These tests were conducted as outlined in 40 CFR Part 1036. Both steady-state fuel mapping, as described in 40 CFR 1036.535, and cycle-average fuel mapping, as described in 40 CFR 1036.540 were conducted. As a Class 8 tractor engine, the 9 default vehicle configurations given in 40 CFR 1065.353 Table 1 were used. Idle mapping was also conducted to support fuel calculations involving Vocational applications. Results are given for both the default (hybrid) mapping approach and the cycle average mapping approach. Fuel maps for the baseline engine and the Low NO_x engine were run on a variety of test vehicle configuration using the EPA Greenhouse Gas Emission Model (GEM). GEM version 3.5.1 was used for these comparison runs. Comparisons were made between these fuel maps for a set of vehicle configurations that EPA utilized to assess stringency for MY 2027 on both Tractor and Vocational applications.

2.4 Low NO_x Aftertreatment Hardware

Advanced AT hardware for this program was supplied in kind by members of the Manufacturers of Emission Controls Association (MECA). The MECA suppliers for this program were organized into two supplier teams, each consisting of a catalyst company, substrate supplier and canning company. Each team was supplied a set of data from SwRI to aid in system design and simulation. These data sets were taken from SwRI engine calibration efforts and projections of expected performance from technologies like CDA. The supplier teams used this data to develop two packages of AT technology offerings, each with several optional elements. This approach provided SwRI with a wide variety of technology to choose from in developing a final AT system approach to reach the NO_x and CO₂ goals of the program. It was understood that these systems were developed with the intention of reaching a 435,000 mile full useful life (FUL). At the time this program was proposed, and when these AT systems were being developed, longer useful life periods had been discussed in concept, but no specific details were yet available, therefore the current FUL requirement of 435,000 miles for heavy-heavy duty engines was utilized for this demonstration.

As was the case in the earlier Stage 1 and Stage 2 demonstration programs, it was clear that a conventional AT system following the current DOC+DPF+SCR architecture would be insufficient to meet the targets for the Stage 3 program on a conventional engine architecture. In addition, the Stage 3 design was developed from the beginning with requirements of the LLC in mind, as well as under the assumption of a broader in-use testing requirement that would consider low load operations. Therefore, additional AT elements explored to deal efficiently with cold-start and low temperature operations.

2.4.1. *Aftertreatment Team 1*

The AT Team 1 architecture was built around the concept of a European-style one-box design for the downstream system. This design features two parallel flow paths for the downstream AT system, and generally results in lower overall system backpressure. The primary Team 1 concept diagram is shown in Figure 6. Unlike a traditional DOC-DPF configuration, a zone-coated Catalyzed Soot Filter (zCSF) was used as the primary oxidation catalyst and particulate filter. This was done to further minimize thermal inertia ahead of the downstream SCR catalysts to aid in warm-up of the downstream SCR. For the purposes of this work, it was assumed that the Platinum Group Metals (PGM) loading on the zCSF was comparable to that of the combined loading from the DOC and DPF. The system also featured a dual path SCR / ASC configuration, which provided higher SCR volume compared to the other evaluated downstream system. As will be mentioned for the other configurations, the upstream and downstream systems are connected by a 1.2 meter exhaust tube. This length represents the typical distance between the engine bay and the designated AT mounting location for the downstream section. Table 2 provides additional catalyst details for this candidate system. Figure 7 shows the packaged downstream unit, as well as the upstream LO-SCR hardware.

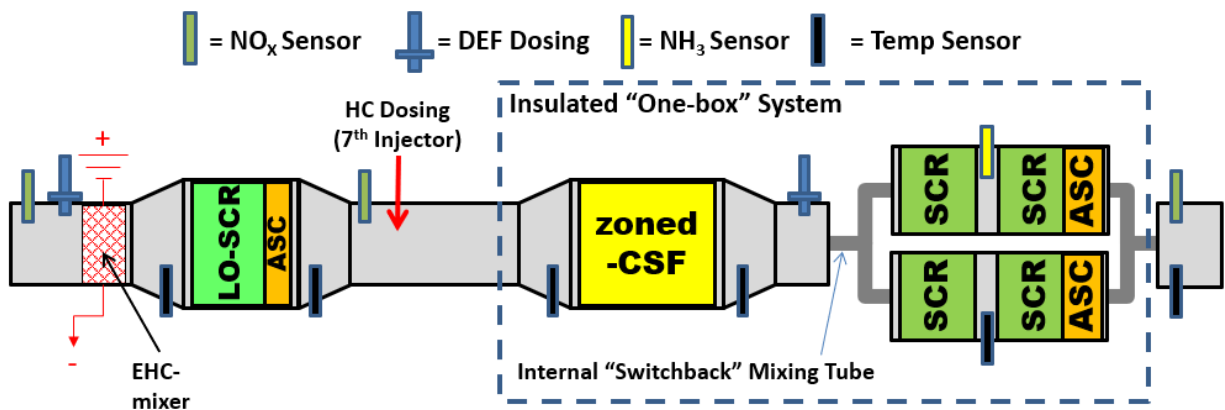


FIGURE 6. TEAM 1 AFTERTREATMENT PRIMARY CONCEPT

TABLE 2: CANDIDATE AFTERTREATMENT SYSTEM 1 CATALYST SPECIFICATIONS

Component	D x L, in	CPSI/Wall, mm	Volume
LO-SCR /ASC	13x7	300/5	15 L
Zoned-CSF	13x7	300/7-ACT	15 L
SCR	(2) 10.5x4	600/4.5	11.5 L
SCR	(2) 10.5x5	600/4.5	14 L
SCR-ASC	(2) 10.5x5	600/4.5	14 L
ACT = Asymmetric Channel Technology			

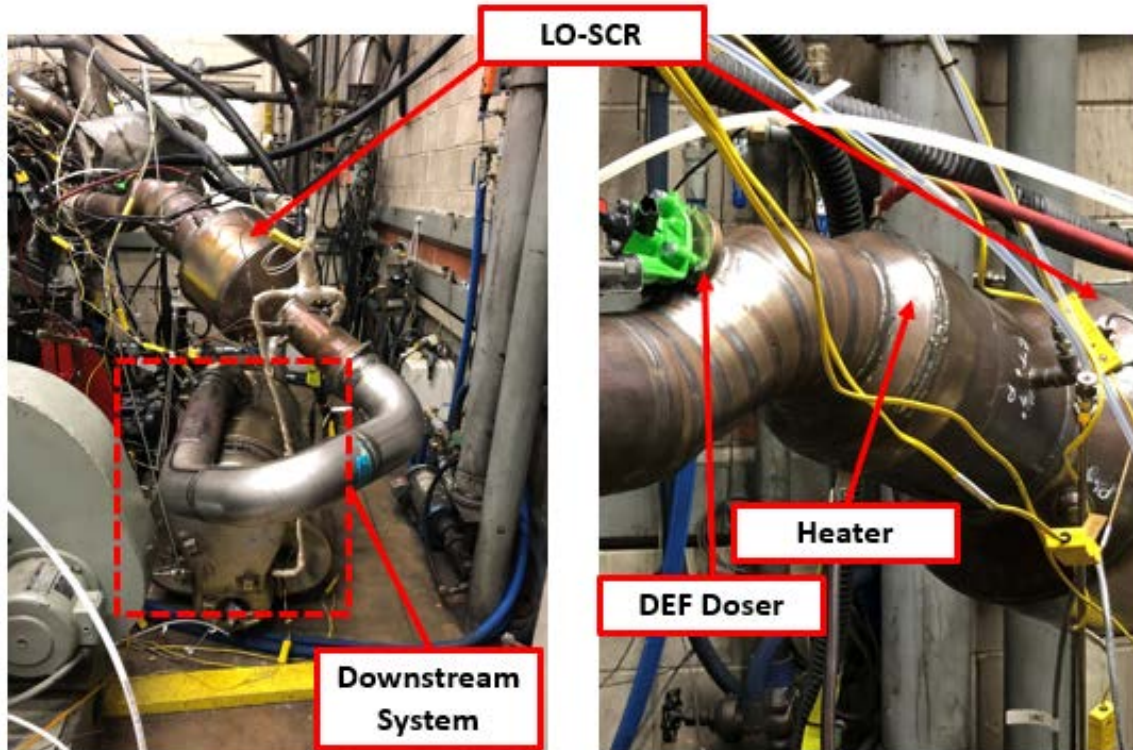


FIGURE 7. CANDIDATE AFTERTREATMENT SYSTEM 1 INSTALLATION

The DEF injection hardware shown in Figure 7 utilized a DEF injector and heater to generate NH_3 at low temperatures for the upstream system. The heated dosing approach in this case was an electric heater built into an electrically heated catalyst (EHC) assembly having only a thin metallic support substrate downstream of the heater assembly to aid evaporation and mixing. The intention of the 2 kW EHC was not to provide significant supplemental heat energy to the bulk exhaust gas, but instead to provide a warm surface for DEF evaporation at lower temperatures. This solution is one of two potential designs proposed to generate NH_3 under low temperature conditions. In this case, the EHC was run at 1.8 kW when the exhaust temperature was low, but was turned off whenever the exhaust temperature at the LO-SCR inlet was above 210°C . The downstream SCR catalysts utilized a conventional DEF injector to deliver the NH_3 . Both of the DEF injectors for this system were supplied by a single pre-production pump designed to supply two dosing nozzles. A single dosing control unit was responsible for low level dosing controls on both systems, and was commanded via CAN from the SwRI Integration Controller.

Figure 8 shows an internal view of the downstream “one-box” configuration of the Team 1 AT system. The internal configuration allows sharing of heat between the various substrates, also provided some internal heating for the integrated mixing tube. The exhaust split chamber was verified to provide a very even split of exhaust flow under both high and low flow conditions. A mixer is incorporated just downstream of the DEF injection point (not shown in this picture). The

completed system incorporates production-style insulation, and no additional insulation was employed on this unit as a result.

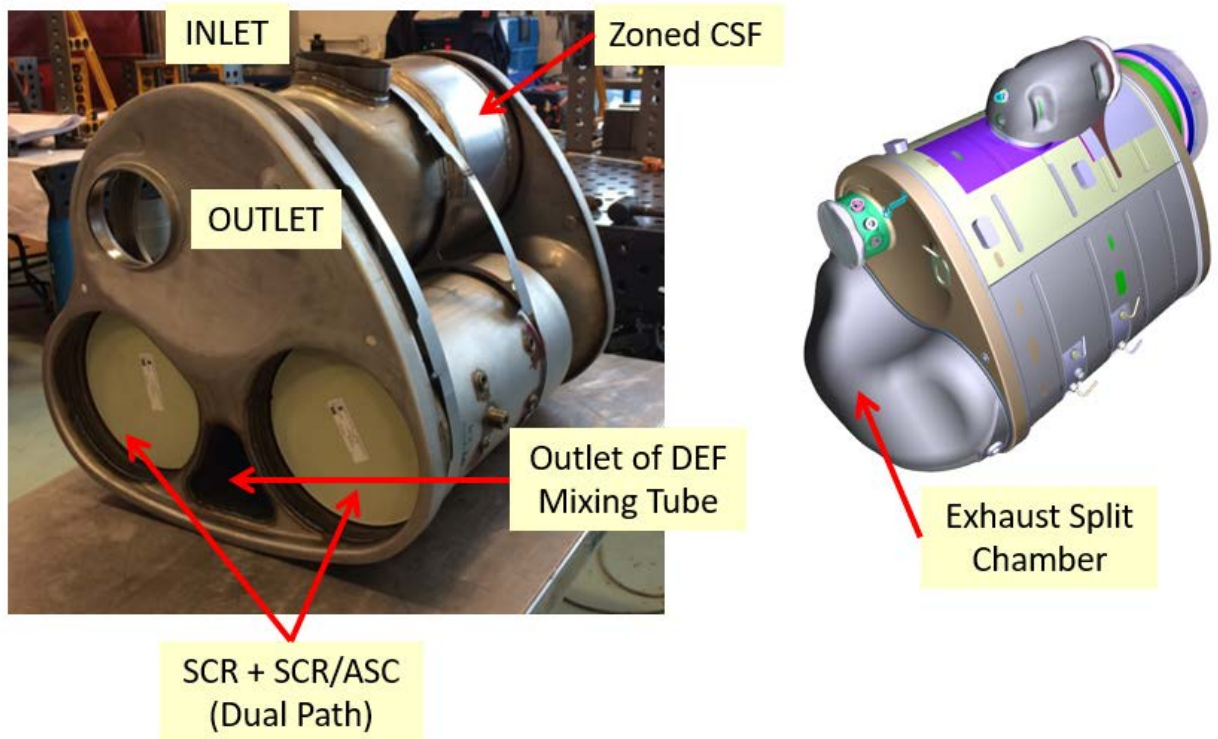


FIGURE 8. INTERNAL DETAILS FOR TEAM 1 DOWNSTREAM “ONE-BOX” SYSTEM

The Team 1 AT system provided several advantages over the other evaluated systems. For example, there are inherent heat retention benefits from the “box” style integration. Though it is not shown in the picture, the SCR catalysts are surrounded by exhaust, which can be beneficial during cool down segments like those observed during the LLC. The integrated dual path SCR configuration also provided lower backpressure helped improved fuel economy, as did the relatively low backpressure mixing tube arrangement. Aside from the system layout, the combination of DOC and DPF into the zCSF component reduced the thermal inertia upstream of the downstream SCR catalysts, reducing light-off time during cold-starts. Assuming that the component characteristics (e.g. PGM loading and washcoat formulation) are consistent with those stated in literature, the passive regeneration performance has been reported as similar to a conventional DOC + DPF configuration.

There are also a few disadvantages that were considered for this system. For example, the LO-SCR DEF injection hardware incorporated a small thermal mass (i.e. the heater and supporting metal substrate) upstream of the catalyst, which could delay the LO-SCR warm up. The additional power draw from the electrical system will also have an inherent fuel penalty and burden,

especially on the low load cycles. The increased burden on the vehicle electrical system will also present integration problems for current and future vehicles. There were also initial concerns regarding the durability of the zone coated CSF, as this component does not yet have a track record in production applications, since most heavy duty systems utilize a DOC-DPF configuration. Some of these concerns included the durability of the NO-to-NO₂ oxidation function for both passive soot oxidation and feedgas preparation, as well as the potential impact of ash loading on this function.

An alternate configuration was also proposed by Team 1, as a contingency in the event that the LO-SCR alone did not provide sufficient improvement in system light-off. This alternate concept including the use of an SCR-on-Filter (SCRF), and is illustrated in Figure 9. This configuration would result in more rapid system light-off, however it would also result in a significant increase on active regeneration frequency due to the loss of most of the passive soot oxidation capability of the system. Therefore, this configuration was only considered as a fallback option. The initial performance of the other systems indicated that this option was not necessary, and therefore it was not evaluated in the test cell.

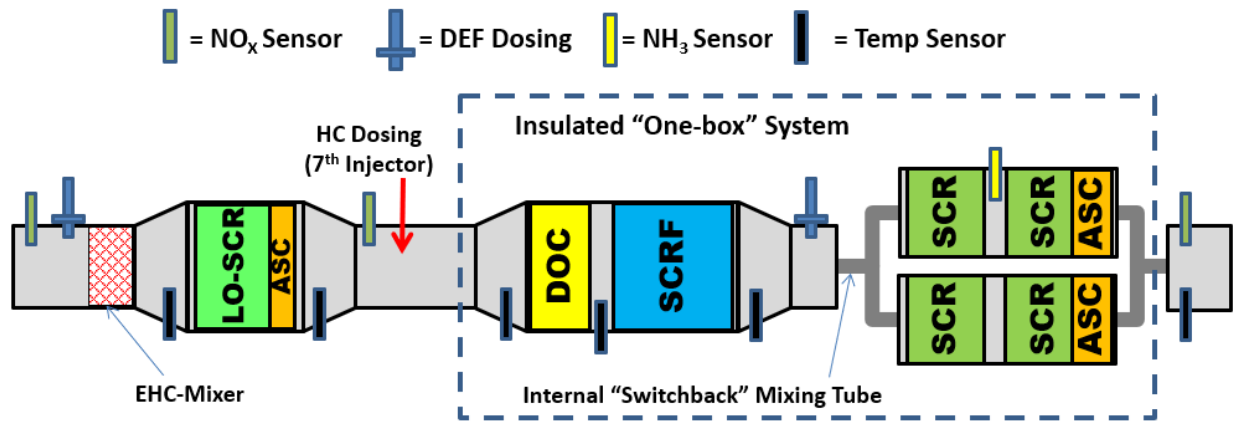


FIGURE 9. TEAM 1 ALTERNATE CONFIGURATION (SCR-ON-FILTER)

2.4.2. *Aftertreatment Team 2*

AT Team 2 designed their system around a single inline module approach, which is also commonly used in many 2017 and later AT systems. This approach has advantages with respect to packaging, and represents a different approach to lowering thermal inertia. Team 2 also provided two different options for the upstream catalyst module. The two configurations supplied by Team 2 are shown in Figure 10 and Figure 11 below. Details of the catalyst sizing and substrates used in the Team 2 system are given below in Table 3.

TABLE 3. TEAM 2 CATALYST SPECIFICATIONS

Component	D x L, in	CPSI/Wall, mm	Volume
LO-SCR /ASC	13x6	400/4	13 L
DOC	13x5	400/4	11 L
DPF (catalyzed)	13x7	300/7-HAC	15 L
SCR	13x6	600/4.5	13 L
SCR-ASC	13x6	600/4.5	13 L

HAC = High Ash Capacity

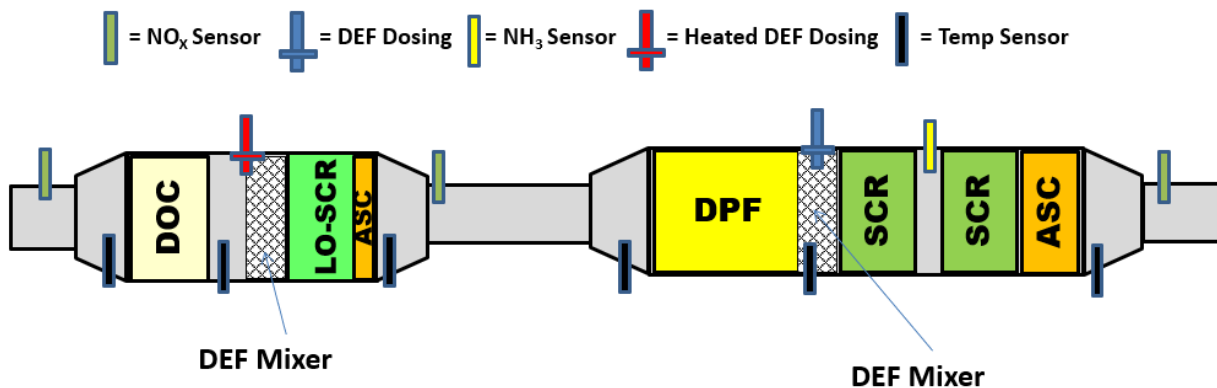


FIGURE 10. TEAM 2A CONFIGURATION SCHEMATIC (DOC UPSTREAM OF LO-SCR)

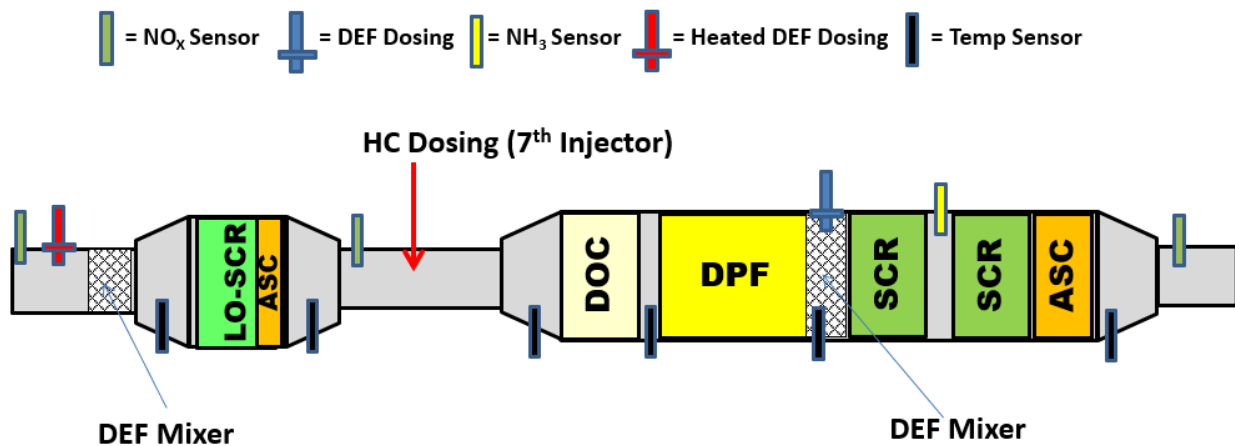


FIGURE 11. TEAM 2B CONFIGURATION SCHEMATIC (NO DOC BEFORE LO-SCR)

Both of the Team 2 configurations used the same DEF dosing hardware. The upstream LO-SCR package utilized a novel heated doser approach, which involved the direct heating of the DEF under pressure. This approach resulted in a very fine droplet distribution and pre-heated fluid, which allowed dosing at temperatures down to 130°C, and high rates of dosing to be used at temperatures under 200°C where dosing would normally be limited due to risk of urea deposits

formation. The heated dosing hardware is shown in Figure 12 below. In Team 2 testing, the system was supplied by a separate commercial dosing pump. However, for the final AT configuration, this unit could be supplied by the same pump that was used to supply the two nozzles of the Team 1 dosing system, replacing the upstream nozzle in the plumbing but operating at the same pressures. Due to proprietary considerations, details of this heated dosing approach cannot be supplied, but as of the writing of this report, the manufacturer is preparing to proceed to on vehicle demonstrations as the hardware moves toward production.



FIGURE 12. TEAM 2 HEATED DOSING SYSTEM HARDWARE INSTALLED AT IN-PIPE LOCATION (USED FOR CONFIGURATION 2B)

For downstream dosing, the Team 2 system utilized the production dosing system that came with the engine. That hardware is shown installed on the Team 2 downstream unit in Figure 13. This unit was supplied by the production DEF pump (not shown), and was controlled via commands sent to the engine ECM. The compact mixer assembly in the Team 2 downstream unit was designed specifically to mount this doser, in a fashion similar to the baseline AT system.



FIGURE 13. PRODUCTION CUMMINS DEF DOSER INSTALLED ON TEAM 2 DOWNSTREAM UNIT

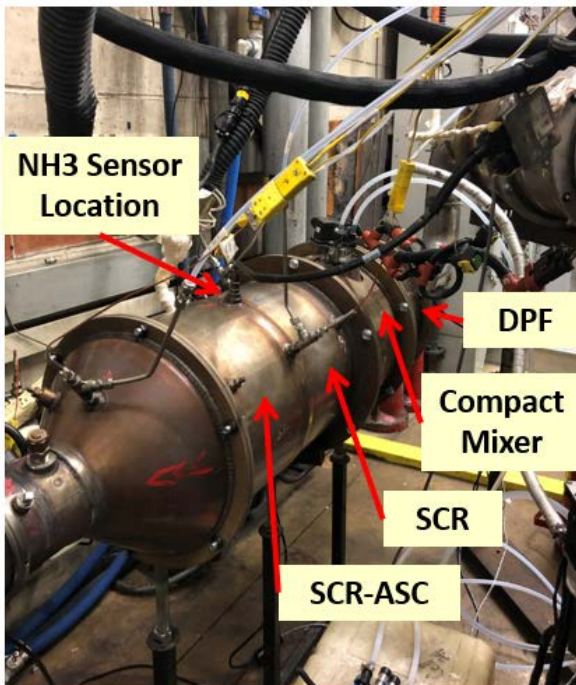
The Team 2A configuration placed the DOC upstream of the LO-SCR catalyst, as shown in Figure 10 and pictured in Figure 14. The primary advantage of this approach is that the DOC upstream of the LO-SCR can be utilized to generate an exotherm to desulfate the LO-SCR. In addition, the DOC can provide NO-to-NO₂ oxidation to optimize the feedgas for the LO-SCR and improve low temperature conversion efficiency. This approach is likely more compatible with the use of post-injection to provide HC for generating exotherms across the DOC. Details of the Team 2A configuration are shown in Figure 15.

However, this approach also has a significant number of disadvantages as well. The use of the DOC also requires the use of a compact mixer approach between the DOC and LO-SCR to enable the upstream DEF dosing. This means that the upstream catalyst module is considerably larger, and would likely result in a very difficult packaging challenge, and might not be practical for under-hood, close-coupled use. In addition, the presence of the DOC and the compact mixer upstream of the LO-SCR adds significant thermal inertia upstream of that catalyst, slowing down light-off under cold-start conditions. The use of a second compact mixer also adds considerably to the overall backpressure of the system. The presence of the DOC upstream of the LO-SCR also means that the exotherm for DPF regeneration will impact the LO-SCR, which would significantly raise the thermal load and potential for thermal degradation on the LO-SCR.



FIGURE 14. CONFIGURATION 2A COMPLETE SYSTEM DURING INSTALLATION

Downstream Package



Upstream Package

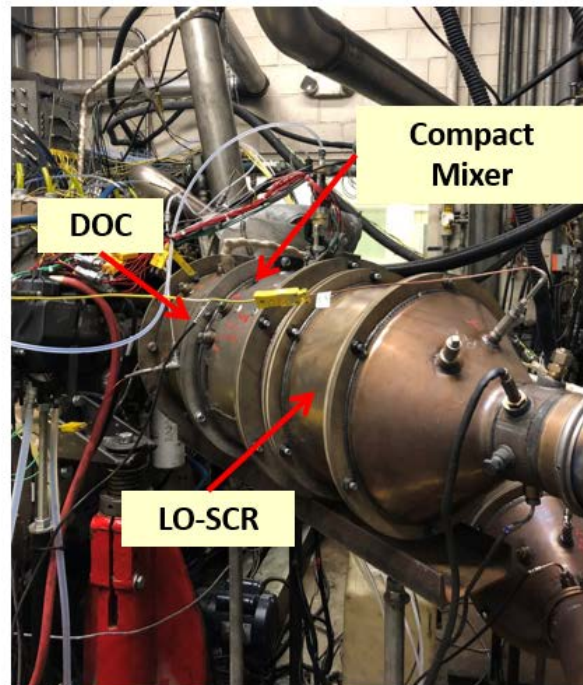


FIGURE 15. CONFIGURATION 2A - DETAILS

One of the largest drawbacks to the Team 2A approach is that, while the DOC enables easier generation of exotherms for desulfation (deSO_x), the presence of the DOC will greatly increase the rate of sulfation on the LO-SCR. This is because of the tendency of the DOC to oxidize SO_2 to SO_3 as sulfates are much more effectively stored as a poison on the LO-SCR. Based on supplier results and information in the literature, it is estimated that the presence of the DOC could increase the required frequency of deSO_x by a factor between 5 and 10. This would result in a significant CO_2 penalty.

As a result of these issues, the Team 2A configuration was considered to be more of a fallback approach, in the event that deSO_x would prove too difficult to accomplish without the DOC. However, it was felt that an alternate arrangement would likely have been needed because the base 2A upstream module was just too large to consider feasible for packaging. In that case, an alternate configuration was proposed as shown below in Figure 16. However, it was never tested given the results of the other tests indicated that the DOC upstream of the LO-SCR configuration was not preferred.

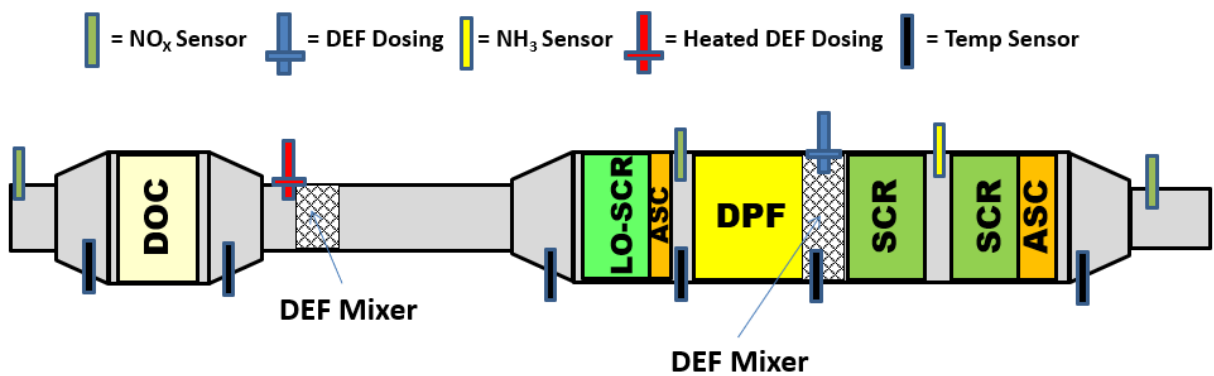


FIGURE 16. TEAM 2A ALTERNATE CONFIGURATION TO RESOLVE PACKAGING QUESTIONS (NOT USED)

The 2A configuration was evaluated in the cell to validate some of its performance characteristics, but was quickly replaced by configuration 2B, shown in Figure 11. The primary advantages of the 2B arrangement included:

- A smaller upstream package size due to the DOC being located in the downstream package, and the use of a smaller in-pipe mixer as a result of this relocation
- Reduced thermal inertia upstream of the LO-SCR
- Less thermal load on the LO-SCR, improving prospects for long-term durability
- Much reduced frequency of deSO_x due to lack of SO_2 -to- SO_3 oxidation
- Lower backpressure given the much reduced mixer hardware requirement
- Lower N_2O emissions due to reliance primarily on “standard” (NO-only) SCR

The reduced package size, although still challenging to package under the hood, nevertheless represents a configuration which is at least feasible for “close-coupled” use. The Configuration 2B hardware is shown installed in Figure 17.

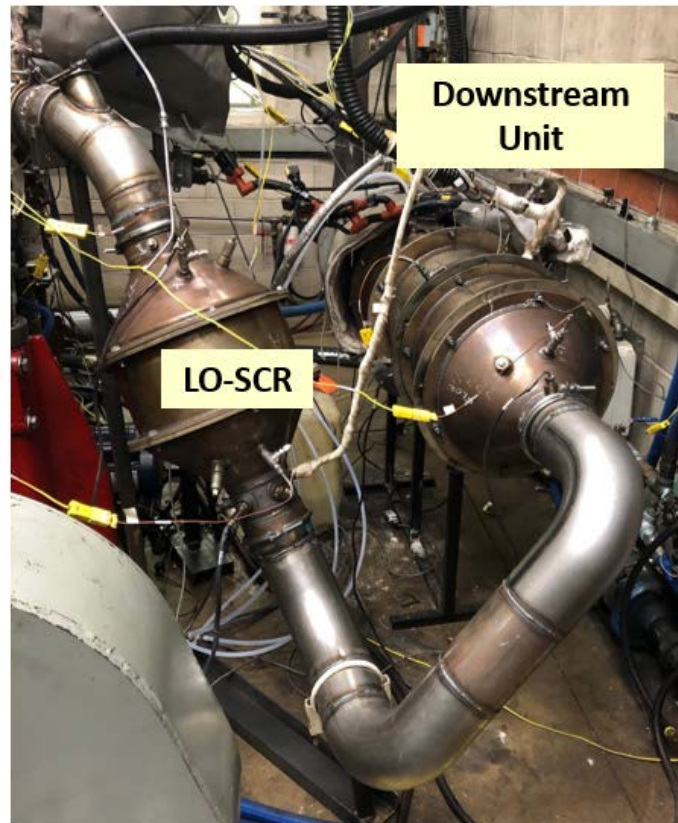


FIGURE 17. CONFIGURATION 2B – TEST CELL INSTALLATION

However, this configuration also has a few drawbacks. The principle issue is that without a DOC to generate exotherms, the heat required for deSO_x must be generated by the engine itself. Given that deSO_x requires temperatures up to 550°C , that could be a considerable challenge, especially at light load. However, this is an area where the use of CDA can help considerably, enabling practical deSO_x under a much wider range of driving conditions. The second issue is that without a DOC, the use of post-injection to supply HC for exotherms during DPF regeneration could be an issue, possibly causing long-term LO-SCR durability issues. The detailed concerns would be direct HC impact on the LO-SCR, possible low temperature fouling due to combined HC and soot impacts, and exotherms across the ASC if one is present on the LO-SCR. However, this is an area which deserves further study to determine whether LO-SCR can be durable enough for heavy-duty applications in a configuration using in-cylinder post injection to support exotherms. Given the uncertainty around this potential issue, it was decided to use in-exhaust HC injection, placed after the LO-SCR (thought still in an under-hood location), to support DPF regeneration on the downstream system. Finally, this configuration does not allow for any feedgas optimization upstream of the LO-SCR, although this is balanced by the lower thermal inertia of this system.

Both configurations were evaluated, as discussed later under the Results section, and ultimately the configuration 2B approach was selected as the optimal choice for the Low NO_x demonstration.

2.4.4. Final Aftertreatment Configuration

In the early stages of the program development, configurations 1, 2A, and 2B were each evaluated separately. The detailed results of those evaluations are discussed later in the Results section. Each of the systems showed advantages and disadvantages. Ultimately the decision was made to combine components from both AT teams to produce the optimal AT configuration. Therefore, the upstream components of Configuration 2B were combined with the downstream components for Configuration 1. This produced the final Stage 3 AT configuration, which is given below in Figure 18. Catalyst details for the final Stage 3 system are given in Table 4.

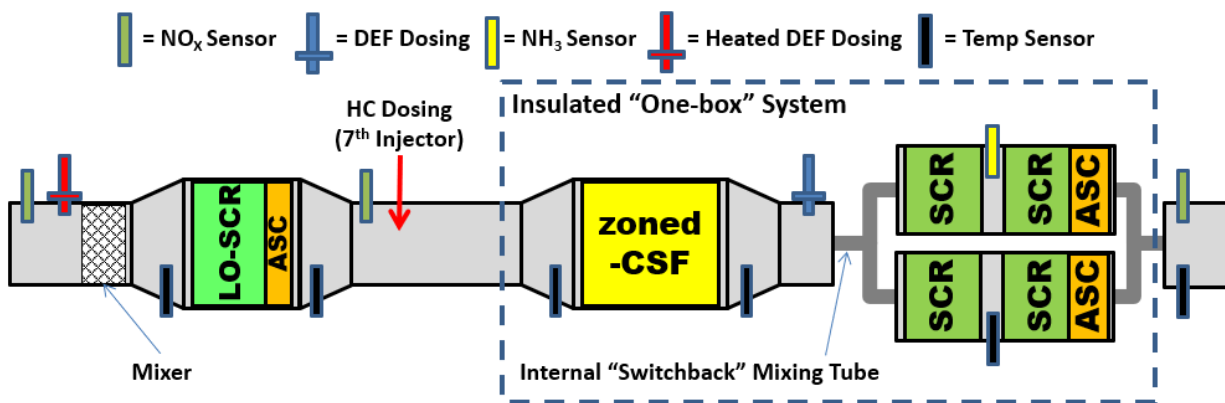


FIGURE 18. FINAL STAGE 3 AFTERTREATMENT CONFIGURATION

TABLE 4. CATALYST SPECIFICATIONS FOR FINAL STAGE 3 AFTERTREATMENT SYSTEM

Component	D x L, in	CPSI/Wall, mm	Volume
LO-SCR /ASC	13x6	400/4	13 L
Zoned-CSF	13x7	300/7-ACT	15 L
SCR	(2) 10.5x4	600/4.5	11.5 L
SCR	(2) 10.5x5	600/4.5	14 L
SCR-ASC	(2) 10.5x5	600/4.5	14 L
HAC = High Ash Capacity			

The final Stage 3 AT configuration uses the upstream LO-SCR hardware and the heated doser from Team 2, and the Team 1 one-box downstream AT system. This system produced the best combination of NO_x performance and CO₂ emissions. The backpressure associated with this system was lower than either of the two systems tested separately. There were still some compromises in the system configuration. In exhaust HC dosing was still utilized to generate the exotherm required for regeneration of the downstream system, and it was necessary to leverage

CDA fully to enable deSO_x on the LO-SCR. Finally, the zoned-CSF had to be utilized despite some of the durability concerns, because a DOC+DPF version of the system was not available at that time. Performance tests had by this time indicated that the lower thermal inertia of the zoned-CSF compared to DOC+DPF was not necessary for cold-start, and that the increased thermal inertia of a DOC+DPF would in fact be helpful in some duty cycles, but the available hardware had to be used.

The final Stage 3 AT hardware set is shown installed on the Stage 3 engine in the transient test cell in Figure 19. The system is shown without the insulation that was later installed on the transfer pipes so that the components can be seen more easily. A second set of hardware from the same batch of catalysts was used to prepare the parts for Final Aging, and these are the parts shown in Figure 19. One modification for the Final Aged parts was made to allow the removal of the zoned-CSF for ash cleaning and weighing, or in the event of problems with the filter. This modified canning is shown below in Figure 20. The transfer pipe from the turbine outlet to the heated doser mounting point is roughly 24 inches in length. It is somewhat longer than would be anticipated for a final installation in part to accommodate the laboratory instrumentation needed for the development work. The transfer pipe from the LO-SCR to the downstream catalyst assembly is 46 inches in length and the length is set to simulate a transfer tube from and under hood location to an underfloor location in a vehicle installation.

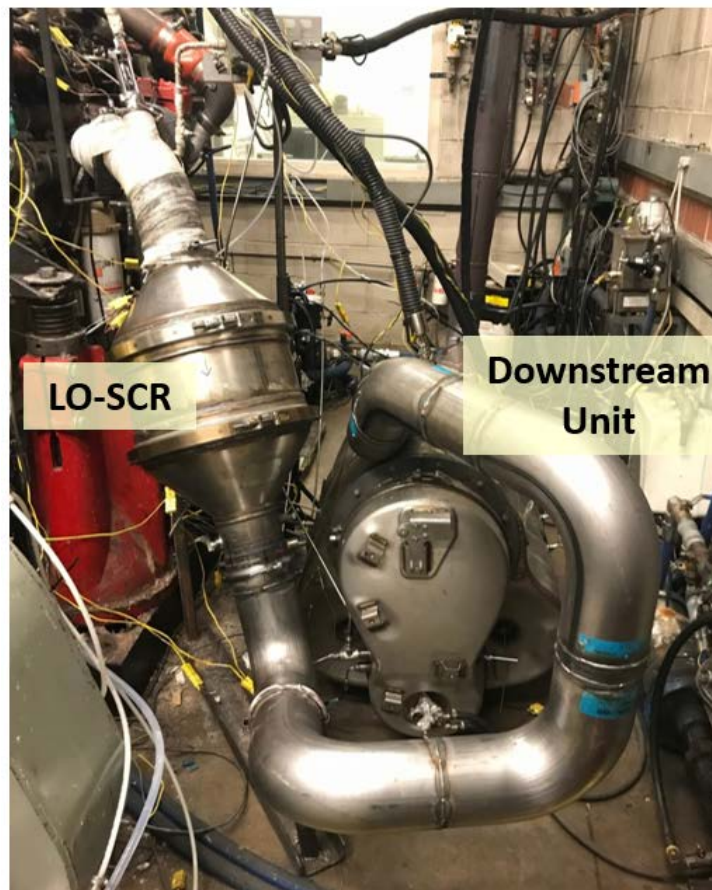


FIGURE 19. STAGE 3 FINAL AFTERTREATMENT CONFIGURATION (SHOWN WITHOUT INSULATION)

It should be noted that the first set of parts, referred to as the Development parts in this report, do not feature a removable zoned-CSF module, and also a bolt flange is utilized on the LO-SCR rather than the more production like v-band clamps used on the Final parts. The aging and preparation of both sets of these parts are detailed later under the Aging methodology section of the report.



FIGURE 20. STAGE 3 FINAL DOWNSTREAM SYSTEM SHOWING REMOVABLE ZONED-CSF MODULE

2.5 Low NO_x Engine Hardware Options

Following some of the early engine calibration efforts, it became apparent that it would be very difficult to reach the NO_x and CO₂ targets for this program simultaneously without additional flexibility on the engine platform that was not included on the base engine. This need was anticipated in the planning stages of the program, and SwRI worked to secure additional scope and funding from several parties that would permit the examination of a number of additional engine hardware options. This effort was sometimes referred to as the Stage 3b engine hardware program. Funding parties in this effort included EPA, MECA, and the SwRI-led CHEDE-VII industry consortium program.

SwRI worked with suppliers to select a variety of different engine hardware modifications that could be examined on the engine in the scope and timeframe allocated for this Stage 3b effort. Those options are given below in Figure 21. Each of these technologies was implemented on the engine and tested to examine its capability to enhance the ability to reach Low NO_x levels and/or reduce the CO₂ impact of engine calibration changes to reach those levels. Implementation details of each of these hardware options is shown below, while the results of the evaluations are discussed in detail later. Ultimately, it was determined that CDA would be utilized in the final Stage 3 configuration. It was also determined that an EGR Cooler Bypass could be valuable for robustness

reasons, but it was not implemented in the final demonstration configuration for performance reasons, as discussed later.

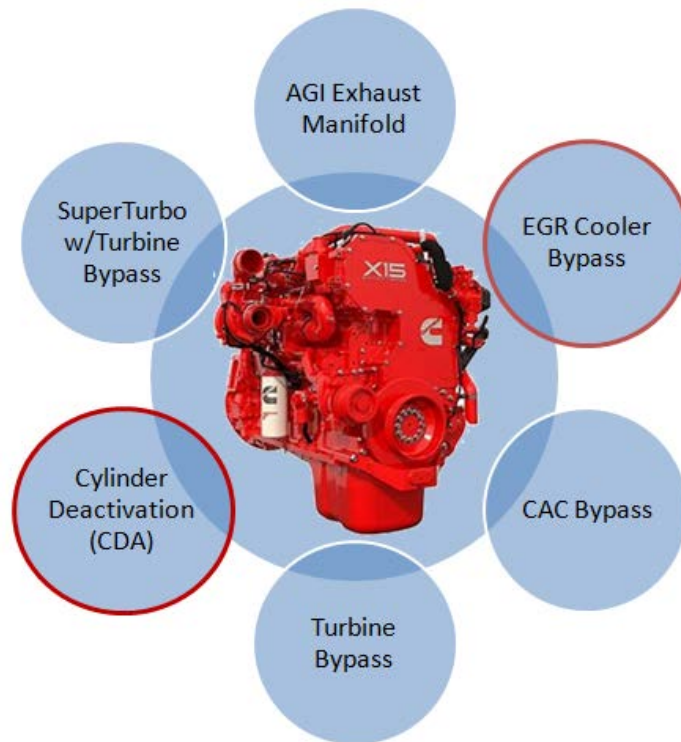


FIGURE 21. “STAGE 3B” ENGINE HARDWARE OPTIONS EXAMINED

2.5.1. Air Gap Insulated (AGI) Exhaust Manifold

An AGI manifold is a technology that uses a specially fabricated exhaust manifold featuring two layers with an air gap to provide extra insulation. The intent is to prevent heat losses from the exhaust manifold and retain more of the exhaust heat in the exhaust. The supplier worked with Cummins and SwRI to design and fabricate a prototype AGI manifold that would fit this engine and mount the stock VGT turbocharger. To prepare for the efficient evaluation of other hardware options shown in Figure 21, the AGI manifold built with preparations in place to also implement both an EGR cooler bypass and a turbine bypass. Additional hardware was used to fully implement these features, and the ports were covered with block-off plate when those options were not being utilized.

The AGI manifold is shown in Figure 22 from different views. The AGI manifold is also depicted in comparison to the stock exhaust manifold in Figure 23. The manifolds had very similar overall internal volume, and both also featured an asymmetric turbine inlet design (not shown due to proprietary details). The AGI manifold was designed to have the same asymmetric proportions between the front and rear cylinders as the stock manifold.

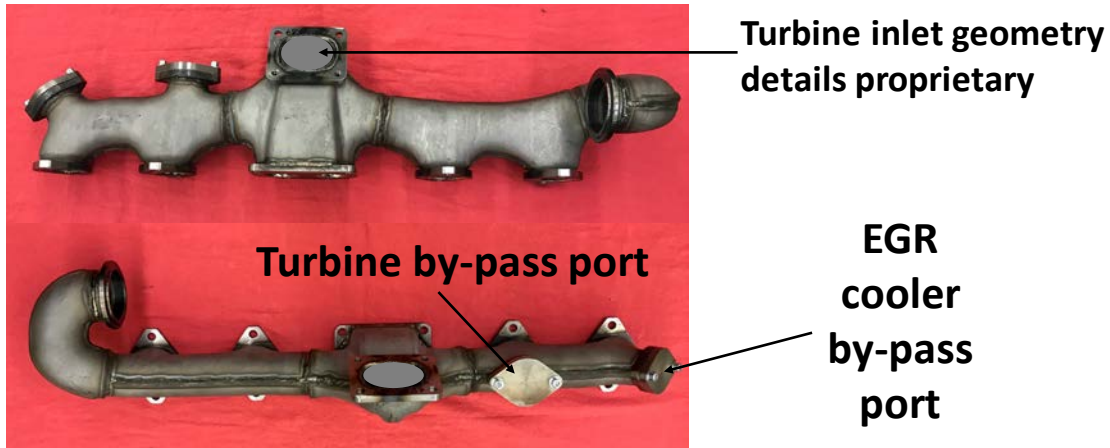


FIGURE 22. AGI EXHAUST MANIFOLD FOR STAGE 3 ENGINE



FIGURE 23. COMPARISON OF AGI AND STOCK EXHAUST MANIFOLDS

The AGI manifold is shown installed on the Stage 3 engine in Figure 24, in this case for initial testing with both the EGR cooler bypass port and the turbine bypass port blocked. One area of difference that needs to be noted between the manifolds pertains to pressure and temperature instrumentation, as shown in Figure 25. It was not possible to instrument the AGI manifold in the same locations without causing sealing problems due to the air gap construction. Therefore, those ports were relocated to the inlet of the turbine housing. However, this does cause some difficulties on comparing turbine inlet temperatures as noted later. The key turbine outlet data measurements, however, are in the same location and are not disturbed by this.



FIGURE 24. AGI EXHAUST MANIFOLD INSTALLED ON STAGE 3 ENGINE

Pre-turbine T Locations for Stock Manifold



Pre-turbine T Locations for AGI Manifold



Turbo Out T Location



FIGURE 25. PRESSURE AND TEMPERATURE MEASUREMENT LOCATIONS ON STOCK AND AGI EXHAUST MANIFOLDS

Given that this was a prototype design which had not been validated for long-term operation yet, additional brackets were installed to help support the weight of the VGT turbocharger and avoid any potential damage to the AGI manifold during operation. It is unclear whether these precautions were ultimately necessary, but there were no mechanical problems with the AGI manifold during the course of testing.

2.5.2. EGR Cooler Bypass

The potential for the EGR cooler bypass was initially evaluated under steady-state experiments in several preliminary arrangements. This was done in part due to the procurement

timing for the final EGR bypass control valve. The cooler bypass was implemented in all cases in a manner that allowed for the engine's normal EGR measurement via venturi after the cooler to function properly. The initial evaluations were done using the AGI manifold, which would also examine any synergy between the two technologies. The first arrangement, shown in Figure 26, was used to examine full (100%) cooler bypass under steady-state conditions. This setup was load limited due to temperature limitations of the venturi differential pressure sensor used by the engine for EGR flow rate measurement, but was still sufficient to examine the concept at light loads where it would be utilized the most.

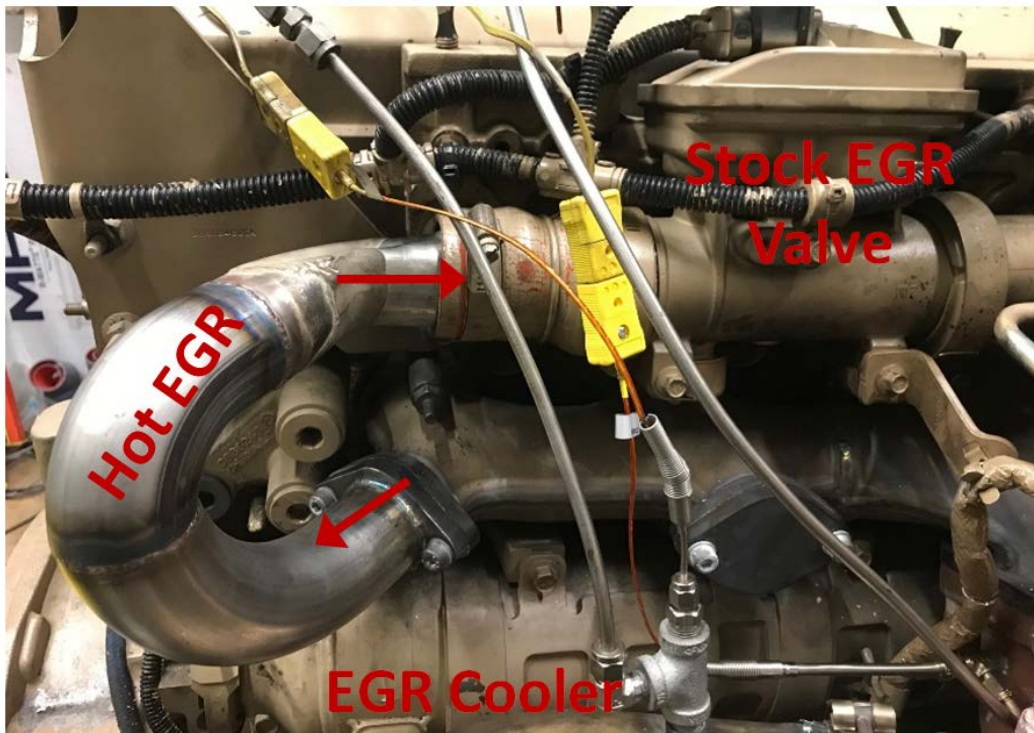


FIGURE 26. EGR COOLER BYPASS DEVELOPMENT SETUP FOR INITIAL EXPERIMENTS WITH 100% BYPASS

Given the temperature limitations noted above, a second preliminary installation, shown in Figure 27, was used to examine a partial bypass, which allowed higher load test points. Ultimately, neither of these arrangements would have allowed transient evaluation, therefore a final configuration was installed after a control valve was procured that would allow for transient control of the bypass leg. This final setup is shown in Figure 28, and it incorporates a bypass valve which was engine water cooled and could be controlled via CAN from the SwRI controller.

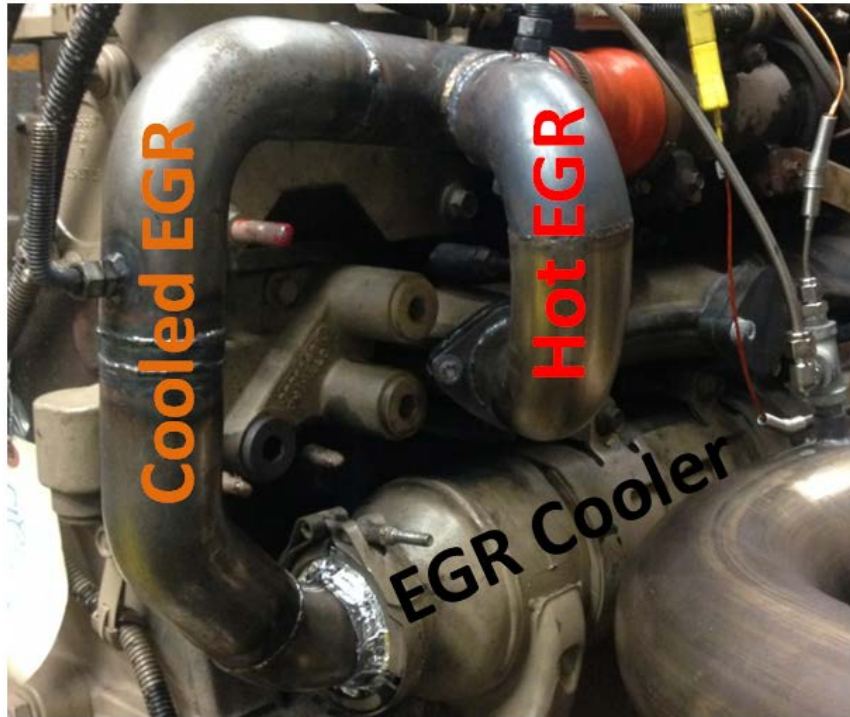


FIGURE 27. EGR COOLER BYPASS DEVELOPMENT SETUP FOR INITIAL EXPERIMENTS WITH 50% COOLER BYPASS – AGI MANIFOLD

It should be noted that this final arrangement did still permit a very small amount of leakage through the bypass leg at high loads (and high manifold pressures), when there was normally no desire for any amount of EGR cooler bypass. In addition, the maximum amount of cooler bypass in this arrangement was still limited by the temperature limits of the EGR venturi dP sensor. Plans were made to implement a fix for this problem to enable continued use if needed, and a preliminary fix was implemented, but it was ultimately decided not to use the EGR cooler bypass on the final configuration in the test cell, and therefore this fix was not fully finalized.

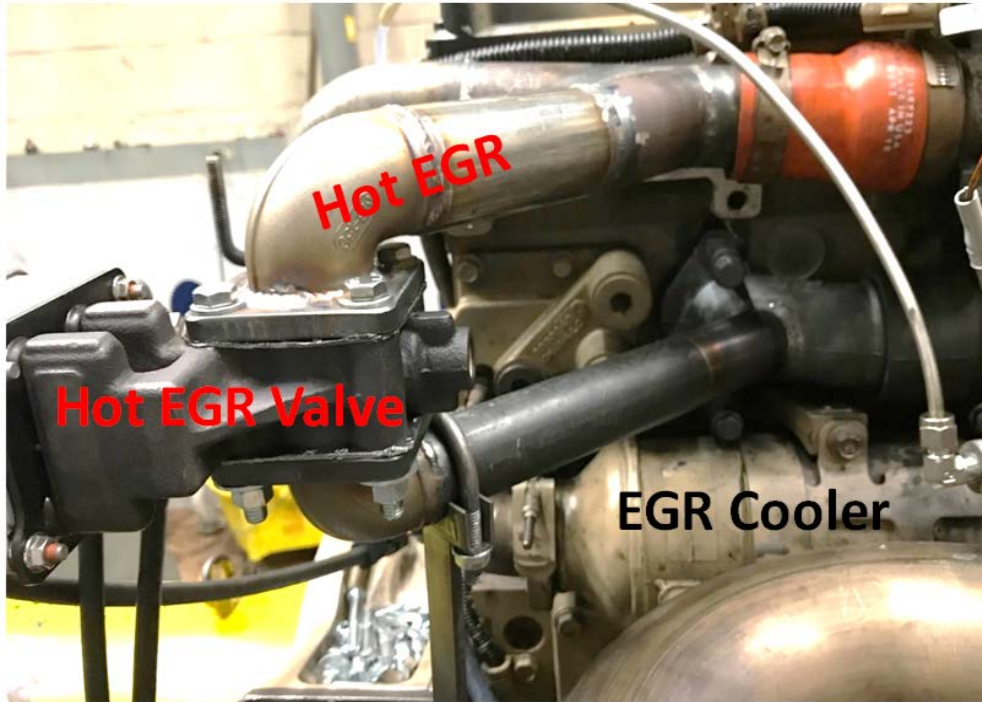


FIGURE 28. EGR COOLER BYPASS FINAL SETUP FOR TRANSIENT EXPERIMENTS WITH CONTROL VALVE – STOCK MANIFOLD

2.5.3. Charge Air Cooler Bypass

In cold-start and low temperature operations, the charge-air cooler (CAC) can potentially result in overcooling of the intake air charge, and it can also represent a significant thermal inertia to overcome during the early cold-start. Some light-duty vehicles use a CAC bypass to assist with cold-start. A CAC bypass could also help prevent overcooling at low loads under low ambient temperature conditions in-use. However, this last benefit is difficult to demonstrate in a normal test cell. Therefore, the primary benefit examined with the CAC bypass for the Stage 3 program was the potential to assist with cold-start warm-up.

For the purpose of the initial experiments, a fixed flow rate bypass (controlled via a butterfly valve) was implemented, as shown in Figure 29. In the event that this technology was adopted in the final Stage 3 configuration, this valve would have been replaced by an electric motor driven valve commanded via CAN. As noted in more detail in the results section later, the CAC bypass did not provide significant improvement to cold-start warm-up for this engine, and therefore the more sophisticated setup was not implemented.

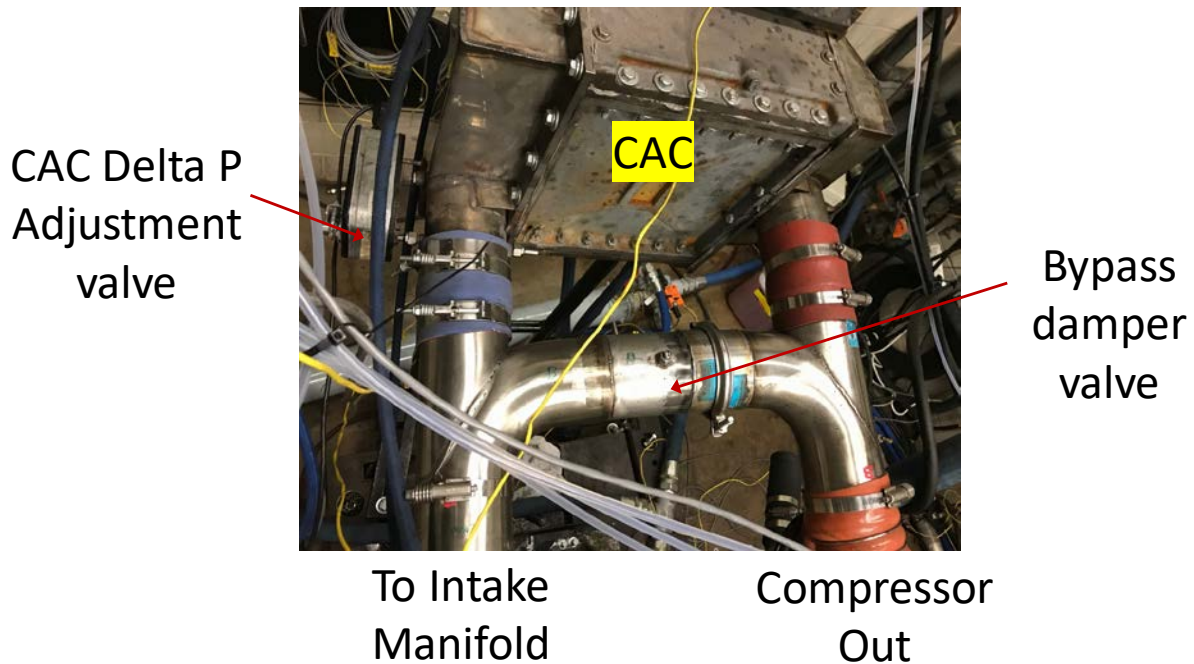


FIGURE 29. CHARGE-AIR-COOLER (CAC) BYPASS

2.5.4. Turbine Bypass

A turbine bypass can be another effective way to deliver exhaust heat directly to the exhaust during cold-start warm-up, as well as potentially under very low load conditions, such as idle. In cold-start this is done by bypassing the thermal inertia of the turbocharger during warm-up. In other conditions, the amount of dilution air in the cylinder can be reduced at lower loads, thus increasing exhaust temperature, and reducing exhaust flow rate. Transient controls must be carefully worked out to preserve acceleration performance.

The experimental installation of the turbine bypass is shown in Figure 30. For the initial turbine bypass experiments, a poppet style wastegate valve was used to ensure a complete positive cell under boosted conditions when the bypass was not wanted. An air actuated valve was used, and for the initial experiments, the amount of bypass was controlled with the valve fully open using several orifices. At low loads, this valve was capable of as much as 100% bypass around the turbine, allowing exploration of the full range of possibilities.

The initial experiments were run using the AGI manifold, which had a bypass port already prepared for this testing. It should be noted that in a production implementation, the turbine bypass would likely be integrated directly into the turbine housing for more compact and efficient arrangement. However, this setup was sufficient to allow SwRI to explore the potential of the turbine bypass. The bypass valve actuator was driven by a 3-way valve commanded by the SwRI controller, allow for automated control over cycles.

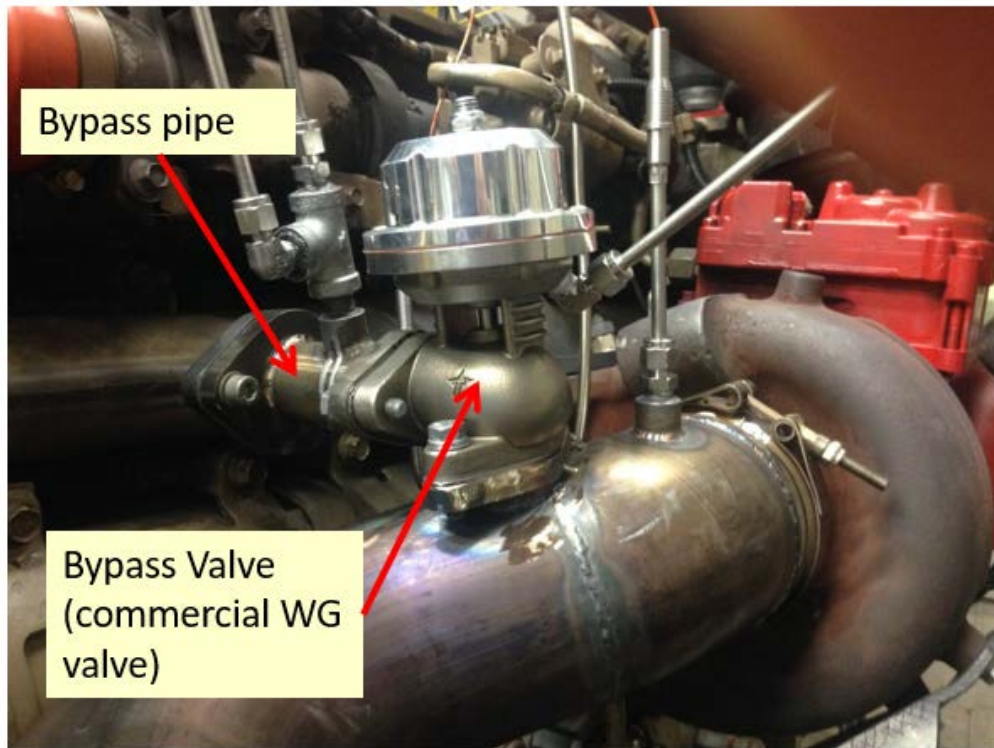


FIGURE 30. TURBINE BYPASS VALVE AND INSTALLATION (AGI MANIFOLD)

2.5.5. *Cylinder Deactivation*

CDA is a technology wherein one or more cylinders can be turned off at light loads. It should be noted that the proper implementation of CDA involves both turning off the fuel to a cylinder and deactivating the valves for that cylinder so that the air does not pass into or out of the cylinder. This is distinct from cylinder cut-out, where fuel is turned off, but the valves continue to operate. CDA is more complicated to implement but has a much larger potential benefit.

CDA was the primary added engine hardware technology retained for the Stage 3 engine. CDA was chosen because of its flexibility in being able to provide both enhanced thermal management and GHG emission benefits at light load.[5][6][7]. CDA also provides additional flexibility in raising temperatures for specialized operations like LO-SCR de-sulfation. These features made CDA a “swing” technology that could provide both NO_x and CO₂ benefits. However, the implementation of CDA on the engine required considerably more effort in terms of both hardware and controls.

The CDA valvetrain system was supplied by Eaton, and it was capable of independently deactivating the valves on all six of the cylinders in the engine. An example of the hardware for one cylinder is shown in Figure 31. The installation of the hardware on the cylinder head for all six cylinders for the X15 engine is shown in Figure 32.

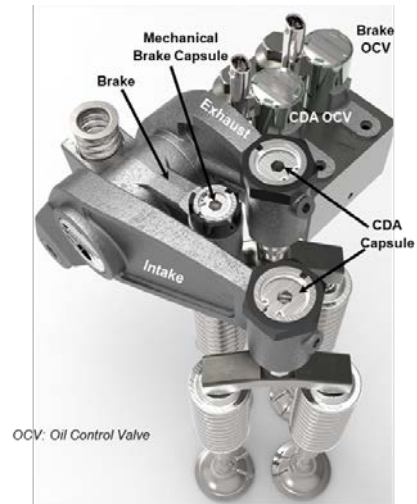


FIGURE 31. EATON CDA HARDWARE FOR ONE CYLINDER (SHOWN WITH ENGINE BRAKE INTEGRATION)



FIGURE 32. X15 CYLINDER HEAD SHOWN WITH CDA HARDWARE INSTALLED FOR ALL SIX CYLINDERS

The Eaton CDA system implemented on the X15 was based on hydraulic actuators that are driven by oil pressure. The prototype system used for this program required more oil pressure than the stock oil system could generate at lower pressures, therefore a supplemental oil pump was utilized to supply the CDA system for this program. This system used oil taken from the engine oil sump and the oil returned to the sump via normal drain paths from the cylinder head. One additional drain was added to insure sufficient drain capacity during all operations. It should be noted that in a production system, this supplemental oil pumping would not be required.

It should also be noted that the prototype system used for this engine was limited to speeds below 1750 rpm, due to concerns over the impact of leaks on system timing at high speeds. This limit is not fundamental to the technology however, and this would not be a problem in production (e.g. subsequent iterations of this prototype hardware have eliminated that problem in other installations already). This prototype limitation manifested for the Stage 3 project when activity entered the low torque/high speed corner of the engine map and represents additional improvement gains expected for a production system.

The integration of CDA required a substantial amount of controls work and significant coordination between Eaton, Cummins, and SwRI. These controls are described later in more detail under the Controls section of the report. An extensive amount of initial work was done to develop the proper timing and controls for the deactivation and reactivation of fueling and valves for the cylinders.

Because the Eaton system allowed for independent deactivation of all six cylinders, this allowed for a great deal of flexibility to fire different combination of cylinders in different engine conditions. This capability was crucial to maximize performance benefits of CDA while at the same time avoiding vibration issues. In this report, CDA modes are identified in terms of the number of cylinders that are firing, with various combinations identified by a letter designation. These modes are illustrated in Figure 33, with the most commonly used modes in this program highlighted with a red border. In addition to the modes shown, SwRI also used a 1 cylinder “breathing” mode for high speed motoring operations to reduce exhaust flow that might cool the AT (labeled 1D and implemented using Cylinder 4).

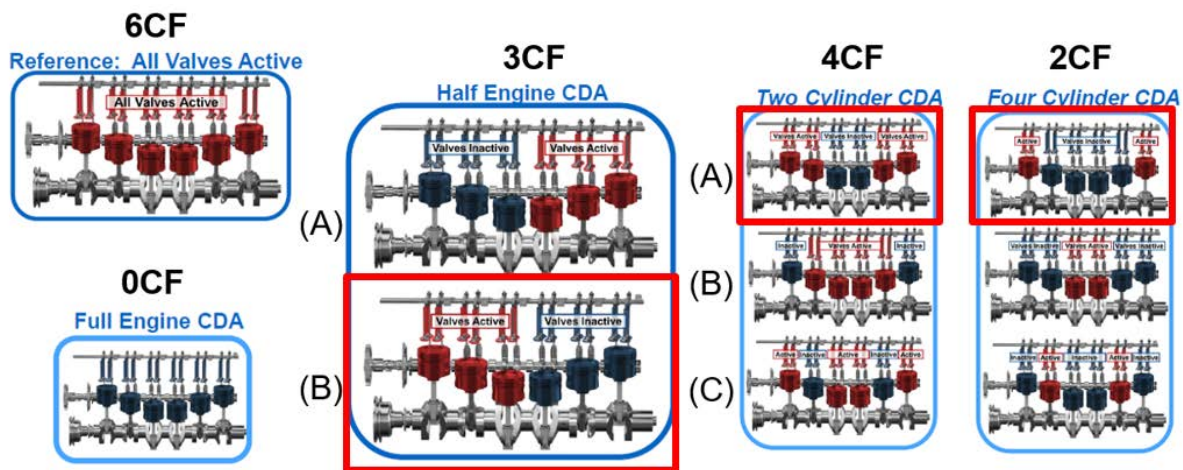


FIGURE 33. ILLUSTRATION OF DIFFERENT CDA MODES

Following the initial installation, Eaton and SwRI did a significant amount of vibration measurement on the CDA equipped engine, looking at both torsional and linear vibration. This work was vital to the development of a CDA control strategy that avoided potential Noise vibration

and harshness (NVH) problems, while delivering maximum performance benefits. These efforts are described in detail in other publications [7][8]. Examples of this effort are given below in Figure 34 and Figure 35, for torsional and linear vibration, respectively.

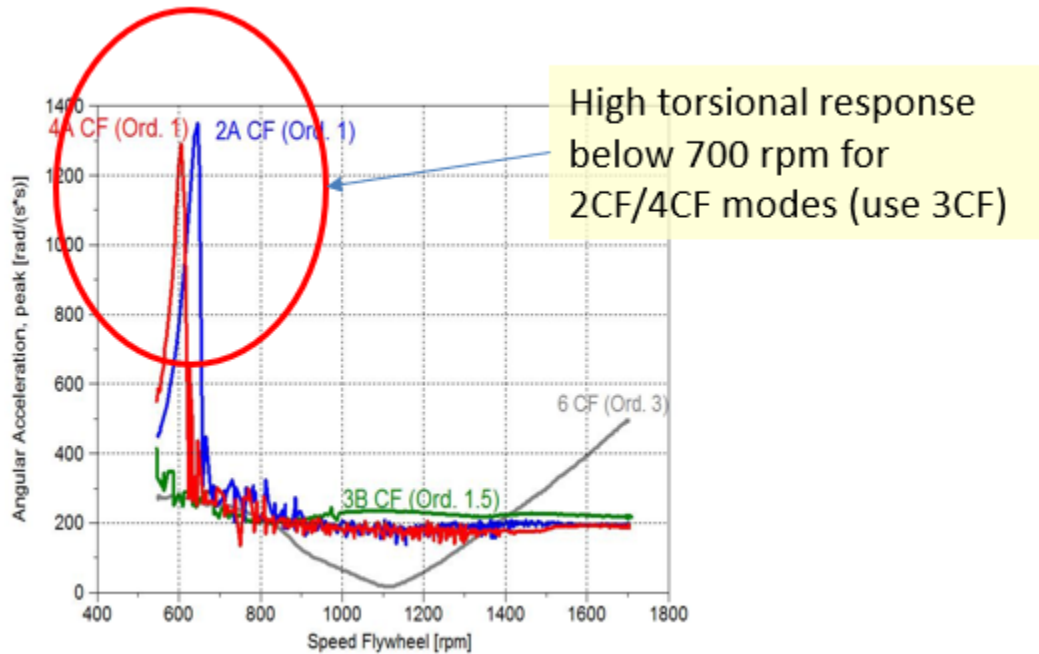


FIGURE 34. EXAMPLE OF TORSIONAL VIBRATION MAPPING AND ANALYSIS FOR CDA

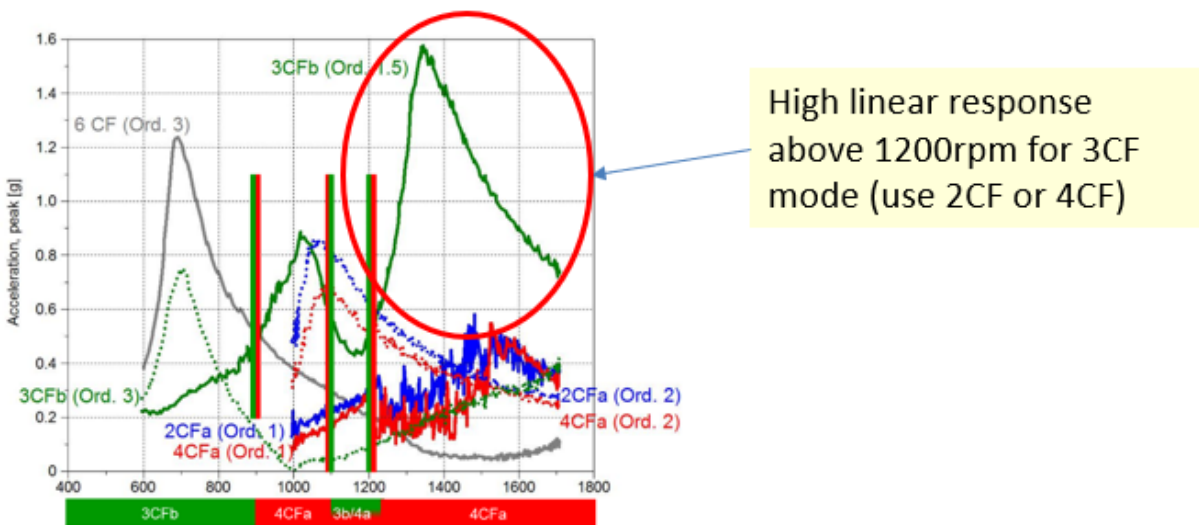


FIGURE 35. EXAMPLE OF LINEAR VIBRATION MAPPING AND ANALYSIS FOR CDA

SwRI implemented a map-based CDA strategy with a number of different modes which were designated by the number and combination of cylinders firing, as outlined in Figure 36. It should be noted that this is the “base” map used for most operating modes. The strategy will

sometimes deviate from these in specific engine modes used for purposes like cold-start warm-up or deSO_x. This strategy allowed SwRI to gain significant benefits from CDA in both thermal management and fuel consumption reduction, while avoiding any vibration issues. As noted earlier, the prototype implemented at SwRI was limited to speeds below 1750 rpm, otherwise the map would have had similar patterns at 1800 and 1900 rpm that are shown at 1700 rpm. This means that the actual benefit available from CDA is somewhat larger than observed in this demonstration (as noted later in some of the Phase 2 GHG cycle results).

		BMEP [bar]					
		Motoring	0	1	2	3	4
Ne [RPM]	600	3B	3B	3B	6CF	6CF	6CF
	700	3B	3B	3B	3B	6CF	6CF
	800	3B	3B	3B	3B	6CF	6CF
	900	3B	3B	3B	3B	3B	6CF
	1000	3B	2A	2A	3B	3B	6CF
	1100	1D	2A	2A	3B	3B	6CF
	1200	1D	2A	2A	4A	4A	6CF
	1300	1D	2A	2A	4A	4A	6CF
	1400	1D	2A	2A	4A	4A	6CF
	1500	1D	2A	2A	4A	4A	6CF
	1600	1D	2A	2A	4A	4A	6CF
	1700	1D	2A	2A	4A	4A	6CF
	1800	6CF	6CF	6CF	6CF	6CF	6CF
	1900	6CF	6CF	6CF	6CF	6CF	6CF

FIGURE 36. FINAL BASE CDA CONTROL MAP IMPLEMENTED FOR STAGE 3 ENGINE

It should be noted that there are more complex strategies that can be implemented to further optimize CDA behavior, such as dynamic skip fire [9], wherein algorithms are running in real time to determine the optimal number of cylinders to fire at any given point, and the particular combination of cylinders varies from one time to the next. This allows behaviors such as alternating between modes to break up potential resonance responses before they can create vibration issues. These kinds of algorithms can be particularly valuable on engines that may have more difficulty implementing CDA, such as 4-cylinder engines. Further details regarding the transient control of CDA are given in the Controls section.

2.5.6. SuperTurbo

Near the end of the hardware evaluation effort, SwRI engaged in a concept demonstration of one more advanced technology approach. It was understood that due to time and budget constraints, this approach could not be implemented for the full Stage 3 demonstration. However, a short proof-of-concept experiment was conducted to highlight the potential benefits of the technology. This effort was supported by SuperTurbo, and they also contributed some funding to help complete the full proof-of-concept effort. SuperTurbo is essentially a turbocharger technology wherein the turbo is mechanically coupled to the crankshaft via a continuously variable transmission assembly that allows it to be driven by the engine when desired, or operate as a normal turbocharger in other conditions. In this way, it combines the functionality of a turbocharger and a supercharger. The SuperTurbo technology is illustrated in Figure 37.

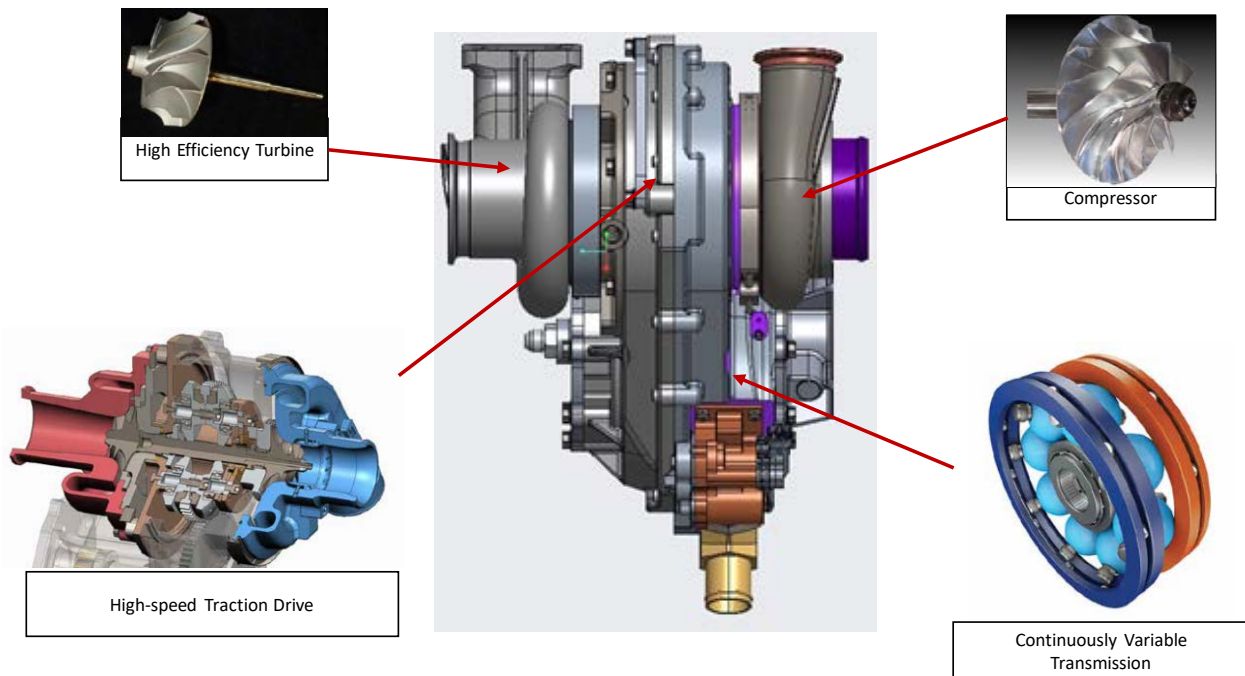


FIGURE 37. SUPERTURBO HARDWARE COMPONENTS

The installation of the SuperTurbo on the Stage 3 engine is shown in Figure 38. The implementation for the Stage 3 proof-of-concept also incorporate a turbine bypass valve. In this case, a belt drive was used to couple the CVT to the engine crankshaft. SuperTurbo Technologies provided the controls for the SuperTurbo hardware, and the control strategy was contained within their proprietary controller. Following initial steady-state mapping, transient controls were implemented, and several demonstration FTP cycles were run.

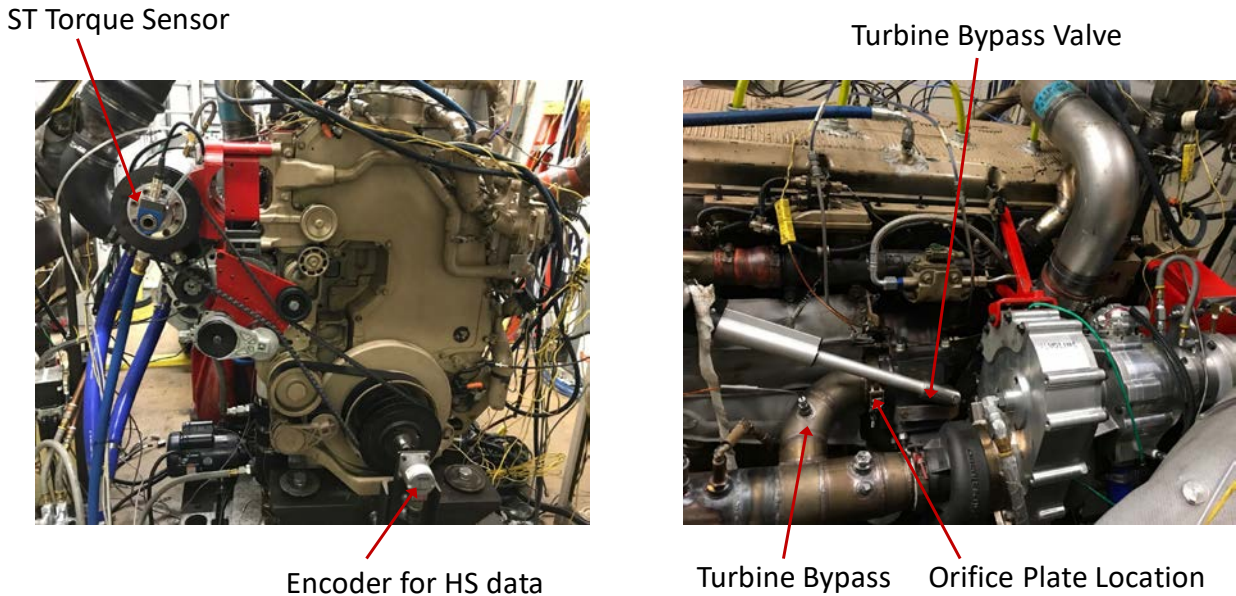


FIGURE 38. INSTALLATION OF SUPERTURBO ON THE STAGE 3 ENGINE

2.6 Low NO_x Controls

A significant portion of the effort in the Stage 3 demonstration involved the development of the hardware and software controls needed to make the combined engine-AT system function, and to provide the flexibility needed to minimize tailpipe NO_x and maximize engine efficiency. Although the controls were implemented in an open development platform, the controls used on the Stage 3 engine were designed using a production-oriented approach based on SwRI's experience working with production engine controls. As with a production controller, a single unified strategy and calibration were developed that could run on any duty cycle without cycle specific tuning.

The basic control architecture for the Stage 3 demonstration is shown in Figure 39. The core strategy and much of the custom controls were operating from the SwRI Controller, which resided in a dSPACE MicroAutoBox (MABx) platform. The SwRI Controller had overall supervisory control of the system, and several key controls were located there. These included the Engine State Machine, the main CDA controller, and the AT Controller.

The SwRI Controller was linked to the engine by two parallel methods. Cummins provided a proprietary high-speed link implemented over a Generic Serial Interface port which allowed high speed commands to be sent to the engine. This high speed link enabled control functions that needed to function at crank-angle speed, such as fueling commands to enable CDA. To preserve bandwidth in the high speed port, a secondary low speed link was also implemented via an ASAP3 link to the engine to enable lower speed overrides, such as to drive various engine state overrides or drive the stock dosing system when it was used. These parallel approaches enabled a flexible

system that allowed SwRI to enact a wide variety of engine control modifications, while at the same time leveraging many of the existing controls built into the ECM. This control approach was combined with changes made to various control maps on the engine ECM itself to implement the final strategy and calibration.

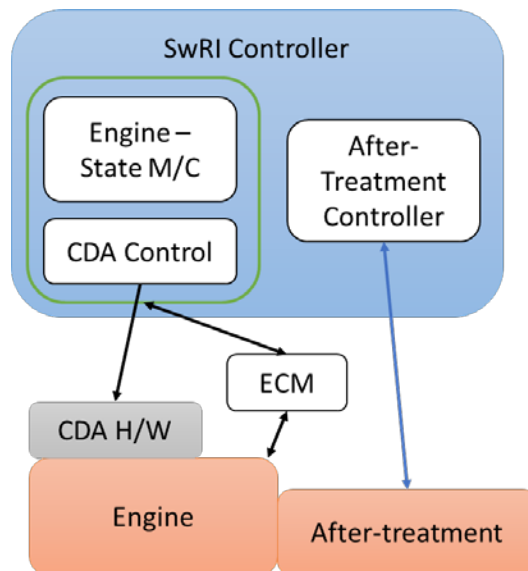


FIGURE 39. HIGH-LEVEL CONTROL STRUCTURE FOR STAGE 3 LOW NO_x DEMONSTRATION

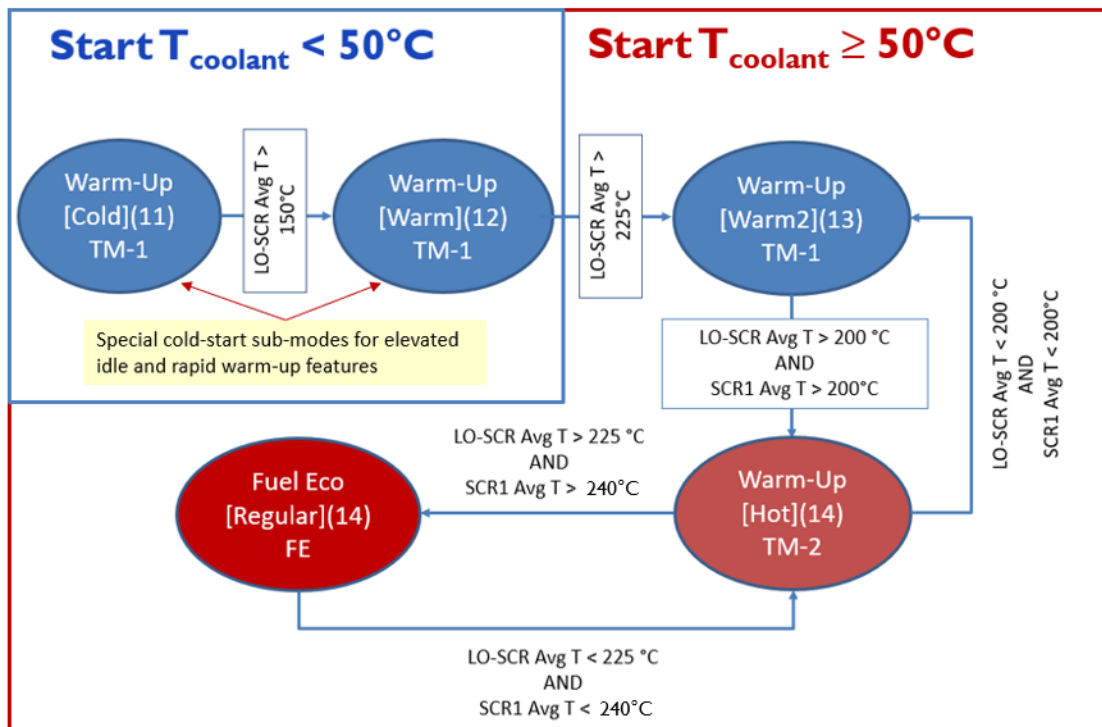
2.6.1. Overall Strategy and Engine State Machine

The Engine State Machine contained the primary Strategy controls for the engine-AT system. The Strategy control was implemented a series of Engine Modes that allowed the implementation of different calibration targets, depending on the state of the system. This strategy was driven by a combination of Engine Coolant Temperature (ECT) and AT system temperatures. In particular, the LO-SCR temperature and the temperature of the first brick of the downstream SCR system (SCR1 in the diagrams) were used to drive state switching. The Strategy is shown in Figure 40 and involved three primary Engine States that were defined as follows:

- **Fuel Economy (FE)** – this mode was the desired endpoint of the strategy and can be considered the “Default” operating mode when the engine and AT system are at optimal temperatures for maximum NO_x efficiency. It has the highest engine-out NO_x emissions and the lowest CO₂ emissions. In some cases, this mode actually was calibrated to higher engine-out NO_x levels than the baseline engine.
- **Aggressive Thermal Management (TM-1)** – this mode was used when both catalyst beds were below optimal temperature, and represent the most aggressive thermal management mode used outside of cold-start. TM-1 had the lowest engine-out NO_x level and the highest CO₂ emissions. Features of this mode included higher EGR rates, significant use of multiple injections, combustion phasing, intake throttling, and modifications to the CDA mode table that prioritized system

temperature at certain speeds. Due to the impact on CO₂ this mode was used only to the degree necessary.

- Low Thermal Management (TM-2)** – this mode was a transitional mode that was added to provide an intermediate point between FE and TM-1. This was used in cases where the AT system temperatures were at temperatures slightly below optimal, but still able to reach high conversion on at least one of the catalyst beds. TM-2 provided a less drastic mode of intervention allowing moderate thermal management and some NO_x reduction, but with significantly less CO₂ penalty than the TM-1 mode. The flexibility added by TM-2 was essential for optimizing CO₂ emissions in part load duty cycles.



FE = Fuel Economy Mode (Highest EO NO_x)
TM-1 = Aggressive Thermal Management (Lowest EO NO_x)
TM-2 = Low Thermal Management (Moderate EO NO_x)

FIGURE 40. ENGINE STATE M/C AND OVERALL STRATEGY CONTROL DIAGRAMS

Under normal operations after engine-start and when ECT was above 50°C, these three modes were the only active modes, and the strategy work cycle between these modes as dictated by the AT system temperatures. Each of these modes was tied to a set of maps in the engine ECM for various systems, leveraging the existing controls within the engine ECM as much as possible. SWRI then recalibrated these maps to implement the desired strategy.

If at engine start the ECT was below 50°C, additional sub-modes (Engine Modes 11 and 12 in Figure 40) were enabled under the TM-1 mode to implement early stages of the cold-start

warmup strategy. These include additional features such as the elevated idle speed targets and modified CDA modes specific to cold-start warm-up. Transition out of these modes was based on ECT and the LO-SCR temperature, given that the primary purpose of these modes was to warm up the LO-SCR as rapidly as possible. An example of the control switching over a cold-start FTP is shown in Figure 41 below. A different duty cycle during cold-start would likely result in a different progression through these modes, as would different ambient conditions, and an example of this behavior over a different cold-start duty cycle with a much longer initial idle is shown later in the Results section.

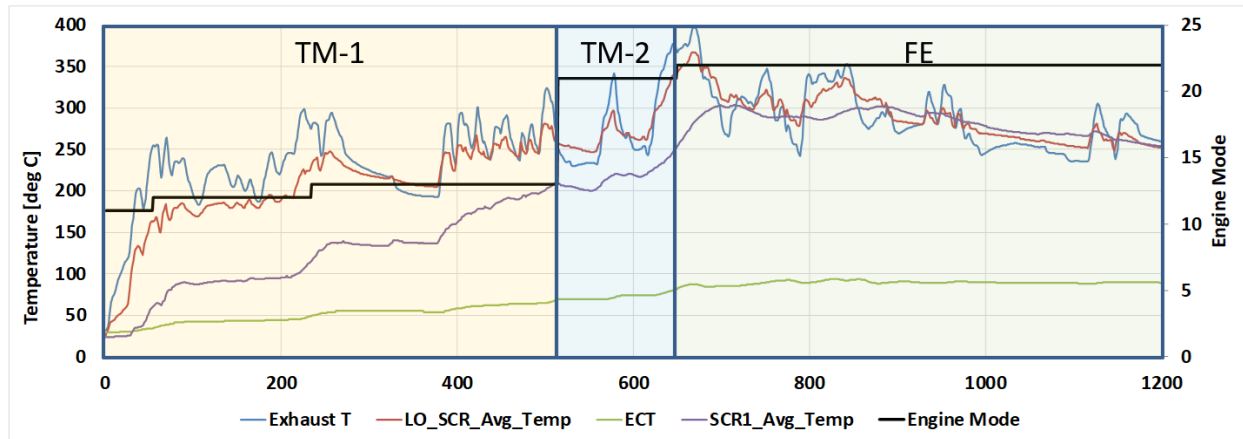


FIGURE 41. EXAMPLE OF CONTROL MODE SWITCHING DURING COLD-FTP

Additional specialized controls modes were also implemented for specific functions, such as DPF Regeneration or LO-SCR deSO_x. DPF regeneration also involved control of the in-exhaust HC injection. More discussion on the strategy associated with these modes is given under the AT Controls section. Due to scope limitations, these specialized modes were not fully calibrated for transient cycle implementation as part of this demonstration program.

2.6.2. CDA Controls

As noted earlier, the base CDA strategy, shown previously in Figure 36 implemented CDA under different combinations of cylinders firing for different speed-load combinations to balance performance targets and vibration constraints. Generally, CDA was only utilized at loads below 3 to 3.5 bar brake-mean effective pressure (BMEP). Modifications were made to this base CDA map under certain engine modes, for instance in early cold-start and TM-1 modes, as well as for specialized operations like LO-SCR deSO_x. However, there was more to CDA control than just the selection of modes under different operating conditions.

The actual implementation of CDA required two different sets of controls:

- Modified fueling commands which included,
 - Turning off fueling in deactivated cylinders
 - Modified fueling commands increasing the fueling quantity in firing cylinders to maintain engine torque and performance
- Valve commands sent to the Eaton CDA valvetrain hardware controller

Fueling commands were implemented through the high speed GSI link to the engine ECM, while valvetrain commands were sent via a set six digital outputs (one for each cylinder) from the MABx to the Eaton CDA controller. The synchronization and logic for timing these commands to properly implement turning on and off cylinders was run from the SwRI Controller. It was critical to time these events properly to avoid the possibility of injecting fuel into a cylinder with deactivated valves, or to avoid a valve deactivation in the middle of a valve lift event. SwRI worked with Eaton based on their previous efforts to devise an approach that worked well under transient conditions and insured the safe activation and deactivation of fuel and valves.

Beyond the basic implementation and CDA mode maps, a number of additional features were developed in the controls to enable transient operation. These features were necessary to avoid excessive switching, maintain CDA benefits, preserve transient torque response, and avoid other potential issues such as excessive oil consumption during sustained CDA events.

An asymmetrical persistence timer was utilized on CDA activation and switching events between CDA modes to prevent excessive mode switching and provide smooth transient control transitions. This was tuned so that a request had to be present for 2 seconds before the system would implement that request. However, a request to turn off CDA in the event of a significant increase in load demand was implemented immediately, for transient torque response. A hysteresis function was built into the controller to avoid potential vibration issues when transitioning between CDA modes.

A “recharge” function was also built into the CDA system to deal with sustained CDA mode operation. As noted earlier, the trapped air charge in deactivated cylinders is critical for realizing the full fuel consumption benefits of CDA. In addition, the positive pressure of the trapped air charge also prevents pulling oil into the cylinder in the expansion stroke. However, the cylinders are not perfectly sealed at the piston rings, therefore the trapped air charge will tend to be pumped away over time. As a result, it is necessary to replenish that air charge periodically during operations where a cylinder stays deactivated for a period of time. Therefore, SwRI built in a control function to periodically reactivate the valves in a deactivated cylinder, and thus replenish the trapped air charge. This recharge function was timed based on a fixed number of engine cycles, and was calibrated based on cylinder pressure measurements and experiments at various engine speeds. This function helped to keep oil consumption comparable to the baseline engine, which was important for AT durability.

2.6.3. Aftertreatment Controller and DEF Dosing Controls

The AT controls for the Stage 3 program were entirely resident on the SwRI Controller on the MABx. In cases where the original stock doser that came with the engine was used for downstream dosing, that dosing command was relayed to the Engine ECM via the ASAP3 channel. All other AT sensors and actuators were interfaced directly to the MABx, and the AT controls in the Engine ECM were disabled. The relationship of the AT Controller to the overall control and the interface to the hardware system are shown in Figure 42. The AT system employed 6 temperature sensors, 3 NO_x sensors, and one NH₃ sensor. All sensors were production sensors, and all were interfaced to the MABx via CAN. For the final configuration there were two dosing controllers, one for the heated dosing and one for the downstream dosing. Low level dosing controls were handled by the individual DEF doser subsystem controllers provided by the system suppliers, and both systems communicated with the MABx over CAN. The SwRI Controller also was used to directly control the heater system for the Team 1 LO-SCR.

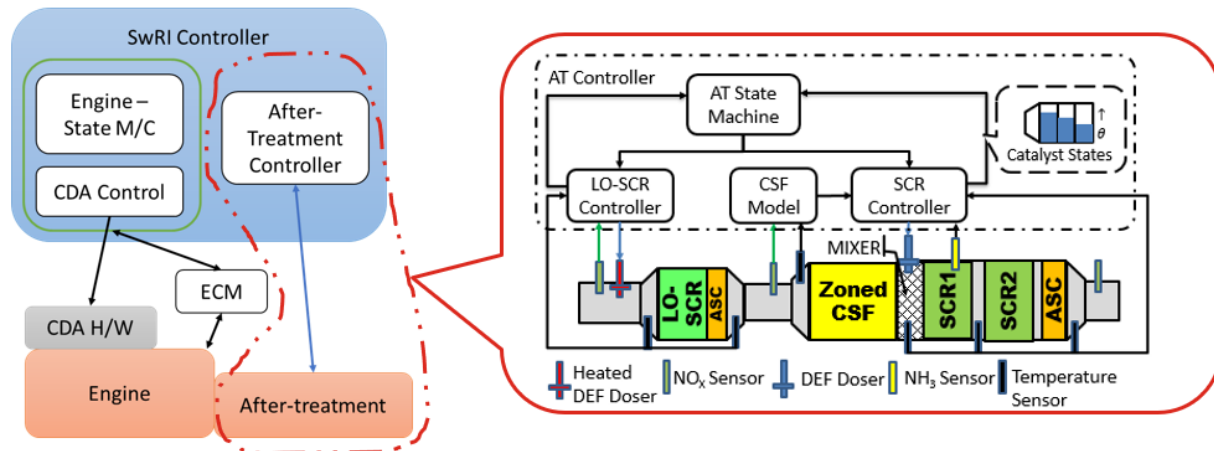


FIGURE 42. AFTERTREATMENT CONTROLLER IN OVERALL CONTROL ARCHITECTURE

The DEF dosing controller was a model-based control approach which was aimed at controller ammonia coverage on the SCR catalysts. The controller has been described in detail in [10], but the major details are given in this report below. A dual-bed, dual DEF dosing system controls architecture was developed for this system, and the overall structure is depicted in Figure 43. The system employed three different ammonia coverage observers, one for the LO-SCR and two for the downstream SCR. Each coverage observer consisted of a 1-D axial model consisting of 7 0-D model cells. This approach meant that the model provided not only a total coverage amount but also an axial profile of coverage in each catalyst section. Both the total coverage and the profile information were used in the controller. The profile tracking allows controls to target a desired profile, and to react to an unfavorable profile that could result in low conversion or ammonia slip as that profile was still developing.

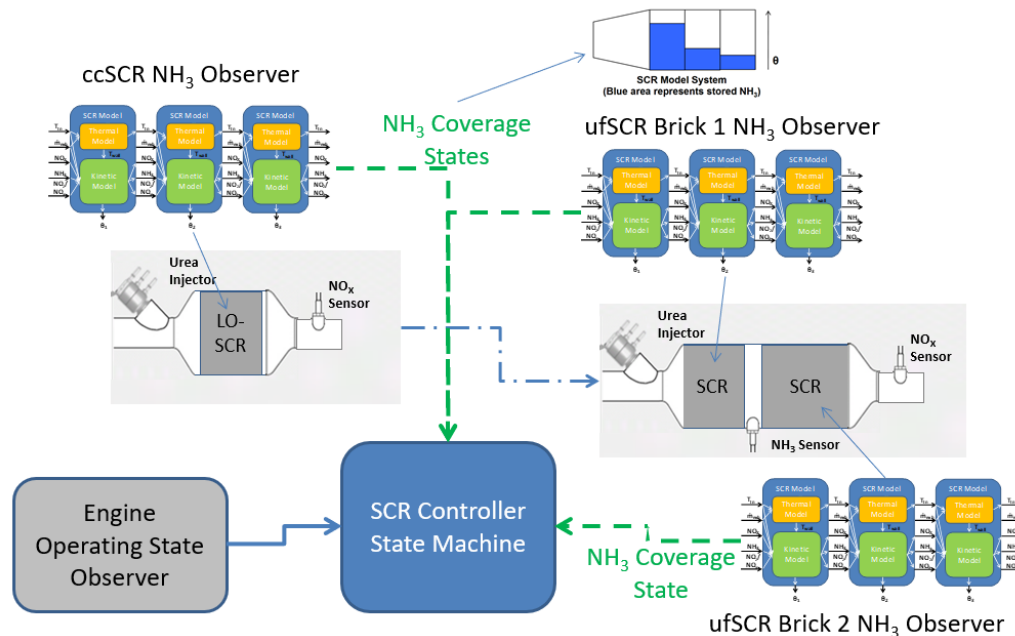


FIGURE 43. DEF DOSING CONTROLS – OVERALL SYSTEM OVERVIEW

The controller also included functions that allowed the system to balance between the two systems, such that one catalyst bed could be used to compensate for the other in cases where coverage might be below target. This flexibility allows the overall system to respond quickly to a wide variety of situations to maintain high NO_x conversion performance in the overall system in a robust manner. The dosing controller also incorporated specialized modes in the state machine for operations that required different targets, such as DPF Regeneration or LO-SCR deSO_x. These specialized modes are discussed more later.

A simplified, control-oriented, lumped parameter model was used as the Coverage Observer to track ammonia coverage on each model cell, and the output of each cell was fed to the input of the next cell. The model consisted of a thermal model tracking temperature through the catalysts, and a kinetic model which solved the SCR reaction equations and tracked ammonia coverage. A single-site storage model was used to simplify the calculations for ECM use, but it provided enough fidelity for control use. The kinetic model incorporated seven reactions given below:

- Adsorption of Ammonia on the surface of the catalyst: $NH_3 + S1 \rightarrow (NH_3)_{S1}$
- Desorption of Ammonia from the surface of the catalyst: $(NH_3)_{S1} \rightarrow NH_3 + S1$
- Ammonia Oxidation reaction at the surface of the catalyst: $4(NH_3)_{S1} + 3O_2 \rightarrow 2N_2 + 6H_2O + 4S1$
- “Standard” SCR (NO only) reaction: $4(NH_3)_{S1} + 4NO + O_2 \rightarrow 4N_2 + 6H_2O + 4S1$
- “Fast” SCR (NO+NO₂) reaction: $2(NH_3)_{S1} + NO + NO_2 \rightarrow 2N_2 + 3H_2O + 2S1$
- “Slow” SCR (NO₂ only) reaction: $8(NH_3)_{S1} + 6NO_2 \rightarrow 7N_2 + 12H_2O + 8S1$
- Nitric Oxide Oxidation reaction: $2NO + O_2 \rightarrow 2NO_2$

In these equations, the variable S1 denotes an ammonia storage site. A series of simplifying assumptions were used to reduce some of the equations to an algebraic form that could be readily solved in the limited computing environment of an engine ECM. This model form has been implemented directly into ECM production code by SwRI in other cases, although for this program the models were run on the MABx.

The LO-SCR sub-controller is shown in Figure 44, and the basic control structure is depicted in Figure 45. The controller incorporated a feedforward ammonia-to-NO_x ratio (ANR), a model-based ANR correction, and an ammonia storage manager function. The dosing controller incorporated a function that limited the maximum dosing rate based on temperature and exhaust flow to avoid risk of deposits. However, it should be noted that with the Heated Doser, this limiting function could be set to much more aggressive dosing levels than would normally be possible for DEF injection, especially at lower temperatures.

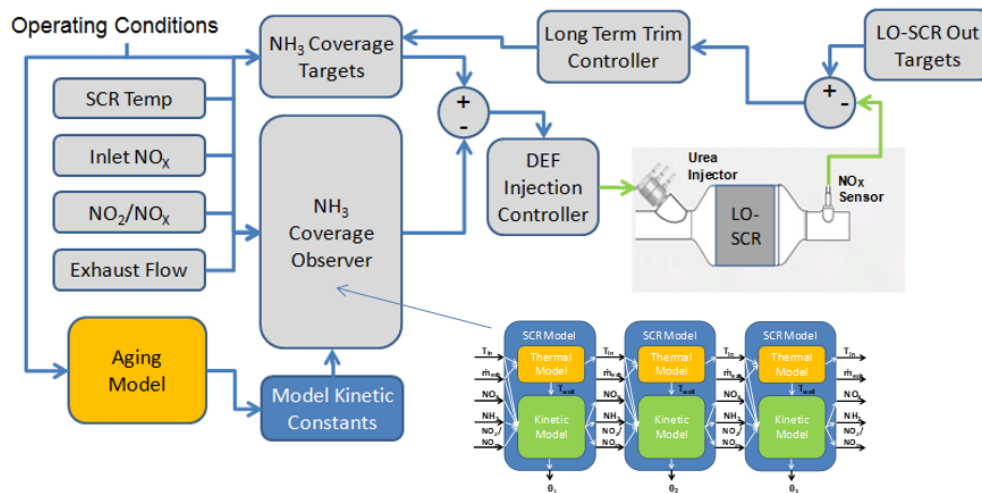


FIGURE 44. LO-SCR DOSING CONTROLLER SCHEMATIC

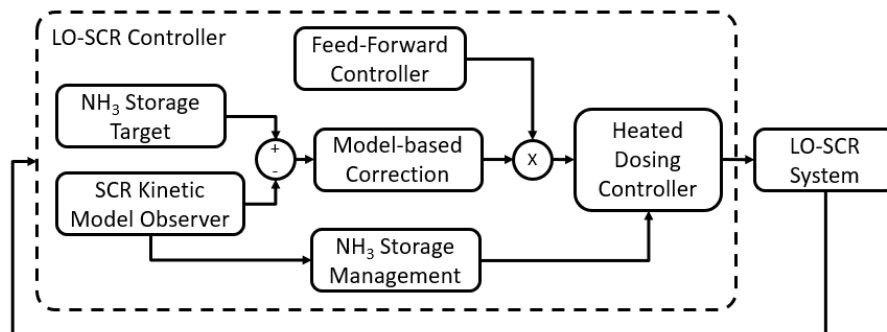


FIGURE 45. LO-SCR CONTROL STRUCTURE

The LO-SCR sub-controller also incorporated a catalyst aging model component and a long-term trim function which adjusted the coverage targets to maintain catalyst performance over time in response to modeling or input errors. It should be noted that the aging model function was not utilized in the Stage 3 program, as sufficient scope was not available to calibrate that model. The long-term trim function was partially implemented for the Stage 3 program, but the coverage target adjustments had to be inserted manually because sufficient scope was not available to fully develop and automate the long-term trim function. This is an area of continuing development at SwRI. For the LO-SCR, the LO-SCR outlet NO_x sensor is the basis for driving long-term trim adjustments.

The ammonia storage manager could also invoke an accelerated dosing mode when coverage levels were significantly below targets to help re-establish coverage quickly, reverting to normal ANR-based control once the coverage was closer to the target levels. This accelerated dosing mode would dose at the maximum DEF rate allowed by the controller for a given temperature and flow condition. This function was especially critical for the LO-SCR controller as the LO-SCR would typically be emptied of stored ammonia at sustained higher temperatures (over 300°C), and the controller had to be capable of rapidly reestablishing coverage as temperatures dropped. The heated Doser allowed this function to be calibrated very aggressively even at marginal dosing temperatures (180°C to 200°C) without the risk of deposit formation.

The downstream SCR sub-controller is depicted in Figure 46, and the basic control structure is shown in Figure 47. Much of the structure is similar to the LO-SCR sub-controller, but there are several unique features. It should be noted that the downstream SCR catalysts were generally used to do most of the conversion at higher temperatures and under high loads. Therefore, the downstream controller required a higher level of precision. Given this, the downstream SCR controller had several added features.

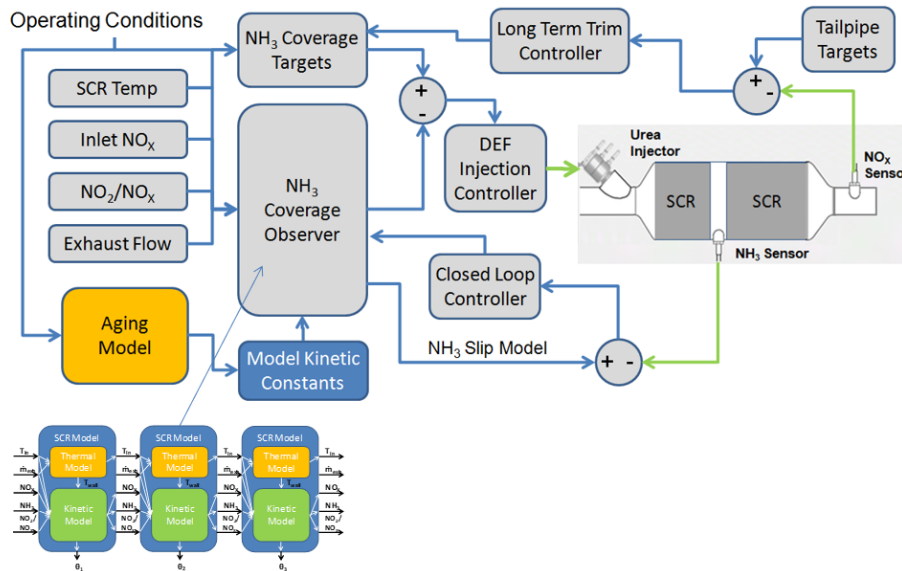


FIGURE 46. DOWNSTREAM SCR DOSING CONTROLLER SCHEMATIC

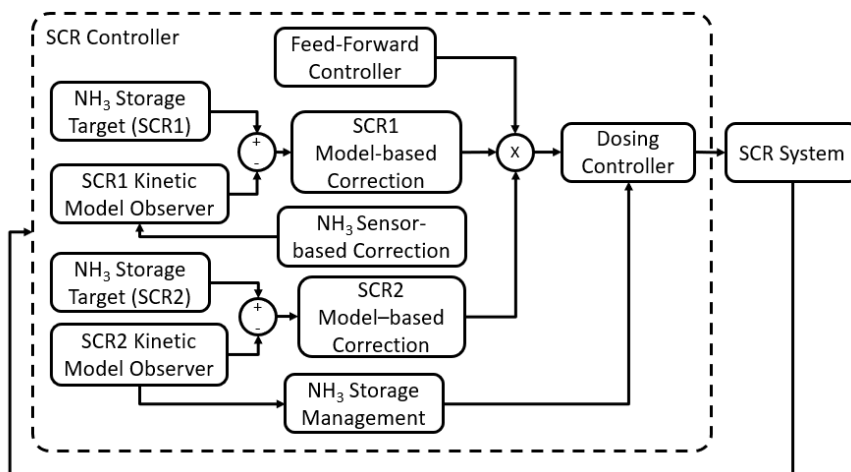


FIGURE 47. DOWNSTREAM SCR CONTROLLER STRUCTURE

As shown in Figure 47, the downstream command is the sum of corrections for both the first downstream SCR bed (dsSCR1) which is before the NH₃ sensor, and the second downstream SCR bed (dsSCR2) after the NH₃ sensor, with each bed having both an average storage correction, and a profile-based correction. However, the two beds target a different desired profile, given that the first bed must provide ammonia to the second bed, while the second bed profile is targeted to avoid tailpipe NH₃ slip. A further bias function is used to help drive coverage to desired levels by allowing the first bed to exceed its targets in cases where the second bed is too far below targets. The downstream catalyst controller also contains the same deposit avoidance limiting of maximum dosing and accelerated dosing features as the upstream controller. Because the downstream system uses normal (un-heated) DEF dosing, the maximum dosing rate function is calibrated more conservatively than for the heated DEF system on the LO-SCR.

The primary added feature was the high-speed feedback element, driven by the mid-bed NH_3 sensor. To meet tailpipe NO_x targets and in-use requirements, the warmed up AT system must be able to maintain NO_x conversion in excess of 99.5%. Given even a small margin for degradation of 0.25%, this translates to a controls demand to be above 99.75% conversion consistently before any degradation. From a control standpoint, maintaining such a high performance level consistently requires a high amount of precision, and it is very difficult to maintain that kind of precision on any system without some form of real-time feedback. Slower long-term trim adjustments, while also important for long-term precision are not enough by themselves. For the model-based DEF controls, the key parameter modeled is ammonia storage, and therefore some real-time feedback element is needed that can provide information about how accurate the storage model actually is. Either NO_x or NH_3 could be used for this purpose. However, the tailpipe NO_x sensor cannot be used for this function because the downstream SCR catalysts itself is such a large filter that any tailpipe sensor signal, whether NO_x or NH_3 , is simply too slow to be of use. A tailpipe NH_3 sensor would have a similar attenuation problem, in addition to the fact that tailpipe NH_3 levels are generally low, and the presence of the ASC would eliminate most of the remaining signal.

For this reason, the downstream catalyst was split into two regions with a mid-bed sensor to provide feedback. At this location a mixture of both high NO_x and high NH_3 is expected, therefore a NO_x sensor would not be useful due to the cross-sensitivity of currently available sensors. Therefore, a mid-bed NH_3 sensors was the only viable option for real-time feedback. However, the currently available production NH_3 sensor is known to have issues with accuracy at lower NH_3 levels (below 30ppm), and is also subject to significant drift over time. It was necessary to use the NH_3 sensor in a manner that was not sensitive to these issues. As shown in Figure 46 above, the mid-bed NH_3 sensor was used for model state correction based on comparison to the model predicted value at the mid-bed location. Because the NH_3 sensor is used as a state sensor, rather than in a traditional feedback loop, the absolute accuracy of the NH_3 sensor is not as important, and the sensor functions primarily to detect the presence of an unexpected ammonia wave, or the absence of a predicted ammonia “wave.” This allows the feedback algorithm to correct storage over a timescale of seconds to minutes, and the more accurate storage prediction allows the controller correct catalyst behavior better.

Figure 48 shows an example of how the ammonia storage profiles look during a typical hot-start FTP cycle. Storage is tracked in the model as the variable “theta,” which is a fractional ratio of ammonia storage compared to the maximum capacity of the system at a reference condition of 200°C. As temperature increases, this coverage ratio (theta) can be seen to drop exponentially. For each catalyst both the actual (black) and target (red) average storage values are shown, along with the actual coverage values for each of the seven model cells on a given bed. As can be seen in the figures, the individual cell coverage values can be very dynamic, and they illustrate how storage evolves through a given catalyst bed over time. This profile information can be very useful for high efficiency SCR control, as it can be used to spot a wave of ammonia moving through the

catalyst, allowing controls to react to that profile to prevent ammonia slip before it occurs, while also maximizing coverage and preparing the next wave of ammonia. In this way, the controls can be thought of as arranging a succession of waves of ammonia to pass through the catalysts as the temperature cycles.

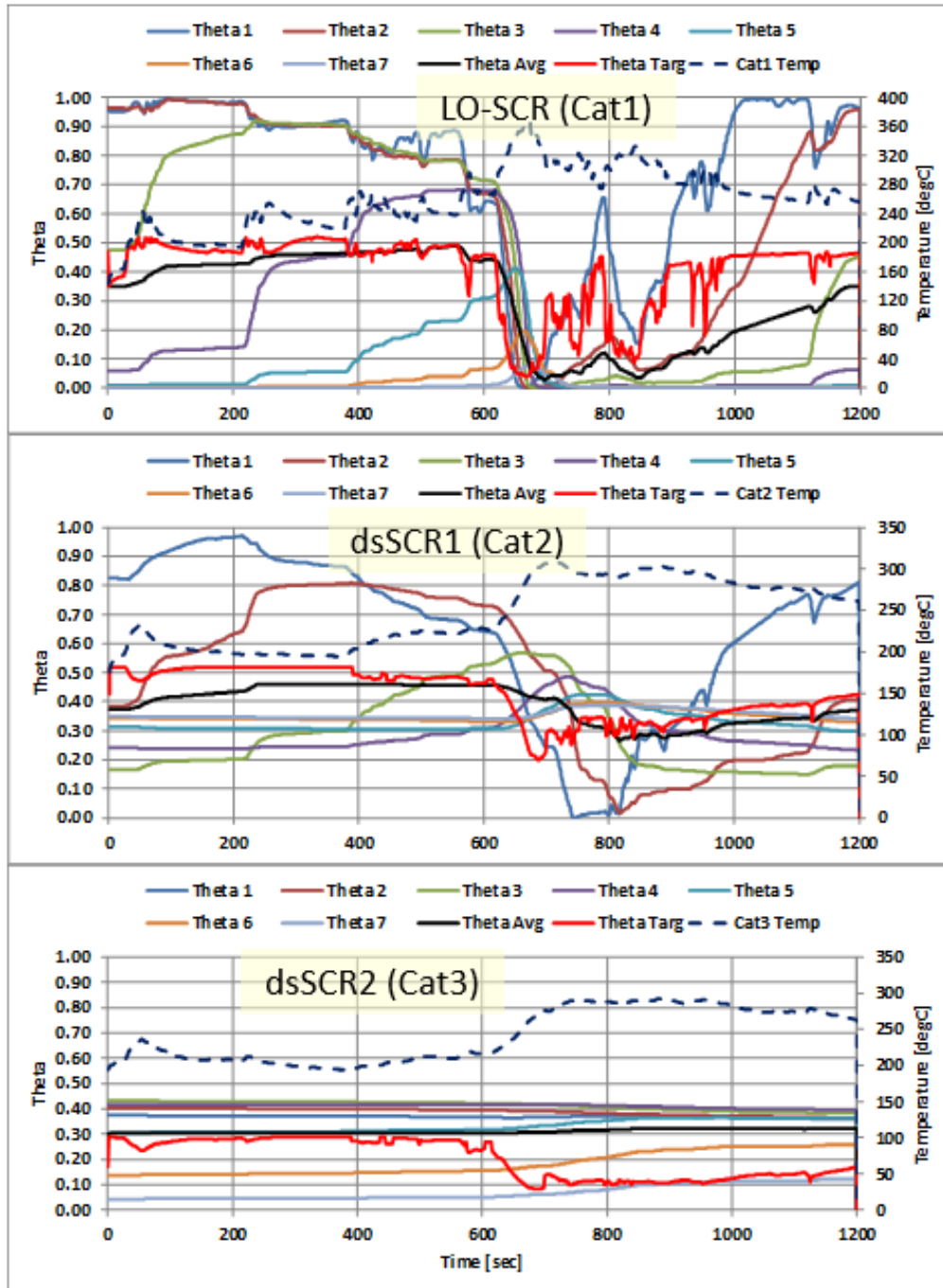


FIGURE 48. EXAMPLE OF AMMONIA STORAGE PROFILES DURING HOT-START FTP TRANSIENT CYCLE

2.6.4. Overall Aftertreatment System Control Strategy

The DEF dosing controls described above allow for a great degree of flexibility in designing a strategy to manage the usage of the two SCR catalysts systems to try to reach the program targets for NO_x and CO₂ in a robust manner. At the same time, other system priorities, such as removal of soot from the DPF, must also be considered. The planned strategy was considered at the time of the AT hardware design, and implemented in the calibration of the DEF dosing controls and the Engine State Machine thermal states.

Under cold-start warm-up conditions, stored ammonia on the surface of the catalysts is crucial to maximizing performance during catalyst light-off. Although the lower temperature capability of the heated dosing is helpful in this case, the high storage capacity of the zeolite SCR catalysts at low temperatures makes it difficult to push enough ammonia through the catalysts to achieve coverage. Therefore, previously stored ammonia is vital for reaching Low NO_x levels during cold-start which creates a design aim to continuously maintain target coverage prior to each (time-unknown) engine shutdown. This is most important for the LO-SCR, and a significant amount of the strategy is designed to enable rapid recovery of LO-SCR storage that will be needed for the next start event. The accelerated dosing modes of the controller and the low deposit risk, high DEF dosing rate capabilities of the heated dosing system are both important features for this to work on an optimal fashion over a wide variety of duty cycles and entry conditions.

At lower temperatures, generally below 300°C, the approach is to leverage the LO-SCR to the maximum amount possible. Storage targets are generally set as high as practical without running the risk of excessive NH₃ slip from the LO-SCR during a sudden thermal ramp. The LO-SCR does the majority of the NO_x conversion in this case, while the downstream system functions provide the incremental reduction needed to reach Low NO_x levels. At lower temperatures where conversion is below optimal, the TM-1 and TM-2 modes are used to reduce the overall demand for conversion, given that the LO-SCR is not as large, and the downstream system is still below optimal temperatures. However, as the system temperature nears and exceeds 300°C, the LO-SCR storage is quickly ramped down by reducing the storage targets, to the point where eventually there is little or no storage on the LO-SCR. At this point, the downstream does the majority of the NO_x conversion. The engine by this point is operating at maximum engine-out NO_x levels, but the downstream SCR system is large enough to handle this higher demand. The LO-SCR is still used during this time but only to convert a small amount of NO_x, as little as 20%-30% conversion under some conditions. Effectively, the LO-SCR operates as a peak shaving device at this point.

The primary reason for backing off on the LO-SCR catalysts at higher temperatures is to allow a significant amount of NO_x to reach the zoned-CSF (or DOC+DPF). This enables passive soot oxidation to function as needed to remove most of the soot from the filter, thus reducing the need for active regeneration, thus improving CO₂. In addition, the periodic removal of stored ammonia from the LO-SCR and operation of the LO-SCR with a high NO input in an under-dosing

situation helps to remove any nitrates and other nitrogen-related compounds that may have formed during low temperature operations where the LO-SCR operates under high conversion demand. This helps maintain long-term LO-SCR performance.

However, as the catalysts begins to cool, it is important to re-establish coverage on the LO-SCR quickly to be ready for the next start event. Because it is not possible to know when the next engine shutdown is coming, the controller leverages accelerated dosing modes and the capability of the heated dosing system to start re-establishing coverage as rapidly as possible whenever temperatures dip below 300°C. This can also be done with un-heated dosing, but at lower temperatures the recovery will be slower due to the need to limit dosing rates more to avoid DEF deposits. Storage recovery on the downstream system is generally easier as the temperature drops because the system is not depleted as often, and also the NO_x conversion demand is not as high, allowing more NH₃ to be used for re-establishing coverage.

The realization of this strategy is illustrated below in Figure 49. This shows an example of the behavior of storage over the course of a hot-start FTP. In this figure, Cat1 is the LO-SCR catalyst bed, Cat2 is the dsSCR1 bed, and Cat3 is the dsSCR2 bed. The dashed lines correspond to the target Theta values. The LO-SCR storage in blue can be seen as the most dynamic over the course of the test, with storage nearly emptying out around the 700-second mark, but then recovering quickly in just a few minutes to the necessary level before engine shutdown. The downstream catalysts go through much less cycling, although dsSCR1 still sees more movement than dsSCR2.

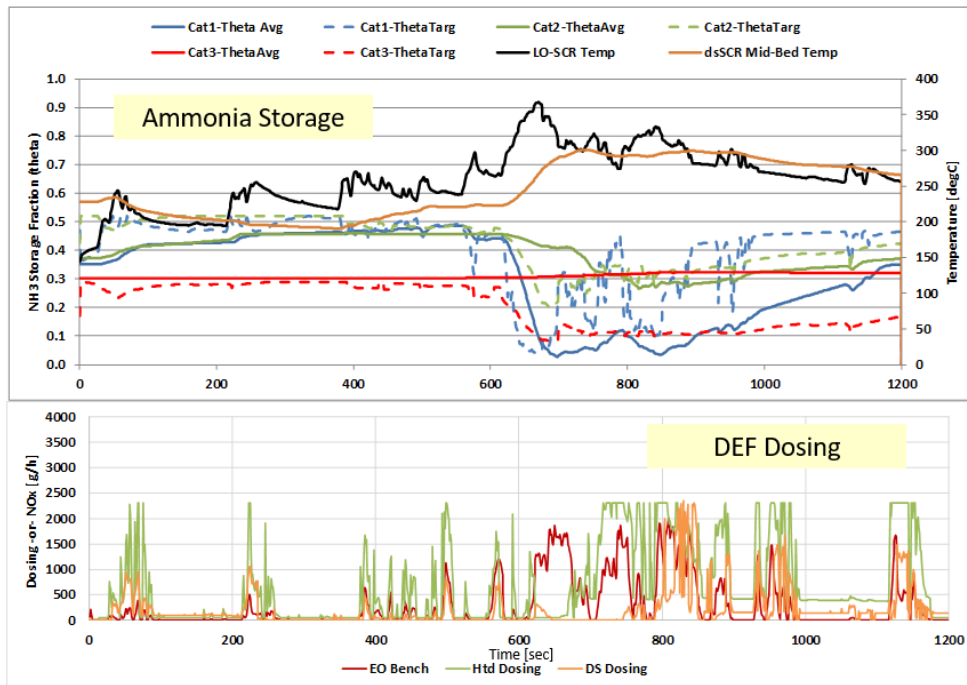


FIGURE 49. EXAMPLE OF AMMONIA STORAGE TRACKING AND DEF DOSING OVER HOT-FTP TRANSIENT CYCLE

Figure 50 shows a different realization of the same duty cycle, this time following a high temperature DPF regeneration when the SCR catalysts were nearly empty, apart from a small amount of coverage on the LO-SCR built up during the brief cooldown period following the regeneration. This data set is taken from the first of two preconditioning runs prior to placing the engine into overnight soak for a subsequent cold-start test. In this scenario it should also be noted that the initial temperatures are quite a bit higher than a normal hot-start test, making it potentially more difficult to build up ammonia storage quickly. In all cases it can be seen the ammonia storage is initially well below targets. Comparing the dosing traces between Figure 50 and Figure 49, it can be seen that dosing is much more aggressive as the controller attempts to force a wave of ammonia through the catalysts to re-establish coverage.

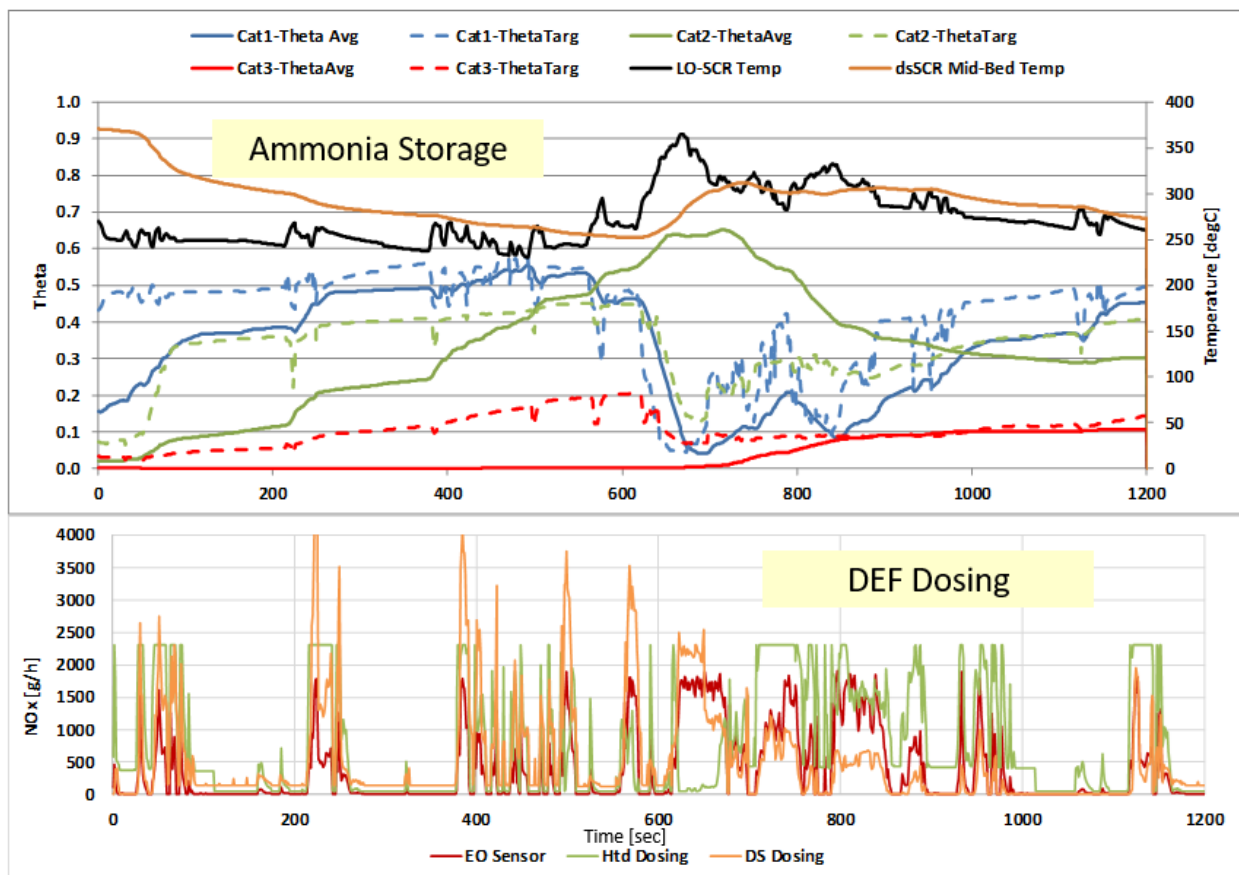


FIGURE 50. EXAMPLE OF AMMONIA STORAGE AND DEF DOSING OVER HOT-FTP TRANSIENT CYCLE – AFTER DPF REGENERATION

Note that dosing is still restrained as needed by allowable limits to avoid deposits, although these are much more aggressive for the heated doser. As the built up wave of ammonia begins to propagate through the downstream SCR catalyst to the second bed, around the 750-second mark, the downstream dosing pulls back as the storage begins to approach targets, so as to avoid future

ammonia slip. For reference, this particular cycle was at a tailpipe NO_x level of roughly 0.05 g/hp-hr according to the tailpipe NO_x sensor measurements (a valid laboratory tailpipe measurement was available for this prep cycle), though this was certainly helped in some part by the elevated temperatures present at the start of the cycle. As aggressive as this dosing was, it should still be noted that storage did not fully reach equilibrium with the duty cycle on the downstream system until the end of the second preconditioning cycle.

A different duty cycle behavior is illustrated below in Figure 51, which shows the same storage and dosing behavior for an RMC-SET cycle, including the preconditioning cycle run immediately before the test for record. This cycle was run following earlier testing on lower temperature duty cycles, and as seen in the figure, the AT begins the duty cycle at higher storage levels, with the targets falling quickly as the cycle ramps aggressively up in temperature. However, it takes some time to consume the stored ammonia on the back of the downstream system, so the controller can be seen pulling back on dosing on the downstream system to prevent a wave of ammonia slip. It should be noted that the peak tailpipe ammonia slip observed during this transition was less than 20ppm (around the 800 second mark), and the event was over quickly. Behavior returned to a more normal dosing pattern at around 1600 seconds. Storage is generally low on this cycle, although occasional ramps in the storage can be seen as the catalysts cool below 300C for short periods. Note that the cycle for record shows a much smaller wave of ammonia through the Cat3 bed shown in red). At the end of the cycle the controller can be seen aggressively re-establishing coverage, especially on the LO-SCR as the catalysts cool down.

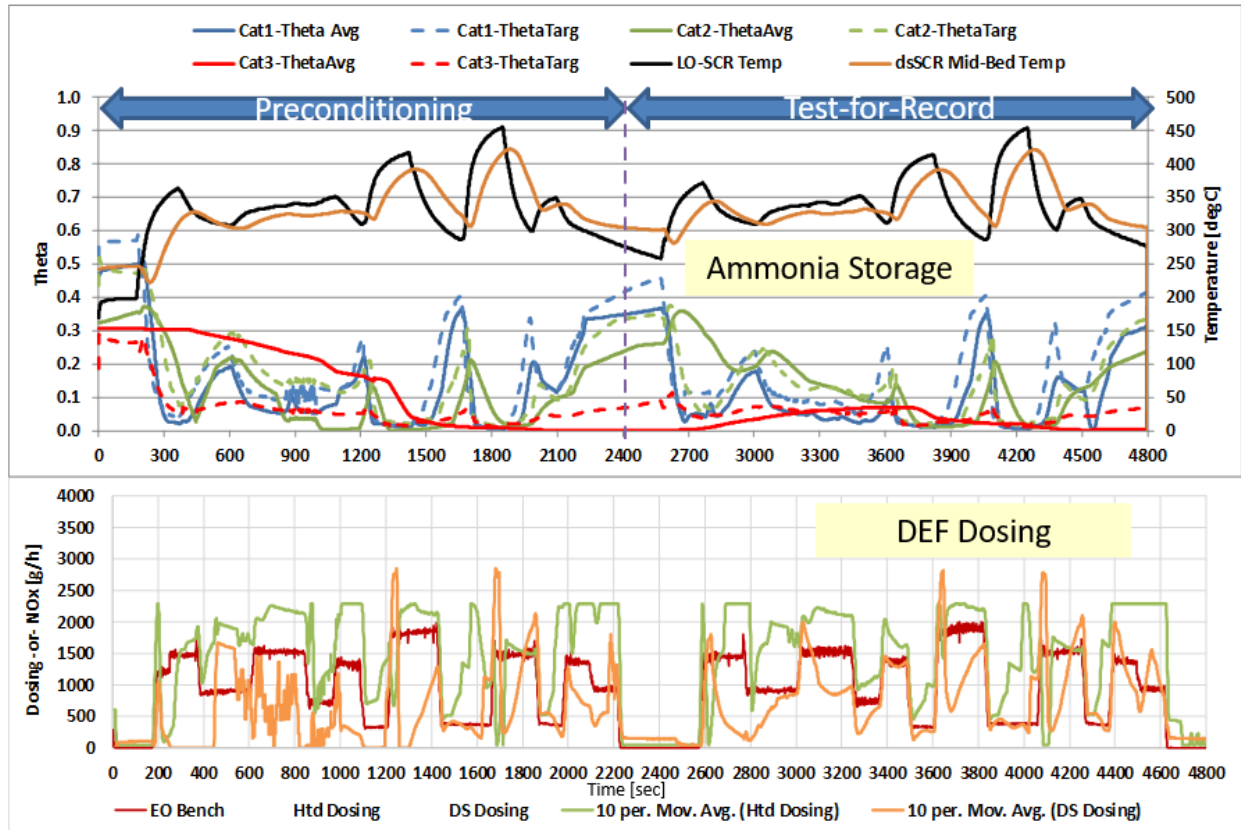


FIGURE 51. EXAMPLE OF AMMONIA STORAGE AND DEF DOSING OVER RMC-SET CYCLE – INCLUDING PRECONDITIONING PORTION

2.7 Aging Methodology

Emissions standards must be met at the end of FUL period that is defined in the regulations as part of the standard. As a result, any demonstration of feasibility in controlling emission must be conducted using hardware which has been aged to represent exposure to FUL operation in the field as closely as possible. Following the advent of the 2010 emissions standards, heavy-duty NO_x and PM emission control performance over time has been dominated by the performance and degradation of the AT. This is even more the case when considering Low NO_x levels. For heavy heavy-duty engines, such as the X15 engine used in this program, the current FUL period is 435,000 miles, and that is the FUL target that was used for this program. It is understood that CARB has pursued longer FUL requirements, but those were not available at the start of this program, therefore the current 435,000 mile target was used. This is equivalent to 10,000 hours of operation, based on Class 8 truck data that was used to scale the aging operations for this program.

A full on-engine demonstration, similar to the deterioration factor (DF) testing done by engine manufacturers over thousands of hours for emission certification, was not possible in this program due to time and budget constraints. Therefore, given the dominant role of AT

performance on emissions control, it was determined that the AT systems would be aged in an accelerated manner to simulate FUL conditions for demonstration. It should be noted that in upcoming standards, both CARB and EPA are considering a similar approach for future certification. The approach that SwRI used in this program is based on the protocols developed in the SwRI-led Diesel AT Accelerated Aging Cycles (DAAAC) consortium program, completed in 2010. This protocol was developed to simulate both thermal and chemical aging of diesel AT systems, and it was designed to achieve a 10X acceleration in aging. Therefore, 10,000 hours of aging could be conducted in 1000 hours, which is a timeframe that was within the scope of budget of the program. The DAAAC protocol methods are designed to simulated real-world aging in as close a manner as possible in the laboratory. As such they generate parts that are representative of the results from more traditional and time consuming methods of aging. In this program, the final DAAAC aging methodology considering both thermal and chemical aging is referred to as Final Aging. The Stage 3 aging approach mirrors that used for the Stage 1/2 system and both aging protocols were discussed with the Program Advisory Group for comment prior to use.

Given the wide variety of AT hardware evaluated in this program, it was not practical to conduct full DAAAC-style aging considering thermal and chemical components on every system, especially those that would not ultimately down-selected for the final system. Therefore, a simplified and faster version of this protocol that considered only the hydrothermal aging mechanism was used for the initial development and calibration efforts. This simplified aging protocol is referred to in this report as Development Aging. The two methods of aging are described in more detail below.

2.7.1. Final Aging (DAAAC)

The intent behind the Final Aging was to be as representative as possible of real-world aging in the field. To meet this objective, SwRI chose to leverage the DAAAC protocol which has been developed for this purpose over the last 12 years. More information on the development of the DAAAC protocol can be found in [11] and [12]. The DAAAC protocol provides a method to develop and run application specific accelerated aging cycles for diesel AT systems in a manner that represents the field as closely as possible. Unlike most other accelerated aging methods, DAAAC considers both thermal and chemical aspects of aging, and does not attempt to replace chemical aging with additional thermal aging. The DAAAC methodology has been accepted for regulatory purposes by the JRC in Europe for aging of diesel AT, and by CARB for aging of retrofit AT hardware. SwRI has previously shown correlation between accelerated DAAAC-aged parts and full-length engine based aging, as well as some field parts in the past. CARB and EPA have also proposed the use of DAAAC methodology for future certification durability demonstrations, and final validation experiments are currently being run to finalize the protocol for regulatory use. SwRI used this methodology to develop the Final Aging for this cycle, however there were some differences between the normal DAAAC protocol and what was done for Stage 3.

The DAAAC protocol typically relies on the use of field data, including field measured AT temperatures, to develop the aging cycle conditions. In this case, there were no field systems to rely on given that this is an early stage technology demonstration. However, there is an option being finalized within the DAAAC methodology to use field data to weight modes developed from standard laboratory cycles. Under this approach, aging conditions are developed using laboratory data from the appropriate regulatory cycles, in this case the FTP, RMC-SET, and LLC. Each cycle is represented by one or more aging modes, and then field and/or application data is used to weight operating time in those modes in a representative fashion. Furthermore, any specialized high temperature events, such as DPF regeneration are included in the cycle, with the frequency and duration of those high temperature events matching the equivalent of FUL.

For the case of the Stage 3 engine, the primary application is a Class 8 tractor. The final weighting chosen between FTP and RMC modes based on field application guidance was 45% and 55% respectively. However, for the purposes of this demonstration there was some attempt to represent a broader range of applications. As such, the low temperature operations of LLC were weighted at 15% of the total, which matched the distribution observed in the fleet data used to develop the LLC. The weighting of the other 85% of time was kept in the 45/55 proportion given earlier. To ensure a proper range of temperature exposure, the RMC was split into an average temperature and high temperature mode, with the high temperature mode representing B100 and C100 operations, and the average representing the rest of the RMC. Those two modes were time weighted in a manner to match their weightings in the RMC cycle.

For the Stage 3 engine there are two forms of elevated temperature operations. These are the Active Regeneration of the downstream zoned-CSF (which also served as deSO_x for the downstream SCR and decrystallization of any potential urea deposits in the downstream system), and the deSO_x of the LO-SCR catalysts. For Active Regeneration mode, it was determined based on experimental measurements of passive soot oxidation behavior, and observation of zCSF differential pressure over time, that the Stage 3 engine would use the same Active Regeneration frequency as the baseline engine. This information was supplied by Cummins for the baseline engine, and it was given as 30 minutes every 100 hours, a frequency of 0.5%. However, for the zCSF, a higher temperature of 600°C at the filter outlet was utilized, based on the need for a more conservative regeneration approach to ensure proper cleaning of the filter over time. This higher temperature was also felt to be beneficial for deSO_x of the downstream SCR, given the higher demand for NO_x conversion for the Low NO_x system.

The LO-SCR deSO_x temperature was initially set as 525°C, based on initial supplier and SwRI experiments. From the same experiments, the LO-SCR deSO_x frequency was set at 30 minutes every 300 hours. This relatively lower frequency was possible due to the fact that there is no DOC upstream of the LO-SCR in the Stage 3 configuration, and therefore the majority of sulfur exposure on the LO-SCR comes in the form of SO₂, which is stored much less efficiently on the zeolite catalysts than SO₃. Following the first 333 hours of aging, performance and deSO_x

tests indicated that the 525°C was not quite sufficient for the desired removal of sulfur, and the temperature setpoint was changed to 550°C, which did prove sufficient. These results are discussed in more detail later.

As discussed earlier, the target for the DAAAC-based acceleration was 10X above the field. Therefore, to simulate 10,000 hours of field aging, the Final Aging protocol ran for 1000 hours. In the DAAAC protocol, thermal acceleration is achieved by leveraging the fact the hydrothermal aging is exponential in nature as temperature increases, according to the Arrhenius equation given below in Figure 52. This relationship essentially means that time at higher temperatures, such as Active Regeneration, dominates thermal deactivation, and therefore it is possible to remove a large amount of operating time at lower temperatures while still reaching the same amount of thermal deactivation. In effect, the DAAAC approach maintains a FUL of Active Regeneration (and in this case LO-SCR deSO_x) exposure, and increases the regeneration frequency by a factor of 10. All of the lower temperature operation, which had minimal thermal impact on the AT, was conducted primarily to create a representative environment for chemical aging, as discussed below.

$$k = Ae^{-\frac{E_A}{RT}}$$

Labels in the diagram:

- rate constant (points to k)
- activation energy (points to E_A)
- kelvin temperature (points to T)
- the gas constant (points to R)
- frequency factor or pre-exponential factor (points to A)
- mathematical quantity, e (points to e)

FIGURE 52. ARRHENIUS RATE LAW EQUATION FOR THERMAL CATALYST DEACTIVATION

The final aging cycle is described in Table 5. The aging temperature targets, are based directly on test cell data for the regulatory cycles. However, it should be noted that exhaust flows were somewhat higher on the DAAAC engine to reach the desired oil consumption exposure. This is discussed more later. The regeneration of the zCSF was conducted as it would be in application by using in-exhaust fuel injection to create an exotherm on the zCSF, and is run for 30 minutes every 10 hours of aging cycle operation (equivalent to 100 hours of field operation). This base cycle with zCSF regeneration is illustrated in Figure 53. This base cycle is repeated three times, and then a LO-SCR deSO_x is run by raising the system inlet temperature to the desired target, resulting in a deSO_x event every 30 hours of aging cycle operation (equivalent to 300 hours of

field operation). The complete Final Aging cycle with deSO_x is shown in Figure 54. Again, it should be noted that the initial target was 525°C, but that was later increased to 550°C to ensure sufficient deSO_x on the LO-SCR. One other change that was noted following the initial aging runs is that it was found that dosing during regeneration on the downstream system (Dos 2) did not result in additional NO_x reduction, and in some cases caused a NO_x increase. Therefore, in later aging operation, the Dos2 ANR was set to 0 during modes 5a – 5c.

TABLE 5. FINAL AGING CYCLE MODE TARGETS

Mode	Mode Descriptor	Time		System Inlet T degC	Exhaust Flow kg/hr	NO _x ppm	Dos 1 ANR	Dos 2 ANR	zCSF Outlet T degC
		min	sec						
1	FTP	74	4440	260	1235	200	0.80	1.00	n/a
2	LLC	27.75	1665	200	739	100	1.05	1.00	n/a
3	RMC-Avg	66.6	3996	340	1370	500	0.30	1.00	n/a
4	RMC-High	16.65	999	425	1500	800	0.20	1.05	n/a
Repeat 1-4 3 times then proceed run 5a-5d once									
5a	Regen prep	5	300	350	800	900	1.00	1.00	n/a
5b	Regen ramp	5	300	350	800	900	1.00	1.00	600
5c	Regen	30	1800	350	800	900	1.00	1.00	600
5d	Regen Cooldown	5	300	350	800	500	1.00	1.00	n/a
Repeat loop of 1-5d X (3-5) times then run 6a-6c once									
6a	deSO _x ramp	5	300	525	900	100	1.00	1.00	n/a
6b	deSO _x	30	1800	525	900	100	1.30	1.00	n/a
6c	deSO _x Cooldown	5	300	260	900	100	1.00	1.00	n/a

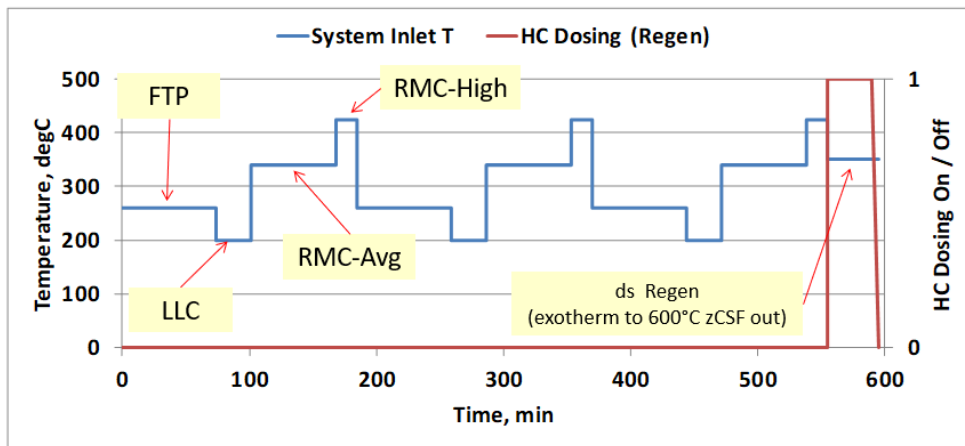


FIGURE 53. STAGE 3 FINAL DAAAC-BASED AGING CYCLE – BASE CYCLE WITHOUT DESO_x

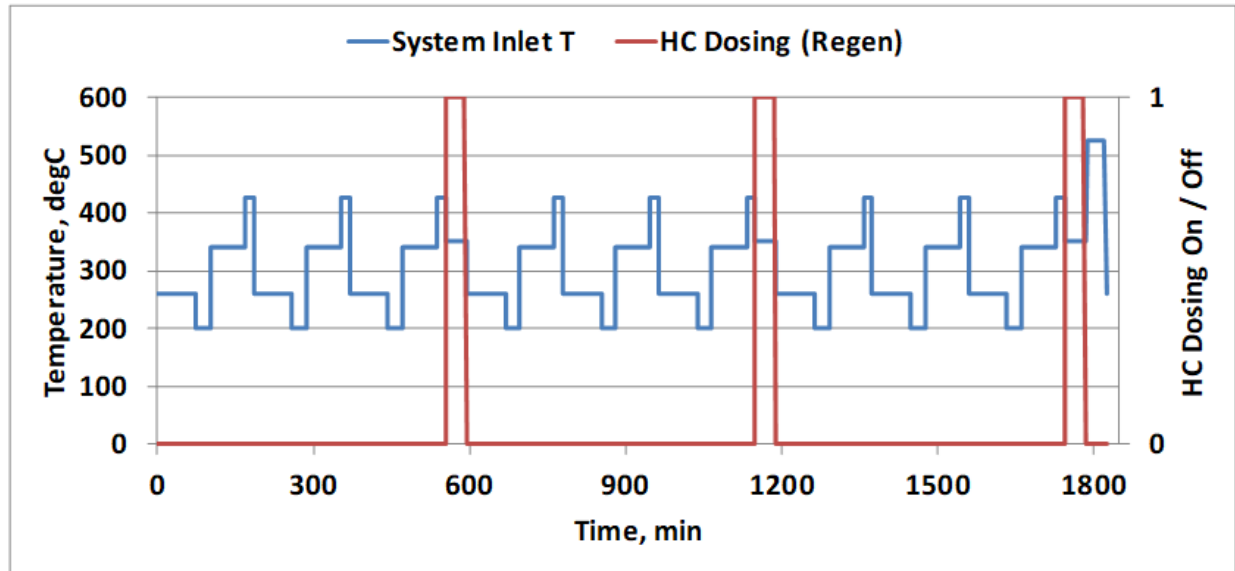


FIGURE 54. STAGE 3 FINAL DAAAC-BASED AGING CYCLE – FULL CYCLE WITH LO-SCR DESO_x

The modes are arranged in an alternating fashion such that there is cycling between high and low temperatures, as would occur in the field under normal operations. This helps to ensure that the deposition and cycle of chemical poisons happens under representative conditions, with periodic high temperature exposure due to Regeneration and deSO_x.

Chemical exposure in the DAAAC protocol takes the form of increased exposure to lubricating oil and sulfur. Previous efforts have validated that it is possible to increase the chemical exposure by a factor of 10 while still getting representative response from the AT system in terms of deposition and cycling of these poisons. Based on data from Cummins, the normal oil consumption rate for this engine in the field is 15 g/hr. Therefore, the oil exposure target for Final Aging was 10X that rate, or 150 g/hr. Following DAAAC methodology, the increased oil consumption was achieved using a combination of raising engine oil consumption via flipped rings, and doping of oil into the fuel. In accordance with DAAAC targets, increased oil consumption on the engine accounted for 65% of this total (~ 100 g/hr), while the fuel-doped oil accounted for the other 35% (~ 50 g/hr). It should be noted that this consumption rate is over the complete cycle, actual exposure on individual modes will vary somewhat with engine operating modes. This rate was verified by periodic measurements of oil consumption through the engine using a specialized measurement rig, and further validated by periodic weights on the filter to examine ash accumulation and ash-finding ratio.

Target sulfur exposure for 10,000 hours of operation was calculated using the weighted fuel flow of the cycle points from the Stage 3 engine data, and the 15 g/hr oil consumption. To be conservative, these calculations assumed a 10ppm fuel sulfur content representing at least a 90th percentile fuel sulfur level, as recently corroborated by California fuel sampling [13]. These

calculated fuel consumption rates were also examined by Cummins to ensure they were representative of normal operations in a broad sense over time. The fuel consumption of the modes in Table 5 was then measured, and it was used to determine a total expected fuel exposure over the 1000 hour aging process. Additional sulfur was then doped into the fuel to make sure that that total sulfur exposure would be 10X the baseline data. This resulted in a target fuel sulfur level of 65ppm, given that average fuel consumption on the aging engine over the DAAAC-based cycle was higher than the normal average for the baseline data.

Final Aging was run in three segments, with intermediate tests points at 333 hours (33% FUL), 667 hours (67% FUL), and 1000 hours (100% FUL). Ash cleaning of the zCSF was planned for the 500-hour test point, at 50% of FUL, and again at the 1000-hr test point, where the system would be tested both before and after ash cleaning.

Final aging was conducted on a DAAAC engine stand, illustrated in Figure 55. DAAAC does not require the use of the exact test engine for aging, but rather uses a specially modified mule engine and test cell setup to create the target conditions for aging. For this test stand, a DAAAC-modified 2009 Cummins ISX 15-liter engine was utilized. The DAAAC cell also contains in-exhaust air-to-air heat exchangers, allow independent control of temperature and flow rate, as well as direct control of several engine elements, such as the EGR valve, to provide the flexibility needed to produce the desired aging conditions. The engine ring pack was modified to increase oil consumption. This DAAAC mule engine can be used to achieve a wide range of engine aging conditions for engines in the range of 11L to 15L, and it was also used for Final Aging in the Stage 1 and Stage 1b Low NO_x programs. Figure 56 shows the Stage 3 AT system installed in the DAAAC aging stand.

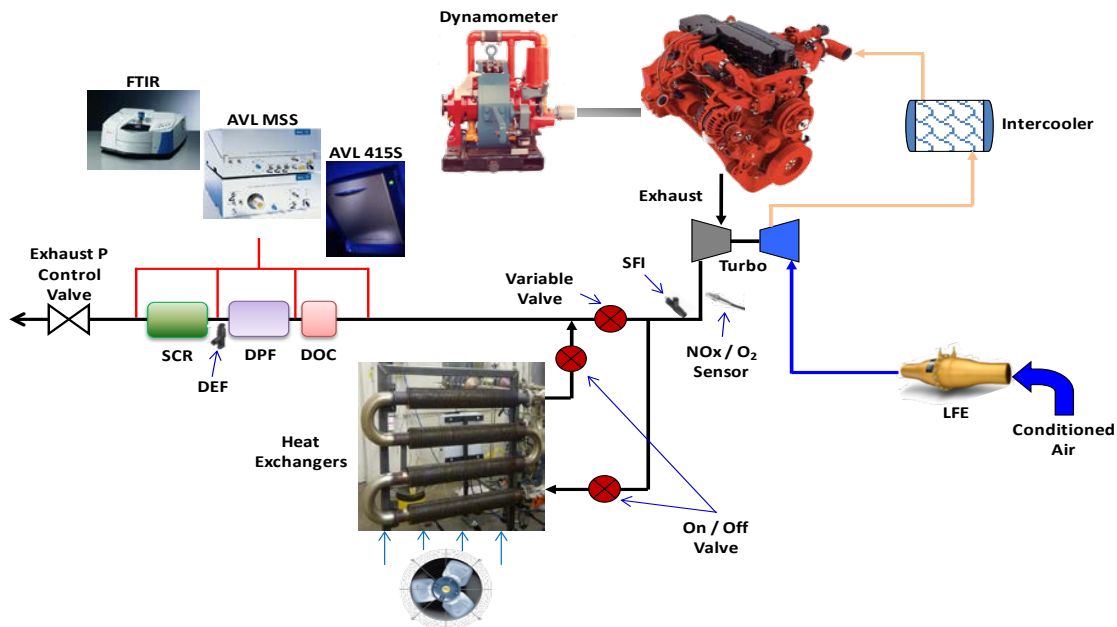


FIGURE 55. SWRI DAAAC ENGINE-BASED AGING CELL



FIGURE 56. STAGE 3 AT SYSTEM INSTALLED IN DAAAC AGING CELL

2.7.2. Development Aging (Hydrothermal Only)

The Development Aging process was designed to simulate of FUL of hydrothermal aging only. The process did vary slightly from one set of hardware to the other, given that there were some differences in key parameters like Active Regeneration target temperature. The basic approach to Development Aging was to again leverage the exponential relationship of temperature and thermal deactivation, but without the extra time for the chemical poisoning elements of DAAAC. In effect, all of the high temperature exposure events were collected together, with little or no time in between. Because the final systems were not yet developed, conservative choices were made regarding regeneration durations and frequencies.

Development Aging was conducted on the ECTO-Lab burner system, illustrated in Figure 57. This system allows the simulation of exhaust conditions of many different engines, and can be used for aging and evaluation of full-size engine AT systems for engines ranging from 3-15L in displacement.

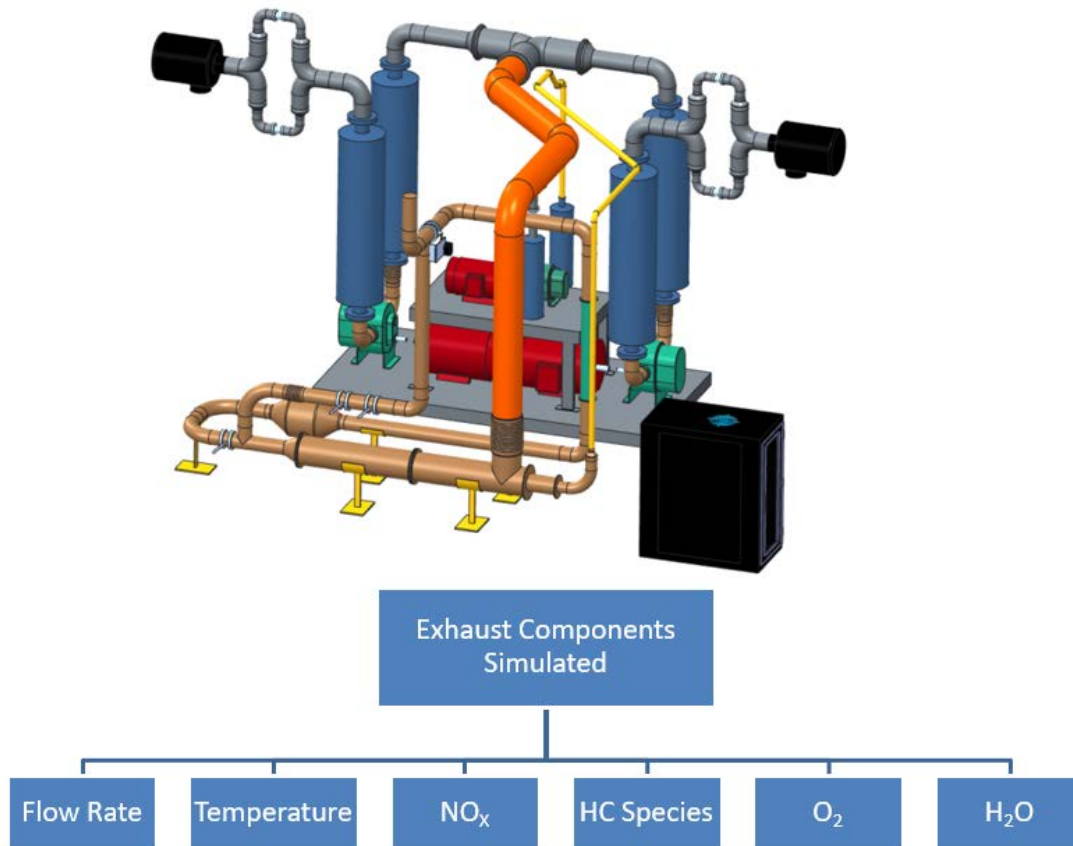


FIGURE 57. SWRI ECTO-LAB™ BURNER-BASED AGING AND TEST STAND

For Team 1 which utilized the zoned-CSF, the estimated regeneration frequency used to scale aging was 1 hour every 80 hours. This worked out to 150 hours of total regeneration over the course of 435,000 miles. The expected temperature exposures over that time were 75 hours at 575°C, 50 hours at 600°C, and 25 hours at 625°C, all measured at the zoned-CSF outlet gas temperature (bed temperatures would likely be higher due to the exotherm). This was later simplified to a final protocol of 100 hours at 600°C plus 25 hours at 625°C. For the Team 1 LO-SCR the expected total deSO_x was 100 hours at 550°C. The first 100 hours of aging were run at a 550°C system inlet temperature and using HC exotherm across the zCSF to reach 600°C at the filter outlet. Under these conditions, the downstream SCR temperature was around 565°C at the mid-bed location. The LO-SCR was then removed, and the last 25 hours of aging were run with an increased exotherm to reach 625°C at the filter outlet, which put the downstream SCR at about 585°C at the mid-bed location.

For Team 2, the system was Development Aged in the worst-case configuration for temperature exposure, which was Configuration 2A with the DOC upstream of the LO-SCR. This meant that all the temperatures associated with Active Regeneration of the DPF would pass through the LO-SCR. An assumption of 1 hour per 100 hours was used for Active Regeneration, and this event would serve as the deSO_x for both of the SCR catalysts. Therefore, a total of 100 hours of aging were used. The target temperature for Active Regeneration was 600°C at the DPF inlet, which was generated using exotherm across the DOC. However, given the system configuration this meant that the LO-SCR was subjected to temperatures of 650°C during these events. A DOC inlet temperature of 400°C was used for the aging, and in-exhaust fuel injection produced the exotherm across the DOC to raise temperatures to the aging target. It was understood that this approach likely produced an LO-SCR that was over aged thermally for the Team 2B configuration where the DOC was downstream of the LO-SCR. However, this was considered acceptable for the initial evaluation and calibration, given that the lack of chemical aging would likely underestimate low temperature performance impacts anyway.

2.7.3. De-greening (Hydrothermal Only)

Prior to the start of the 0-Hour tests on the Final Aged system, some degreening was necessary to prepare the catalysts for this initial test. This degreening was also conducted on the ECTO-Lab burner system. This degreening process involved 50 hours of aging at a system inlet temperature of 400°C. Every 25 hours, in-exhaust HC injection was used to raise the temperature at the zoned-CSF outlet to 600°C for 30 minutes to simulate an Active Regeneration. After this, the system inlet temperature (before the LO-SCR) was raised to 550°C to simulate an LO-SCR deSO_x event. Therefore, two of each of these elevated temperature events were run during the course of the degreening process. This was considered sufficient to stabilize emission performance prior to the initial tests.

3.0 RESULTS AND DISCUSSION

3.1 Baseline Engine Testing

At the beginning of the laboratory effort in this program, the baseline emissions of the production 2017 Cummins X15 engine were characterized in detail. This was done to provide a basis for comparison for later Low NO_x engine configurations. Baseline testing was conducted on the engine as-received from Cummins with the production AT system installed. The AT system was received having already been de-greened at Cummins, and no further aging was conducted as SwRI. The baseline results on criteria pollutants served as a point of comparison as well as verifying the proper operation of the baseline engine. The tailpipe CO₂ emissions measured during the baseline tests are used as the basis for calculating the impact of the Low NO_x technology on GHG emissions.

The engine was torque-mapped to generate both full-load and motoring torque curves, as needed for subsequent baseline test cycle generation. The baseline initial tests involved only the FTP and RMC-SET test cycles. Later, when the final LLC became available, a baseline was conducted using the LLC, and that was later updated when the final procedures regarding accessory load at idle were finalized. In addition, when the task was added to evaluate the impact of the Low NO_x configuration on vehicle CO₂ emissions using the Phase 2 GHG methodology, a baseline was run for the fuel mapping process in 40 CFR Part 1036.

Tailpipe BSNO_x emission results for the initial test are shown in Figure 58. Detailed individual cycle emission results for all pollutants are given in Appendix A. The average baseline NO_x results are summarized in Figure 59, with the error bars showing one standard deviation.

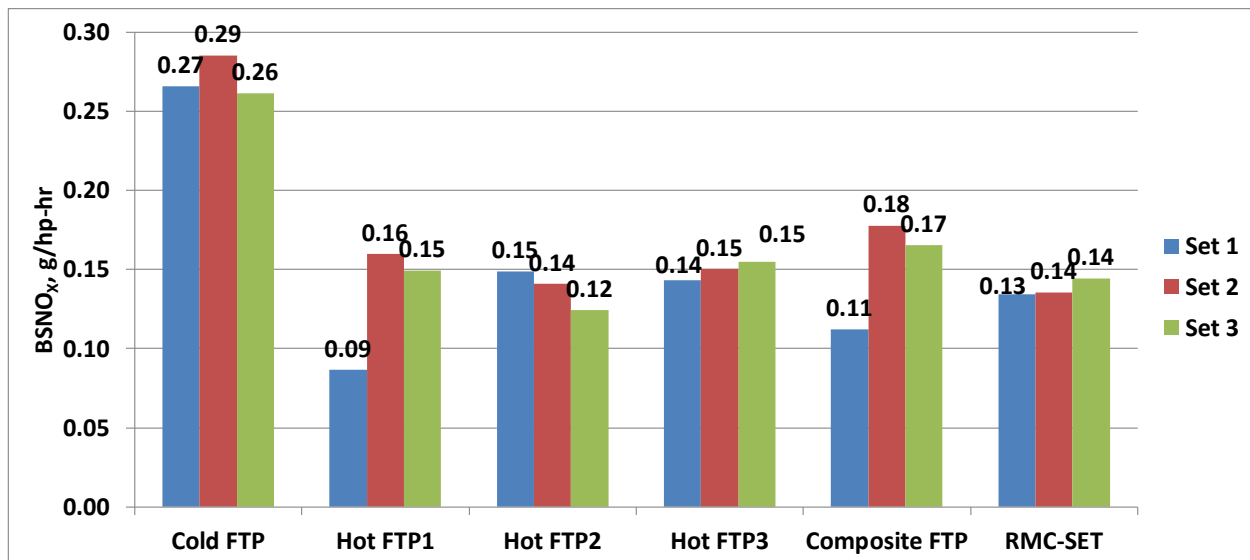


FIGURE 58. BASELINE TAILPIPE BSNO_x EMISSIONS FOR 2017 CUMMINS X15 ENGINE

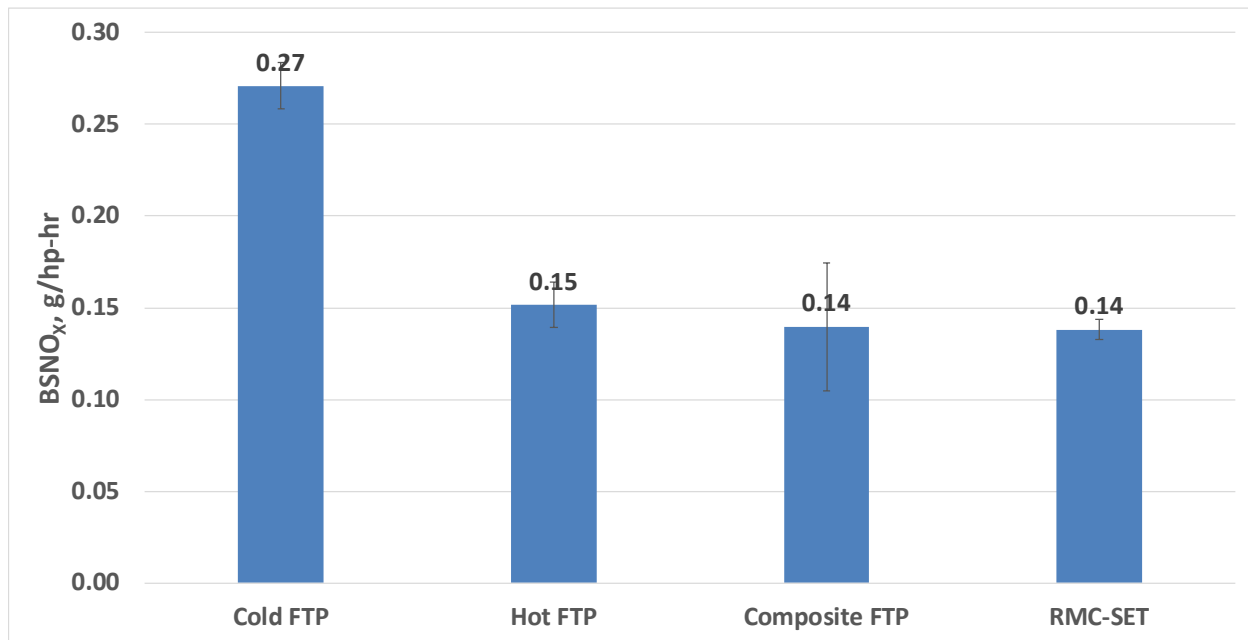


FIGURE 59. BASELINE TAILPIPE BSNO_x SUMMARY

It was noted that on the first baseline test sequence, tailpipe NO_x on the first hot-start was significantly lower than for all of the subsequent hot-start repeat tests. It was later determined that on the initial test sequence, thermal management was active for a longer period of time than on the subsequent runs, which is result on a higher CO₂ levels for that particular test. However, this was never observed again, and subsequent hot-start run showed more consistency. The baseline engine levels were compliant with 2010 heavy-duty standards, although it was noted that the margin on some of the FTP repeats was smaller than anticipated for a degreened system. After consultation with the engine manufacturer, the results were deemed representative and the program continued with engine calibration efforts.

Given the length of the program, the test plan included a baseline repeat that was conducted near in time to the final Low NO_x demonstration testing with Final Aged parts. At this point nearly 2 years had elapsed from the original baseline measurement, and nearly 800 hours had been run. It had been noted during development testing that a small upwards drift may have occurred on engine-out CO₂ levels. A comparison of the two baselines from 2018 and 2020, for both NO_x and CO₂ is given in Figure 60. It should be noted that the 2020 values for CO₂ have been corrected to account for any difference in carbon balance error from the 2018 measurements, so that the values may be directly compared. The comparisons indicated that there had been an upwards shift in CO₂ from the engine, on the order of 1 to 1.2% depending on duty cycle. The final impact of the Low NO_x configuration on CO₂ for the Final Aged parts was determined based on these later baseline repeats, because they were conducted much closer in time. This increase was also confirmed by examining proprietary engine fueling data, indicating a small increase in fuel consumption.

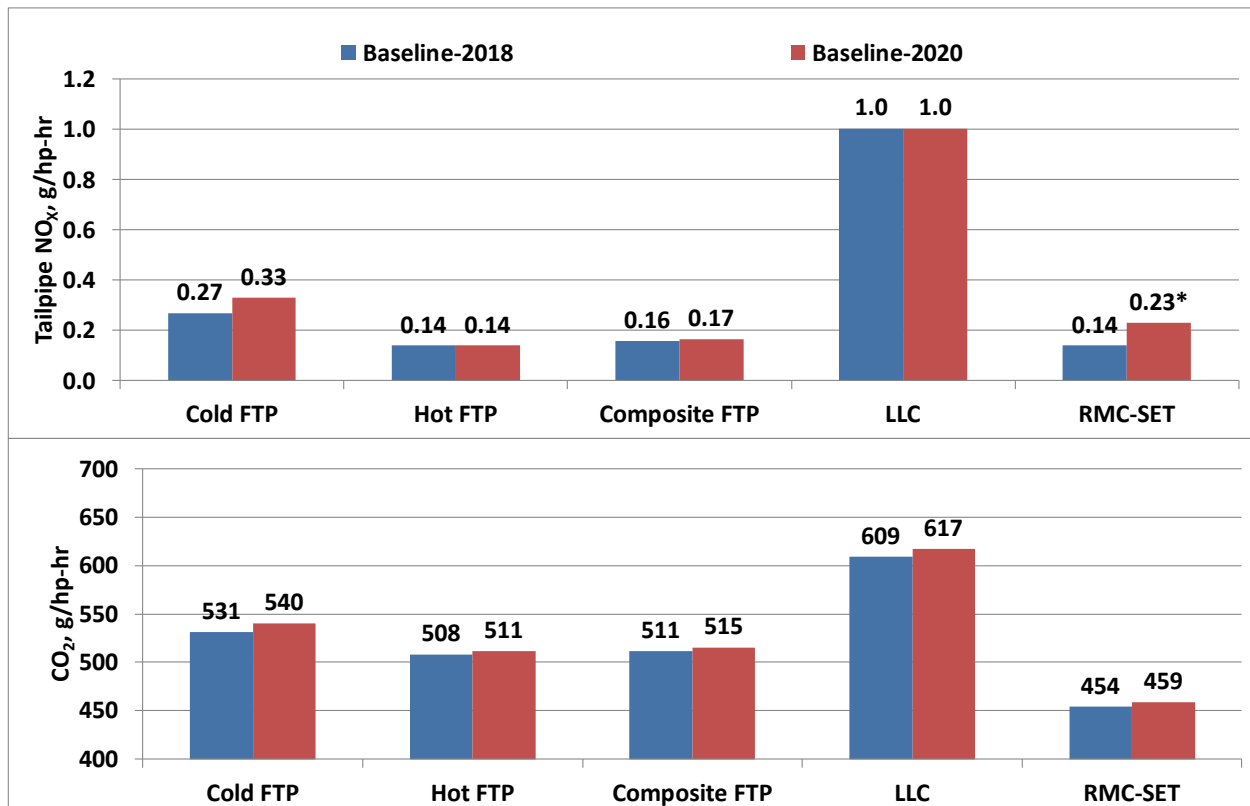


FIGURE 60. COMPARISON OF INITIAL AND FINAL BASELINE TAILPIPE NO_x AND CO₂ MEASUREMENTS

It should be noted on the baseline repeat tests that the value measured on the RMC-SET was not below the 2010 standard. Analysis indicated that this appeared to be due to a shift upward in engine-out NO_x at high load modes on the baseline engine, resulting in slightly higher NO_x breakthrough at the tailpipe. Despite some diagnostic efforts with the engine manufacturer, the root cause of this shift was not determined. It should be noted that if the engine-out NO_x had been lower in those modes, the CO₂ would likely have been slightly higher, and this should be considered when using that value for comparison, though this cannot be quantified from the available results.

Baseline tests were later added, as shown in Figure 60 for the LLC, and these were also run during the 2020 baseline repeat. The baseline results shown are for the LLC run in the finalized form with a 3kw accessory load added at idle. However, earlier baseline tests, and some development tests were carried out without this idle load, because that modification had not yet been finalized for the LLC at that time. The LLC BSNO_x without accessory load was 1.4 g/hp-hr, and the LLC BSCO₂ without accessory load was 624 g/hp-hr. It was noted that the 3kw accessory load had a very significant impact on LLC emissions for the baseline engine.

Later baseline tests also included the performance of triplicate Phase 2 fuel mapping tests, conducted in accordance with procedures given in 40CFR Part 1036. Steady-state fuel maps and idle fuel maps were conducted as outlined on 40CFR 1036.535, and cycle average fuel maps for all three duty cycles were conducted as specified in 40CFR 1036.540. This allowed final fuel consumption values for vehicles to be produced using GEM for either the default approach, combining steady-state maps for the two Cruise cycles and cycle average maps for the ARB transient cycle, or the cycle average approach (for all three cycles). In deference to the engine manufacturer, the full baseline fuel map data is not presented in this report. Rather, the results of Phase 2 GHG fuel mapping will be discussed later by examining relative differences between fuel mapping results for the final Low NO_x configuration and the baseline engine. This approach allows the impact of the Low NO_x changes on vehicle CO₂ to be assessed without disclosing sensitive engine information in a public manner. It should be noted that the fuel mapping baselines were conducted in parallel with the later baseline repeat tests conducted in 2020.

3.2 Modified Base Engine Calibration Updates

This section describes the development of a modified engine calibration to be used when SCR temperatures are too low to allow high NO_x conversion efficiency. Low SCR temperatures are encountered during cold-starts as well as extended low load operation. Therefore, since the goal of the Stage 3 program was to demonstrate ultra-low NO_x regardless of test cycle, engine operation beyond the cold FTP had to be considered so use of the modified calibration during warmed-up conditions was also planned. The initial modified calibration leveraged the available engine-based measures of multiple fuel injections, air-handling actuators such as EGR, intake throttle and VGT positions, and idle speed to simultaneously increase exhaust gas temperature and reduce engine-out NO_x emissions. The Cummins's proprietary calibration software Calterm® was used for engine actuator control, idle speed setting, calibration table manipulation, and ECM calibration file management. In addition, combustion quality was monitored with cylinder pressure measurement in at least one cylinder.

3.2.1. Steady-state Test Point Selection

To explore the trade-offs available with the available engine measures, several steady-state speed and load conditions were selected that were representative of both the early portion of the HD FTP and several vocational cycles that were tested in the previous Stage 1 program. The calibration development test points are listed in Table 6 and are plotted on a speed and load scatter plot in Figure 61 which includes data from the first 400 seconds of the HD FTP and several vocational cycles. It should be noted that the additional idle speeds of 800 and 1000 RPM (base idle speed was 600 RPM) were included due to the effectiveness of elevated idle speed for cold FTP observed in the original Stage 1 program.

TABLE 6. ENGINE SPEEDS AND LOADS FOR SELECTED STEADY-STATE TEST POINTS

Test Point	Engine Speed	Load	
		BMEP [bar]	Torque [Nm]
-	[RPM]		
1a	600	0	0
1b	800	0	0
1c	1000	0	0
2	800	2.5	297
3	800	5	595
4	800	10	1190
5	1000	2.5	297
6	1000	5	595
7	1000	10	1190
8	1500	2.5	297
9	1500	5	595
10	1500	10	1190
11	1500	20	2379
12	1700	2.5	297
13	1700	5	595
14	1700	10	1190

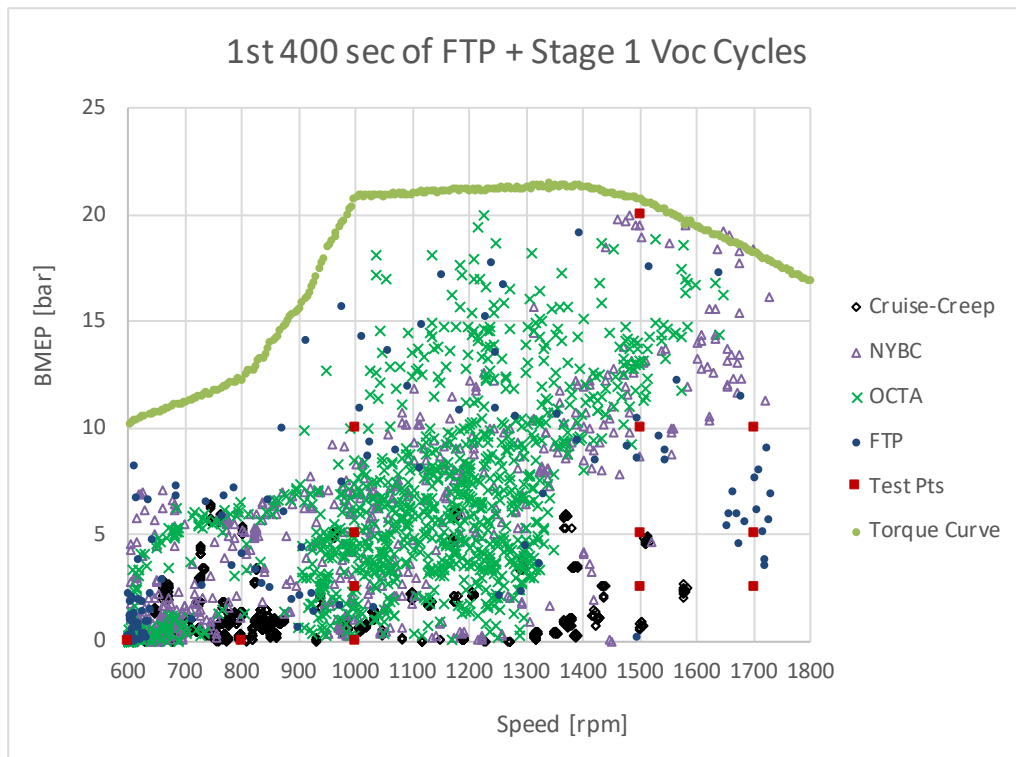


FIGURE 61. RELATION OF SELECTED CALIBRATION TEST POINTS TO FIRST 400 SECONDS OF FTP AND VARIOUS VOCATIONAL TEST CYCLES

3.2.2. *Steady-state Testing for Modified Engine Calibration Development*

Steady-state testing at the selected test points was conducted at cold coolant temperatures (+25-35°C) to simulate the early part a cold-start FTP and to ensure robust combustion during all of the planned test cycles. Maintaining cold coolant was achieved by a combination of a blocked open engine thermostat and an additional coolant heat exchanger plumbed to chilled water. The first step for the testing was to document the performance of the baseline cold calibration and then explore the calibration space using the engine measures listed previously. For brevity, only results obtained at idle and a few loaded test points are shown in the following sections.

3.2.2.1 - Test Point 1: Idle

Test results obtained at idle under cold coolant conditions (+25°C) are shown in Figure 62 for the baseline cold calibration, at the base 600 and elevated idle speeds of 800 and 1000 RPM, and the modified calibration at 1000 RPM. The y-axis parameters include exhaust mass flow rate, turbine outlet temperature, normalized engine-out (EO) NO_x mass flow rate relative to the baseline cold calibration, EO filter smoke number (measured via AVL 415S) and fuel flow rate relative to the baseline. These key parameters are plotted against exhaust energy (exhaust mass flow rate * exhaust specific heat * exhaust temperature) since exhaust energy is also a key parameter for catalyst warm-up.

Simply increasing the idle speed with the baseline calibration resulted in a significant increase in exhaust flow and hence energy; however, only a 20°C exhaust temperature increase was obtained which would hinder warm-up of a LO-SCR. In addition, EO NO_x increased by over a factor of 5 and fuel consumption was 2.3 times the baseline fuel flow at 1000 RPM. The modified calibration at 1000 RPM, which incorporated additional thermal management strategies, gave a 100°C exhaust temperature increase with a manageable NO_x and smoke increase. However, a significant fuel penalty of 3.4 times the baseline was measured.

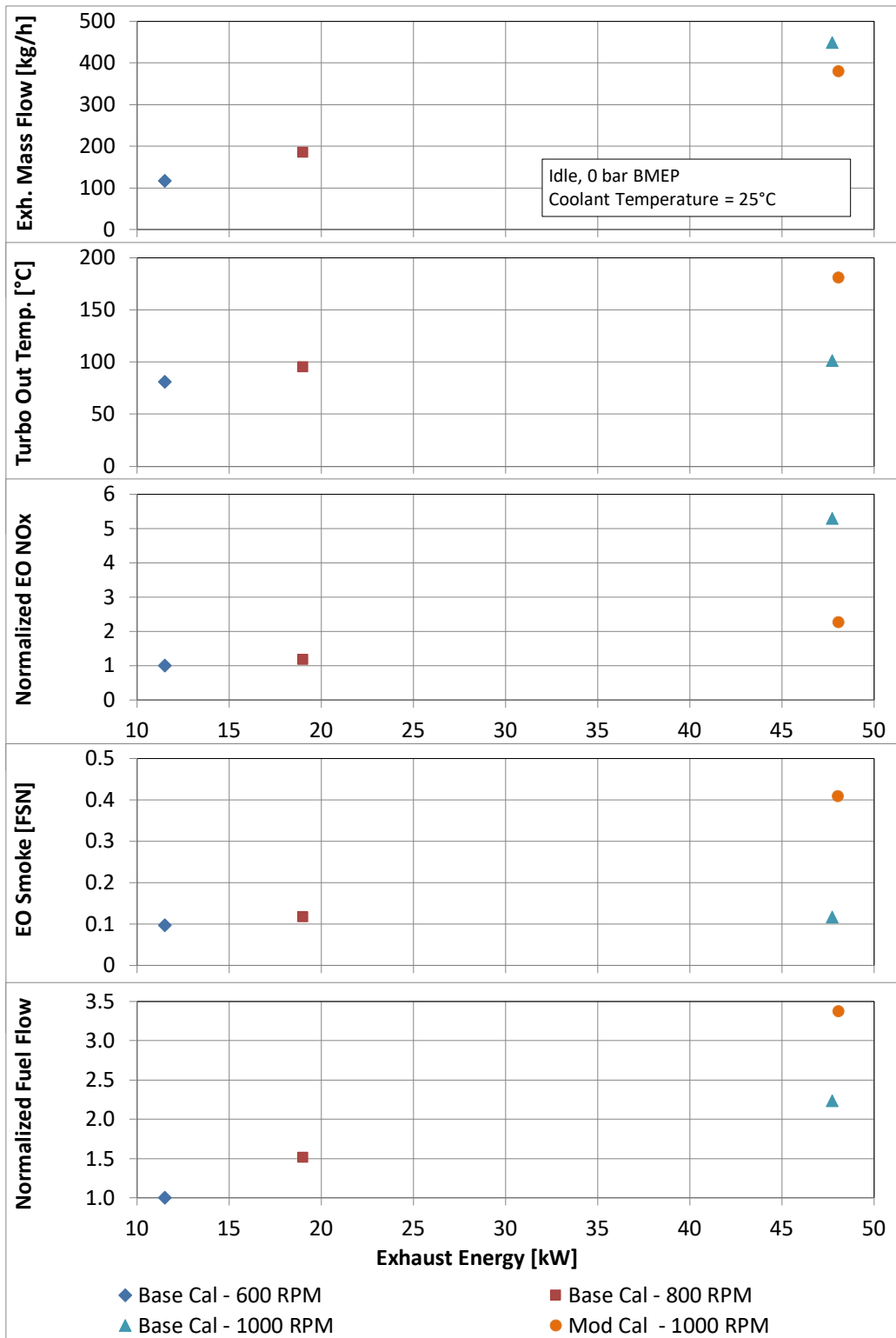


FIGURE 62. IDLE TEST POINT RESULTS FOR BASELINE AND MODIFIED CALIBRATION

3.2.2.2 - Test Points 5-7: 1000rpm, 2.5, 5, and 10 bar BMEP

Steady-state results obtained at 1000 RPM and three engine loads: 2.5, 5, and 10 bar BMEP, are shown in Figure 63, Figure 64, and Figure 65, respectively, to illustrate the typical trade-offs that were encountered while developing the modified calibration off idle. The results shown include the baseline cold calibration, exploratory tests, and the modified calibration tuning. As for the idle tests, these tests were conducted with low coolant temperature (between 25 and 30°C) and the x-axis in the plots is exhaust energy. The “R9” in the legend for the modified calibration represents the ninth revision of the modified calibration. The y-axis parameters include turbine outlet temperature, EO brake-specific (BS) NO_x relative to the baseline cold calibration, BSFC relative to the baseline, and EO soot mass flow rate (computed from AVL 415S soot concentration measurements) relative to baseline. The targets for both turbine outlet temperature and engine-out BSNO_x shown as horizontal dashed lines were based on projections from the Stage 1 project achievements.

The R9 version of the calibration included a combination of a number of elements including changes to EGR rate, fuel injection parameters, VGT position, and intake throttling. All of these modifications were generally undertaken to increase exhaust temperature and reduce engine-out NO_x under cold aftertreatment temperature conditions. Under some conditions, the R9 calibration also uses multiple injections to achieve a later combustion phasing to produce additional exhaust heat.

Both the turbine-out temperature and engine-out NO_x targets were achieved with the modified calibration at all of the conditions. However, small reductions in the exhaust energy were caused by reduced exhaust mass flow rates associated with increased EGR to reduce NO_x. The fuel consumption penalty varied with load and was as high as 15% at the 2.5 bar BMEP load and was between 5 and 10% at the higher loads. In addition to higher fuel consumption, achieving the target NO_x levels with higher EGR levels generally resulted in higher engine-out soot mass flow rates, especially at the 10 bar BMEP condition where an increase by a factor of 7 compared to the baseline was estimated. Although not shown, the maximum AVL Filter Smoke Number (FSN) was limited to 2.5 FSN during development of all modified calibration revisions. Similar exploratory testing was conducted at the other calibration development test points which were used to develop a modified cold calibration suitable for transient evaluations.

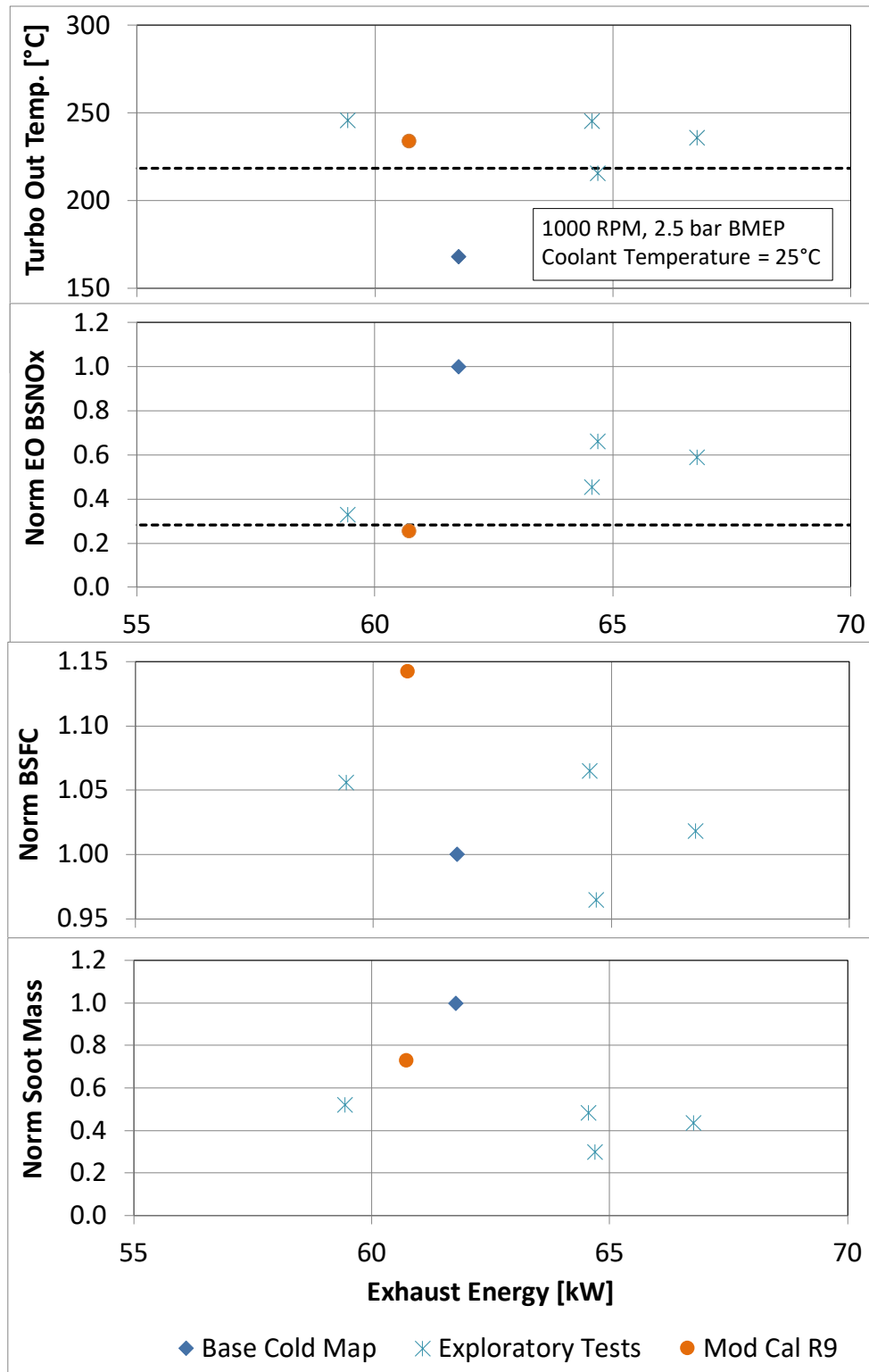


FIGURE 63. COLD COOLANT TEST RESULTS FOR BASELINE, EXPLORATORY, AND MODIFIED CALIBRATIONS AT 1000 RPM AND 2.5 BAR BMEP

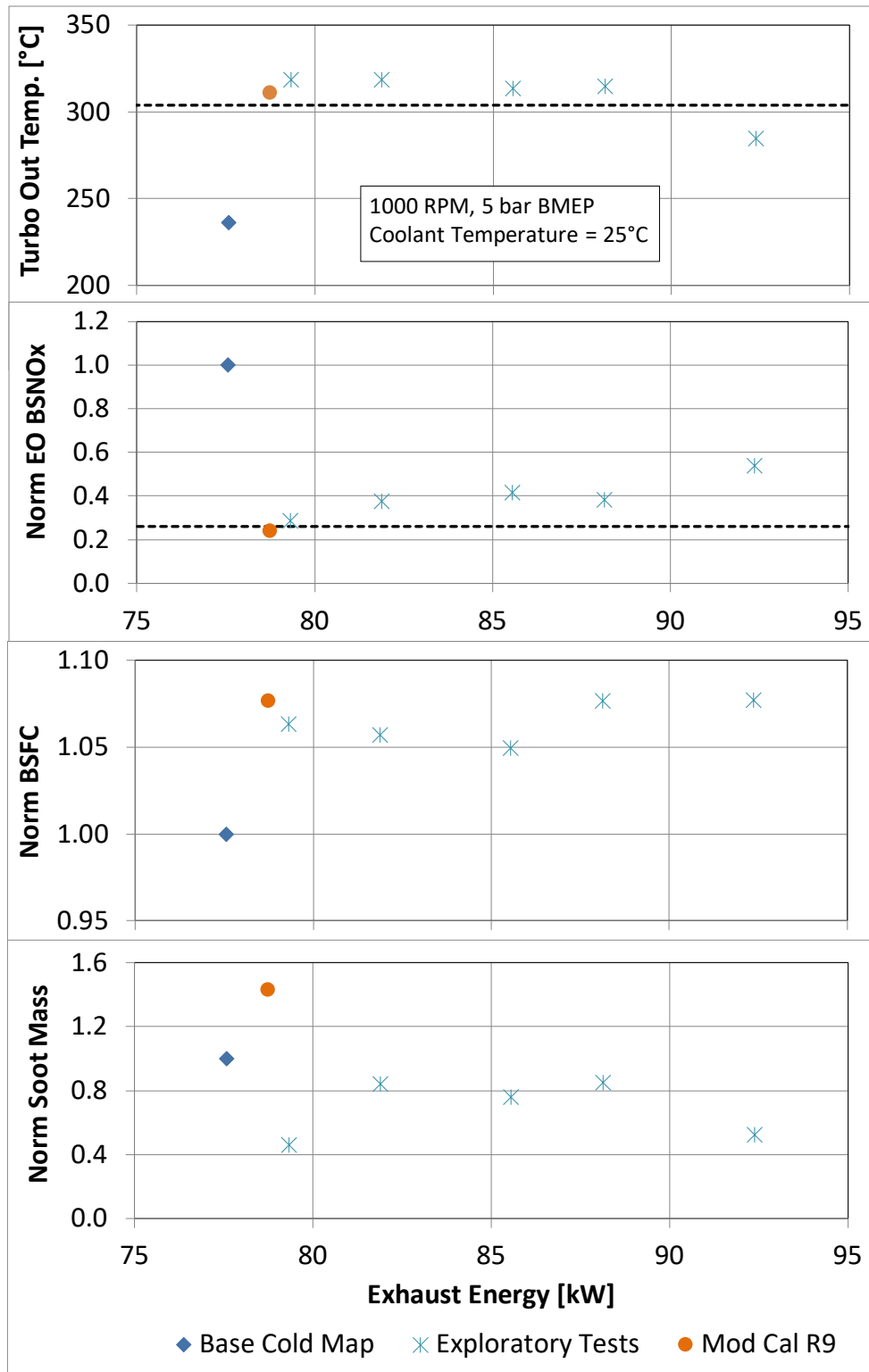


FIGURE 64. COLD COOLANT TEST RESULTS FOR BASELINE, EXPLORATORY, AND MODIFIED CALIBRATIONS AT 1000 RPM AND 5 BAR BMEP

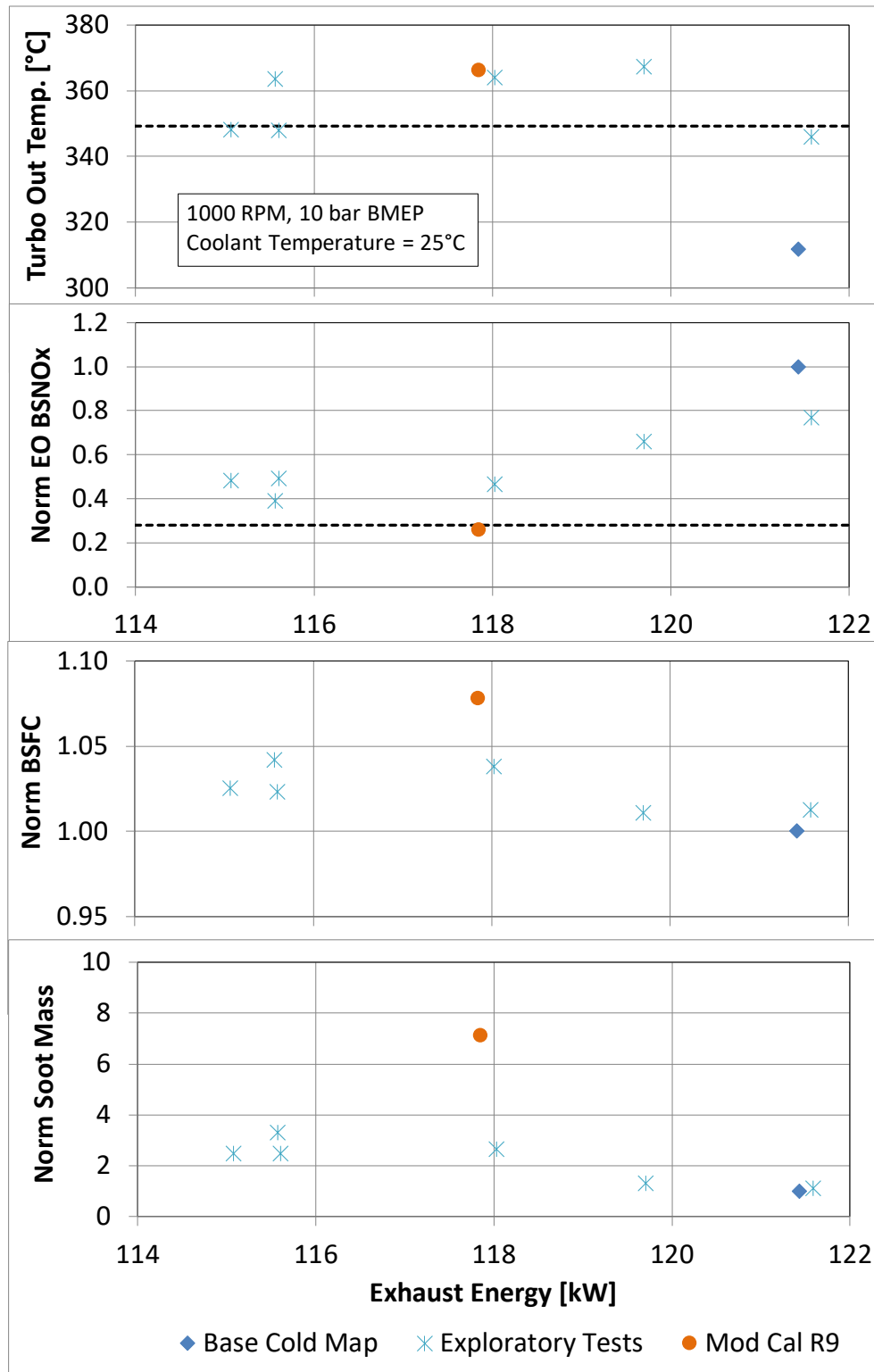


FIGURE 65. COLD COLLANT TEST RESULTS FOR BASELINE, EXPLORATORY, AND MODIFIED CALIBRATIONS AT 1000 RPM AND 10 BAR BMEP

3.2.3. *Transient Evaluations for Modified Engine Calibration*

Based on the steady-state results, a full transient calibration was developed and evaluated over the cold FTP. During the transient evaluations, several iterations or revisions of the modified calibration were performed mainly to reduce the engine-out NO_x spikes associated with the early torque events. Reducing engine-out NO_x early in a cold FTP is critical for achieving the low NO_x target since it is unlikely that even a LO-SCR would be at sufficient temperature to provide high NO_x conversion efficiency. Engine speed, torque and engine-out NO_x emissions are shown in Figure 66 for the baseline and two versions of the modified engine calibration over the first 400 seconds of the cold FTP. The engine speed traces illustrate the use of elevated idle with 1000 RPM used for the first two idle segments and 800 rpm for the third segment. The effectiveness of the increased EGR and later combustion phasing with the modified calibrations on reducing engine-out NO_x is clearly shown. A slightly more aggressive EGR during the torque tip-ins was used for the “ModCal2-R2978” calibration which led to a small degradation in torque response.

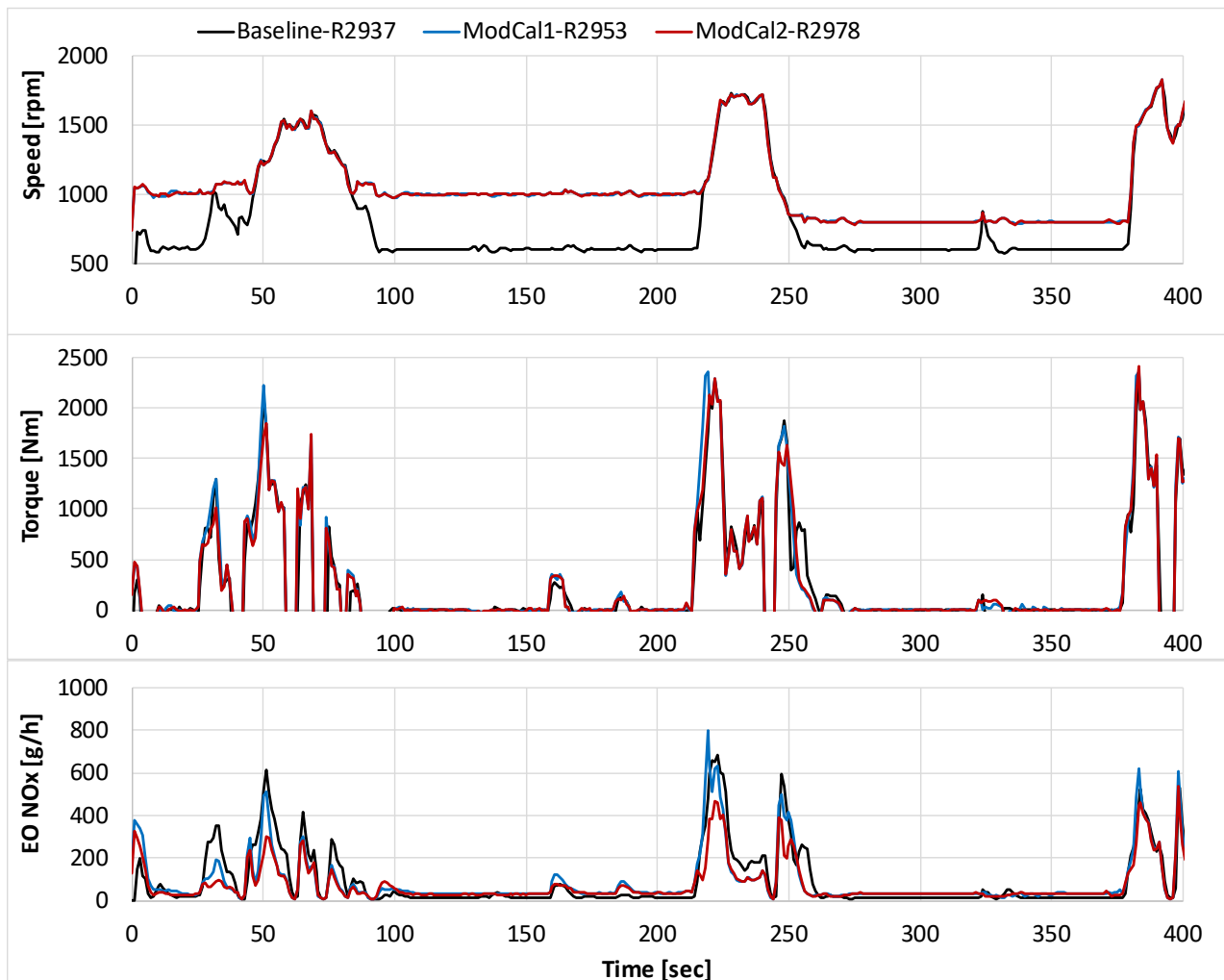


FIGURE 66. COLD FTP RESULTS WITH BASELINE AND TWO MODIFIED CALIBRATIONS – ENGINE SPEED, TORQUE, AND ENGINE-OUT NO_x

The other goal of the modified calibration was to increase exhaust gas temperature and enthalpy to heat the planned LO-SCR as quickly as possible in order to achieve catalytic NO_x control. The effectiveness of the modified calibrations for this purpose can be observed in Figure 67 where engine speed (for cycle reference), turbine-out and stock DOC out temperatures obtained over the first 400 seconds of the cold FTP are shown. The stock DOC was the first catalyst in the stock AT package, so it is representative of a LO-SCR.

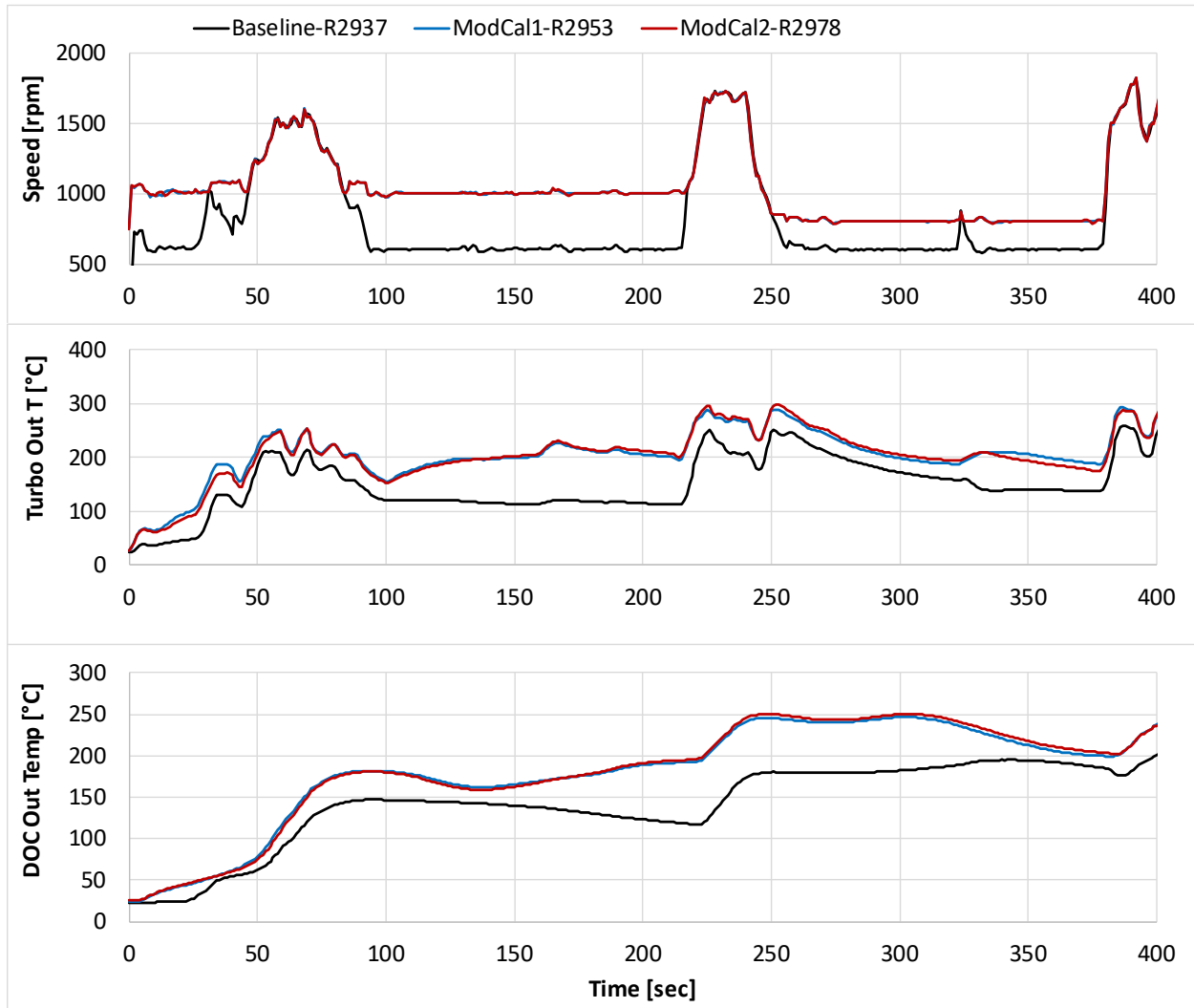


FIGURE 67. COLD FTP RESULTS WITH BASELINE AND TWO MODIFIED CALIBRATIONS: ENGINE SPEED, TURBINE OUT AND STOCK DOC OUT TEMPERATURES

As shown in the steady-state results, the engine measures used to achieve the reduced engine-out NO_x and increased exhaust gas temperatures were not fuel neutral. To summarize the transient results and provide insight into the fuel penalty associated with the modified calibration, several key parameters obtained from the three cold FTP cases are presented in Table 7. Note that the baseline AT and control were used for these tests. For the ULN solution, it is expected that the

modified calibration would be used until sufficient LO-SCR temperature is reached for effective NO_x control after which the more fuel efficient baseline calibration would be used.

TABLE 7. FTP RESULTS WITH BASELINE AND MODIFIED CALIBRATIONS

FTP	Cold			Hot
Engine Calibration	Base	Mod1	Mod2	Base
SwRI Run Number	2937	2953	2978	2737
Time 180°C Turbo Out T (TOT), sec	50	34	48	N/A
Cum EO NO _x at 180°C TOT, g	1.7	1.0	1.1	N/A
Time to 150°C DOC Out T, sec	233	68	70	N/A
Cum EO NO _x at 150°C DOC Out T, g	6.3	2.5	2.0	N/A
Cycle EO NO _x , g/hp-hr	2.0	3.0	3.2	2.6
Cycle TP NO _x , g/hp-hr	0.27	0.27	0.32	0.14
Cycle NO _x Conv Eff, %	87	91	90	95
Cycle CO ₂ , g/hp-hr	531	549	552	505
Delta CO ₂ (from base), %	N/A	3.4	4.0	N/A
FTP	Composite			
Engine Calibration	Base	Mod1	Mod2	
TP NO _x , g/hp-hr	0.16	0.16	0.17	
CO ₂ , g/hp-hr	509	511	512	
Delta CO ₂ (from base), %	N/A	0.4	0.5	

The effectiveness of the modified calibrations in catalyst warm-up are highlighted in the times to reach 150 °C DOC outlet temperature. This is a key temperature since it represents when a significant portion of the LO-SCR would begin providing some level of NO_x conversion. The cycle EO NO_x results for the modified calibrations are higher because the engine calibration was changed to a more fuel efficient calibration with higher EO NO_x at around 600 seconds in order to “buy back” some of the fuel penalty associated with the modified calibration. It is expected that the Low NO_x AT would be capable of handling the higher EO NO_x. Despite the use of this strategy, the modified calibrations had fuel penalties on the order 3-4% for the cold FTP. However, due to the 1/7 cold FTP weighting factor, the composite penalty was 0.4-0.5%. Since the goal of the Stage 3 program was to demonstrate ULN with minimal fuel penalty, an add-on task with additional funding sources was organized with the purpose of exploring the potential of additional engine hardware technologies to provide a more favorable exhaust temperature versus fuel penalty trade-off. This add-on task is referred to as Stage 3b and is discussed in the next section.

3.3 Engine Hardware Evaluations (Stage 3B)

An additional task, Stage 3B, was added to the overall project plan with the purpose of evaluating the potential of several engine HW technologies to improve the exhaust gas characteristics, emissions, and fuel consumption trade-offs. The modified calibration discussed in the previous section was used for the evaluations and the HW technologies tested are shown in Figure 68. Details of the test cell implementations of the HW options are provided in [Appendix A](#). The evaluations consisted of both steady-state and transient testing. However, transient evaluations were only conducted with HW options that demonstrated strong potential during the steady-state evaluations or if transient testing required minimal engine recalibration.

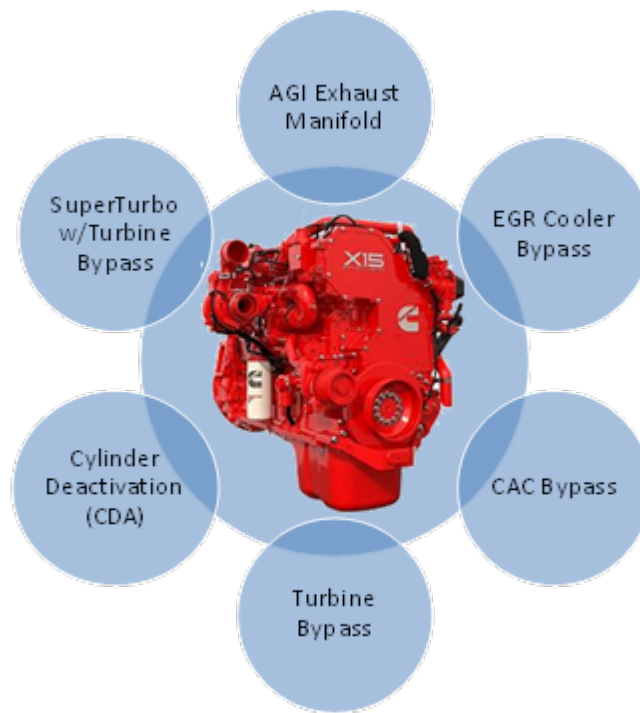


FIGURE 68. ENGINE HARDWARE TECHNOLOGIES EVALUATED IN THE STAGE 3B TASK

3.3.1. *Steady-State Hardware Testing*

The steady-state testing was conducted with cold coolant temperature (+25-35°C) conditions to simulate the early portion of a cold-start FTP using a blocked-open thermostat and an additional coolant heat exchanger.

3.3.1.1. 1000-rpm Elevated Idle

As discussed in the modified calibration section, the use of 1000 RPM elevated idle was an effective strategy for AT warm-up and temperature maintenance early in the cold FTP cycle. Therefore, this idle condition was used to evaluate several of the HW options with coolant temperature maintained around 25°C. The target torque for all idle tests was 0 Nm. Before the test results are shown, a description of the legend labels is provided below.

1. Mod Cal R9 = modified cold calibration as described in previous section (R9 indicates ninth revision).
2. AGI Exh Man = air-gap-insulated exhaust manifold obtained with modified cold calibration.
3. 100% EGR Cooler BP = EGR cooler was completely bypassed.
4. 100% EGR Cooler BP+CAC BP = same settings as above, but with charge-air-cooler (CAC) also bypassed.
5. 50% EGR Cooler BP = two exhaust gas extraction points from exhaust manifold, one through EGR cooler and one that bypasses the cooler. Both combine before the stock EGR valve.
6. Turbo Bypass = wastegate valve in turbine bypass is opened.
7. CDA3B = cylinder deactivation mode where the rear three cylinders are deactivated (fueling and valves).
8. SuperTurbo wTurboBP = SuperTurbo with turbine bypass fully open (no flow through turbine) and SuperTurbo clutch not engaged.

The key cold-start parameters, turbine outlet temperature, engine-out NO_x mass flow and fuel flow rates, are plotted against exhaust energy in Figure 69. The NO_x and fuel flow results were normalized with respect to the baseline cold calibration results obtained at 600 RPM. In addition to the test results, rough targets for turbine outlet temperature and engine-out NO_x are included in the plots as black dashed lines. Engine-out soot results are not included as the smoke was generally low for all cases.

Both CDA and 100% EGR cooler bypass (including CAC bypass) resulted in increased turbine outlet temperatures over the modified calibration alone. Depending on the air-handling actuator settings, a temperature increase could also be obtained with 50% EGR cooler bypass at the expense of fuel consumption. The SuperTurbo and conventional turbine bypass cases had lower exhaust temperature due to lower exhaust backpressure which improved fuel consumption. Engine-out NO_x was generally well controlled except for the 100% EGR cooler bypass cases where NO_x increased due to hot EGR gas with low density and increased intake manifold temperature. For this engine condition, the CAC bypass provided only a small temperature increase with a NO_x increase. Fuel consumption generally increased with increasing exhaust energy. Only CDA provided a measurable temperature increase without a large fuel penalty albeit at lower exhaust energy.

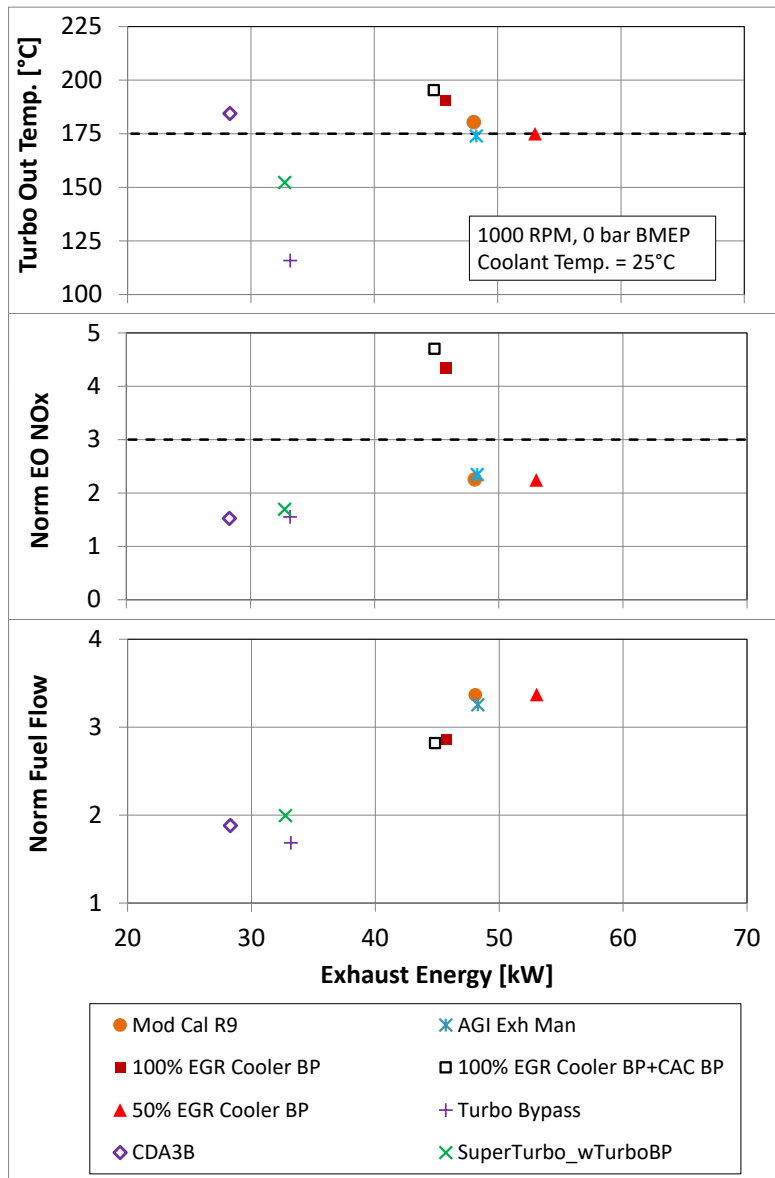


FIGURE 69. STEADY-STATE HW EVALUATION RESULTS AT ELEVATED IDLE SPEED OF 1000 RPM AND 25°C COOLANT TEMPERATURE

3.3.1.2. 1000-rpm 2.5 bar BMEP

Additional steady-state testing with cold coolant was performed at several other engine speed and load conditions. For brevity, only test results obtained at the same engine conditions as was shown in the modified calibration section are presented, namely 1000 RPM and 2.5, 5 and 10 bar BMEP. Results obtained at 2.5 bar BMEP are shown in Figure 70.

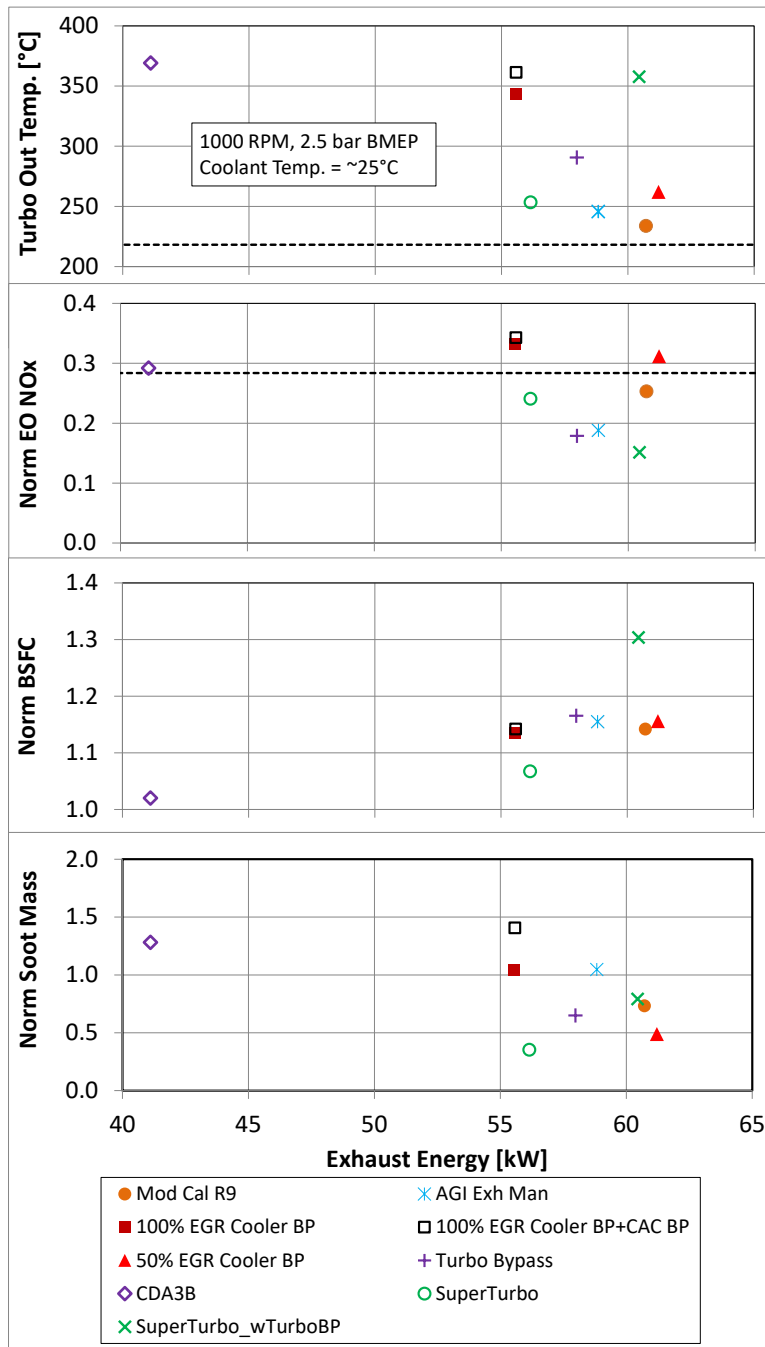


FIGURE 70. STEADY-STATE HW EVALUATION RESULTS AT 1000 RPM, 2.5 BAR BMEP WITH 25°C COOLANT TEMPERATURE.

At 2.5 bar BMEP, all HW options achieved an increase in exhaust temperature compared to the modified calibration only. As was the case for the idle condition, the AGI manifold provided a relatively small temperature increase of 12 °C, which was likely partly due to increased exhaust backpressure associated with the smaller flow area as both the NO_x and exhaust energy decreased slightly and the BSFC and soot mass increased. The 100% EGR cooler bypass provided a significant temperature increase of 100°C without any additional fuel penalty and with only a small

NO_x and soot mass increase and a reduction in exhaust energy. When the CAC was also bypassed, another 18 °C increase in temperature was obtained with some soot increase. For the 50% EGR cooler bypass case, a near 30 °C temperature increase was achieved with little change to the other parameters except for a beneficial soot mass reduction. The conventional turbine bypass resulted in a near 60 °C temperature increase with a NO_x and exhaust energy decrease, a small BSFC increase, and a slight soot mass reduction. CDA resulted in the second highest temperature increase behind the 100% EGR cooler bypass cases with only a small NO_x and soot mass increase, but had a significant exhaust energy reduction due to the lower exhaust mass flow rate. However, CDA also had the lowest fuel penalty of all the HW options. Two SuperTurbo results are shown: one with exhaust flowing through the turbine and one with the turbine bypassed. With the bypass closed, a of 20 °C temperature increase was obtained due to lower airflow, which resulted in reduced exhaust energy and fuel consumption. Both NO_x and soot mass were well controlled. When the bypass was opened, the heat loss associated with the turbine was removed and the SuperTurbo went into “Supercharger” mode requiring power from the crank to maintain airflow leading to increased fuel consumption. The combination of these two actions resulted in a 70 °C temperature increase without a reduction in exhaust energy, but a significant 30% fuel penalty was measured.

3.3.1.3. 1000-rpm 5 Bar BMEP

Results obtained at 5 bar BMEP are shown in Figure 71. Some of the HW options were load limited so CDA and 100% EGR cooler bypass could not be tested at this load. In addition, the SuperTurbo was not evaluated above 2.5 bar BMEP due to project time constraints. As before, the AGI exhaust manifold provided a small temperature increase over the stock manifold. In addition, small reductions in NO_x, fuel consumption, soot mass, and exhaust energy were observed. The 50% EGR cooler bypass provided a near 50 °C exhaust temperature increase with only a small NO_x increase, no additional fuel penalty and small reductions in both soot mass and exhaust energy. A 60 °C temperature increase was obtained with the turbine bypass without a NO_x increase, but at a significant BSFC penalty and a small soot increase. A reduction in exhaust energy was not observed for the turbine bypass.

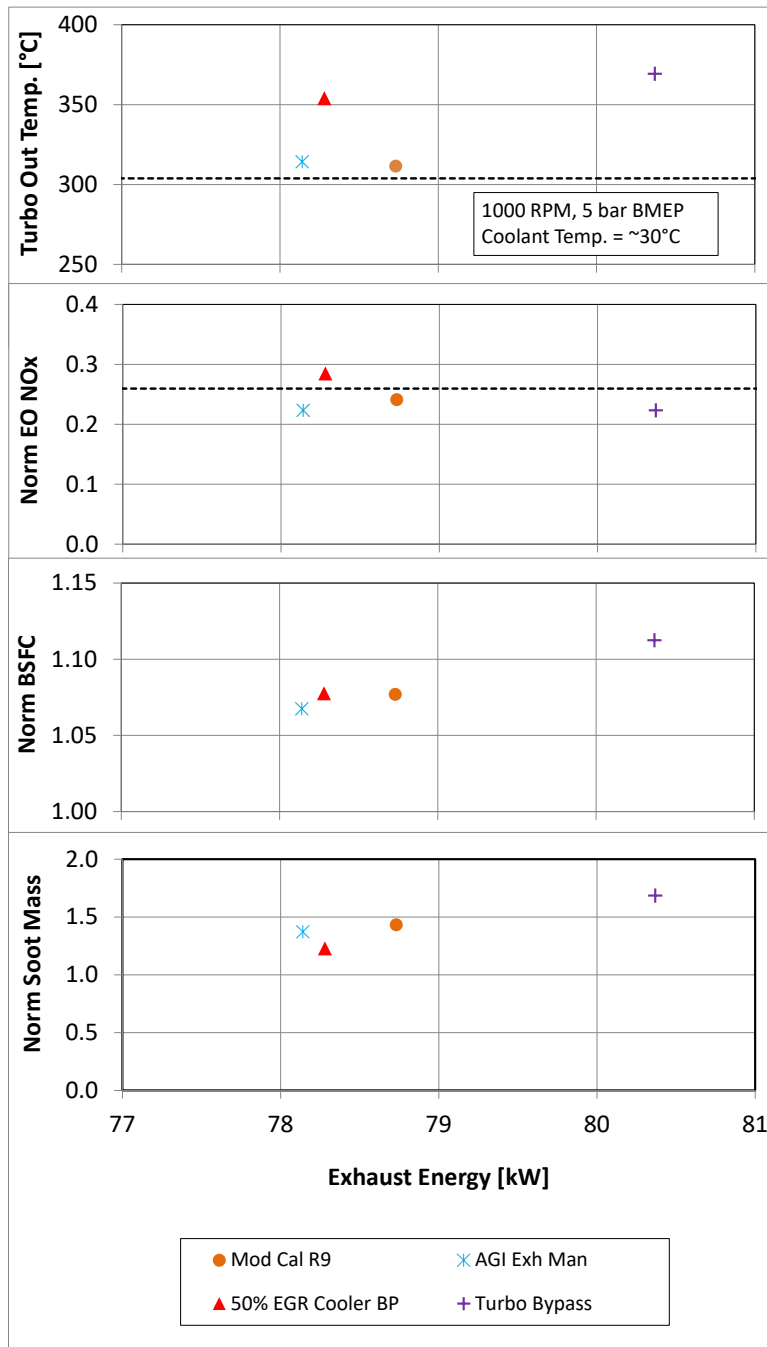


FIGURE 71. STEADY-STATE HW EVALUATION RESULTS AT 1000 RPM, 5 BAR BMEP WITH 30°C COOLANT TEMPERATURE.

3.3.1.4. 1000-rpm 10 Bar BMEP

Results obtained at 10 bar BMEP are shown in Figure 72. This load could not be achieved with the turbine bypass due to temperature and smoke constraints. Starting with the AGI manifold, a 4 °C temperature increase was observed; however, again this was likely due to reduced charge mass as a small reduction in exhaust energy suggests. Small reductions in NO_x, BSFC, and soot

mass were also observed. A 30 °C exhaust temperature increase was measured for the 50% EGR cooler bypass case along with a slight NO_x increase, small BSFC and soot mass reduction, and a slight exhaust energy increase.

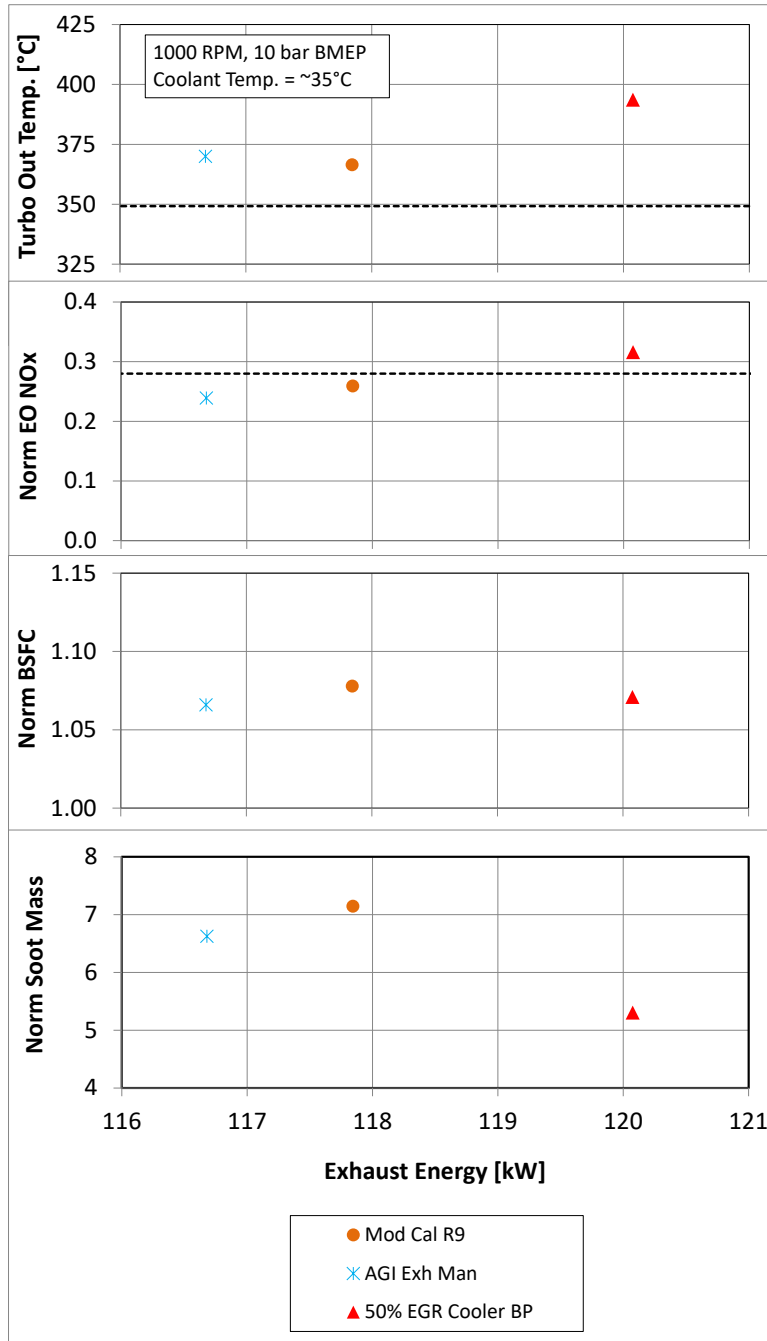


FIGURE 72. STEADY-STATE HW EVALUATION RESULTS AT 1000 RPM, 10 BAR BMEP WITH 35°C COOLANT TEMPERATURE.

3.3.2. *Transient Hardware Testing*

Although the steady-state results obtained with 100% EGR cooler bypass were promising, NO_x control was compromised, and certain EGR system components had to be removed to allow testing due to exceeding their temperature limits. Transient EGR control by the stock ECM was not possible without these components. For these reasons, 100% EGR cooler bypass was not selected for transient evaluation, but the steady-state results show its potential. Similarly, it was decided that the turbine bypass results did not warrant the additional effort required for transient evaluation due to a mixed temperature benefit and an excessive fuel penalty at 5 bar BMEP. Therefore, transient evaluations were conducted with the AGI exhaust manifold, 50% EGR cooler bypass, CDA and SuperTurbo. Cold FTP results are shown in the next sections for each HW option.

3.3.2.1. *Transient Evaluation of AGI Exhaust Manifold*

Cold FTP results obtained with the stock and AGI exhaust manifolds, both with the modified cold calibration, are shown in Figure 73. Only the first 400 seconds are shown since this is the focus area for AT thermal management. Engine speed, torque, engine-out NO_x, turbine outlet and DOC outlet temperature traces are shown for the comparisons.

Compared to the stock exhaust manifold, the AGI manifold had:

- no measurable torque response impact,
- no impact on engine-out NO_x, and
- small increases in both turbine and DOC outlet temperatures, especially at the beginning of both long idle segments.

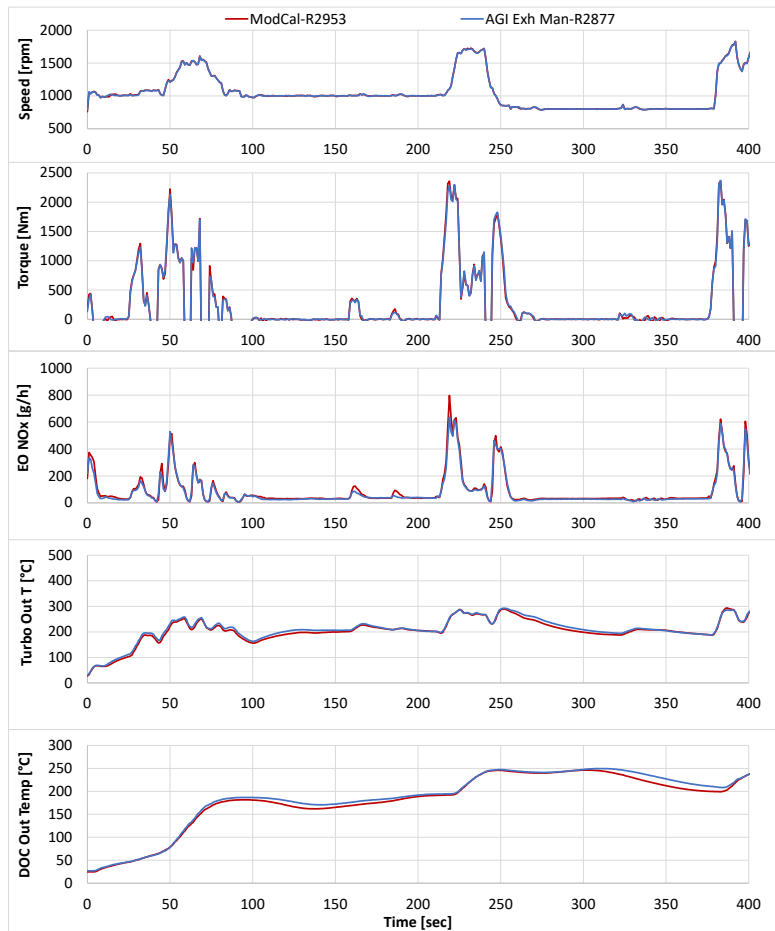


FIGURE 73. TRANSIENT EVALUATION RESULTS WITH STOCK AND AGI EXHAUST MANIFOLDS.

3.3.2.2. *Transient Evaluation of 50% EGR Cooler Bypass*

Cold FTP results obtained with the 50% EGR cooler bypass and corresponding calibration are compared to the modified calibration only in Figure 74. The stock exhaust manifold was used for both calibrations and a slightly different modified cold calibration with further reductions in engine-out NO_x was used for the comparison.

Compared to the modified cold calibration only, the 50% EGR cooler bypass calibration had:

- a small torque response degradation,
- no impact on engine-out NO_x, and
- small increases in both turbine and DOC outlet temperatures during the first long idle and second acceleration segments.

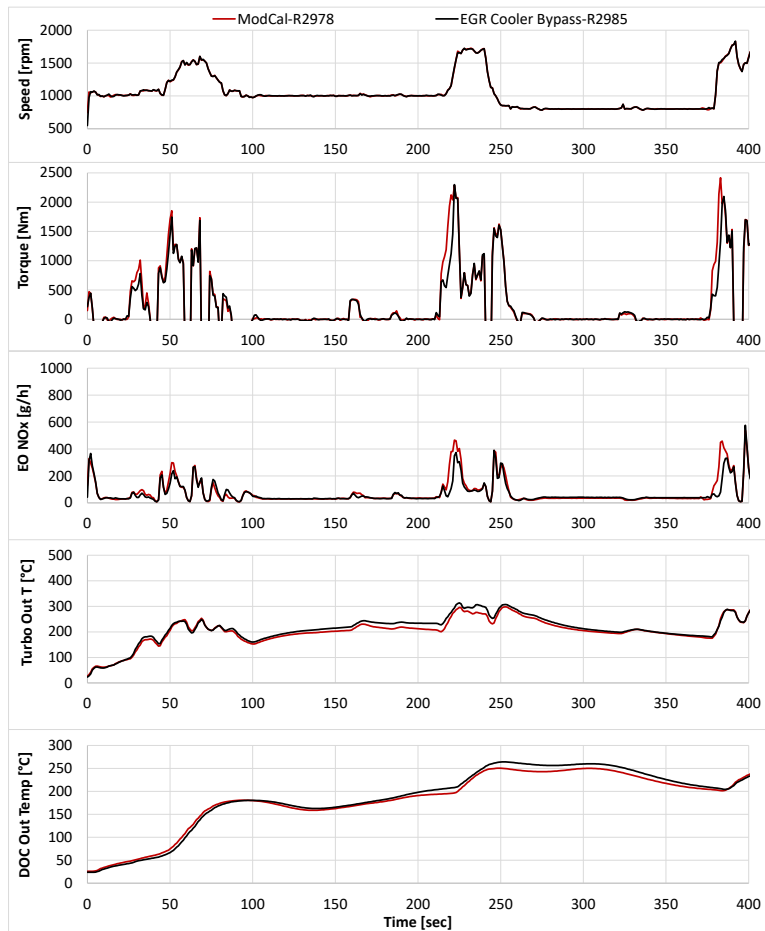


FIGURE 74. TRANSIENT EVALUATION RESULTS WITH MODIFIED AND 50% EGR COOLER BYPASS CALIBRATIONS, BOTH WITH STOCK EXHAUST MANIFOLDS.

3.3.2.3. Transient Evaluation of CDA

Although only CDA results obtained with three cylinder operation (CDA3B) were shown in the steady-state results section, this CDA mode could not be used throughout the engine speed range due to potential interactions between engine firing and driveline resonances. Therefore, a CDA mode map, or recipe, was developed based on NVH measurements conducted on the test engine. The resulting recipe uses CDA modes that avoid the engine resonances. More details on the NVH testing and resulting CDA recipe can be found in [7]. Using this CDA recipe and calibration at loads below about 3 bar BMEP, a cold FTP was conducted, and the results are compared to the modified calibration only in Figure 75.

Compared to the modified cold calibration only, the CDA calibration had:

- minimal to no torque response degradation,
- no impact on engine-out NO_x during CDA operation (torque below 357 Nm), and
- a mixed impact on temperatures but no impact on the time to reach 150 °C DOC outlet temperature.

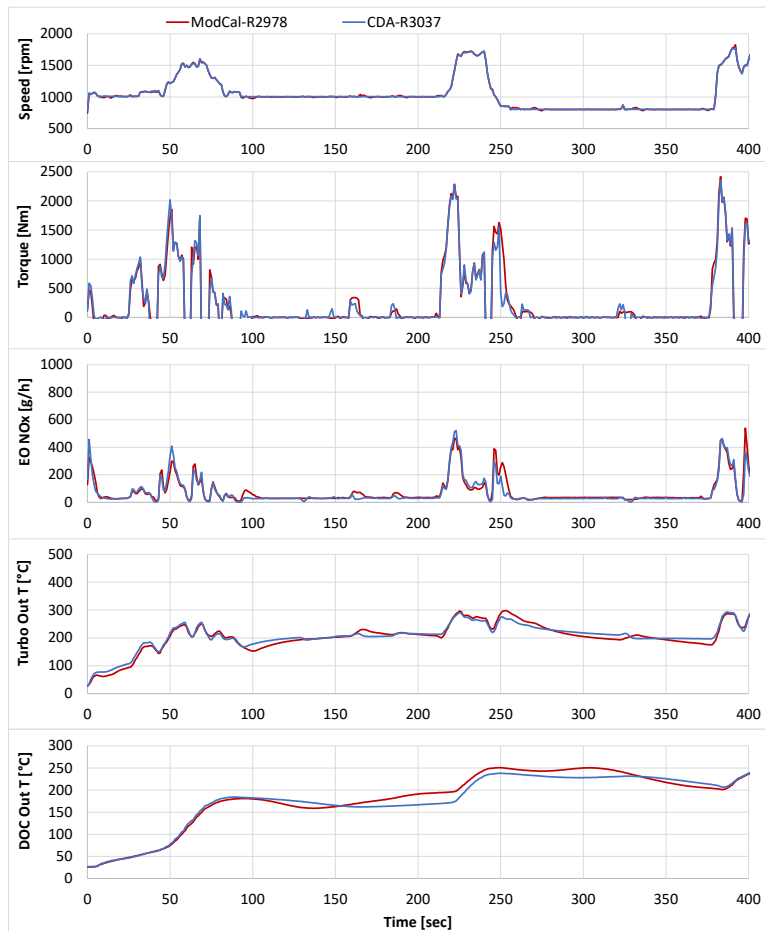


FIGURE 75. TRANSIENT EVALUATION RESULTS WITH CDA AND MODIFIED COLD CALIBRATIONS.

3.3.2.4. *Transient Evaluation of SuperTurbo*

The SuperTurbo had its own controller and for the initial transient proof-of-concept it was controlled using a combination of time-based commands for the clutch and turbine bypass, and a model-based charge flow controller that handled the CVT and other elements. This was integrated with the SwRI engine controller using the modified engine calibration discussed earlier. It should be noted that in a final implementation, these controls would all be automated and integrated with the overall strategy. With these available levers, a proof-of-concept cold-start FTP strategy was developed to demonstrate the potential benefits of the SuperTurbo, and the resulting behavior during a cold-start is summarized as follows:

- At engine start, the SuperTurbo is clutched-in and the turbine bypass is open.
- Within the first hill and before the second acceleration (FTP time = 40 seconds), the turbine bypass is closed to help meet the airflow and torque demand.
- After this second acceleration, the turbine bypass is opened.
- At the start of the first long idle segment, the SuperTurbo is clutched-out.

- Prior to the start of the second hill, the bypass is closed and the clutch is engaged.
- At the start of the second long idle segment, the SuperTurbo is clutched-out and the turbine bypass is opened.
- Prior to the start of the third hill, the bypass is closed and the clutch is engaged for the remainder of the cycle, with the exception of clutched-out operation during extended idle periods late in the cycle.

Following this strategy, cold FTP results for the SuperTurbo and modified calibration only are shown in Figure 76. It should be noted that the modified calibration used for comparison was the same as was used for the AGI exhaust manifold (higher engine-out NO_x) since this was the engine calibration used for the SuperTurbo evaluation.

Compared to the modified cold calibration only, the SuperTurbo results had:

- some torque degradation when the turbine bypass was open (no help from turbo),
- some loss of NO_x control during the second acceleration of the first hill due to less exhaust backpressure to drive EGR compared to the stock VGT, and
- significant increases in both turbine and DOC outlet temperatures.

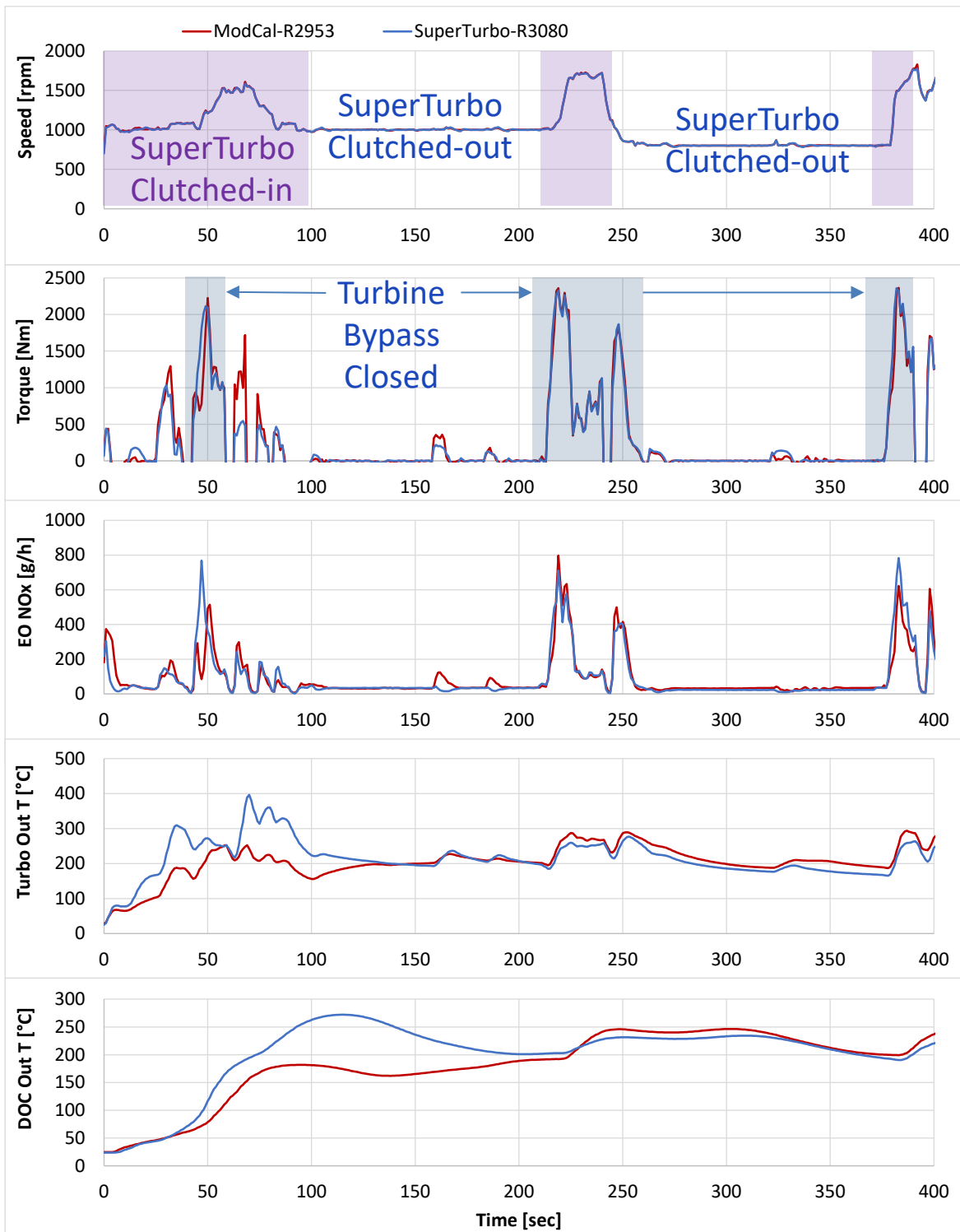


FIGURE 76. TRANSIENT EVALUATION RESULTS WITH SUPERTURBO AND MODIFIED COLD CALIBRATIONS.

3.3.3. Cold FTP Hardware Performance Summary

To conclude the HW evaluation discussion, the key parameters obtained during the cold FTP tests are listed in Table 8. Finally, a simple ranking was applied based on some of the summary results. The rankings and penalty thresholds are listed in Table 9. As shown, CDA ranked the highest mainly due to its fuel consumption reduction. The SuperTurbo was a close second with a high fuel penalty paid for the turbine bypass operations. Therefore, CDA was selected to be used for the remainder of the Stage 3 program.

TABLE 8. SUMMARY OF KEY PARAMETERS FROM COLD FTP HW EVALUATIONS

	Mod Cal	AGI Exh	EGR Cooler	CDA	Super Turbo
SwRI Run Number	2978	2877	2985	3037	3080
Time to 180°C Turbo Out T (TOT), sec ¹	48	33	35	34	28
Cum EO NO _x at 180°C TOT, g	1.1	0.8	0.7	0.8	0.5
Time to 150°C DOC Out T, sec ²	70	67	72	68	56
Cum EO NO _x at 150°C DOC Out T, g	2.0	2.3	1.8	2.0	2.0
Cycle CO ₂ , g/hp-hr	552	547	553	538	550
CO ₂ Increase from Baseline, %	4.0	3.0	4.1	1.3	3.6
Composite CO ₂ Increase from Baseline, %	0.6	0.5	0.6	0.2	0.5
Cycle Work Difference, %	-1.9	-1.5	-3.5	-2.7	-1.8
¹ This temperature represents when DEF dosing could begin upstream of a close-coupled SCR					
² It is expected that the entire LO-SCR has reached minimum operating temperature for NO _x control at this temperature					

TABLE 9. SUMMARY OF KEY PARAMETERS FROM COLD FTP HW EVALUATIONS

	Mod Cal	AGI Exh	EGR Cooler	CDA	Super Turbo
SwRI Run Number	2978	2877	2985	3037	3080
Penalty if Time to 180°C > 30 sec	2	1	1	1	0
	(0:T≤30, 1:30<T≤40, 2:40<T≤50)				
Penalty if Cum EO NO _x at 180°C TOT > 1g	1	0	0	0	0
	(0:NO _x ≤1, 1:1<NO _x ≤2)				
Penalty if Time to 150°C DOC Out T > 65 sec	1	1	2	1	0
	(0:T≤65, 1:65<T≤70, 2:70<T≤75)				
Penalty if Cum EO NO _x at 150°C DOC Out T > 2 g (2g = 0.06 g/hp-hr which is cold FTP limit)	0	1	0	0	0
	(0:NO _x ≤2, 1:2<NO _x ≤2.5)				
Penalty if CO ₂ Increase from Baseline > 2%	4	2	4	0	4
	(0:CO ₂ ≤2, 1:2<CO ₂ ≤2.5, 2:2.5<CO ₂ ≤3, 3:3<CO ₂ ≤3.5, 4:CO ₂ >3.5)				
Penalty for Torque Response (Work Diff >2%)	0	0	2	1	0
	(0:Diff≤2, 1:2<Diff≤3, 2:3<Diff≤4)				
Total Penalty Sum	8	5	9	3	4
CFTP Ranking	4	3	5	1	2

3.4 Aftertreatment Evaluations

The AT options that were offered by the various MECA supplier teams for this program were described earlier in detail under Section 2.4 of the Methods portion of the report. This section discusses the results of the initial evaluations of those technologies, leading to the down-selection of the final Stage 3 AT configuration. It should be noted that all of these evaluations used the engine with CDA installed and operating according the strategy outlined under Section 2.6 of the Methods portion of the report. Some additional modifications were made to the strategy along the way for each configuration, such as changing the temperature switch points of various thermal management triggers.

All of the initial AT evaluations were carried out on the Development Aged parts. The primary intent behind these initial tests was to evaluate the various technology options provided by the teams, and to provide sufficient data to allow a meaningful comparison between them so that a final configuration could be chosen. From the outset, it was planned that the final configuration could either be one of the technology packages supplied, or some combination of the options supplied by both teams, as turned out to be the case. The development targets for this stage of the system evaluations was to achieve emission below 0.06 g/hp-hr on the cold-start FTP, and below 0.01 g/hp-hr on the hot-start FTP and RMC-SET.

3.4.1. Team 2A Results

The first configuration evaluated on the engine was the Team 2A configuration. Although shown earlier in the report, the schematic is shown again below in Figure 77 for ease of reference. This was the configuration initially recommended by the Team 2 supplier, and the advantages and drawbacks of this configuration were discussed earlier in detail. The primary performance question for this system was whether the LO-SCR could be warmed up quickly enough to reach cold-start targets, given that it was downstream of the considerable thermal inertia of DOC and the compact mixer assembly.

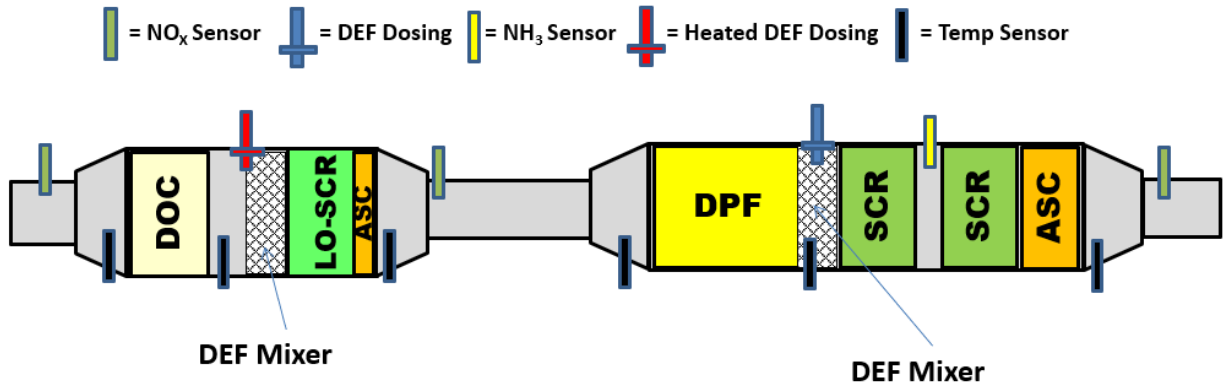


FIGURE 77. TEAM 2A SCHEMATIC

Following initial calibration tuning, initial cold-hot FTP cycles were run, and an example of the results is given below in Figure 78. It should be noted that the x-axis of the continuous result plots shown below correspond to elapsed cycle time in seconds, unless otherwise noted. The LO-SCR inlet cross 150°C after 60 seconds, and 200°C after 80 seconds, while the LO-SCR outlet did not cross 200°C until 245 seconds. This means that the LO-SCR did not light off until after the first acceleration, and it was not quite hot enough in the initial part of the second acceleration to achieve high conversion under high space velocity conditions. This was only good enough for 0.12 g/hp-hr, twice the target level, with a CO₂ at 538 g/hp-hr, 1.3% above the baseline cold-start value.

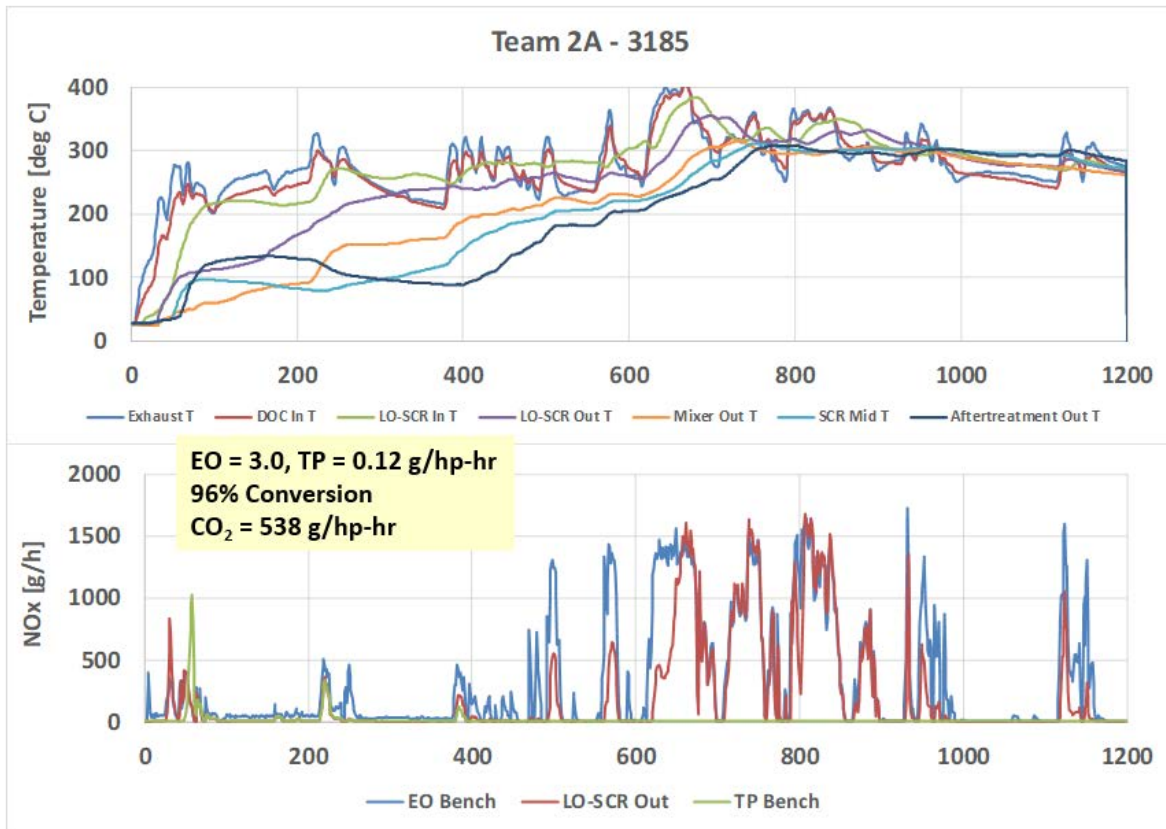


FIGURE 78. COLD-START FTP RESULT FOR TEAM 2A

In attempt to mitigate this, a revised calibration was utilized to lower engine-out NO_x further in the early portions of the cold cycle, before the LO-SCR had reached light-off. A comparison of results between the two calibration for Team 2A is shown in Figure 79. This change did reduce the cold-start FTP NO_x to 0.09 g/hp-hr. However, CO₂ also increased to 542 with this change, and it was noted that further reductions under this cold operation condition were not possible due to concerns over combustion stability and condensation. It was apparent that this configuration would only be successful with a much larger initial thermal input, and this was difficult to achieve while maintaining engine-out NO_x levels this low. This would likely also be at a CO₂ penalty that would be too large to sustain, or else would have involved even higher elevated idle speeds which were not considered feasible.

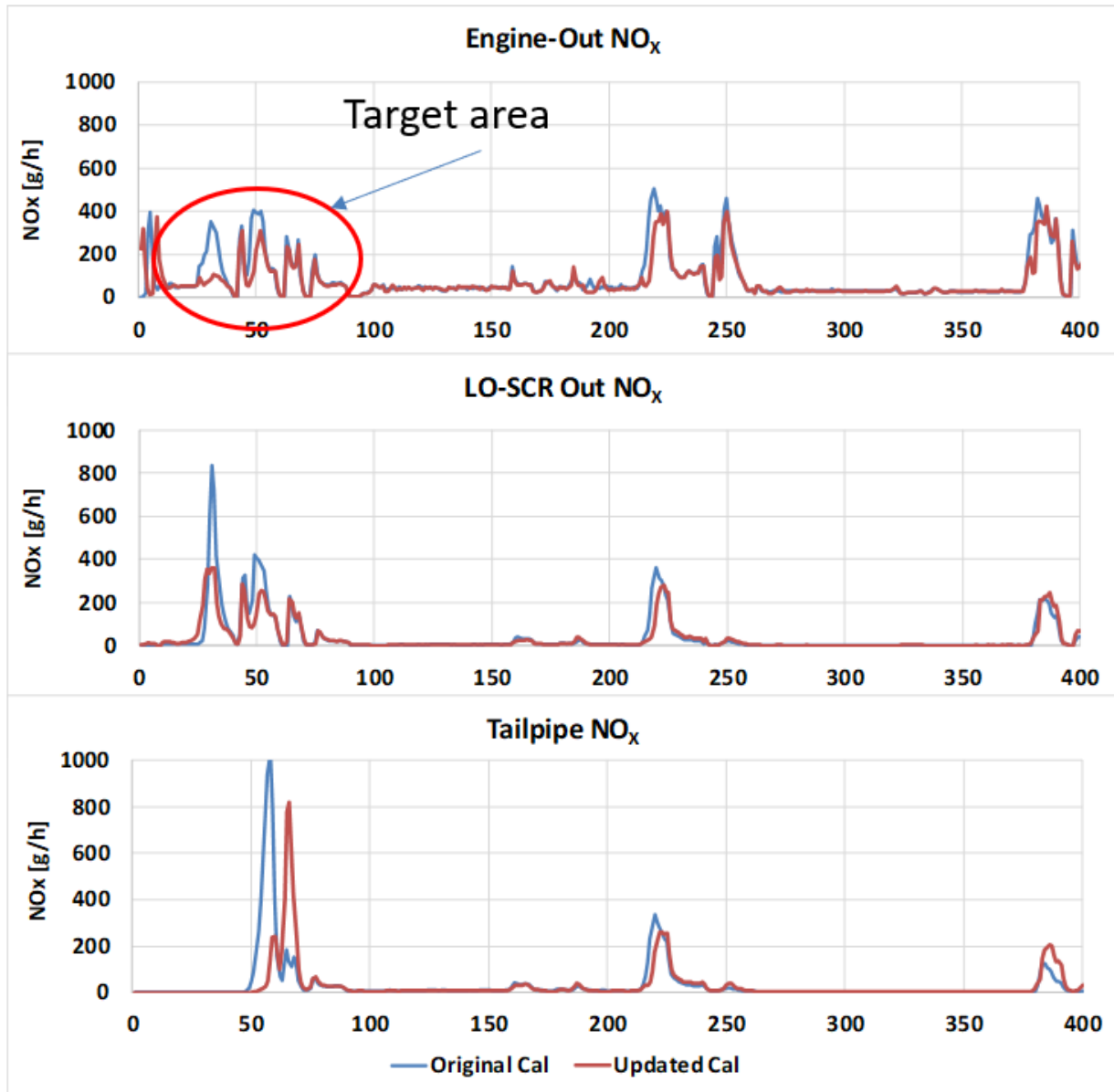


FIGURE 79. TEAM 2A IMPACT OF UPDATED CALIBRATION – LOWER EARLY ENGINE-OUT NO_x

As a result, testing moved on to the Team 2B configuration which was favored by the development team. One other important data noted for configuration 2A was that the backpressure was at 40 kPa on maximum flow rate. This was in part due to the fact that there were two compact mixers in the system. This backpressure represented a significant increase from the 22 kPa observed for the baseline system. Although the RMC-SET was not tested in this configuration, the elevated backpressure would likely have caused a fuel consumption and CO₂ increase at high load. Previous backpressure testing during base engine calibration suggested that this increase would be on the order of 1.5%.

3.4.2. Team 2B Results

The Team 2B configuration is discussed in detail in Section 2.4 of the Methods portion of the report, and is shown again in Figure 80 for ease of reference. This configuration has the LO-SCR upstream, with the heated DEF doser now installed in a smaller in pipe mixer, and the DOC is moved to the downstream assembly. This greatly reduced the thermal inertia ahead of the LO-SCR allowing for much faster light off. However, the downside to this configuration is that the heat for deSO_x must now be generated directly from the engine. Therefore, some deSO_x proof-of-concept work was performed as part of this evaluation, as discussed later.

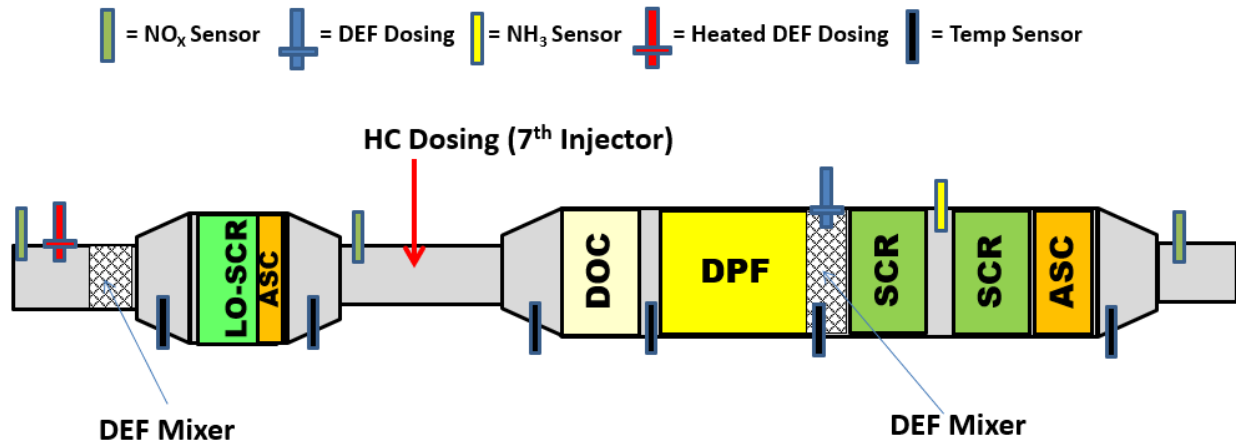


FIGURE 80. TEAM 2B CONFIGURATION

Figure 81 shows a comparison of LO-SCR temperatures in the early cold-start FTP between configurations 2B and 2A. The time to inlet temperature above 200°C is reduced by 30 seconds to the middle of the first acceleration, and the time to outlet temperature above 200°C is reduced by 85 seconds, so that it occurs before the start of the second acceleration. These changes meant that the LO-SCR begins to help conversion even in the first acceleration, and is fully at temperature in time to achieve high conversion in the second acceleration.

This change results in a substantial improvement in tailpipe NO_x emissions, as shown in Figure 82. Tailpipe NO_x on the cold FTP was improved from 0.09 g/hp-hr for 2A to 0.05 g/hp-hr for 2B. Further optimization of the 2B calibration resulted in a final cold-start NO_x of 0.043 g/hp-hr with a CO₂ of 542 g/hp-hr. These values are within the target range, and therefore this configuration was considered acceptable as a final candidate for selection. An example of data from the final cold FTP runs for configuration 2B is shown in Figure 83. That figure also shows the balance between reliance on LO-SCR conversion early in the cycle, and the downstream SCR later in the cycle.

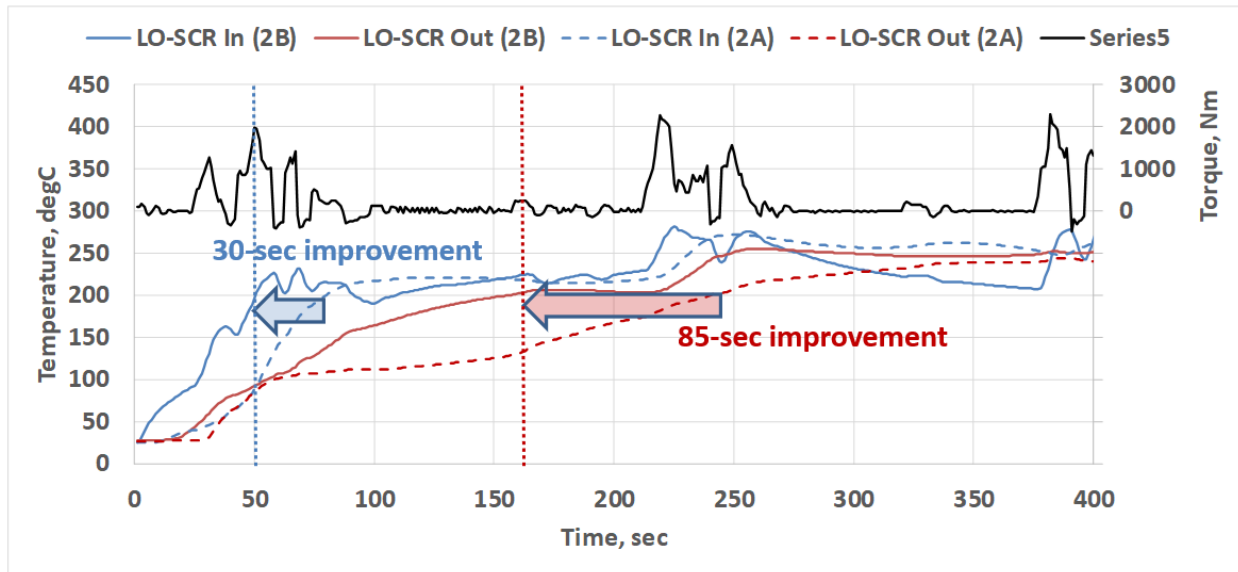


FIGURE 81. COLD-START LO-SCR TEMPERATURE IMPROVEMENTS FROM 2A TO 2B CONFIGURATION

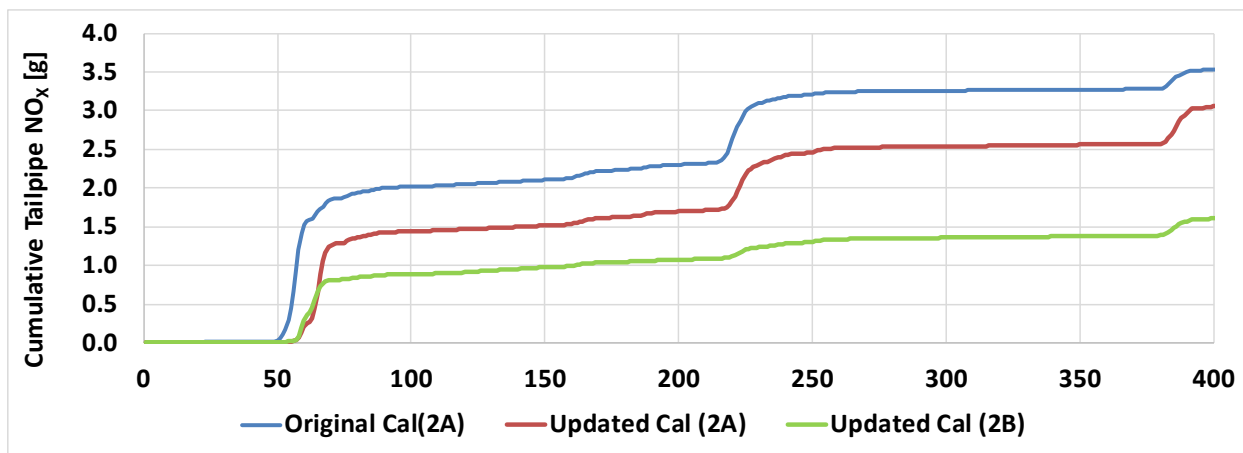


FIGURE 82. CUMULATIVE NOX MASS IN EARLY COLD-START FTP – COMPARISON OF 2A AND 2B

By this point in the development, the warmed-up engine calibration and thermal management timing was completed, and this allowed better evaluations of hot FTP and LLC cycles. Preliminary tuning was done on the hot FTP, and those results are shown in Figure 84. Note that the tailpipe NO_x is shown in the right axis magnified by a factor of 20 so that it can be seen. With this preliminary tune, the Team 2B NO_x results was 0.014 g/hp-hr with a 1% fuel consumption benefit compared to the baseline. Note that the downstream SCR never goes below 200°C, and only a few small breakthroughs of NO_x happen in the vicinity of 400 seconds, where both catalysts are only slightly above 200°C

This was not considered a low enough hot-start number to reach targets, but it was also clear that there was room for additional thermal management tuning to be done while still reaching a GHG-neutral calibration. This was considered sufficient for the configuration screening, and further optimization would be done after the final down-selection.

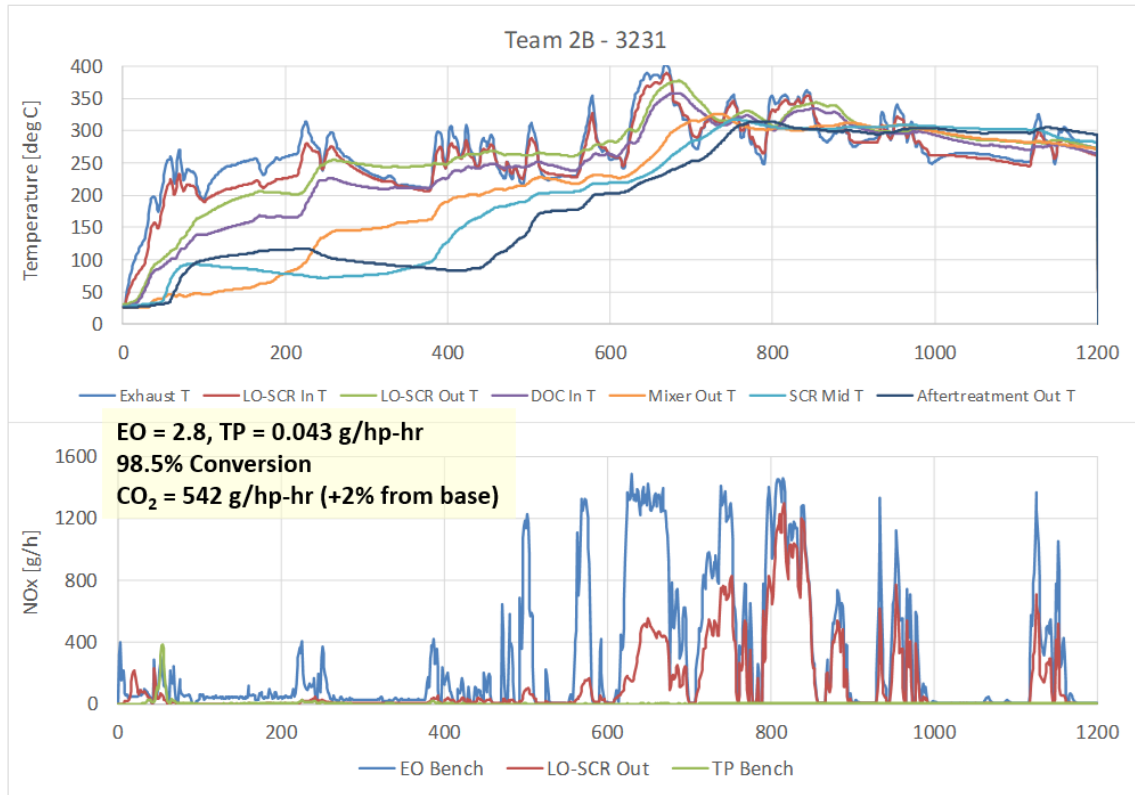


FIGURE 83. COLD-FTP RESULTS FOR OPTIMIZED CONFIGURATION 2B

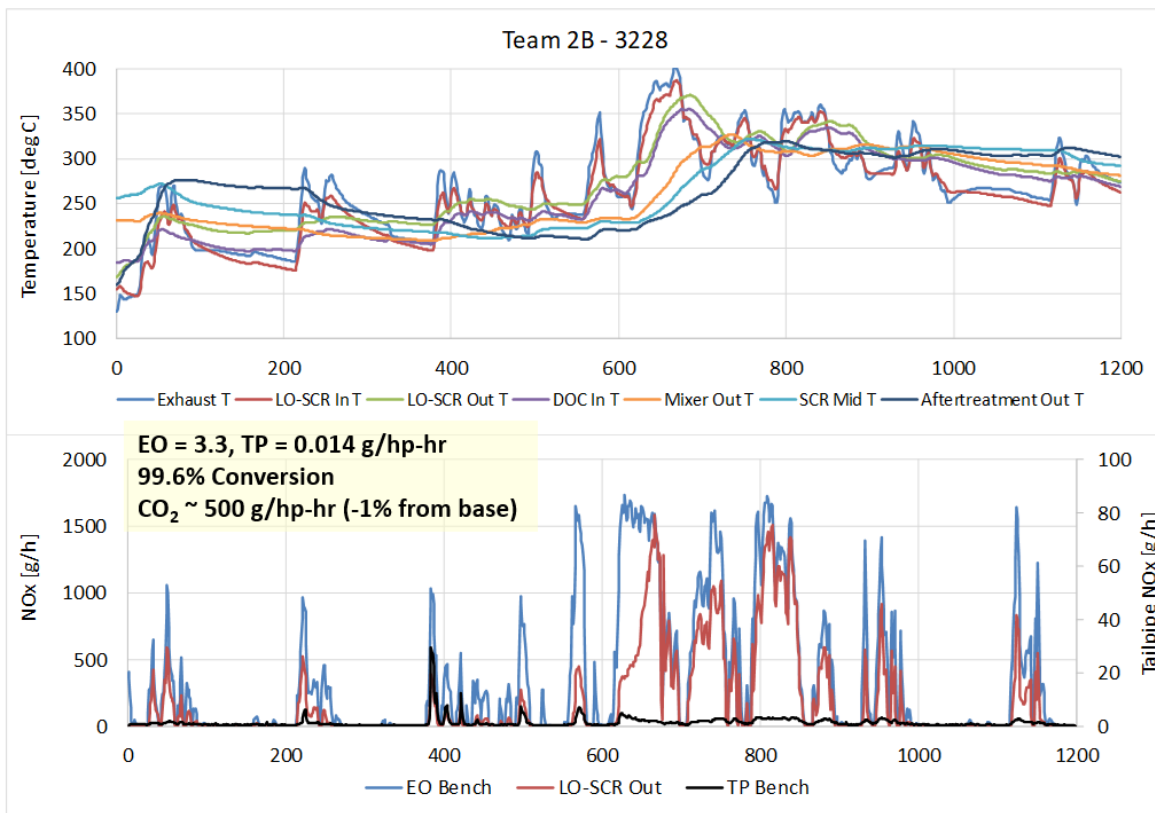


FIGURE 84. HOT-START FTP RESULTS FOR CONFIGURATION 2B

The LLC was also tested on this configuration, given the promising FTP results. Results are shown in Figure 85 after several iterations of thermal management tuning. Tailpipe NO_x levels were near the desired target level, and fuel consumption was essentially the same as for the baseline engine, nearly a 20X drop in tailpipe NO_x. Although more margin would likely be needed for catalyst durability, this result was sufficient for catalyst comparison purposes. It should be noted that these early LLC results do not yet include the idle accessory load of 3.5 kw, because that procedural decision had not yet been made. The observed trends are still generally similar, however. Note that this cycle spends much more temperature at between 150°C and 250°C, and it was clear that in final tuning more thermal management would be needed to provide an acceptable margin in this cycle.

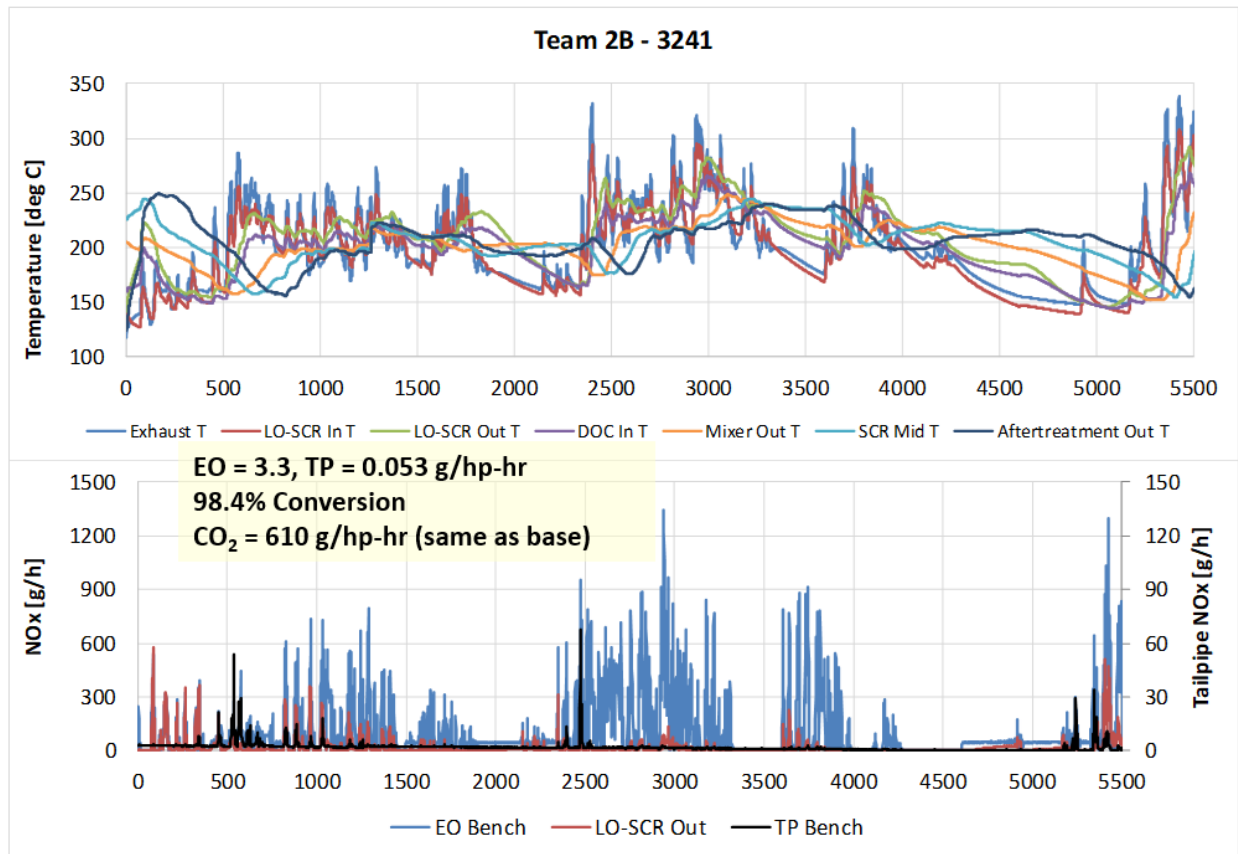


FIGURE 85. LLC RESULTS FOR CONFIGURATION 2B

The RMC-SET was not run on this configuration during the initial screening tests because it was clear that sufficient temperature would be present for high efficiency NO_x control. However, it was noted that backpressure at high load was relatively high in this configuration at 35 kpa, which is a significant reduction from the 40 kpa observed for configuration 2A, but still well above the 22 kpa of the baseline system. This was still enough of an increase to cause concern that a significant increase in CO₂ could be expected. Based on earlier backpressure test results during baseline engine calibration, a 1% increase on fuel consumption was anticipated due to this. This was an important consideration for the later system comparisons.

As noted earlier, a key question for this configuration was how deSO_x would be performed without the aid of a DOC upstream to generate an exotherm via post-injected HC from the engine. To proceed with configurations which involved placing the LO-SCR first in the system, it was felt that a level of validation was needed regarding the feasibility of generating the required temperatures over a range of operating conditions. Without the upstream DOC, the heat for deSO_x would need to be generated directly from the engine. It was anticipated that temperatures of at least 525°C, and potentially as high as 550°C, would be needed for effective removal of sulfur from the LO-SCR. These temperatures could likely be generated at high load using engine calibration changes, but practical deSO_x during normal operations would require a much wider operating range.

It was felt the CDA would be a key enabler for extending the practical deSO_x range to lower loads, but this had not been demonstrated. Given the key importance of answering this question, additional mapping was conducted at this point in the program to validate whether deSO_x conditions could be generated at lower loads. A series of steady-state conditions were run using various CDA modes to examine this question.

Figure 86 shows the result of some of this mapping for one example condition at relatively low load point of 3.1 bar BMEP (roughly 15% load). It is clear from the mapping that engine calibration changes alone would not be likely to approach the desired temperatures. Some increase is possible using a near post-injection, but that would likely only be able to increase temperatures by another 50°C to 75°C. On the other hand, the reduced air-fuel (A/F) ratio from going to CDA mode 5B was able to generate temperatures near 500°C. At this level, it was possible to use some additional near post injection to trim the temperatures into the desired range of 525°C to 550°C. At this load, 2-cylinder firing conditions could not be used due to smoke limitations, and it was decided that a filter smoke number (FSN) of 2 would be used as the limiting line for this mode. Normally this would be too high for sustained operations, but it was felt that for a deSO_x mode that would only be used intermittently, FSN 2 was still a reasonable limit without putting too much soot into the DPF.

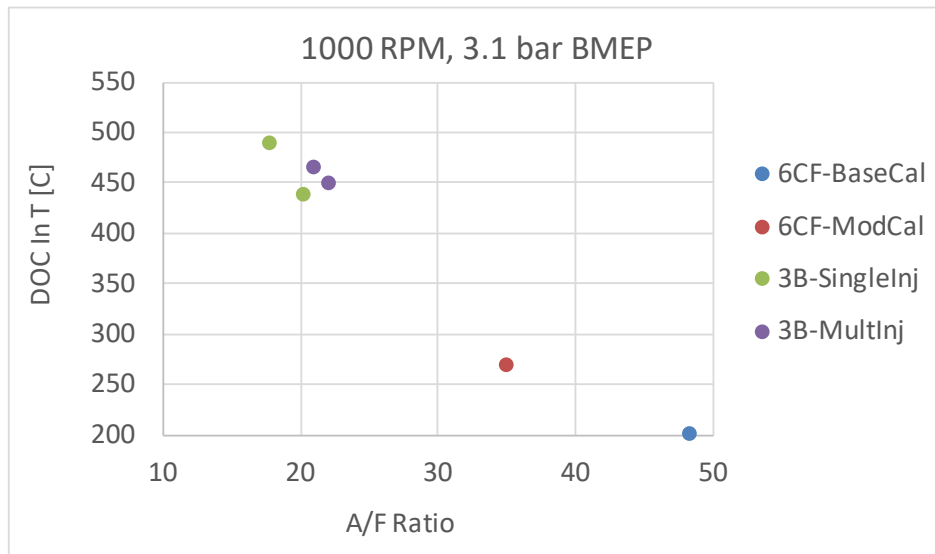


FIGURE 86. DESO_x MAPPING AT 1000 RPM 3.1 BAR BMEP

Similar mapping was conducted at a variety of load points at both 1000 rpm and 1600 rpm, to span most of the speed range. The results of this mapping are summarized in Figure 87. The results show the different CDA modes that were used under different speed and load conditions. The results indicate that temperature near 500°C could be achieved at loads as low as 1.5 bar BMEP (about 7% load), without any aid from additional near post-injection. DeSO_x is a case where CDA would be used even at loads above 3 bar, although it was understood that this would result on some fuel penalty. However, it was noted that the fuel penalty would be less than the amount required to generate such elevated temperatures by other means. It should be noted that given the lowered air-fuel-ratios of these modes, deSO_x would need to be run in a mode where EGR was essentially turned off. However, the elevated temperatures and relatively low exhaust flow rates meant that the SCR system should be very effective in reducing NO_x emissions under these conditions, and this was proven out in subsequent testing. Air-fuel ratio and FSN for these modes is shown below in Figure 88 and Figure 89, respectively.

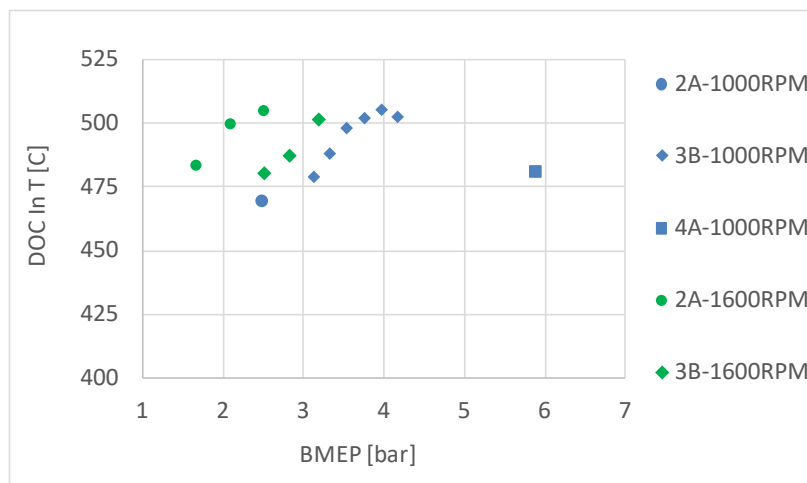


FIGURE 87. DESO_x MAPPING – IDEAL CDA MODES AT VARIOUS ENGINE CONDITIONS

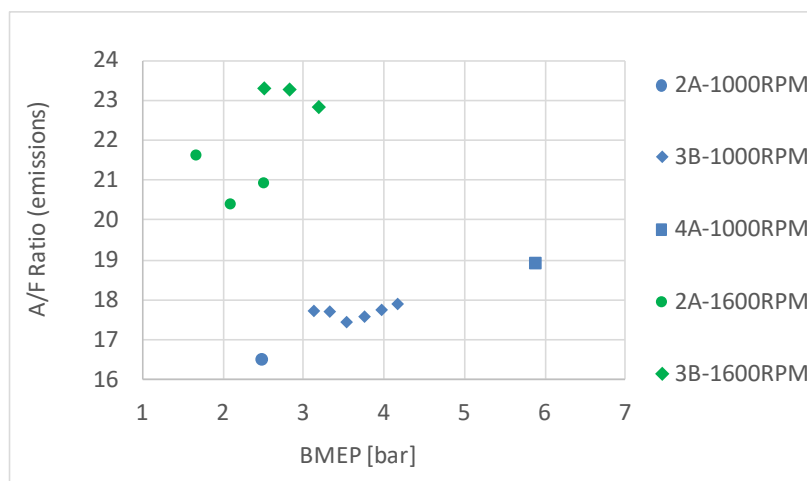


FIGURE 88. DESO_x MAPPING – AIR-FUEL RATIO AT VARIOUS CDA-ENABLED DESO_x CONDITIONS

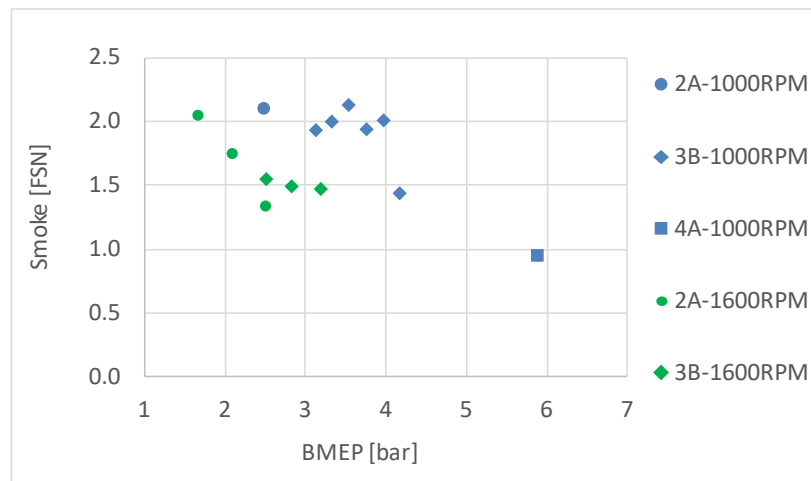


FIGURE 89. FILTER SMOKE NUMBER (FSN) AT VARIOUS CDA-ENABLED deSO_x CONDITIONS

At loads above 8 to 10 bar, it was possible to generate these temperatures without using CDA by leveraging engine calibration changes and near post-injection alone. Given that both CDA and post-injection can be changed on a cycle by cycle basis, this mode of operation is usable under transient operations, and because the usable range goes down to loads around 2 bar, CDA-enabled deSO_x should be compatible with a wide variety of driving conditions.

During later deSO_x experiments, a deSO_x mode at 525°C was run at 1200 rpm, 4 bar BMEP (500 Nm torque or about 25% load), using CDA Mode 3B without any near post-injection supplement. Exhaust flow was nominally 300 kg/hr, and engine-out NO_x was high (400 g/hr), however the AT was able to reach in excess of 99.5% conversion so tailpipe NO_x was on the order of 0.03 g/hp-hr. It should be noted that under deSO_x, the upstream doser is run at this high temperature (which is different from the normal strategy) at an ANR of 1.3 to facilitate sulfur removal through chemical deSO_x. Therefore, given the infrequent use of this kind of operation, this mode can be run with little or no impact on tailpipe NO_x. Fuel consumption was increased by 11% over the most efficiency engine operating mode (FE mode) normally available. Given that this mode of operation is expected to be run roughly 30 minutes out of every 300 hours of operation, this overall fuel consumption impact of this mode would be minimal. Near post-injection could be used to trim the value further to account for factors such as low ambient temperatures, although this would increase the fuel consumption impact.

A second example of deSO_x mode was run at 550°C, 1400 rpm, and 6.6 bar BMEP (800Nm torque or about 33% load), using CDA Mode 4A, again without any near post injection supplement. Exhaust flow was nominally 560 kg/hr, and engine-out NO_x was about 650 g/hr. Again, however, the AT was able to achieve 99.6% conversion so the tailpipe NO_x was 0.03 g/hp-hr. The fuel consumption impact in this mode was a 12.5% increase over the normal FE mode operation.

The examples indicate the CDA could be leveraged to enable deSO_x conditions engine-out over the majority of the engine operating map using rapidly switchable functions that would be compatible with transient operation. High AT efficiency can be maintained, in part due to the dual-bed SCR architecture (because the downstream bed is at somewhat lower temperatures), so

this deSO_x can be conducted without impacting fuel consumption. The overall fuel penalty is anticipated to be in the range of 10-15%, however if this mode is run 0.2% of the time (30 minutes every 300 hours), the overall life cycle fuel consumption and CO₂ increase would be less than 0.03% (assuming a 15% penalty).

With this validation completed, it was felt that the program could proceed forward using a LO-SCR catalyst with a DOC upstream. Examples from the program showing successful removal of stored sulfur are given later.

3.4.3. Team 1 Results

The Team 1 AT hardware was actually received after the Team 2 hardware, and therefore it was evaluated second. The primary Team 1 configuration was described in detail on the Methods section of the report, and is shown below in Figure 90 for easy reference.

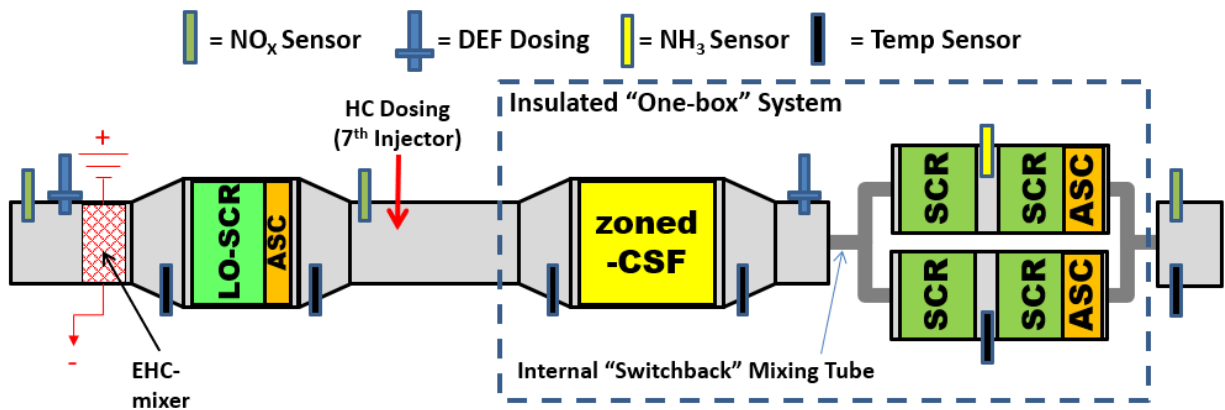


FIGURE 90. TEAM 1 AFTERTREATMENT CONFIGURATION

One of the distinctions of the Team 1 system that required additional effort in evaluation was the approach to heated dosing. In the Team 1 system, heated dosing was implemented by using a normal DEF doser that was targeted at an electrically heated catalyst (EHC) assembly. The EHC assembly included only a very small supporting metal substrate behind the heater element. The only purpose of this system was to provide a hot surface to aid in evaporation of urea, and the supported substrate also provided additional mixing. The heater had a capacity of 2 kw at 24 V, and for this initial experiment it was run at 1.8 kw but it was only used at temperatures up to 200°C. After that the heater would be turned off, thus limiting the overall power consumption through a given cycle.

The heater was powered by a test cell power supply, but given this level of power consumption, it was necessary to account for that power properly in terms of fuel consumption and CO₂. SwRI implemented a test cell approach to ensure an accurate and realistic method of accounting for this. The electrical power consumption was measured in real-time over the cycle, and then translated using an assumed alternator efficiency into an engine power demand. That demand was then used to calculate an equivalent torque demand using the current engine speed. The torque was then subtracted from the measured engine output torque in real time. As a result, the engine had to work harder, and burn more fuel, to reach the target torque for any given cycle.

setpoint, but the extra work was not included in the cycle work calculation. This approach also properly factors in the heat generated in the exhaust to support that electrical load, but forcing the engine to actually burn an appropriate amount of fuel. In this way, the electrical power demand of the heater is accounted in a realistic manner, and the cycle CO₂ results accurately reflect the impact of the heater for any cycle or heater control approach.

One key early point of comparison in the evaluation of Team 1 was that the backpressure at maximum flow rate was 25 kPa, much lower than the 35 kPa for Team 2B, and only slightly higher than the baseline system backpressure. As a result of this, high load fuel consumption for the Team 1 system was similar to what was observed on the baseline engine. This shift was primarily due to the lower backpressure mixing approach, as well as the dual parallel path SCR design for the downstream system, which gave it an effective flow area equivalent to a 15-in diameter substrate.

Following controls tuning and some strategy optimization with the heater controls, demonstration tests were conducted for the Team 1 configuration. Cold-start FTP results are illustrated in Figure 91. The system was able to reach the cold-FTP target of less than 0.06 g/hp-hr, although performance was slightly worse than for Team 2. It was noted that the LO-SCR performance was slightly worse for the Team 1 configuration, as compared to Team 2. The Team 1 system appeared to have a larger CO₂ penalty than the Team 2 system, showing a 3% increase of over the baseline values. This was due in large part to the power requirement to drive the heater. The heater power consumption is also shown in Figure 91. The heater was only functioning for a short period of time in the cold-start, but this was still enough to account for an additional 0.5% to 1% CO₂ impact.

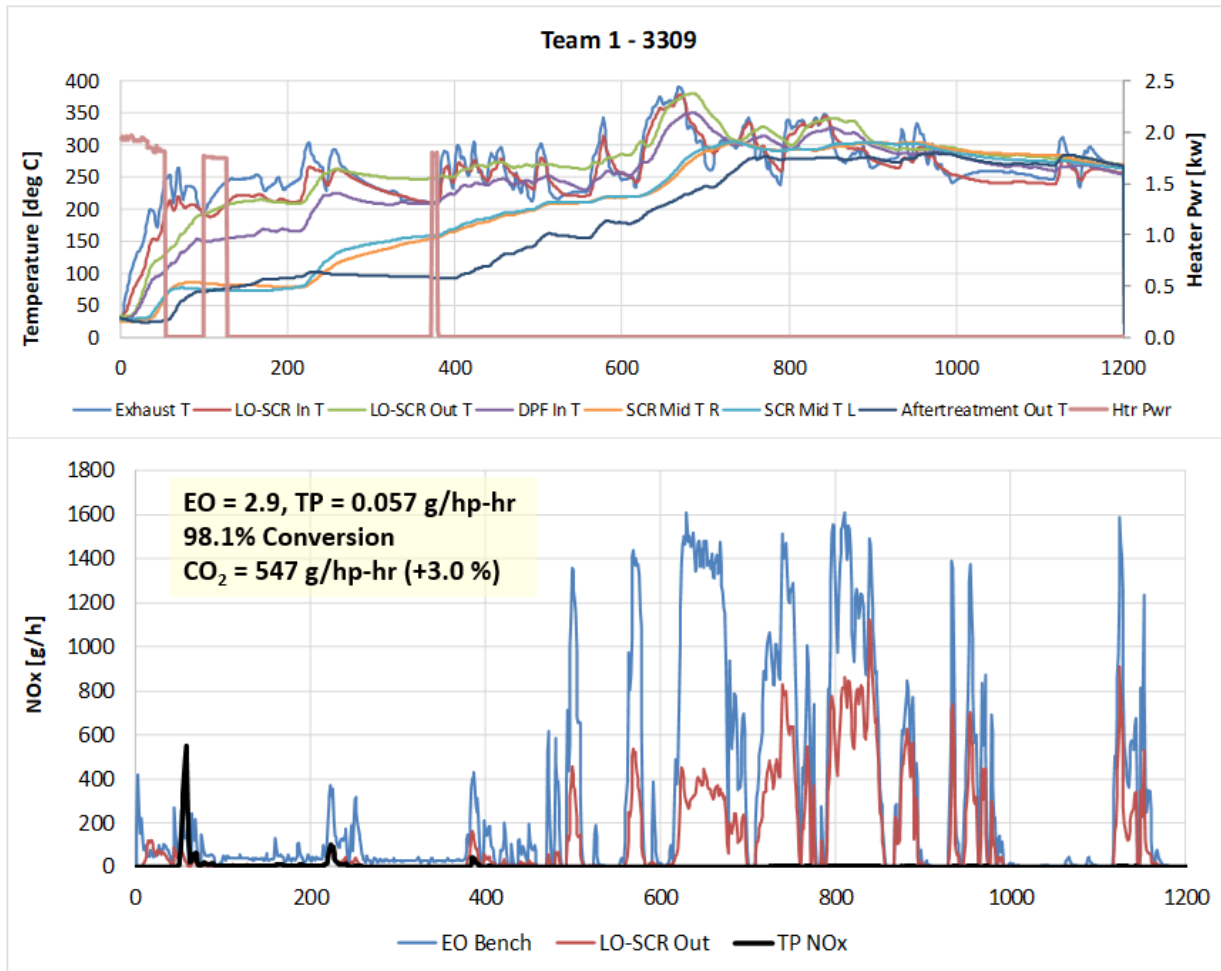


FIGURE 91. COLD-START FTP RESULTS FOR TEAM 1 SYSTEM

Preliminary hot-start FTP results are shown in Figure 92. The tailpipe NO_x in this initial evaluation was 0.016 g/hp-hr, which was not enough to reach the composite FTP target. However, given the heater never ran and considering the lower backpressure and CDA, CO₂ was actually more than 2 % lower than the baseline on this cycle. It is likely that this improvement would be reduced somewhat with further thermal management to reach the target. It was noted that the LO-SCR performance at temperatures below 250°C at high space velocity was not quite as good for Team 1. As noted earlier however, it is worth noting that Team 1 used a 300 cpsi LO-SCR substrate, while Team 2 used a 400 cpsi LO-SCR substrate.

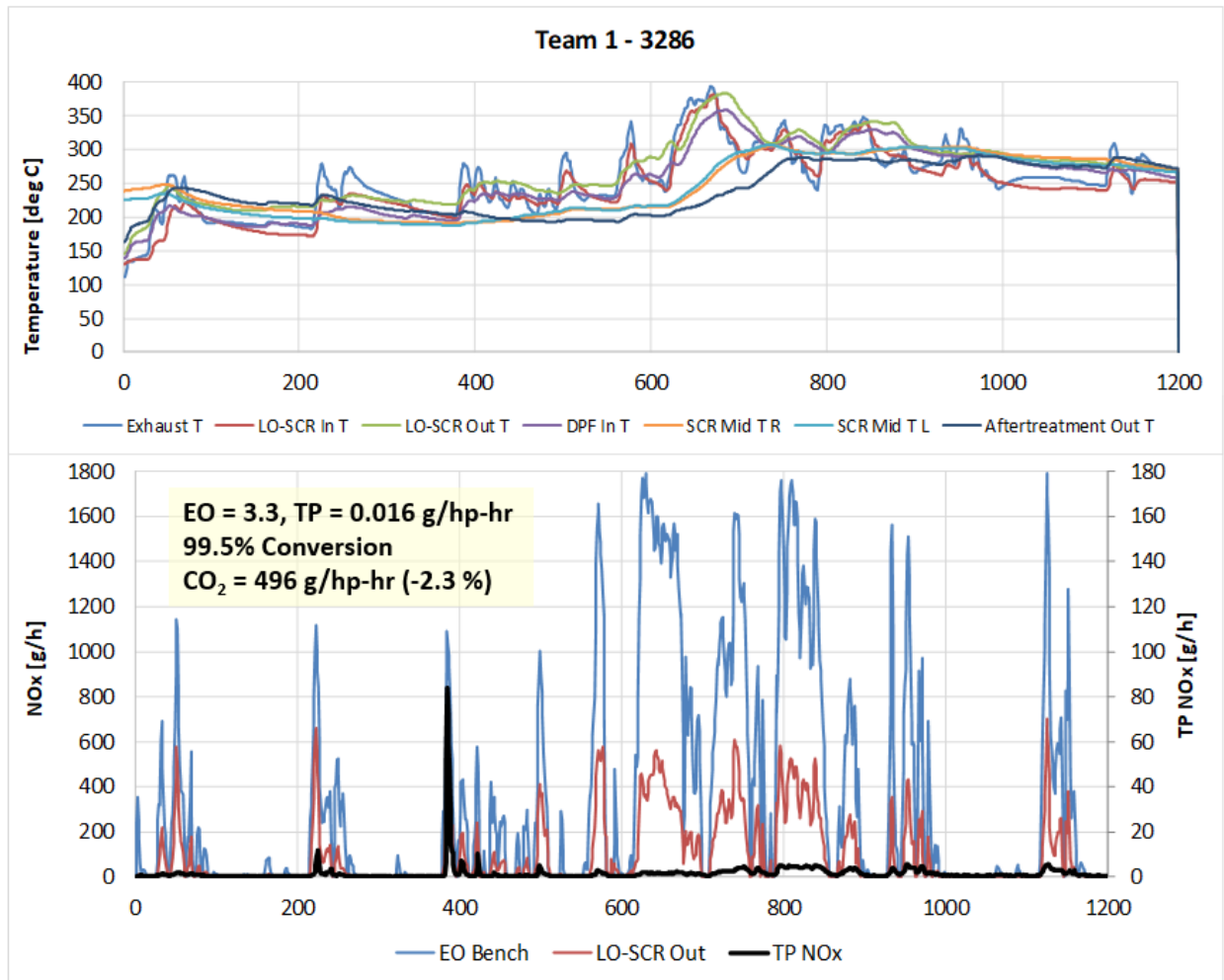


FIGURE 92. HOT-START FTP RESULTS FOR TEAM 1 SYSTEM

LLC results for the Team 1 configuration are shown in Figure 93. The system was able to reach 98% NO_x conversion and a tailpipe level on the LLC below 0.06 g/hp-hr. However, even with CDA operating, there was a CO₂ increase of 2.5% compared to the baseline. This was due mainly to the large amount of heater operation that occurred during the LLC, especially in the long idle segments. As seen in Figure 93, the heater would cycle on and off during longer idle segments as the SCR inlet cross over the trigger threshold. It is possible that this amount could be reduced through a more optimized control strategy, but it was still clear that its use would still result in some form of CO₂ penalty. In addition, a lower tailpipe NO_x level would likely be needed to provide sufficient margin for AT degradation, which would result in a further CO₂ increase. Under these conditions, it was again noted that LO-SCR performance was not quite as good as for the Team 2 LO-SCR, which would likely require more thermal management, and therefore CO₂, to offset.

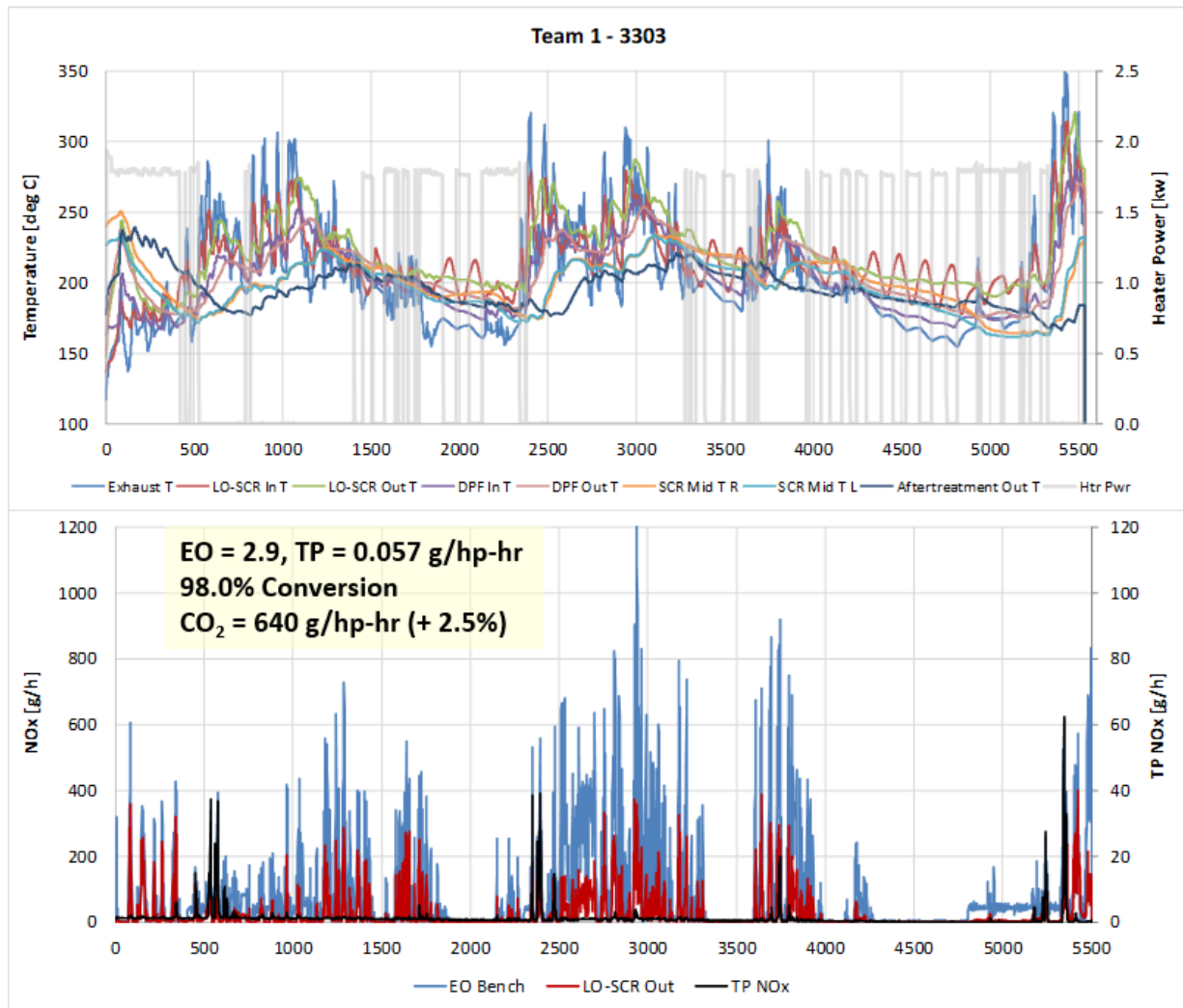


FIGURE 93. LLC RESULT FOR TEAM 1 SYSTEM

The Team 1 system was evaluated over the RMC-SET cycle, and the results are shown in Figure 94. It should be noted that at this point the calibration had not been set to leverage some conversion over the LO-SCR to help the downstream system at high space velocity. Despite that, the downstream Team 1 system was still able to reach emission relatively close to target. With some additional high load assistance from the LO-SCR to trim the conversion demand (as would be implemented later) it was clear this system would be able to reach the desired tailpipe NO_x levels on the RMC-SET. In addition, measured CO₂ was identical to the baseline system, consistent with the fact that the Team 1 system had backpressure nearly the same as the base AT. The results also indicated that the Team 1 downstream system had the potential for higher conversion at high loads, despite the lower backpressure.

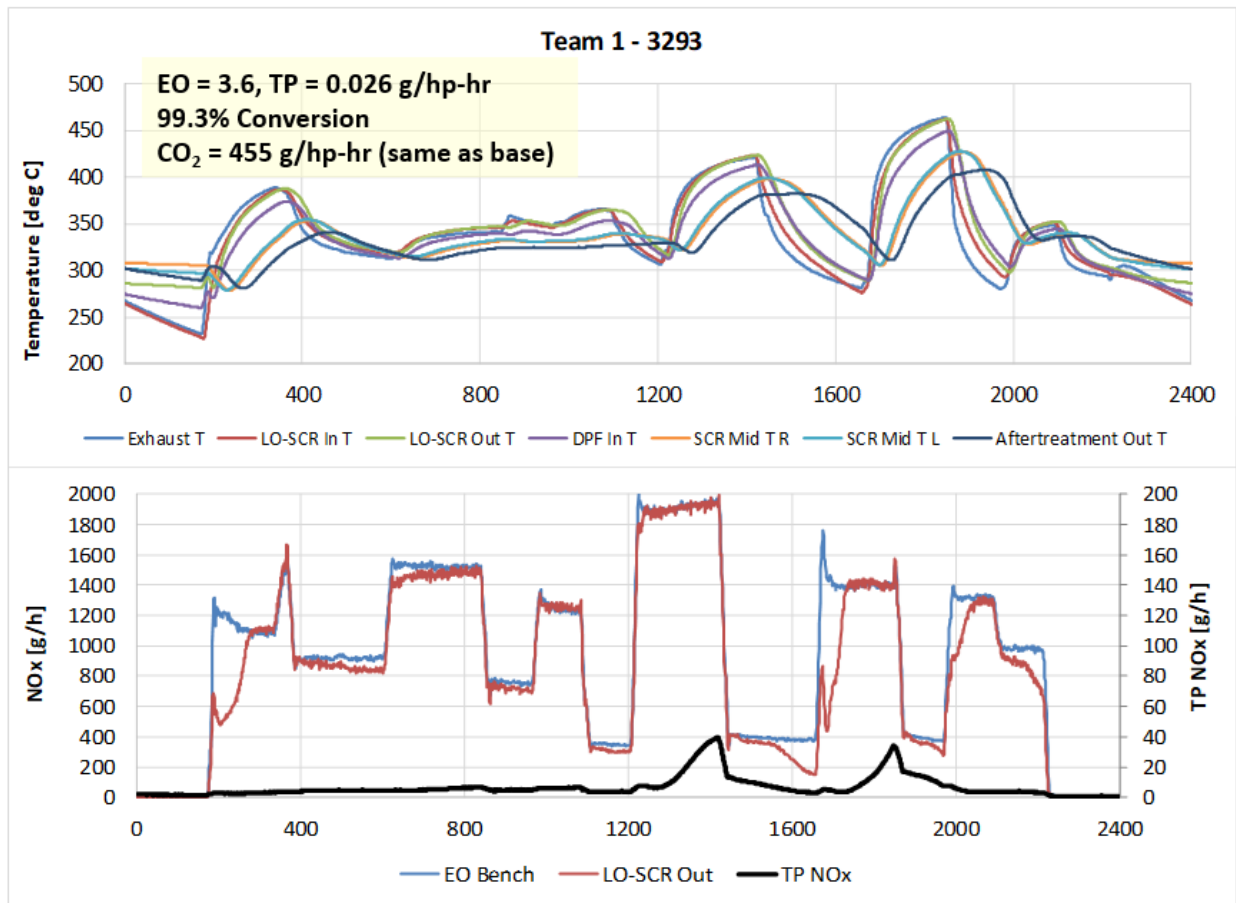


FIGURE 94. RMC-SET RESULT FOR TEAM 1 SYSTEM

3.4.4. System Comparisons – Final System Down-selection

Following the screening tests conducted on the systems provided by both teams, SwRI conducted further analysis to compare the pros and cons of both systems. It was necessary to down-select the final technology package that would be used for the Stage 3 demonstration and carried forward into final optimization, aging, and demonstration testing.

A comparison of critical performance data between the best package for each team is given in Table 10. The Team 2 system clearly had better overall performance on lower temperature cycles, and also lower CO₂ emissions on those cycles. This was due primarily to better low temperature performance from the LO-SCR, and consequently less need for thermal management, which help keep CO₂ lower. This was more the case for the LLC than the FTP. On the other hand, the Team 1 system had significantly lower backpressure, while still having more than enough conversion capacity at high load. This was important for RMC-SET performance and CO₂. Although Configuration 2B was not actually tested over the RMC-SET, it was clear that a CO₂ penalty was expected due to the higher backpressure, likely on the order of 1% to 1.5%. In addition, the Configuration 2B downstream SCR was slightly smaller and therefore would likely have somewhat less conversion margin at high load, high space velocity conditions.

TABLE 10. COMPARISON OF KEY PERFORMANCE DATA FOR TEAM 1 AND TEAM 2 SYSTEMS

		Baseline	Config 2B	Config 1
Cold FTP NO _x	g/hp-hr	0.27	0.043	0.054
Cold FTP CO ₂	g/hp-hr	531	542	545
Hot FTP NO _x	g/hp-hr	0.14	0.014	0.012
Hot FTP CO ₂	g/hp-hr	505	500	502
LLC NO _x	g/hp-hr	1.4	0.12 / 0.053	0.16 / 0.057
LLC CO ₂	g/hp-hr	624	598 / 610	614 / 640
Backpressure	kpa	24	36	25
RMC-SET NO _x	g/hp-hr	0.15	-	0.026 (no upstream help)
RMC-SET CO ₂	g/hp-hr	454	- (but likely higher)	454

An important consideration in this comparison was whether the likely increase in CO₂ from Configuration 2B could be offset using engine calibration. However, an examination of the previous engine mapping data from earlier calibration indicated that this would likely be difficult to achieve with the current engine hardware. Such a calibration change would likely involve increasing engine-out NO_x further at high load in an effort to improve fuel consumption. It should be noted that at the high load modes, the modified engine calibration was running at a level of nominally 4 g/hp-hr. Exploratory runs made at 5 g/hp-hr did not produce any substantial CO₂ benefit. Increasing NO_x by reducing EGR rates further resulted in increased exhaust flow rates and increased losses. At high flow it was clear that efficiency was limited by the flow capacity of the turbocharger, which was matched on the base engine in part for the ability to pump EGR using the VGT. Therefore, any gains in combustion efficiency appeared to be offset by higher pumping losses. On the other hand, in-cylinder data indicated that for the 500 hp 2500 Nm rating of this engine, attempting to increase NO_x via timing advance to improve efficiency would lead to increased peak cylinder pressures. It was felt that this engine was near enough to cylinder pressure limits that a further increase would have represented a poor calibration choice that might compromise mechanical durability. As a result of these limits, it was not feasible to offset the CO₂ penalty from a substantial backpressure increase using engine calibration. However, it should be

noted that with an engine architecture that could sustain higher firing pressures, there would be more room to optimize NO_x and fuel consumption, given that the aftertreatment had the capacity to handle higher NO_x rates at high loads.

The primary concern with the choice of the Team 1 downstream system was uncertainty regarding the durability of the zoned-CSF. It was apparent that with a LO-SCR in place, the reduced thermal inertia of the zoned-CSF was not really necessary. However, a change to a DOC+DPF design was not available within the time constraints of the program. There was also some concern with the larger package size of the Team 1 system, but it was understood that this could be optimized to a smaller level because the design had been prepared somewhat larger in part to accommodate a DOC+SCR configuration.

Ultimately it was decided to combine the best features of both systems to produce the final Stage 3 AT system. The upstream package from Team 2, including the superior LO-SCR and lower power consumption heated dosing approach was paired with the downstream package from Team 1 which featured lower backpressure and a larger high load performance margin. Although there was some risk associated with the zoned-CSF, this was preferable to the significant fuel consumption penalty at high load for the Team 2 downstream package. This penalty would likely have increased over time with ash loading and soot load on the DPF. Given that it was not feasible to offset the RMC-SET CO₂ penalty due to the engine architecture limits mentioned earlier, the Team 1 system was deemed to be the preferred choice between the two.

3.5 Final Aftertreatment System Performance with Development Aged Parts

The details of the final Stage 3 package were described earlier under the Methods section of the report. This system was assembled onto the engine to begin the final stage of calibration and optimization. The final Stage 3 configuration is shown again below in Figure 95 for ease of reference. At this point in the program, a second set of parts from the same batch was being canned for final aging, while the Development Aged parts were used for final calibration tuning and optimization.

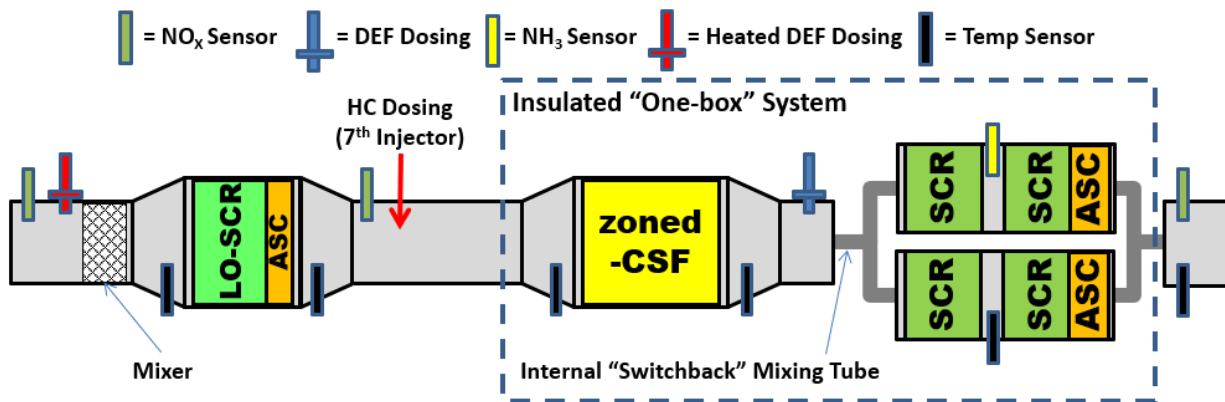


FIGURE 95. FINAL STAGE 3 AFTERTREATMENT CONFIGURATION (TEAM 2B+1)

Following the final down-selection, final development and optimization was carried out over a period of 10 weeks. The controls and strategy were fully automated to be able to run from a single unified calibration on any duty cycle, as would be the case in a production system. Several features were added to the controls and refined, such as the upstream-downstream balance modes, and the accelerated dosing features. System gains were tuned and feed-forward ANR and storage targets were tuned. This effort was coupled with continued refinement of the thermal management strategy and mode changing thresholds. The balance between tailpipe NO_x performance and CO₂ was refined and further optimized.

Figure 96 shows an example of the final cold-FTP performance on Development Aged parts following this optimization process. Similar results are shown in Figure 97 for the hot FTP, Figure 98 and Figure 99 for the LLC, and Figure 100 for the RMC-SET. In the case of the LLC, results are shown both with (in Figure 99) and without (in Figure 98) the 3.5 kw accessory load. It should be noted that the results with accessory load are considered official, while the results without can be compared to the previous screening results that were run prior to this procedure being finalized. The higher load at idle did help to reduce the overall thermal management requirement somewhat, therefore BSCO₂ values were actually lower, although this was also the case even for the baseline engine.

In the case of the FTP, the finalized calibration resulted in a composite FTP NO_x level of 0.017 g/hp-hr. There was concern that this would not be sufficiently low to allow for AT degradation during Final Aging. However, this calibration also demonstrated at 2.5% improvement in CO₂ compared to the baseline engine. As a result, it was decided to move forward with durability with this calibration, to see if this benefit could be preserved. If degradation proved to be too large, some of this benefit could be traded away in the form of increased thermal management to maintain NO_x performance. It was, however, important to at least maintain a GHG neutral performance level compared to the baseline.

Another calibration point to be discussed is the balance between LO-SCR NO_x conversion and downstream NO_x conversion. This balance varies by duty cycle, but in general, the initial approach was to use the minimum amount of LO-SCR conversion needed to reach NO_x targets, especially at catalyst temperatures above 300°C. This was done to enable the maximum amount of NO_x possible to reach the zCSF to promote passive soot oxidation. For the Development Aged parts, LO-SCR conversion was calibrated to 65% to 70% on the FTP, 40% to 45% on the RMC-SET, and 85% on the LLC. At these levels, the zCSF would generally be cleaned out from a moderate level of soot loading, and the FTP generally experienced a slow rate of soot load increase, similar to or slightly slower than what was observed on the baseline engine. Temperatures on the LLC were low enough that there was not significant passive soot oxidation in any configuration. It was also noted that this was another calibration point that could be adjusted over time to help compensate for degradation.

There was not measured tailpipe NH₃ slip on any of the cycles. Tailpipe N₂O levels were on the order of 0.04 to 0.06 g/hp-hr depending on the duty cycle, although nearly 0.07 was observed on the LLC. Generally, N₂O was somewhat lower on the Low NO_x engine than it was on the baseline engine. This was primarily due to the LO-SCR, because the LO-SCR operates mostly on the “standard” (NO only) SCR reaction because engine-out NO_x is primarily NO. Much of the N₂O generation on zeolite-SCR catalysts is via the formation of nitrates at lower temperatures (and later decomposition of those nitrates at higher temperatures), which requires the presence of NO₂. In the Stage 3 system, LO-SCR eliminates a significant amount of NO_x as NO, especially at lower temperatures where this N₂O formation mechanism is most active. Therefore, the opportunity for N₂O formation is greatly reduced. The more LO-SCR is used, the lower N₂O emissions generally are.

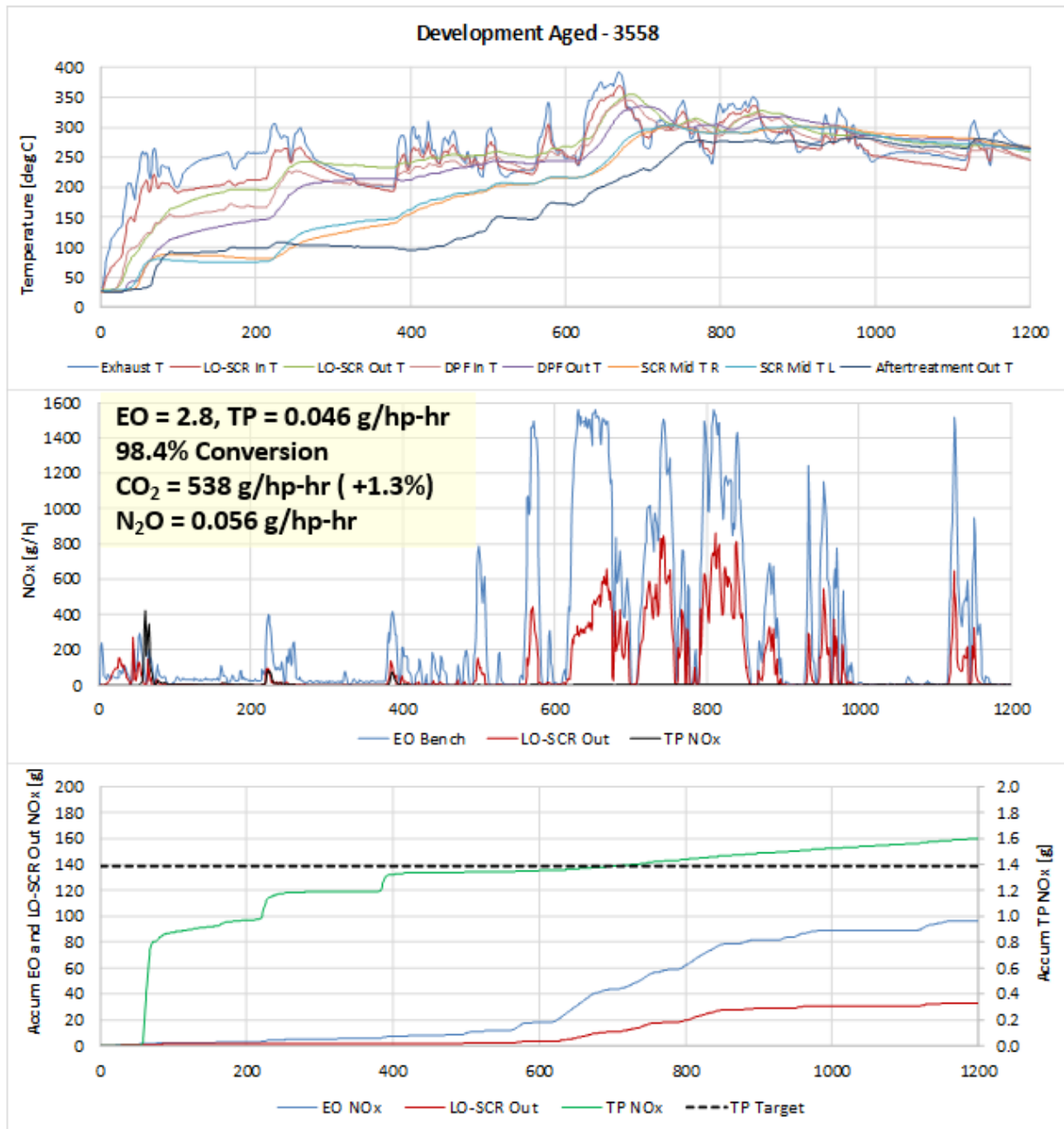


FIGURE 96. COLD-FTP FINAL RESULT ON FINAL STAGE 3 DEVELOPMENT AGED PARTS AFTER OPTIMIZATION

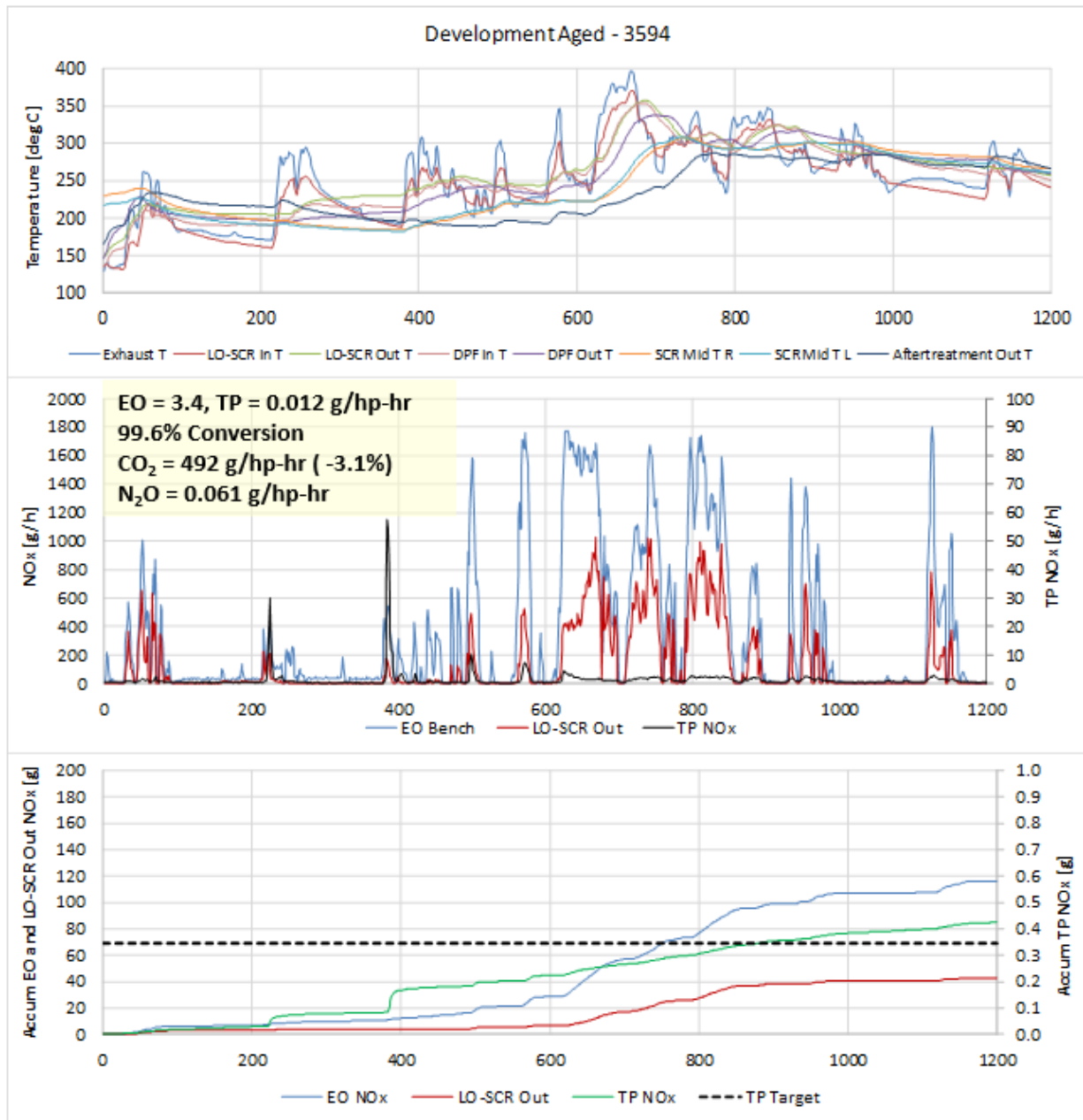


FIGURE 97. HOT-FTP FINAL RESULT ON FINAL STAGE 3 DEVELOPMENT AGED PARTS AFTER OPTIMIZATION

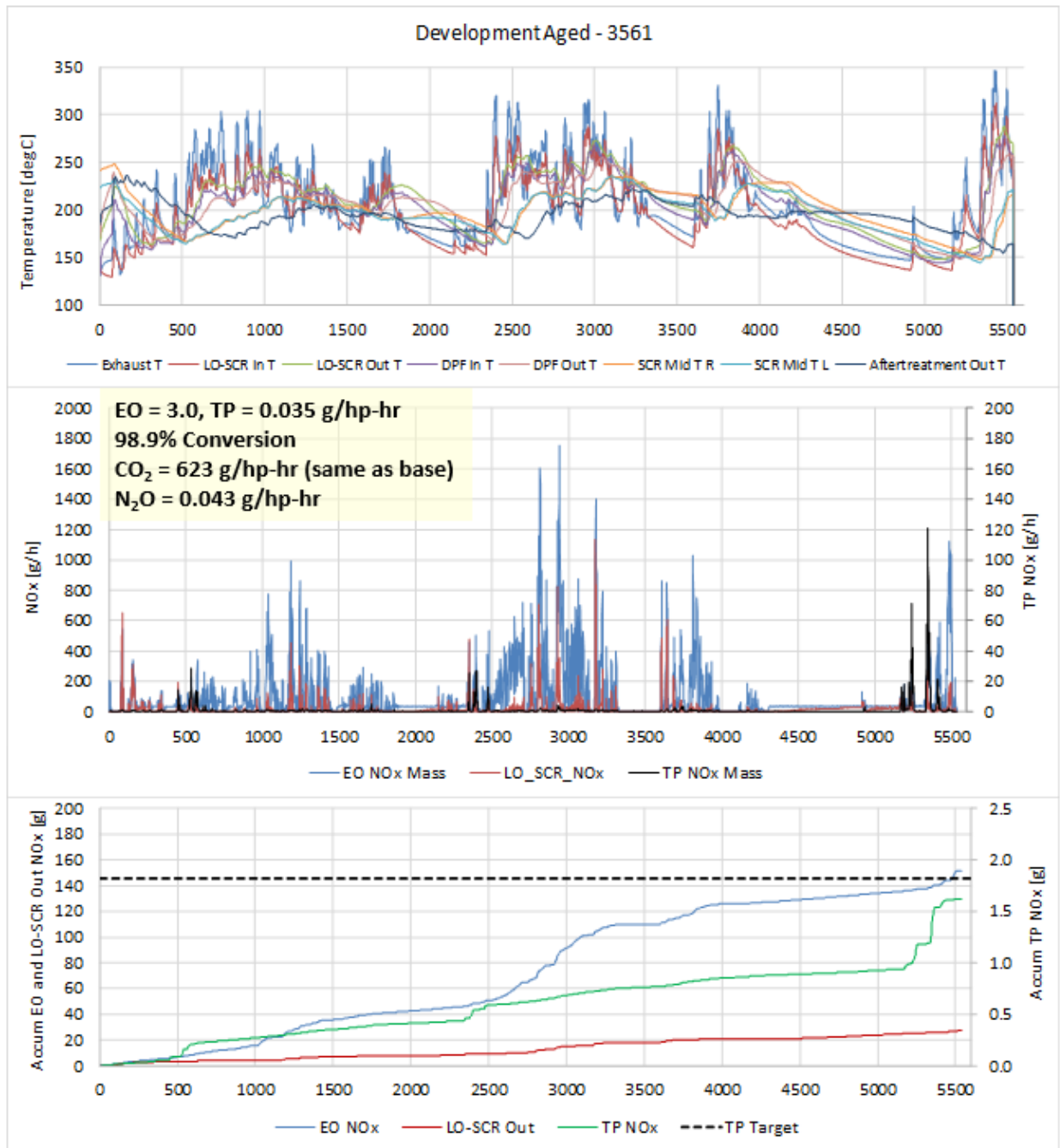


FIGURE 98. LLC RESULT WITHOUT ACCESSORY LOAD – FINAL STAGE 3 DEVELOPMENT AGED PARTS

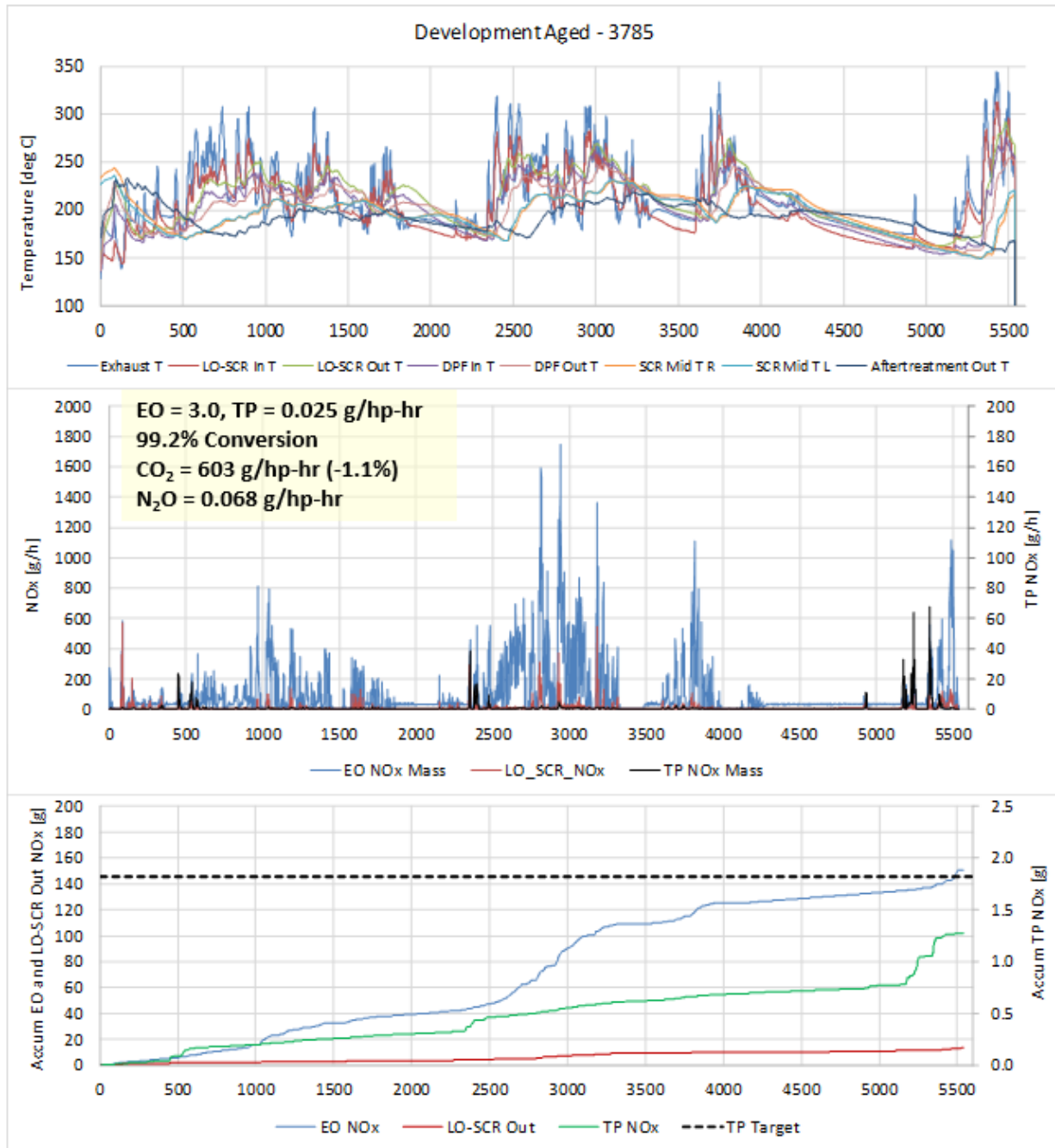


FIGURE 99. LLC RESULT WITH ACCESSORY LOAD – FINAL STAGE 3 DEVELOPMENT AGED PARTS

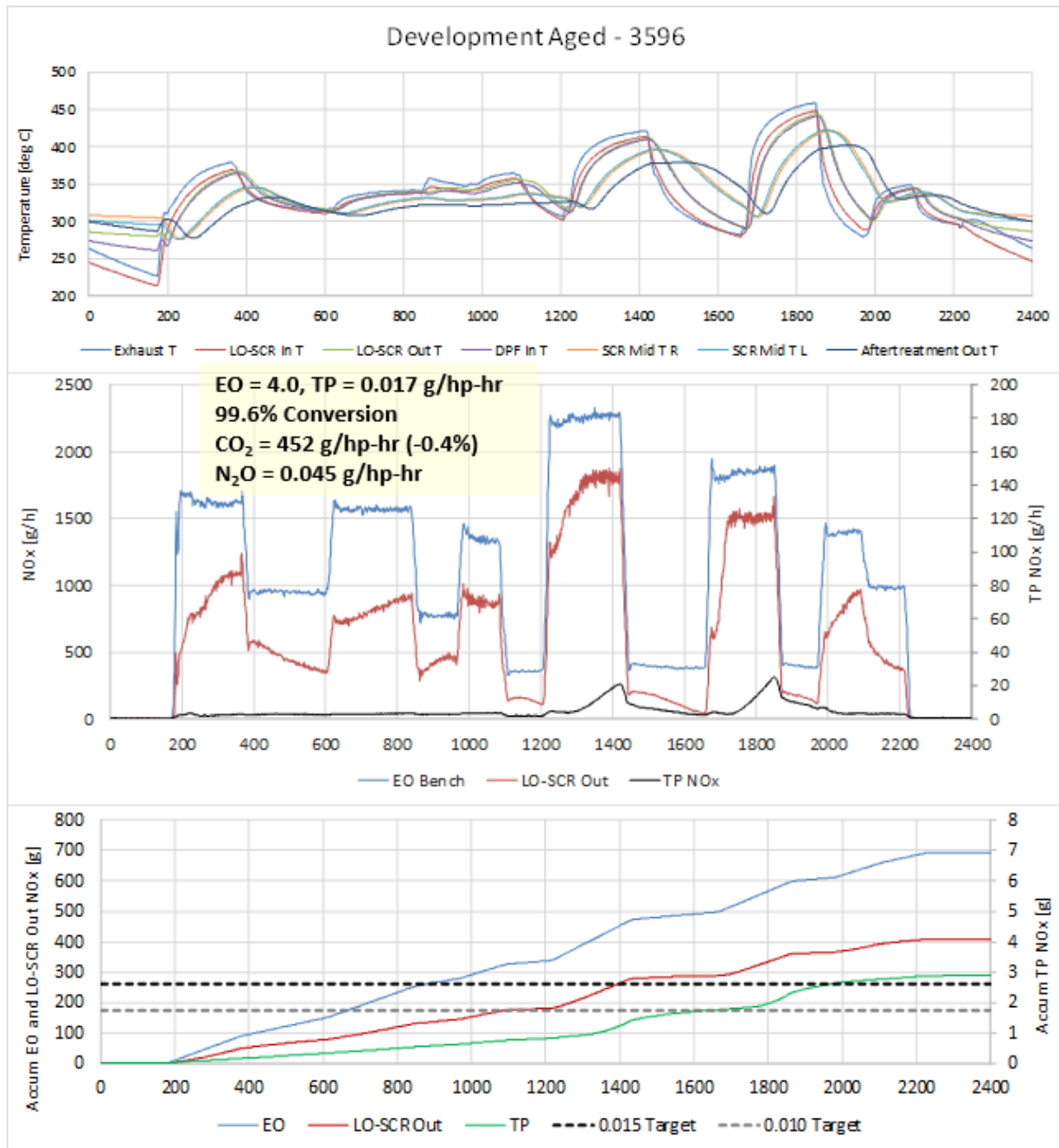


FIGURE 100. RMC-SET RESULTS FOR FINAL STAGE 3 SYSTEM WITH DEVELOPMENT AGED PARTS

A summary of the Development Aged results after optimization is given in Figure 101. In general, these results were roughly 90% below the baseline engine NO_x levels, or 20X lower in the case of the LLC. NO_x conversion was generally at or above 99.5%. This calibration demonstrated improved CO₂ on all cycles, although as noted earlier more margin might be needed to account for chemical degradation during the full DAAAC Final Aging. It was decided to preserve the CO₂ benefits observed, proceed forward to Final Aging and adjust thermal management further if significant additional degradation was seen.

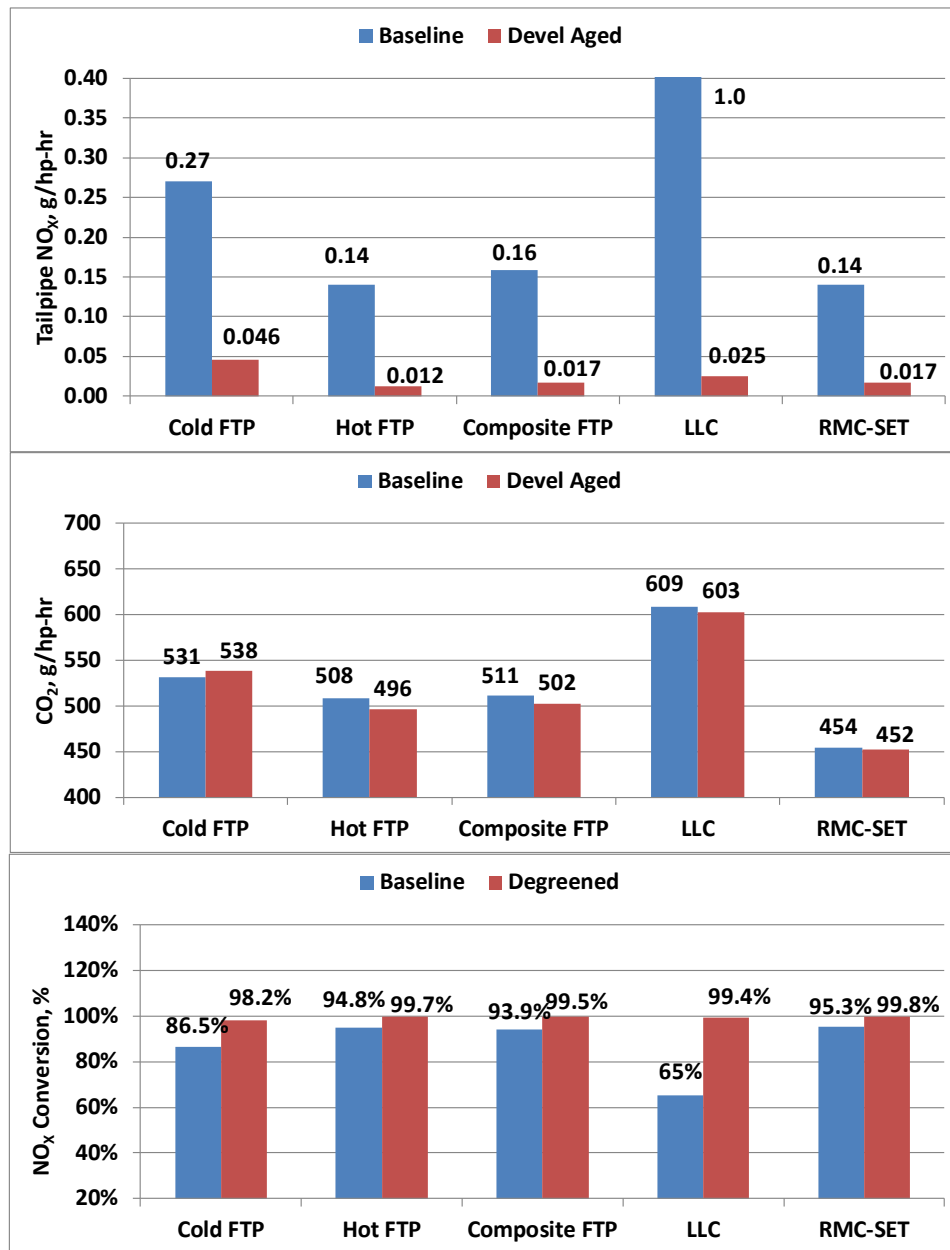


FIGURE 101. COMPARISON OF STAGE 3 DEVELOPMENT AGED AND BASELINE RESULTS

At this point, the Development Aged parts were removed and the degreened Final Aged parts were installed for 0-hour testing. Later in the program, the Development Aged parts were reinstalled for several additional purposes:

- Testing of the Low NO_x engine over the Phase 2 GHG fuel mapping process
- Evaluation of field replay cycles
- Additional idle testing requested by EPA
- Evaluation over the 2021 version of the RMC-SET cycle
- Testing of the final calibration used on the 1000-hr Final Aged parts to examine for comparison to the previous calibration shown in Figure 101.

3.6 DAAAC-Based Final Aging

The Final Aging was conducted on a DAAAC-modified mule engine, as discussed earlier in the Methods section of the report. The details and derivation of the Final Aging cycle are discussed in detail in that section. This section of the report discussed the observations made during the aging itself. Emission test results at various points in the Final Aging process are discussed in the next report section.

As noted earlier, 1,000 hours of aging were run, which were equivalent to 10,000 hours (435,000 miles) of field operation, including chemical and sulfur exposure. The regeneration and deSO_x frequency was 10X normal, so zCSF regeneration was conducted every 10 hours, and LO-SCR deSO_x was conducted every 30 hours. Figure 102 shows a sample of data from the actual aging, taken in this case from a cycle early in the first 333-hour segment of aging. Key temperatures are shown, as is the differential pressure across the zCSF, which gives an indication of soot loading and regeneration. As seen in the traces, soot loading was observed at the lower temperature FTP and LLC derived modes, and passive soot oxidation was observed at the higher temperature RMC-SET derived modes. Early in aging, the filter was mostly cleaned of soot via passive soot oxidation, but it was noted that later during aging the rate of passive soot oxidation slowed, and the system relied more on the Active regeneration event for cleaning.

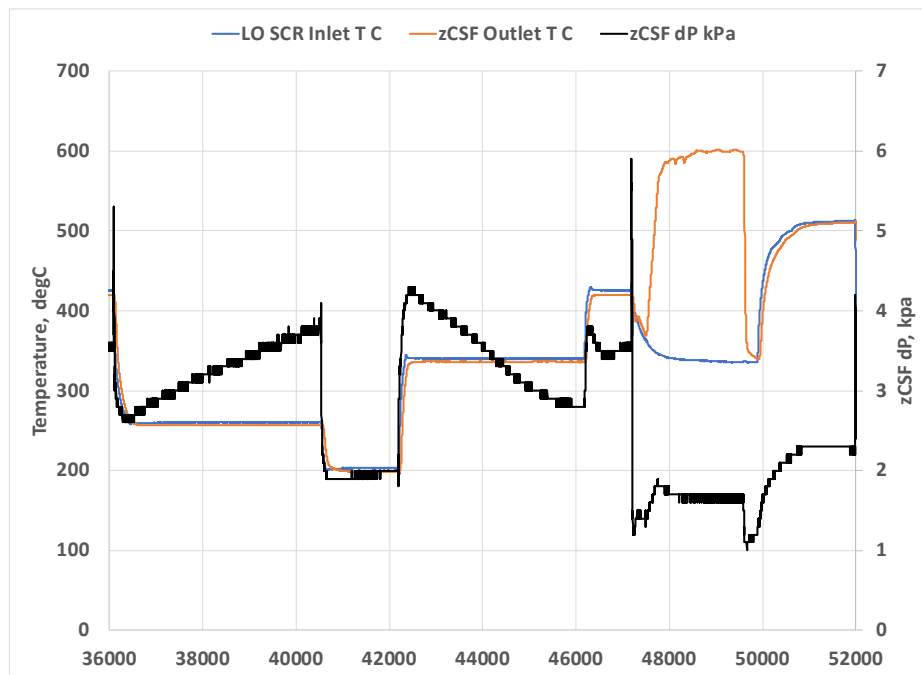


FIGURE 102. EXAMPLE OF SINGLE BASE AGING CYCLE – INCLUDING ZCSF REGENERATION AND LO-SCR DESO_x EVENT

A longer segment of aging, covering roughly 40 hours of aging duration, is shown in Figure 103. This shows the regular cycling of soot loading on the filter, as well as the relative frequency of downstream (zCSF) Active Regeneration events, and LO-SCR deSO_x events. As can be seen,

the overall differential pressure across the zCSF is stable on this timescale, although it should be noted that a slow increase could be seen over time as ash was slowly building up on the filter.

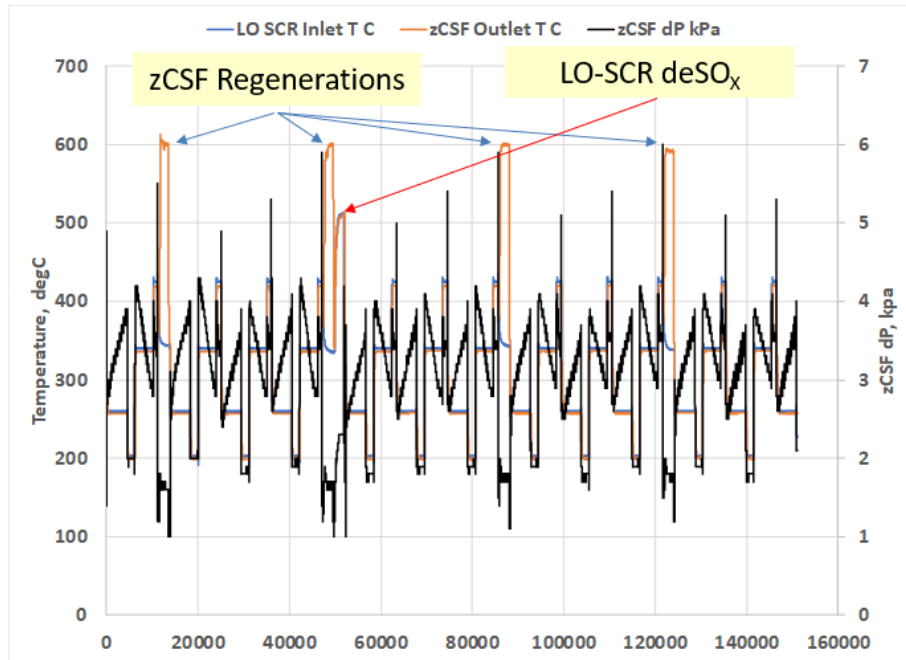


FIGURE 103. 40-HOUR SEGMENT OF FINAL AGING CYCLE DATA

For the first 333-hour segment of aging, the temperature target for deSO_x was 525°C. However, there were some issues implementing this temperature on the aging mule engine, and therefore that target was not always reached. The impact of this is discussed more in Section 3.8 which discusses deSO_x results in detail. This issue was corrected for the second 333-hour segment of aging. However, this temperature proved to be insufficient for complete deSO_x, and therefore the temperature was increased to 550°C for the final 333-hour segment of Final Aging.

Although laboratory NO_x instrument measurements were not taken during aging operation, the three system NO_x sensors were monitored continuously during aging. This NO_x sensor data can provide insights into long term trends, as well as highlight AT behaviors during events like Active Regeneration and deSO_x that were not conducted in the emissions cell. Figure 104 shows an example of NO_x sensor data from 40-hours of aging during the first 333-hour aging segment. The DEF dosing was set at fixed ANR setpoints to match what the Stage 3 model strategy would have targeted, although these were later refined to match the model more closely. The majority of NO_x conversion at low temperature is done by the LO-SCR, while at higher temperatures, the LO-SCR only does some conversion and the downstream system does the bulk of the NO_x reduction work.

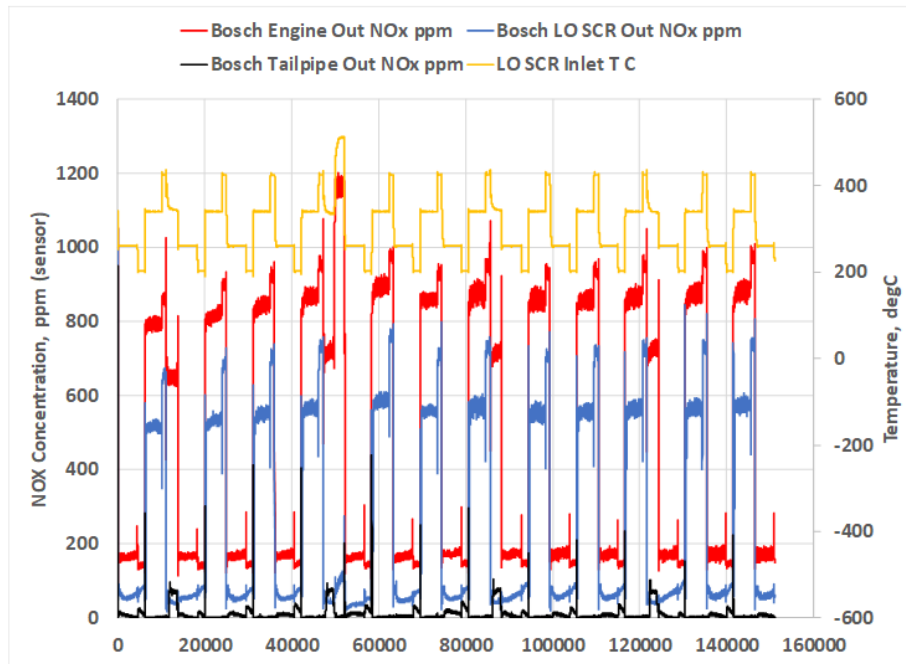


FIGURE 104. EXAMPLE NO_x SENSOR DATA OVER 40 HOURS OF FINAL AGING – EARLY DATA SETS

The behavior during Active Regeneration is of particular interest. Even though this mode is at a system inlet temperature of 350°C, conversion over the LO-SCR is calibrated to be high, because it is expected that the downstream system will struggle to convert NO_x during Active Regeneration of the downstream system. However, dosing was initially targeted to attempt some conversion of the downstream system. As seen in Figure 104, this does not work well, as the tailpipe NO_x (black) actually rises above the LO-SCR outlet NO_x (blue) during Active Regeneration. The downstream SCR is at 575°C during this mode, and it is apparent that the relatively small amount of ammonia being dosed is oxidized into NO_x under these conditions, rather than reducing the remaining NO_x coming from the LO-SCR. This that the downstream system cannot participate effectively in NO_x reduction during Active Regeneration. This information is important for later Infrequent Regeneration Adjustment Factor (IRAF) calculations, because it means that tailpipe NO_x can only be as low as the LO-SCR alone can achieve. This can be minimized somewhat by using the TM-2 mode during regeneration, but it still means there will likely be some impact, as noted later in Section 3.11.

On the other hand, during LO-SCR deSO_x, the ANR is set to 1.3 at the LO-SCR, and that catalyst still does a substantial amount of NO_x conversion, even in later 550°C runs. The downstream system is only at 475°C at this point, and is easily able to remove whatever NO_x remains after the LO-SCR. This helps to confirm previous assessments that LO-SCR deSO_x can be done without impacting tailpipe NO_x performance negatively.

Aging proceeded without incident until roughly the 200-hour mark. At this point there was a failure on the aging-mule engine relative to the EGR control valve. This failure caused excessive soot loading in the zCSF, and there was a subsequent large exotherm on the filter. Ultrasound diagnostics revealed a crack near the back of the filter around part of the radius. Aging was stopped, and it was determined that the exotherm was localized to the zCSF and did not impact the downstream SCR. The filter was deemed to be too fragile to continue aging, but the rest of the system was unaffected. Therefore, a spare zCSF could be installed in the system to continue the experiment. However, this would mean that the zCSF would be less aged than the rest of the system. It should be noted that in a production engine, a failure of this sort would likely be detected prior to reaching to point of causing damage, either by EGR diagnostics or by the filter differential pressure sensors. In this laboratory prototype situation, the long-term behavior of the zCSF was not yet understood, and aging mule engine did not itself has robust EGR diagnostics active. Diagnostics were added to the aging stand to prevent another failure of this kind moving forward.

To continue the experiment, a replacement zCSF was installed in a dedicated canning setup, and placed downstream of a spare LO-SCR in exactly the same position it would be in during normal aging. In this manner, 200 hours of aging were run to “catch up” the zCSF to the rest of the system, using cycling identical to the normal Final Aging process. This was completed, and ash weights confirmed a similar amount of ash load as the previous zCSF. At that point, the catch-up aged zCSF was reinstalled in the Stage 3 system, and aging proceeded forward as normal. Additional safeties were added to the aging stand to prevent a recurrence of the problem, and also the regeneration was modified to include a more conservative staged ramp up to temperature. This would later prove important as passive soot oxidation was observed to deteriorate somewhat in the later aging segments.

The system was emission tested at 333 hours, 667 hours, and 1000 hours of aging. In addition to this, an ash cleaning was performed on the filter at 500 hours, as it was assumed that at least one ash cleaning would be needed over the course of 435,000 miles, which is typical for current production. At the 1000-hour point, the system would be tested both before and after ash cleaning. In this way test points were conducted at a wide variety of ash loading points, up to the peak of 35 g/L. Table 11 summarizes several descriptive statistics tracked over the course of aging at various break-points.

TABLE 11. AGING STATISTICS FOR VARIOUS TEST POINTS DURING STAGE 3 FINAL AGING

Aging Point	% FUL	Equivalent Miles	Ash Load	Oil Exposure	Sulfur Exposure	Notes
334	33%	145,000	26 g/L	53.1 kg	1070 g	Emission Test
500	50%	217,500	35 g/L	65.7 kg	2134 g	Ash Cleaning
667	67%	290,000	12 g/L	89.6 kg	3200 g	Emission Test
1000	100%	435,000	33 g/L	138.2 kg	1600 g	Emission Test

These tracked elements give a sense for the overall exposure to various potential drivers of degradation. By the end of Final Aging at the 1000-hr point, the LO-SCR had been exposed to 183 grams of sulfur per liter of catalyst (not including the ASC volume), and 18 g/L of phosphorous (P). Much of this exposure was at temperatures below 250°C, and the temperature cycling resulted in a realistic deposition of poisons. By the end of the aging process, the downstream system had been exposed to 67 hours of Active Regeneration (including ramping time), and the LO-SCR had been exposed to 20 hours of deSO_x. These values are consistent with the expected regeneration frequency over 10,000 hours of real-world operation, and the number of events and exotherms would also match 435,000 miles of field operation.

Figure 105 shows an example of aging data from 20-hour long segment near the end of the aging run, at about the 900-hour mark. Note from this data that at the RMC-average mode around 365°C there is little evidence of passive soot oxidation, where it had been working quite well when the zCSF was newer. However, Passive soot oxidation is still very active at the 425°C RMC-high mode. These indicate some loss of NO-NO₂ oxidation capability at lower temperatures across the zCSF, coupled with the impact of ash loading. There is evidence of slowly increasing differential pressure from one base cycle to the next, until the filter is cleaned off during Active Regeneration. Even though there is less overall high temperature exposure on these parts than for the Development Aged parts, the combination of real exotherm ramps and especially exposure to chemical poisons has significantly impacted lower temperature performance.

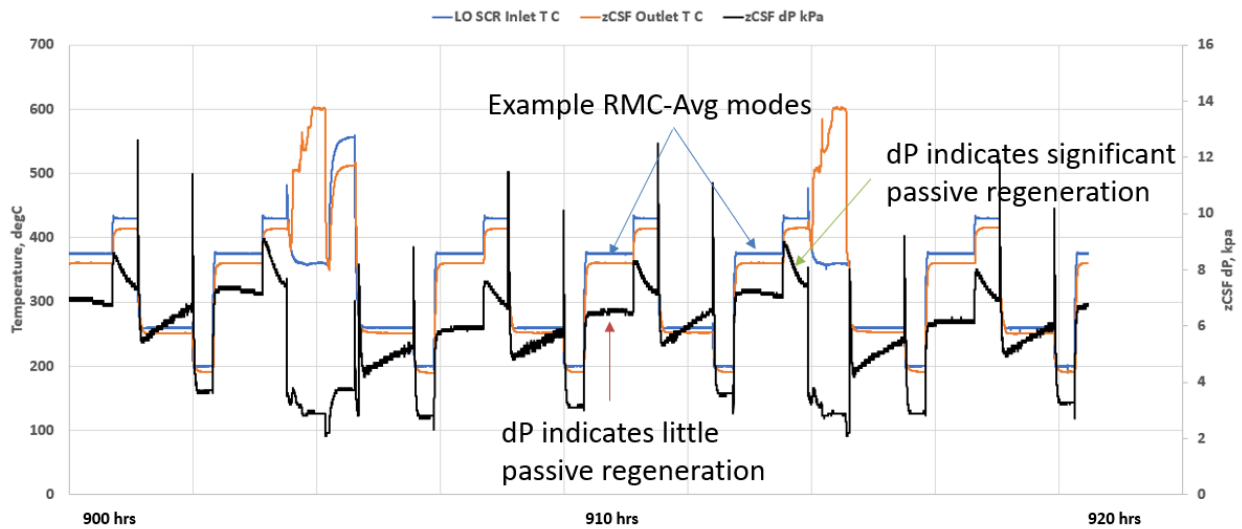


FIGURE 105. EXAMPLE OF AGING DATA NEAR THE END OF 1000-HOUR FINAL AGING

Figure 106 shows an example of visualization of ash loading inside the filter. This image is taken via a CT-scan, which can produce an image of actual buildup of ash in the channels of the filter. This image was taken at the 500-hour mark prior to ash cleaning, when ash load was at 35 g/L. Following ash cleaning, subsequent scans indicate this material has been removed. CT-scan images of parts like this from the field indicate similar patterns, and this image verifies the buildup of lube-oil related material in the AT system during aging.

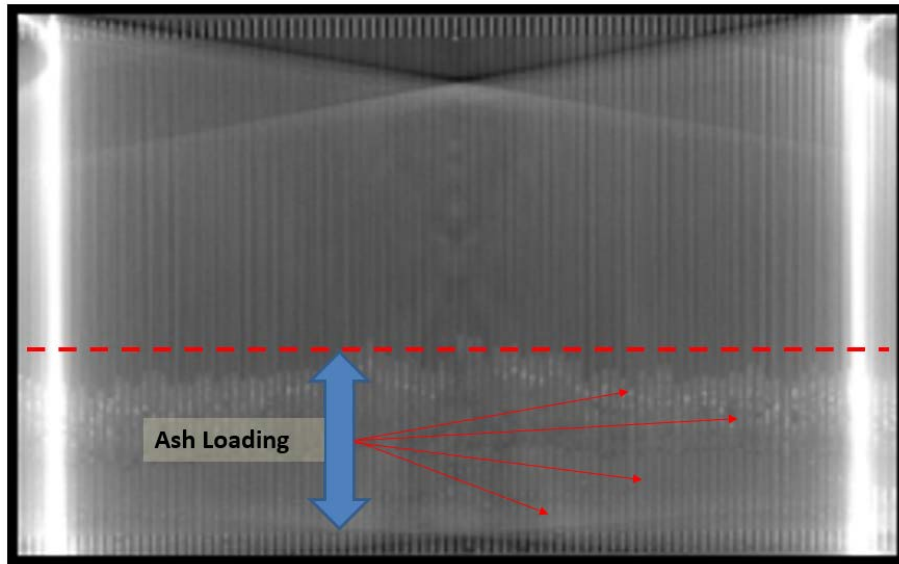


FIGURE 106. EXAMPLE OF FILTER ASH LOADING VISUALIZATION VIA CT-SCAN (500 HOURS, 35 G/L ASH LOAD)

Figure 107 shows an example of NO_x conversion of the LO-SCR before and after the high temperature deSO_x event. A clear difference in NO_x conversion at the low temperature modes (235C and 200C) can be seen before and after the deSO_x at 525°C. This demonstrates the build-up and cycling of sulfur on the catalysts during aging.

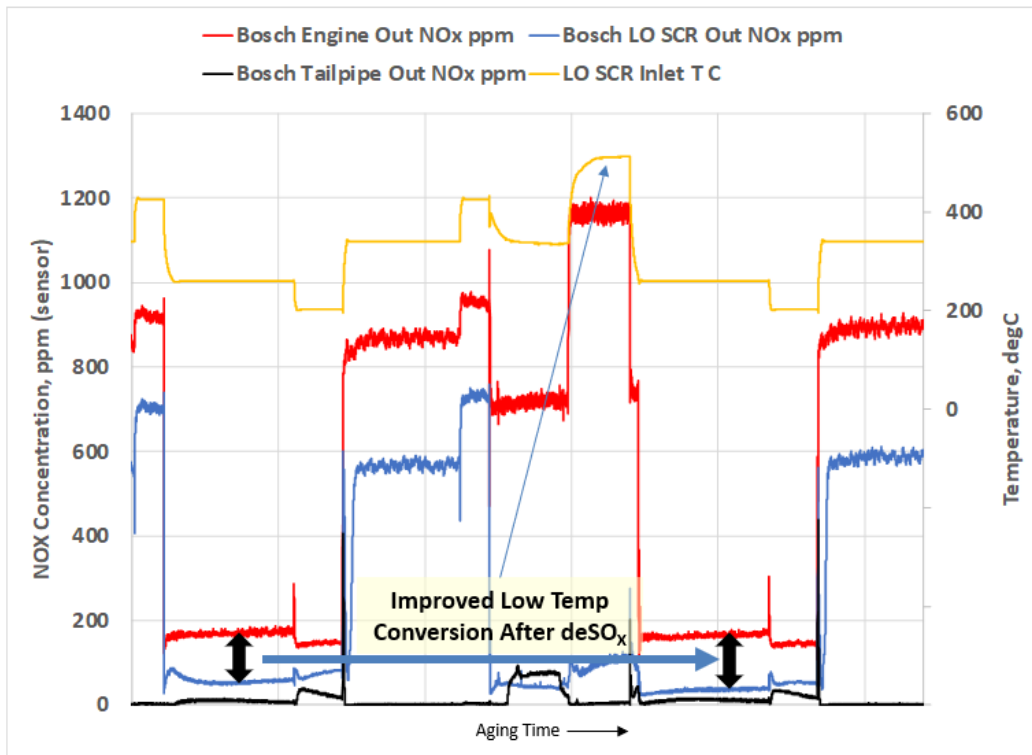


FIGURE 107. LO-SCR CONVERSION BEFORE AND AFTER DESO_x DURING AGING

Behaviors like these illustrated the impact of the chemical aging portions of the DAAAC-based Final Aging protocol, and they also serve to highlight the importance of including these factors in a robust FUL demonstration.

3.7 Emission Performance of Final Aged Parts at Various Test Points

Emission performance of the Stage 3 system was evaluated at 0-hr, 333-hr, 667-hr, and 1000-hr test points, with the final 1000-hr test point representing 435,000 miles of equivalent field operation. These test points helped to illustrate the impact of AT degradation on the performance of these systems. Over the course of the Final Aging experiment, a better understanding of the impact of thermal and chemical aging was gained, the management of sulfur was examined, and a better understanding of the margins needed to reach Low NO_x levels was developed. While the Development Aged parts captured some of the impacts of aging, the Final Aged results indicated the importance of a robust durability approach that also captured the chemical aspects of aging.

3.7.1. Initial (0-Hour) Performance

Figure 108 shows the performance of the degreened system prior to the start of Final Aging in comparison to the Development Aged parts, which were hydrothermally aged with the equivalent of 435,000 miles of regeneration and deSO_x operation. In general, the 0-hour parts performed similarly on the FTP, slightly better on the LLC, and significantly better on the

RMC-SET. The hydrothermal aging on the Development Aged parts appeared to have the most impact on the high load high space velocity conversion capability of the system, especially the downstream system. On the other hand, the lower temperature NO_x conversion of the LO-SCR was not impacted as much, given the lower temperature exposure experienced by the LO-SCR.

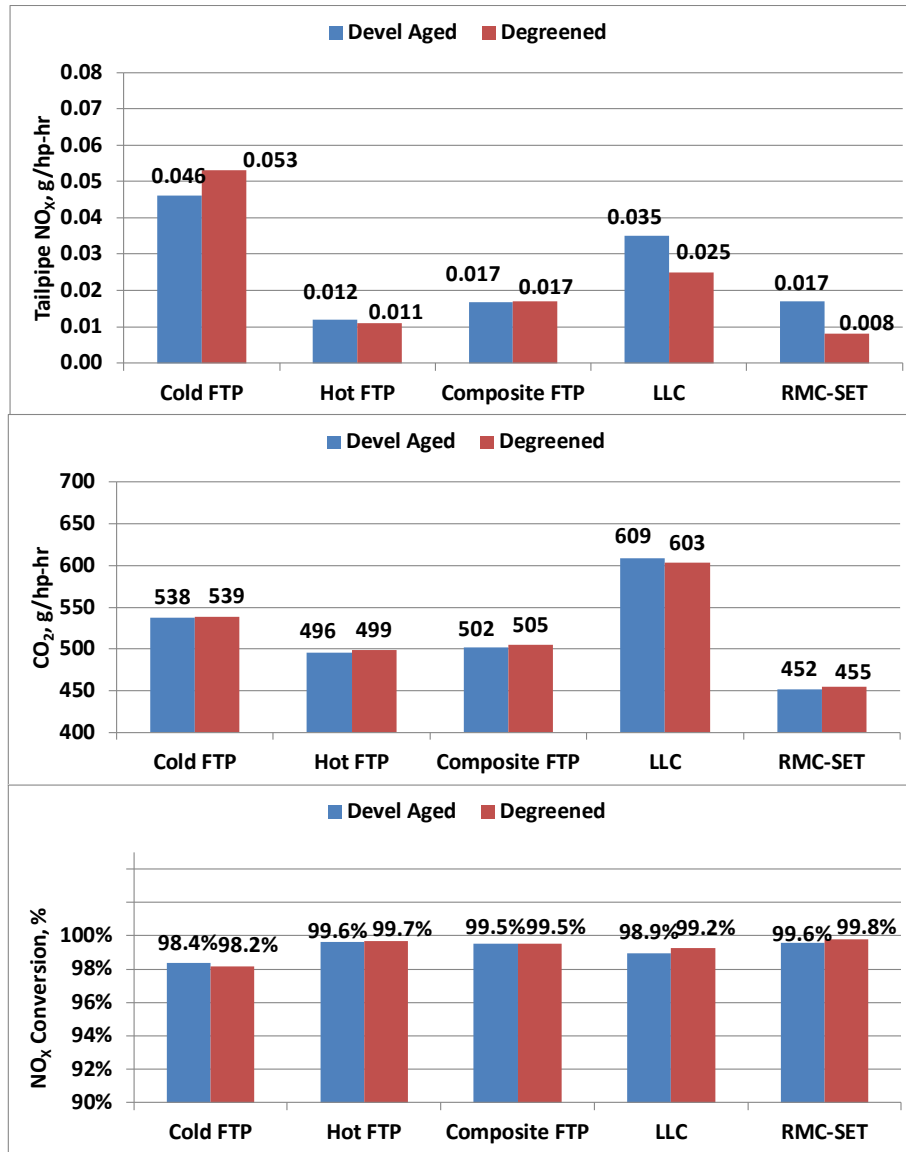


FIGURE 108. COMPARISON OF DEVELOPMENT AGED PARTS AND 0-HOUR FINAL AGED (DEGREENED) PARTS

3.7.2. Intermediate Emission Test Points (333-hour and 667-hour)

The intermediate test points allowed an opportunity to look at system performance and how it might degrade over time, prior to the final test points. They also allowed for corrections to the strategy or to the aging conditions based on what was observed. As mentioned earlier, it was not

clear how much margin would be needed at the beginning of the program, and therefore adjustments might need to be made.

Detailed emission test results for each of these test points are given in Appendix A. Figure 109 depicts a summary of tailpipe NO_x performance at various points during the evaluation, and following key experiments at the intermediate test points. It shows hot-start FTP tailpipe BSNO_x at several conditions, and the various evaluations and adjustments made along the way.

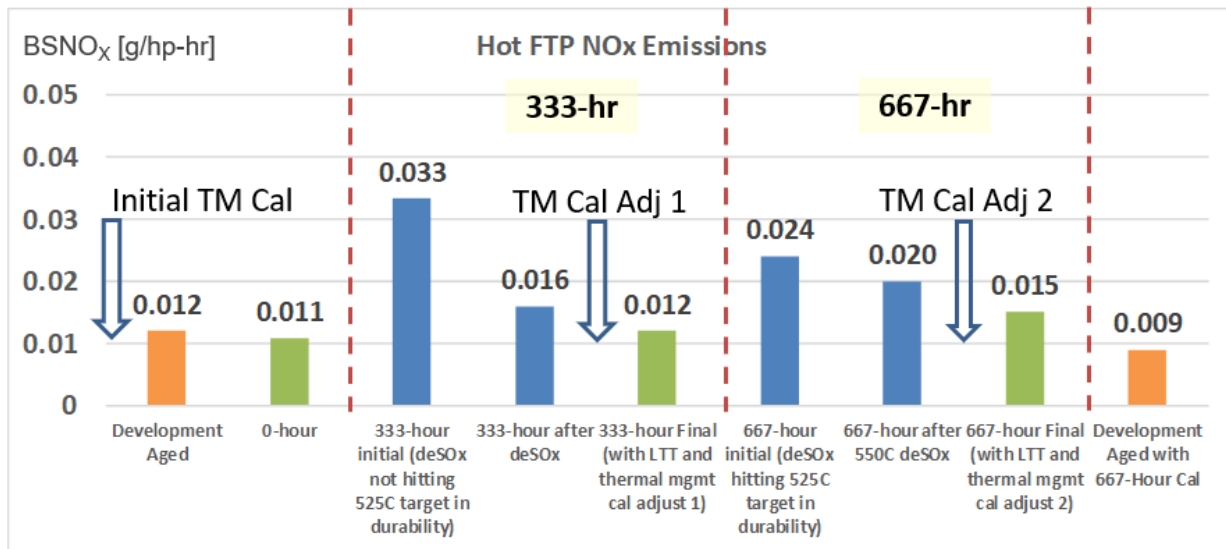


FIGURE 109. HOT-START FTP TAILPIPE NO_x LEVELS AT VARIOUS INTERMEDIATE TEST POINTS

Following the first 333-hour durability (33% FUL), the initial emission runs indicated a substantial drop in LO-SCR performance, with hot-start FTP tailpipe NO_x at 0.033 g/hp-hr (99.1% NO_x conversion, and 68% conversion across the LO-SCR). It was further noted that the LO-SCR appeared to have lost some conversion capability in regions of low temperature (near 200°C) and high space velocity. However, as noted earlier, it had been observed that the deSO_x modes had not been reaching the target temperature of 525°C during this aging run. Figure 110 shows a summary of deSO_x temperatures hitting during the first 333 hours of Final Aging. The data show that the LO-SCR was not actually reaching the 525°C target for a significant portion of the first aging period. As a result of these low temperatures, there was concern that excess stored sulfur was still present on the LO-SCR, even though the last few deSO_x events were corrected prior to the end of the aging period.

Desulfation experiments were conducted to examine the degree to which stored sulfur may have impacted LO-SCR performance, given the fact that correct deSO_x temperatures were not consistently reached. There was also the question of whether performance was recoverable. Details of these deSO_x experiments are given later in Section 3.8. As noted in Figure 109, hot-start performance after these deSO_x experiments was 0.016 g/hp-hr (99.5% conversion and 73%

across the LO-SCR). This indicated that the excess sulfur that had not been removed was impacting performance, and that reaching a proper deSO_x temperature could recover that performance.

However, the tailpipe NO_x level was still higher than the 0-hour level of 0.011 g/hp-hr. After the deSO_x, the long term trim (LTT) was applied to the storage targets, although in this case the changes were minor and involved only adjustments on the LO-SCR at lower flow rates between 275°C-325°C. At this point, LO-SCR performance matched the 0-hour data set, but there appeared to have been some loss in downstream SCR performance. DeSO_x experiments were run on the downstream system, as detailed in Section 3.8, but these indicated there was no issue with residual sulfur storage on the downstream system.

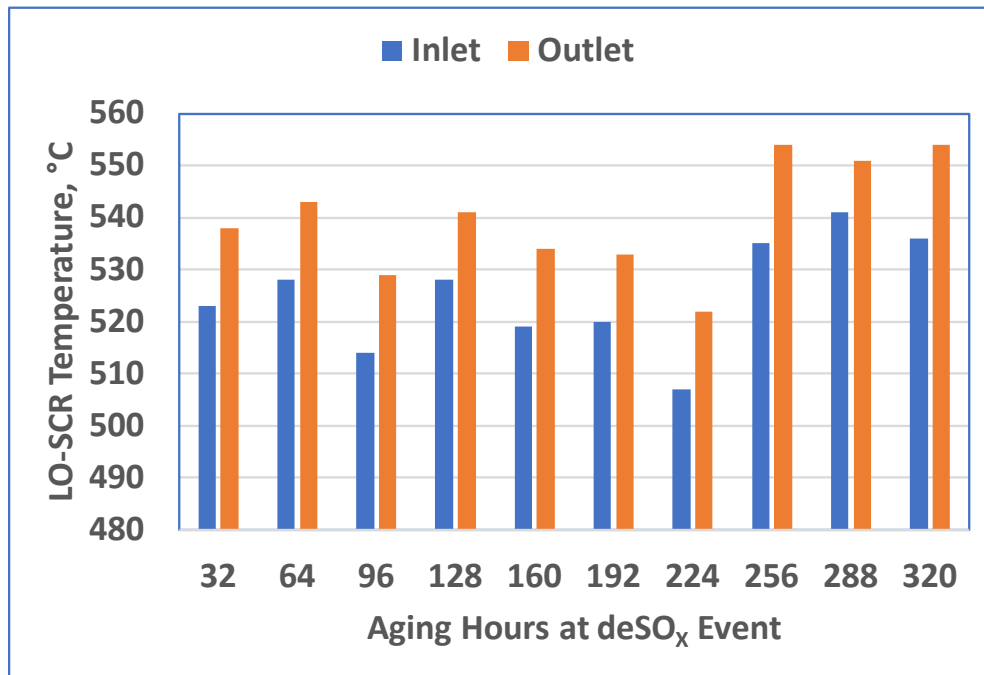


FIGURE 110. TEMPERATURES DURING DESO_x EVENT FOR FIRST 333 HOURS OF FINAL AGING

Therefore, it was determined that the initial thermal management calibration did not create sufficient margin for degradation. The temperature switch points were modified to widen the operating range of the TM-2 mode slightly, and a small modification was made to the engine calibration in that mode. This resulted in improved emissions, as documented in Figure 109, to 0.012 g/hp-hr, which is nearly the same as the 0-hour level. However, this change resulted in a 1% shift upwards in CO₂ due to increased thermal management. This still left the system with a 1% improvement compared to the baseline engine.

At the 667-hour point, performance was checked using the same calibration that was utilized for the 333-hour point. The initial emission results indicated a hot-FTP level of 0.024 g/hp-hr. It was noted again that the LO-SCR indicated a loss of performance at low temperature

and high space velocity. In this run, the aging engine operation had been adjusted so that the deSO_x was reaching 525°C reliably. However, subsequent deSO_x experiments, documented in Section 3.8, revealed that a temperature of 550°C was really necessary to fully manage long-term sulfur accumulation. Following the deSO_x, hot-start FTP performance was at 0.020 g/hp-hr. Figure 111, shows an example of the improved LO-SCR performance after deSO_x in the lower temperature parts of the hot-start FTP.

Application of the long-term trims to the storage targets did improve performance to 0.017 g/hp-hr, and this time the trim adjustment routines did indicate changes on the downstream SCR system, as the tailpipe deviations were now large enough to be spotted in some areas. Storage targets on the downstream system were increased in several areas of the map, which did help with performance.

However, this improvement was not enough to restore performance to the levels observed at the 333-hour test point, and it was apparent that there had been a further loss of performance on the downstream SCR system. Again, it was apparent that the thermal management calibration did not provide sufficient margin for AT degradation, and further modifications were made.

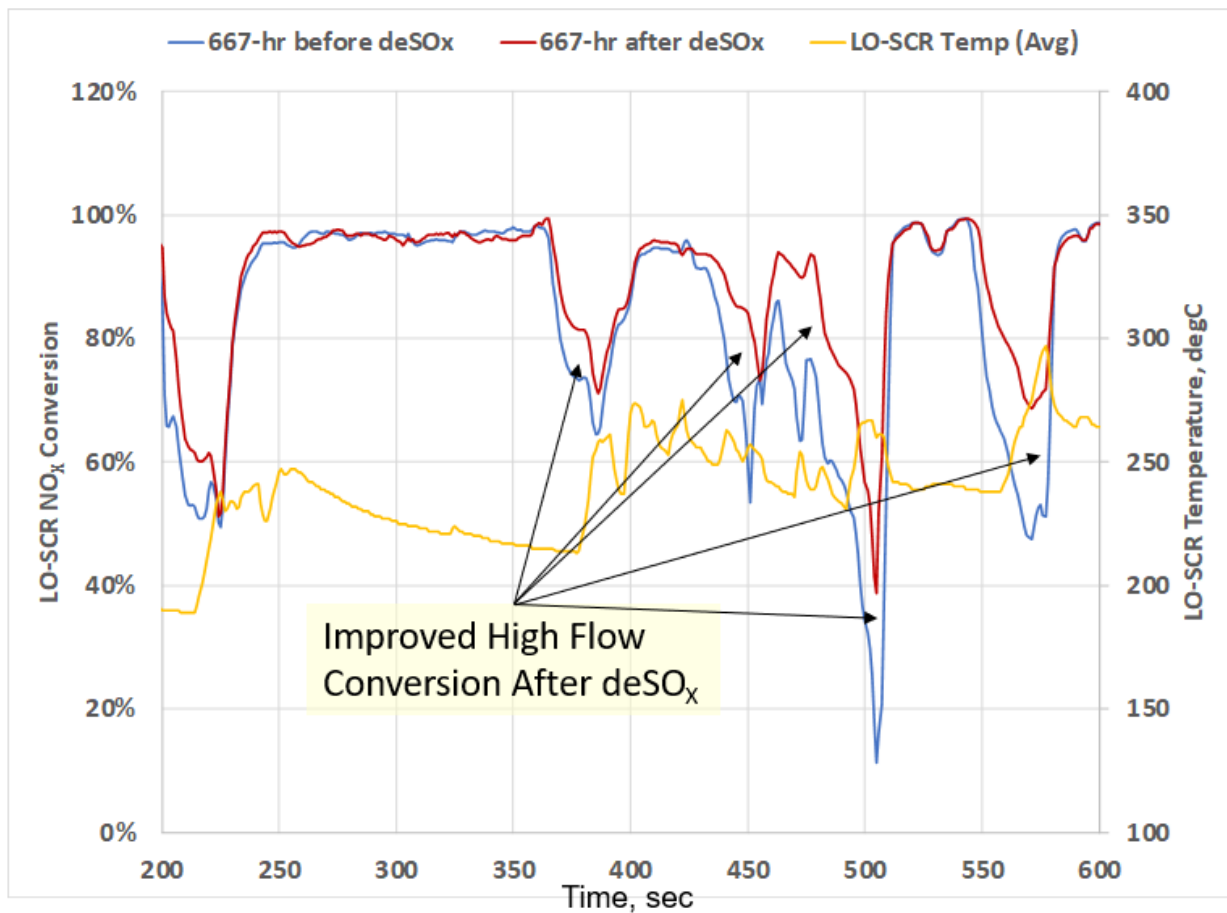


FIGURE 111. EXAMPLE OF IMPROVED LO-SCR CONVERSION AT HIGH SPACE VELOCITY AFTER 550°C DESO_x AT 667 HOURS

The temperature thresholds on the thermal management were adjusted to retain the TM-2 mode longer during transition periods, where previously the switch to the low CO₂ FE mode was more aggressive. This reduced engine-out NO_x somewhat at moderate temperatures, allowing the system to control NO_x better. These changes are illustrated in Figure 112, and they reduced the burden on the downstream system in areas where that system is at marginal temperatures. This not only reduced NO_x spikes in that area, but allowed a small reduction in low temperature storage that reduce late cycle NO_x from post-SCR slip. However, this change was made not without cost, and it resulted in a further 0.5% increase in CO₂. At this point, the CO₂ on the FTP was comparable to the baseline engine. The changes were somewhat larger on the LLC, as noted below.

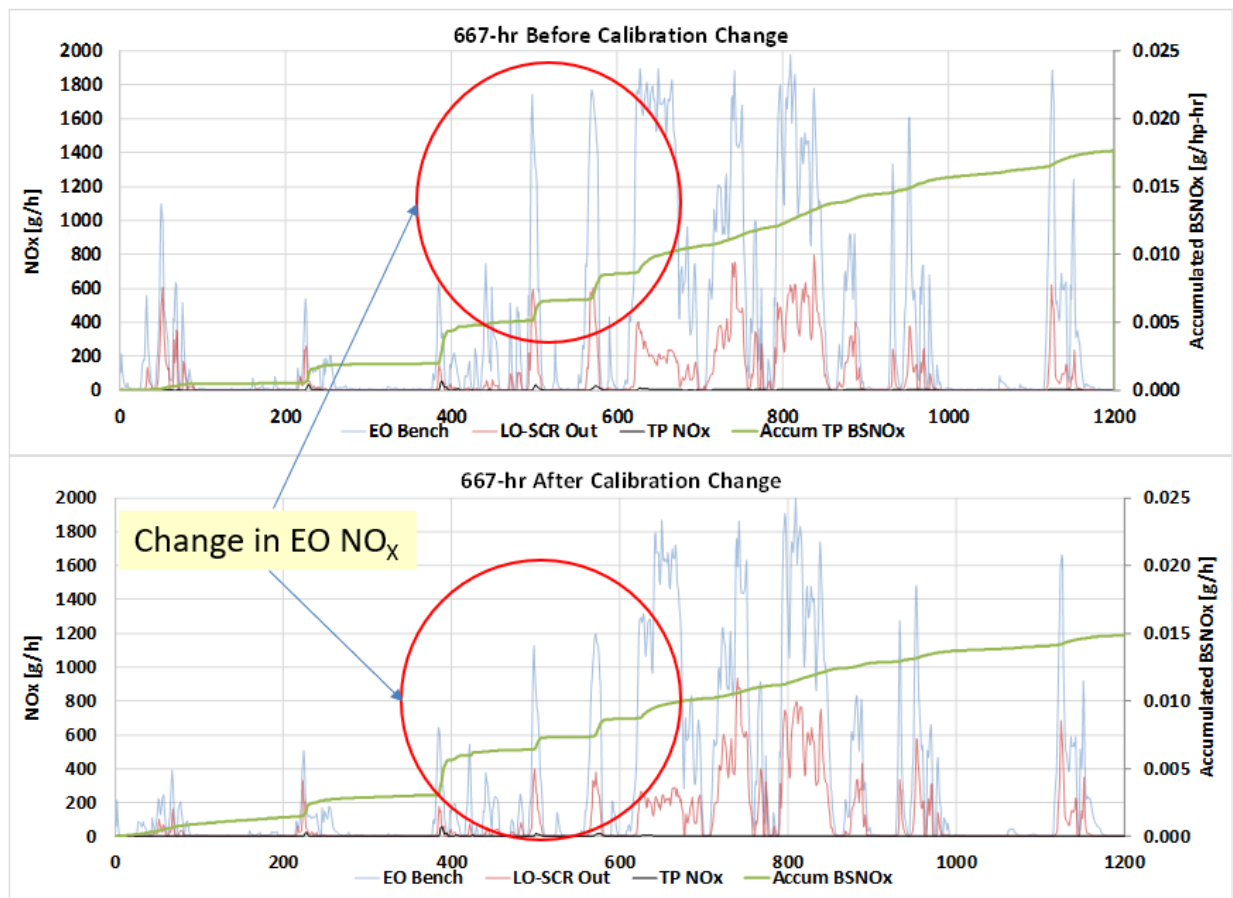


FIGURE 112. EMISSION IMPACT OF 667-HOUR CALIBRATION CHANGE

At this point, as seen in Figure 109, hot-start FTP NO_x was at 0.015 g/hp-hr, and composite FTP NO_x was at 0.022 g/hp-hr, above the 0.02 g/hp-hr target. It is likely that further thermal management modifications could have been made to lower NO_x further. However, these would have increased CO₂ emissions further, and that would have resulted in a net penalty to CO₂. It was felt that understanding the system capability at a CO₂-neutral level of fuel consumption was a critical output. Therefore, the 667-hour data was generated at this point, and further thermal management modifications were not made.

A change in performance was also noted in the high load high space velocity regions of the RMC-SET. At the 333-hour point, there had been some movement in high-load conversion, but the RMC-SET tailpipe NO_x was still at 0.015 g/hp-hr. However, further movement was seen as aging continued, and therefore initial test results on the 333-hour calibration indicated a NO_x level of 0.023 g/hp-hr. This was due entirely to increased tailpipe NO_x at the B100, C100, and C75 modes, the highest temperature and space velocity modes. The original calibration relied very heavily on only the downstream SCR under these conditions, however this did not provide sufficient margin for degradation on the downstream SCR catalyst. The increases were found to be due to ammonia slip and a small loss of selectivity in the ammonia oxidation function on the ASC. The long term trim adjustments which increased storage pushed this function harder.

As a countermeasure to this change, the balance between the catalysts was shifted at high temperatures (above 400°C) to rely more on the LO-SCR. This did not affect other cycles which did not operate in this area. Figure 113 shows a comparison of RMC-SET emissions at both test points. As can be seen, light-off SCR conversion is significantly higher in the period between 1200 to 1400 seconds, and between 1650 and 1850 seconds. It should be noted that this shift did not compromise passive soot oxidation as the NO_x-to-soot ratio at the zCSF inlet in these areas was still well over 150:1. Due to flow rate limitations on the prototype heated doser, a small adjustment was made to engine-out NO_x at B100 and C100, but this did not impact CO₂ by more than 0.1% as NO_x was still in the 4 g/hp-hr range.

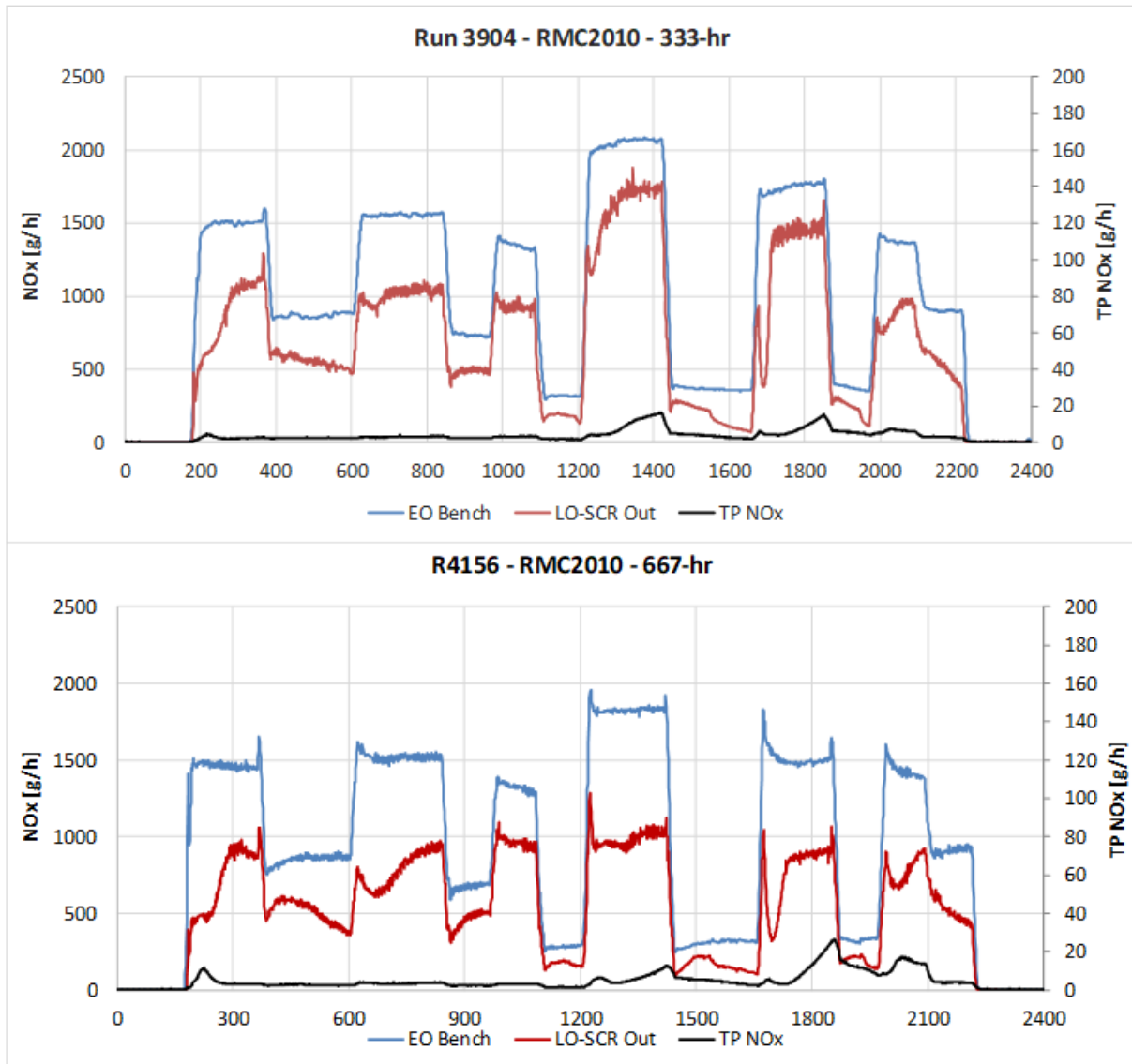


FIGURE 113. COMPARISON OF RMC-SET EMISSIONS – 667-HOUR VERSUS 333-HOUR SHOWING SCR SYSTEM BALANCE

Figure 114 shows a summary of tailpipe NO_x and CO₂ emissions considering both of the intermediate test points. It was noted that the shift in CO₂ compared to the baseline was larger than what had been expected at the 667-hour point baseline on the development data. During the aging to the 1000-hr point, the baseline AT was reinstalled and the engine was put back into stock configuration to support a check of baseline emissions and Phase 2 GHG baseline testing. At this point, it was noted that the engine itself had shifted upwards in CO₂ by about 0.7% from the original baseline. Starting with the 667-hour data, all subsequent GHG comparisons were made by comparing to the Baseline Repeat CO₂, rather than the original baseline. This was done so that the underlying engine shift would not disturb the comparisons. It should be noted that at this point, roughly 1000 hours of operation had been conducted on the X15 engine.

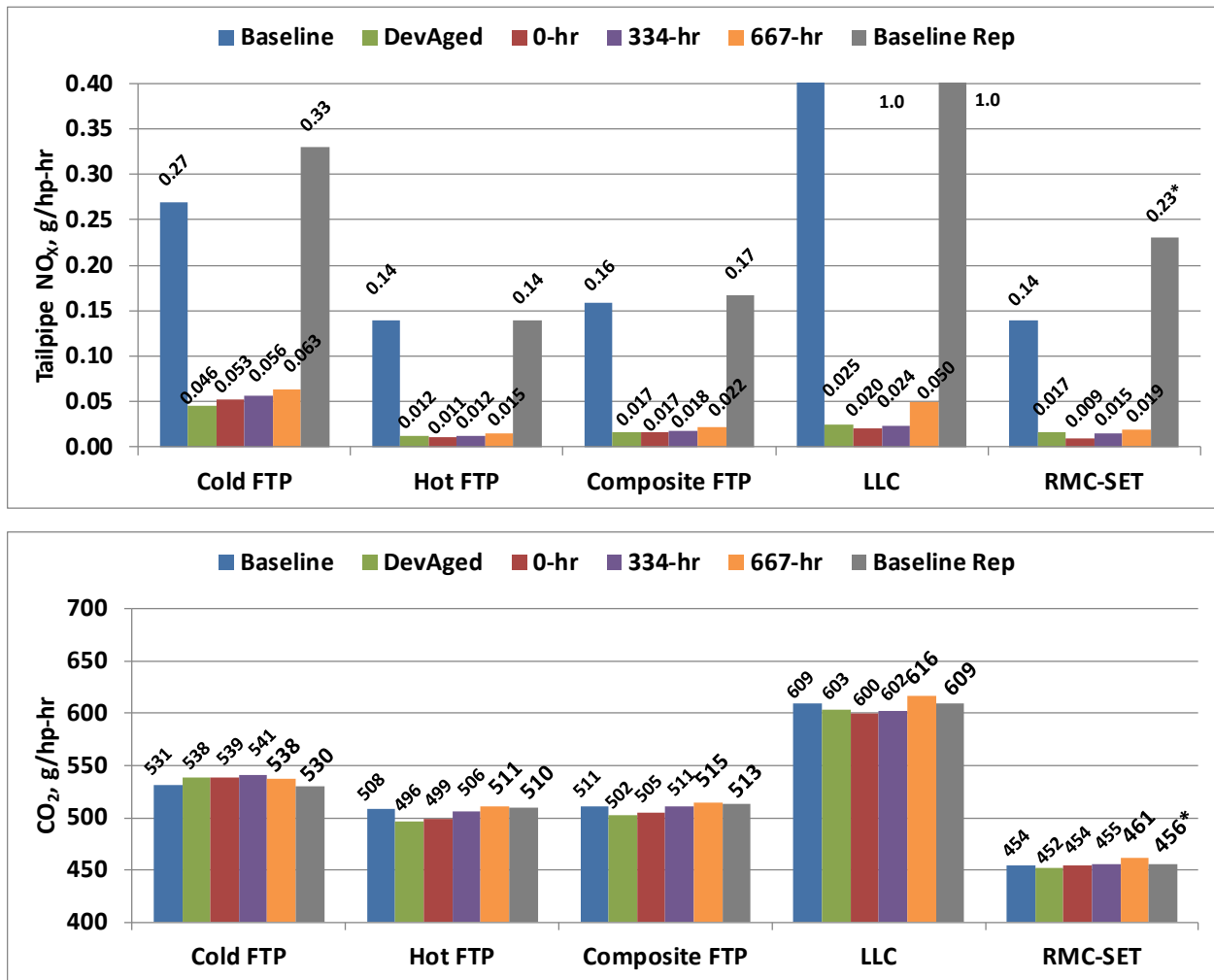


FIGURE 114. EMISSION SUMMARY FOR INTERMEDIATE TEST POINTS ON ALL CYCLES

It was noted that at this point, FTP emissions were at 0.022 g/hp-hr. The LLC was still well below target at 0.024 g/hp-hr at 333 hours, but saw considerable loss of performance at the 667-hr mark, even after the 667-hour calibration change (which also resulted in a 1% increase in fuel consumption at 667 hours on the LLC). At the 667-hour point, LLC emissions were right at 0.05 g/hp-hr. There had also been some loss of high temperature performance on the higher load RMC-SET, with levels just below target at 0.019 g/hp-hr.

3.7.3. Full-Useful Life Emission Tests

The final emission evaluations were conducted at the end of the 1,000-hour aging period, when the AT system had the equivalent of 435,000 miles of aging accumulated. At this point, the filter was also near the peak ash load of 35 g/L. Emission evaluations were conducted both before and after ash cleaning. Detailed emission results for all measured pollutants are given in Appendix A for both test points. As noted earlier, in this segment, the deSO_x temperature was raised to

550°C during aging because it had become clear that 525°C was not sufficient to fully control long-term sulfur accumulation to acceptable levels.

In addition, at the 1000-hr point, it was arranged to stop the aging operation about halfway between deSO_x events, so that an additional experiment could be conducted to examine the use of shorter and more frequent deSO_x events. Furthermore, the cycle was stopped at the end of the low temperature points, such that the 425°C mode had not yet been run. This meant the equivalent of nominally 35 hours of low and moderate temperature operation were seen on both SCR catalysts, such that even loosely bound sulfur might be present. This allowed an examination of the need for a secondary, lower temperature event if the regular duty cycle did not take the temperature above 400°C periodically. These experiments are discussed on more detail in Section 3.8.

Prior to this partial deSO_x, emission performance was checked, and the hot-start level observed was 0.024 g/hp-hr. This indicated that a more frequent deSO_x was desirable, and that sustained low temperature operation in the field would likely require short periods of temperature over 400°C to be generated to liberate loosely bound sulfur, as noted in Section 3.8. Following the short deSO_x, hot-start tailpipe NO_x was observed at 0.019 g/hp-hr, indicating the recovery of SCR performance after this event. Figure 115 shows a NO_x emissions in the region of the hot-FTP where both catalysts are at relatively low temperatures. Both the LO-SCR and the downstream SCR (dsSCR) show more NO_x breakthrough before deSO_x, and both show recovery after. This indicated that both catalysts were impacted by the loosely bound sulfur that was stored at lower temperatures, and both recovered quickly.

Following this experiment, long term trims were applied to the storage targets for the dosing controller. These resulted in increased storage targets at low temperature for the LO-SCR, small decreases in storage on the front portion of the downstream SCR, and small increases in low temperature targets on the rear portion of the downstream SCR. These resulted in very little change in the FTP performance, which remained at 0.019 g/hp-hr on the hot-start, but there were some small improvements in the RMC-SET performance from 0.028 g/hp-hr to 0.022 g/hp-hr. This meant that both the FTP and RMC-SET NO_x emissions were above the 0.02 g/hp-hr level. However, no additional changes were made to thermal management because the CO₂ was already at a level equivalent to the baseline engine, and any increase would result in a net penalty. It should be noted that the storage target long-term trim changes did result a shift towards higher LO-SCR conversion on the FTP.

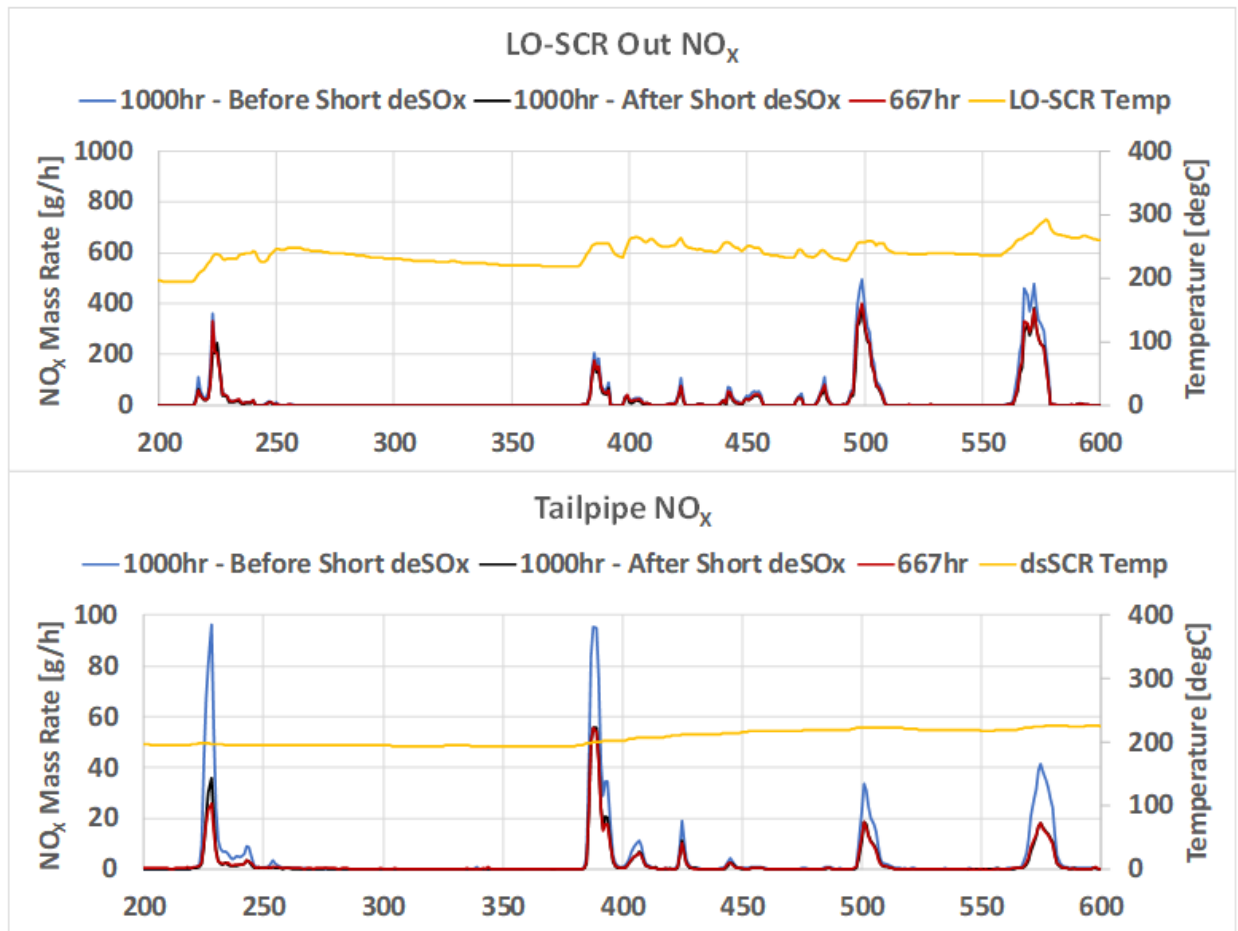


FIGURE 115. INITIAL 1000-HOUR TESTS BEFORE AND AFTER SHORT DESO_x EXPERIMENT

Figure 116 shows a summary of cycle emission results for all test points including the Final Aged 1000-hr data at 435,000 miles. The 1000-hr results are shown both before and after ash cleaning of the zCSF. There was continued movement on the FTP, with tailpipe NO_x at 0.025 g/hp-hr before ash cleaning. A slight improvement was seen after ash cleaning to 0.023 g/hp-hr, which was entirely due to improved downstream SCR performance, likely due to improved NO-to-NO₂ oxidation across the zCSF with the ash removed. Compared to the 667-hour performance, there was another slight drop in downstream SCR conversion, while the LO-SCR had similar performance to the previous result. The RMC-SET also saw another small drop in conversion at high temperature conditions, with the tailpipe emissions ending at 0.022 g/hp-hr. The LLC remained the same as the 667-hour point at 0.050 g/hp-hr, likely reflecting the lack of further movement in LO-SCR performance.

CO₂ emissions remained essentially unchanged from the 667-hour point, given that no further engine or thermal management changes were made. A slight increase in RMC CO₂ was noted when the parts were fully ash loaded, likely due to high backpressure, but this went away after ash cleaning. At the end of the experiment, FTP CO₂ emissions were equivalent to the

baseline engine, while on the LLC, CO₂ was a little over 1% higher than the baseline. The RMC-SET appears to also show an increase even at the 667-hour point, and no further change at the 1000-hr point after ash cleaning. That shift occurred at the same time as the shift in the baseline engine. However, the updated baseline RMC-SET result is somewhat compromised in that the tailpipe NO_x is above the 2010 standard, due to increased engine out NO_x at high load. At an equivalent NO_x level, CO₂ would likely have been shifted slightly higher as was observed for the FTP. Therefore, the conclusion was that RMC-SET CO₂ for the Low NO_x engine would likely also be at a level comparable to the baseline engine, when that baseline was operating properly.

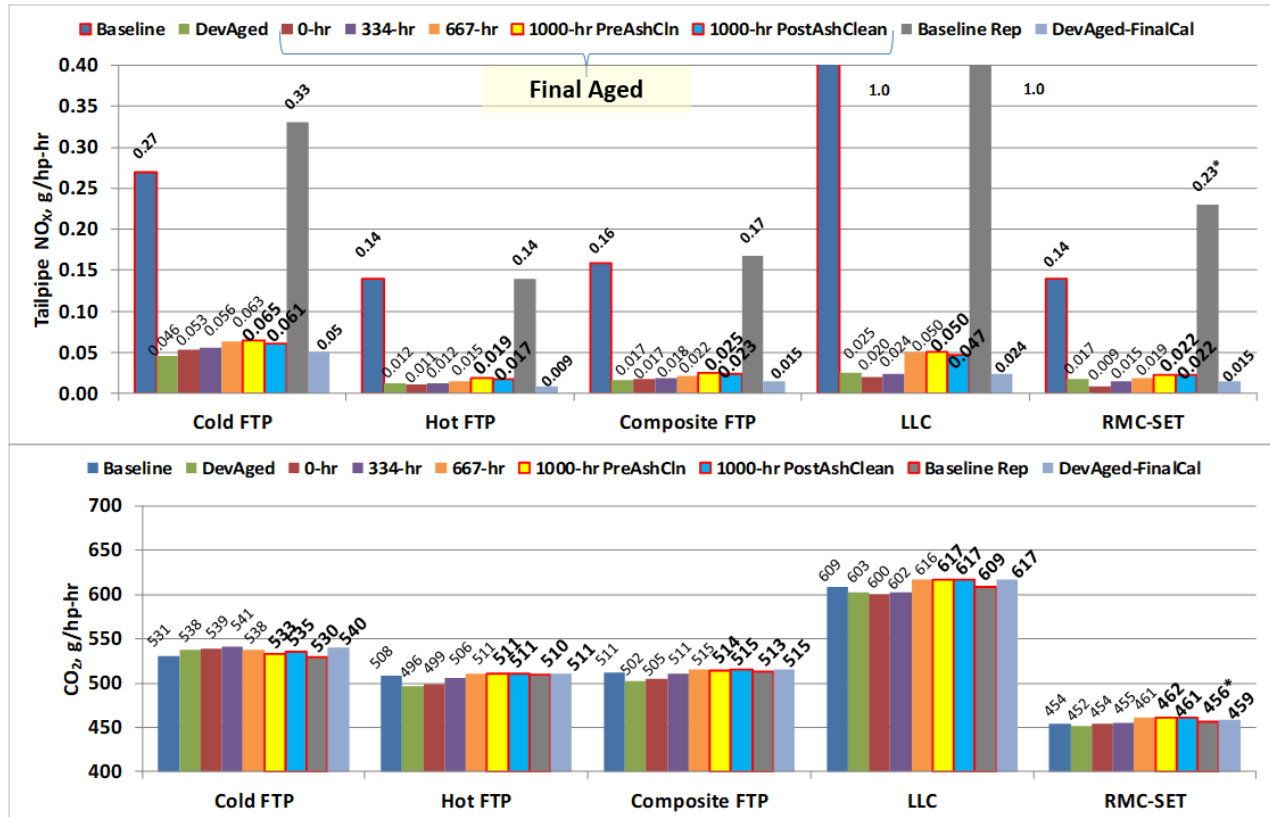


FIGURE 116. FINAL SUMMARY OF STAGE 3 CYCLE EMISSION RESULTS

While the final FTP and RMC values are slightly above the 0.02 g/hp-hr target, it is nonetheless worth noting that, at these levels, the Stage 3 engine achieved an 85% reduction in tailpipe NO_x compared to the baseline engine on these cycles, with no penalty to CO₂ and fuel consumption. On the LLC, the Stage 3 engine reduced tailpipe NO_x by a factor of 20 from the baseline engine, with a 1% penalty to fuel consumption, which on the LLC is already quite low due to the light loads. These reductions were proven durable enough to be achieved at the end of a 435,000 mile useful life. As noted later in some of the off-cycle evaluations, these reductions over such a broad range of duty cycles will translate into large real-world reductions.

Figure 117 shows the results in terms of NO_x conversion efficiency for full-useful life aged parts, comparing the Final Aged parts at 1000 hours, which were exposed to thermal and chemical aging, and the Development Aged parts which were subjected only to thermal aging. These data illustrate the importance of a robust aging protocol that includes the chemical element of aging in achieving representative results. It was noted earlier that the degreened emission performance levels, at the 0-hr point, essentially indicated a durability margin for 0.2% loss in NO_x conversion efficiency on the FTP and RMC to meet a 0.02 g/hp-hr target, and 1% loss in NO_x conversion on the LLC to meet a 0.05 g/hp-hr target. The Final Aged parts demonstrated a 0.4% loss of NO_x conversion on the FTP and RMC, and a 1.5% loss of conversion on the LLC. This indicates that in order to meet a 0.02 g/hp-hr target, the AT will need to be made more robust, such that AT degradation would be reduced by about half. However, there are several potential improvements that could be made to the Stage 3 system to improve AT system durability, as discussed later in the Conclusions. Indeed a number of these are all ready being explored in follow-on projects leveraging these Stage 3 results.

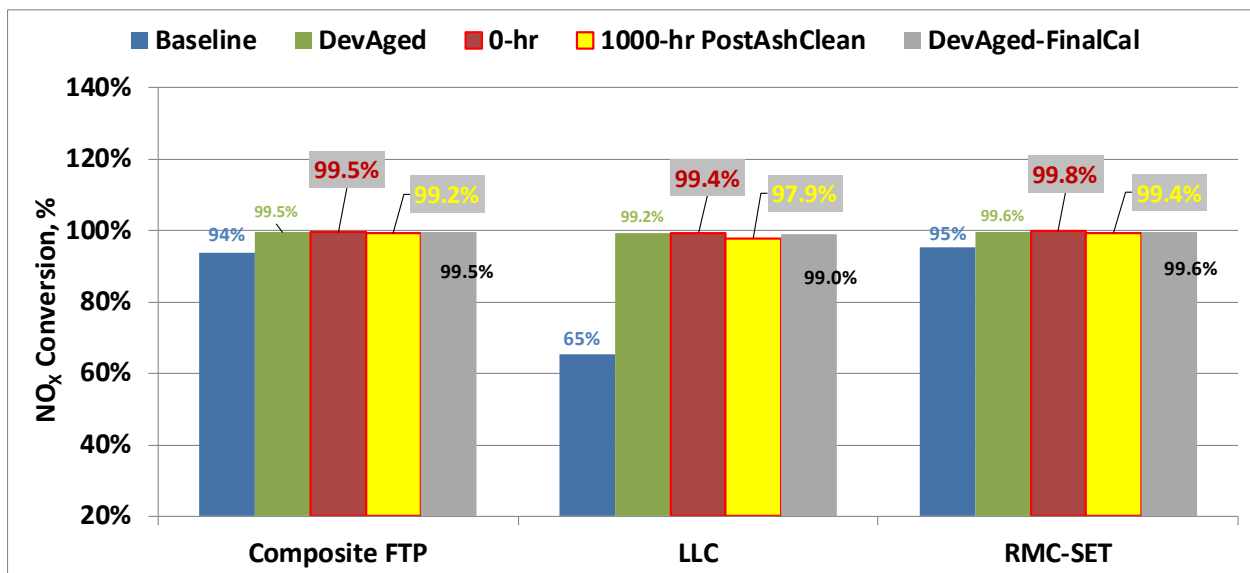


FIGURE 117. CYCLE NO_x CONVERSION EFFICIENCY AT VARIOUS TEST POINTS

Continuous data examples are shown in Figure 118 for the cold-start FTP, Figure 119 for the hot-start FTP, Figure 120 for the RMC-SET, and Figure 121 for the LLC, respectively.

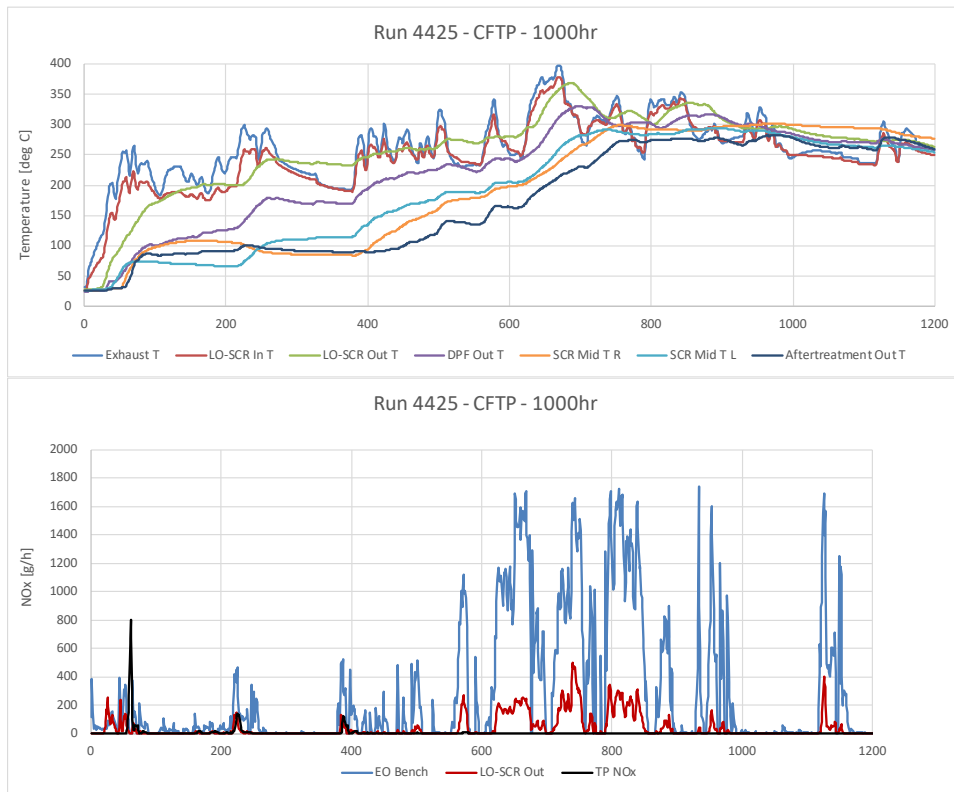


FIGURE 118. COLD-START FTP RESULT AT 435,000 MILES AFTER ASH CLEANING

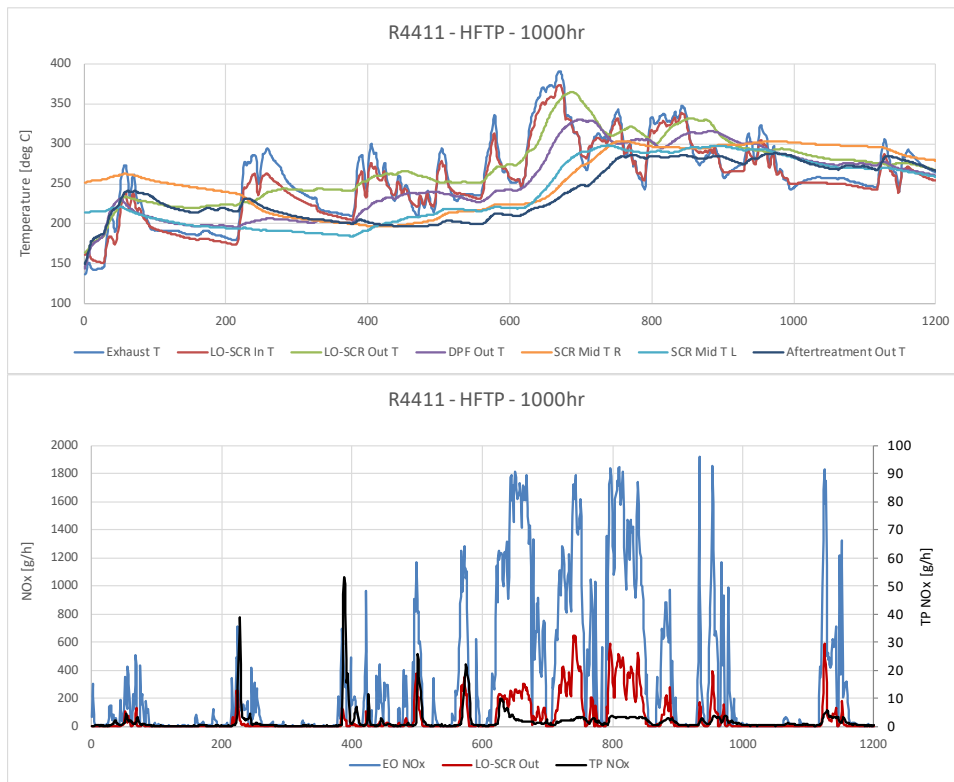


FIGURE 119. HOT-START FTP EMISSION RESULT AT 435,000 MILES AFTER ASH CLEANING

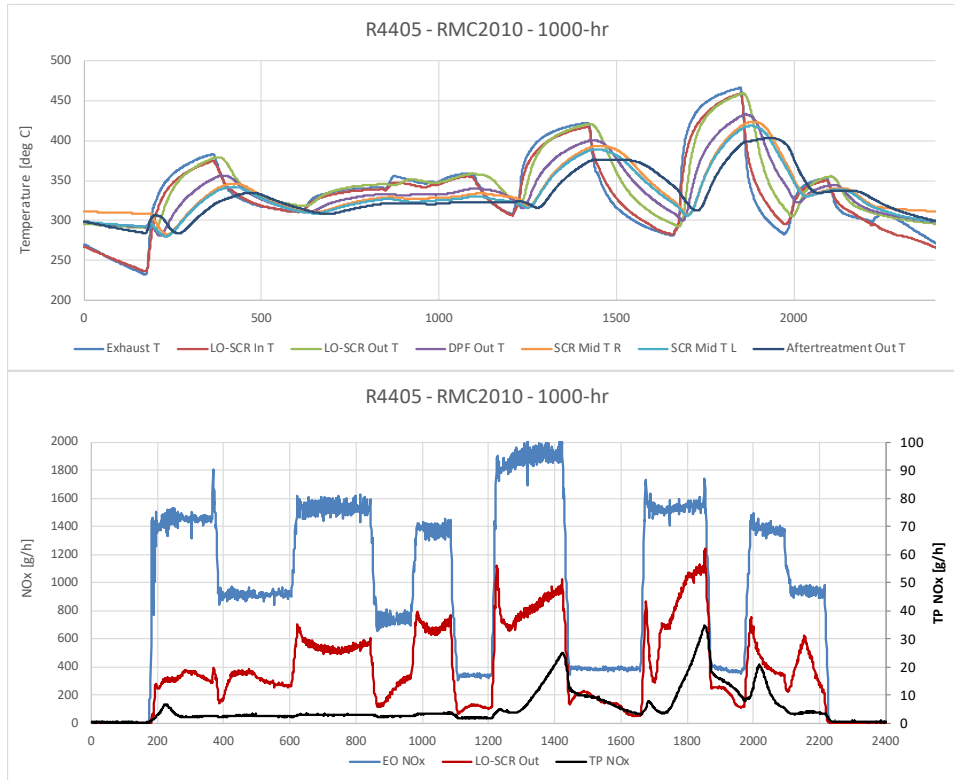


FIGURE 120. RMC-SET EMISSION RESULT AT 435,000 MILES AFTER ASH CLEANING

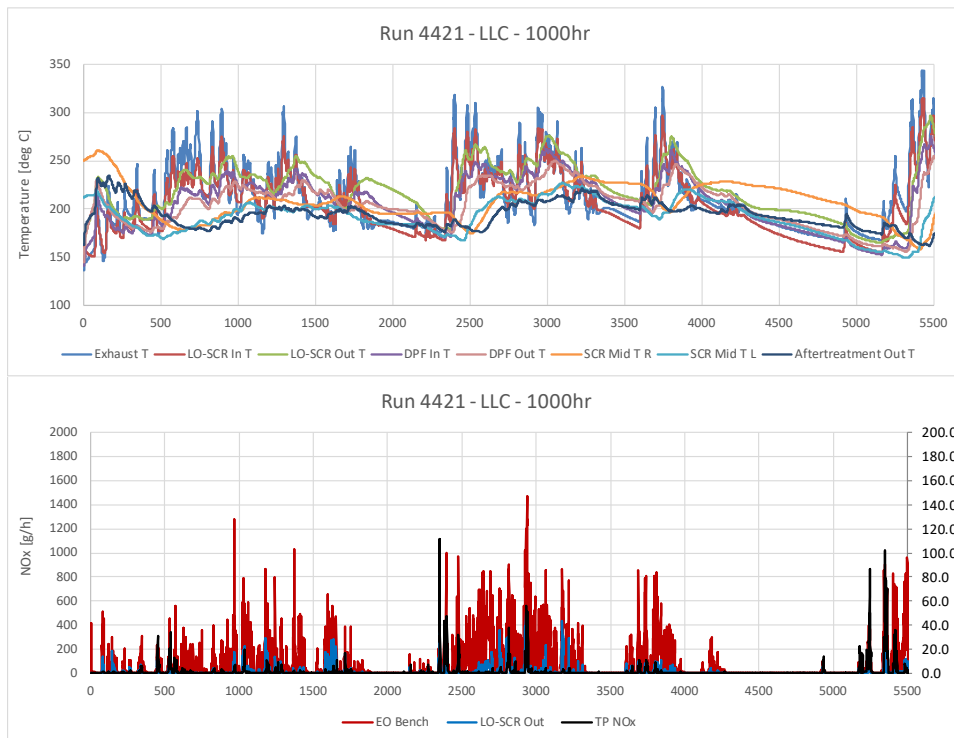


FIGURE 121. LOW LOAD CYCLE (LLC) EMISSION RESULT AT 435,000 MILES AFTER ASH CLEANING

These continuous data examples show the system temperatures on the various duty cycles, as well as the relative usage of the upstream LO-SCR and the downstream SCR. The locations of the few remaining small NO_x breakthroughs are also evident.

The CARB extended idle test was also run at the 1000-hour test point. The cycle was run using the FTP as a preconditioning, followed immediately by a 30-minute idle at the regular curb idle speed of 600 rpm, followed by a 30-minute idle at the elevated (PTO) idle speed of 1100 rpm. The Mode 1 (curb idle) results was 0.1 g/hr tailpipe NO_x, while the Mode 2 (1100 rpm idle) result was 0.3 g/hp-hr tailpipe NO_x. This is a major reduction from the 20-30 g/hr level observed for most current engines.

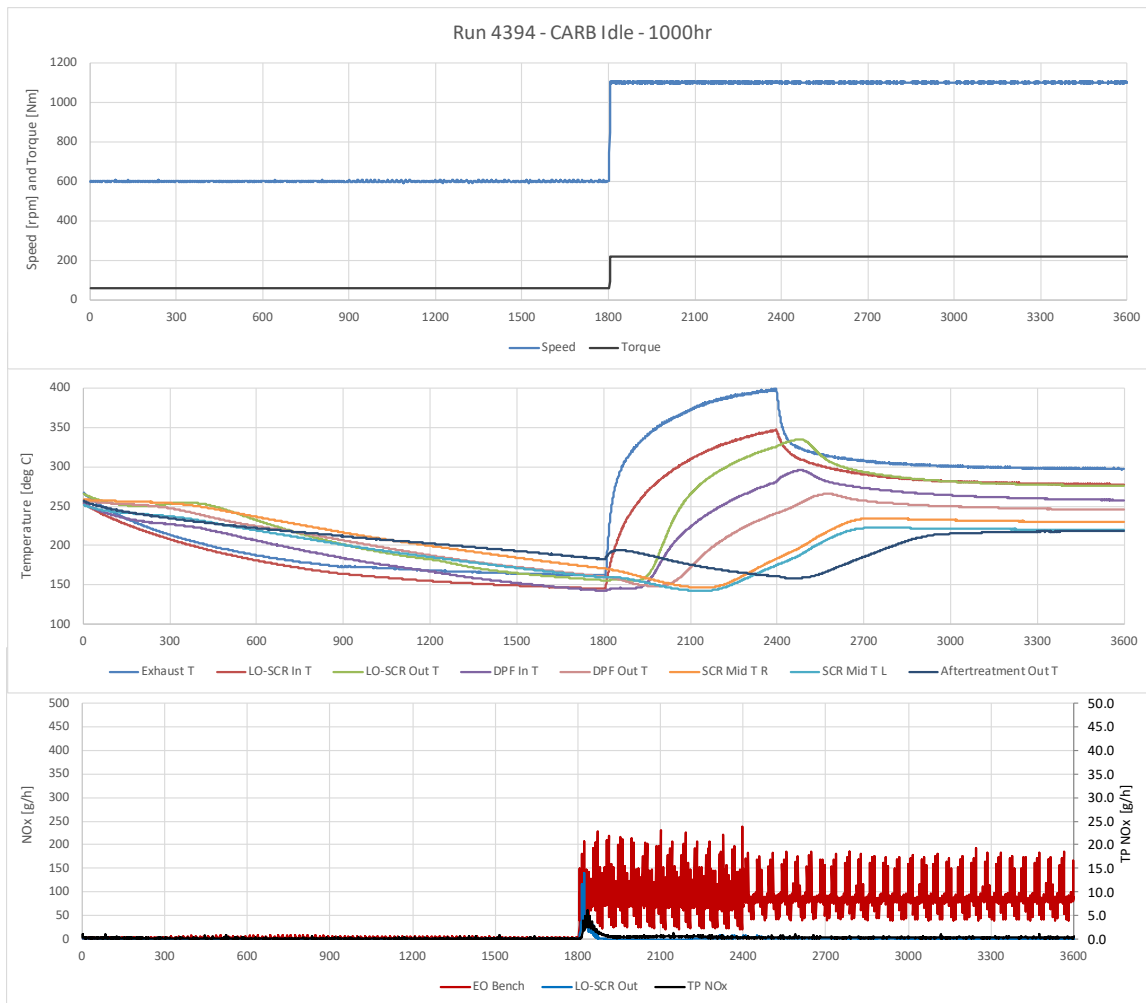


FIGURE 122. CARB EXTENDED IDLE TEST RESULT FOR STAGE 3 LOW NO_x ENGINE AT 435,000 MILES

Figure 123 shows tailpipe N₂O emissions for all of the various test configurations and aging points. In general, the Stage 3 engine had lower N₂O emissions than the Baseline engine, and N₂O generally tended to go down a bit with aging, although some of this was due to increasing reliance

on LO-SCR as the system aged. This lower N₂O emission rate can be ascribed to the use of LO-SCR, especially on the lower temperature cycles. As mentioned earlier, the LO-SCR primarily operates using the “standard” (NO-only) SCR reaction because engine-out NO_x is primarily NO, which serves to reduce N₂O production that occurs at low temperatures via nitrate formation and decomposition. Generally, N₂O for the Stage 3 engine was around half the level observed from the Baseline engine, though this varied by duty cycle and was sometime nearly the same, and sometime less than a third of the Baseline level.

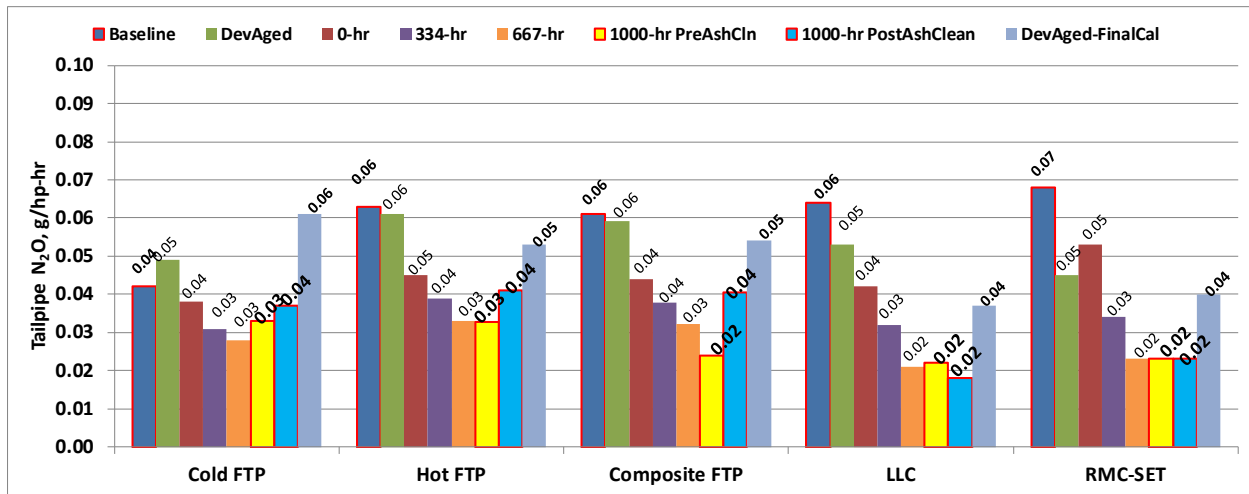


FIGURE 123. CYCLE N₂O EMISSIONS

3.8 Sulfation and Desulfation Experiments

One of the key concerns that needs to be addressed in any Low NO_x AT system that utilizes zeolite SCR catalyst technology is the management of sulfur. It is well understood that zeolites, and in particular copper-based zeolites can store sulfur, especially at lower temperatures, and over time the stored sulfur can block active sites. Given that Low NO_x will require maintaining NO_x conversion in excess of 99.5% over time, an approach must be available to periodically remove that stored sulfur. Typically deSO_x requires elevated temperatures, and it can be aided by either rich conditions or a localized source of hydrogen (such as hydrogen liberated from ammonia during oxidation). In most current production on-highway systems that employ copper-based zeolite SCR catalysts, periodic deSO_x is usually accomplished during periodic Active DPF regeneration events, and in fact the timing of these events is sometimes controlled by the need to deSO_x the downstream SCR.

This issue is particularly important for the LO-SCR catalyst in the Stage 3 system because it is upstream of any other catalyst, including the DOC. Not only is it the first catalyst in the system but the most straightforward means of generating elevated temperatures through exotherm induced by HC introduction in front of the DOC (either in exhaust or via post injection) is not available. At the same time, because the LO-SCR has no DOC upstream of it, the majority of the

sulfur exposure is in the form of SO₂, which is not stored at nearly the same efficiency as SO₃. This means that desulfation frequency is much lower because a significant amount of sulfur will either pass through the LO-SCR, or else will only be loosely bound at lower temperatures. At the same time, periodic deSO_x is likely to be the only truly high temperature exposure the LO-SCR experiences, therefore the frequency, temperature, and duration of these events has a direct impact on hydrothermal aging.

Given the importance of this issue, several deSO_x experiments were performed during the course of the Stage 3 program, and the results of these are detailed in this section of the report. Taken together, these experiments provide documentation that sulfur can be managed on the LO-SCR, and they also provide insight into the requirements and frequency of these events.

Based on data from the LO-SCR supplier, the initial target for deSO_x was set at 525°C at a frequency of 30 minutes every 300 hours. This was used to set the deSO_x modes for the Final Aging process. However, as noted earlier, during the first 333-hour aging segment, the mule engine had difficulty reaching this target consistently. As a result, the LO-SCR came from aging with enough sulfur poisoning to have a measurable impact in NO_x performance, as noted earlier in Section 3.7.

An initial deSO_x experiment was carried out at 525°C on the Stage 3 engine, using CDA to reach the temperature at relatively light load. During this deSO_x, the upstream dosing was set to an ANR of 1.3 to provide excess ammonia which would ensure that ammonia oxidation would be occurring in the catalyst to help facilitate sulfur removal. Figure 124 shows the result of this experiment by looking at SO₂ as measured by FTIR at the outlet of the LO-SCR. It should be noted that this LO-SCR has an ASC coating on the back, and therefore some of the sulfur that comes off as SO₂ is likely to be oxidized to SO₃. Therefore, the measured SO₂ likely only represents a portion of the removed sulfur. At the same time, a “rotten egg” odor was detected during this operation in the cell, indicating that at least some sulfur was likely also coming off the catalyst as H₂S, likely due to the presence of excess ammonia (this was primarily in the early stages of the deSO_x). Significant amounts of sulfur began to come off when the LO-SCR reached above 425°C, and the deSO_x was run until SO₂ had returned back to base level, which in this case required nearly 2 hours. As noted on the chart, this resulted in a significant improvement in NO_x performance, but not quite enough to fully recover hot-start FTP tailpipe to previous levels.

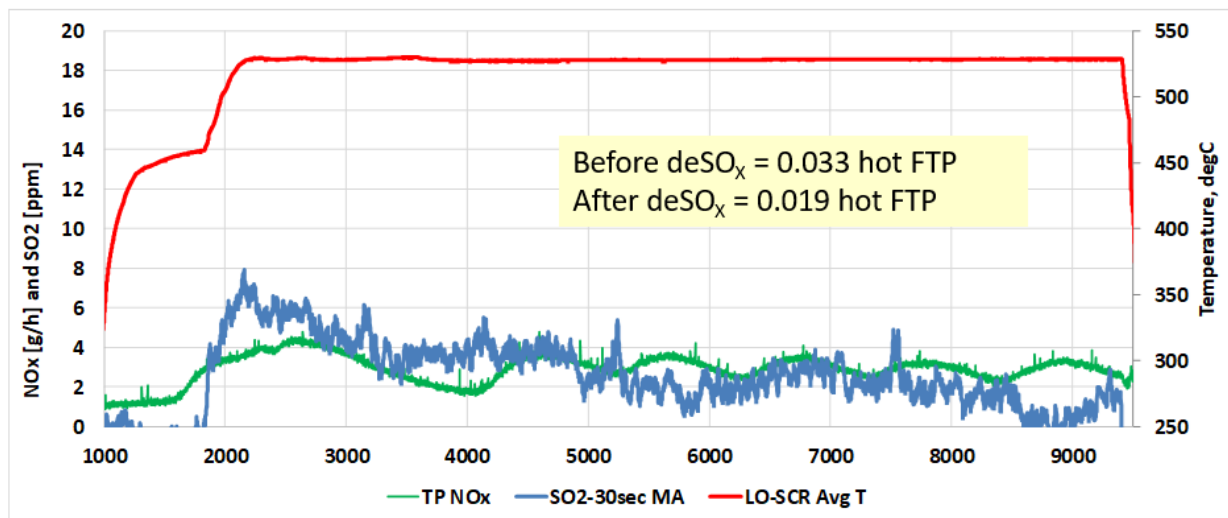


FIGURE 124. DESO_x AT 525°C AFTER EXCESS SULFUR STORAGE DURING FIRST 333-HOUR AGING SEGMENT

A second experiment was run at 550°C, to determine if more sulfur could be driven off at the higher temperature. Figure 125 shows the result of this experiment. There was an initial short burst of sulfur removal when temperatures first reached 550°C, but this ended about 900 seconds later, and no additional sulfur was removed. This indicates that there was some residual left after the 525°C deSO_x, but only a relatively small amount. Nevertheless, hot-FTP tailpipe NO_x performance showed an additional incremental improvement.

Because the tailpipe NO_x performance was still at 0.016 g/hp-hr at this point, a deSO_x experiment was also conducted on the downstream SCR to determine if there was any residual stored sulfur left on the catalysts following the multiple repeat Active Regenerations. This was considered unlikely given that the downstream SCR regeneration temperatures were typically on the order of 565° to 575°C for at least 30 minutes, but the experiment was still run to verify this.

A deSO_x experiment was conducted on the downstream system using the ECTO-Lab burner stand to generate the desired temperature. Experiments were conducted up to 650°C at the zCSF outlet. This final temperature was beyond the normal regeneration temperatures, just to be sure that there was no residual sulfur left behind. Figure 126 shows the result of this experiment, again shown as SO₂ measurement, though in this case the measurement was made upstream of the system ASC. Even at 650°C there is no significant evidence of additional sulfur removal. Additionally, there was no change in downstream SCR performance after this experiment. These results indicated that the Active Regeneration event conducted at 600°C zCSF outlet for 30 minutes every 100 hours was sufficient for deSO_x on the downstream SCR.

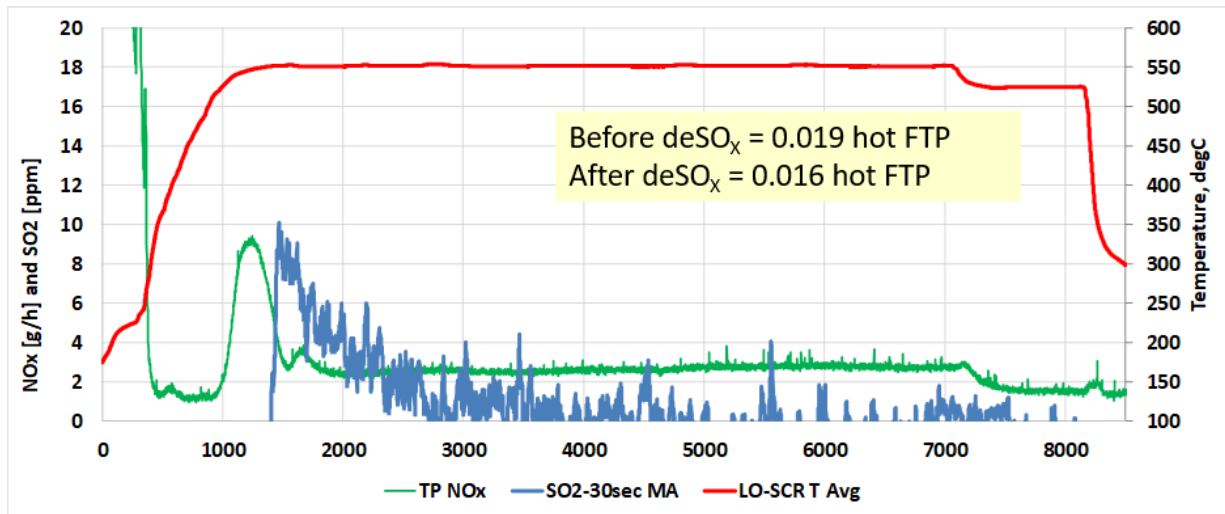


FIGURE 125. DESO_x AT 550°C AFTER EXCESS SULFUR STORAGE DURING FIRST 333-HOUR AGING SEGMENT

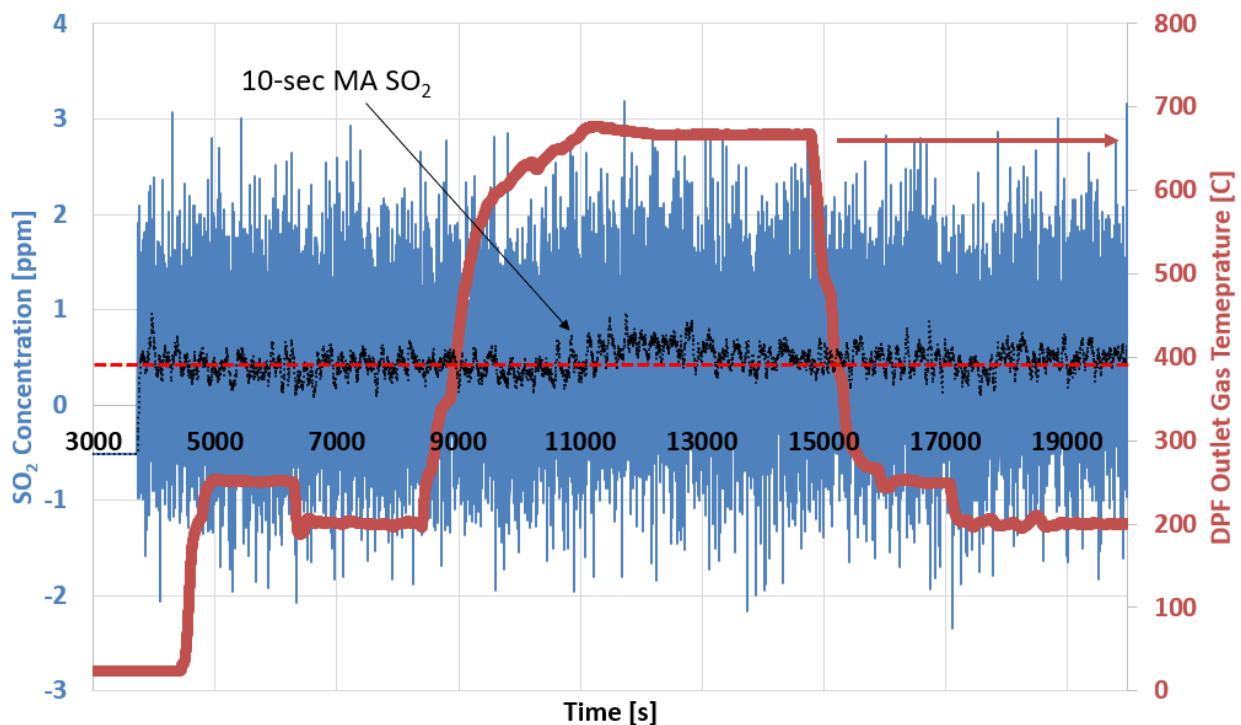


FIGURE 126. DOWNSTREAM DESO_x EXPERIMENT AT 650°C

Because the first aging segment was run at abnormally low deSO_x temperatures, it was decided to run the second aging segment to 667 hours with deSO_x targets still at 525°C to properly understand whether the 525°C temperature target was sufficient for long-term sulfur management or not. Following this second aging segment, it was noted that LO-SCR was still retaining enough sulfur to impact NO_x performance, indicating that 525°C was in fact not quite a high enough

temperature. Another deSO_x experiment at 550°C was conducted, and the results are shown in Figure 127. Again, it can be seen that sulfur begins to come off the catalysts at LO-SCR temperatures around 450°C, although there is not nearly as much sulfur as was present at the 333-hour mark when deSO_x events were not reaching 525°C. Still sulfur continued to come off, with SO₂ peaking briefly as the temperature reached 550°C before slowly moving back down over the course of 20 minutes. This is a clear indication of sulfur removal, and it was noted that following this event, LO-SCR performance was improved.

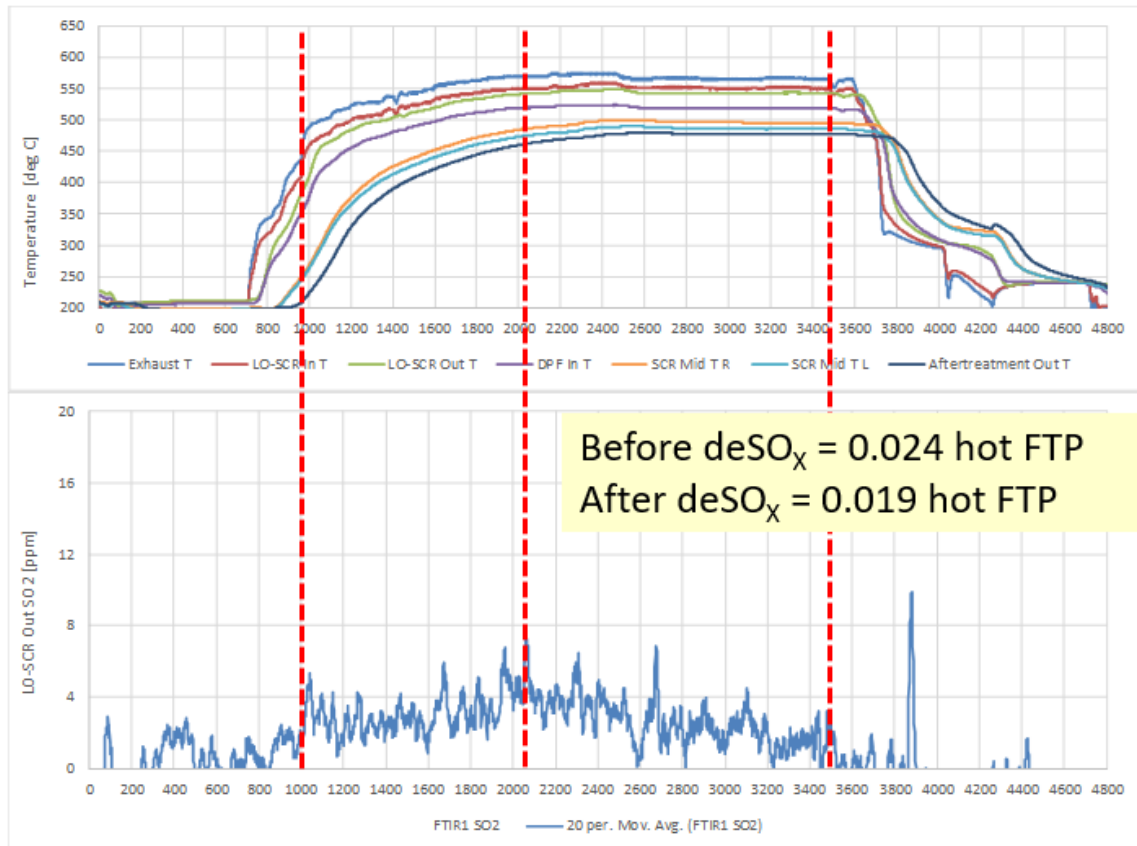


FIGURE 127. DESO_x AT 550°C AFTER REPEATED 525°C DESO_x EVENTS DURING 667-HOUR AGING SEGMENT

It was clear that for Low NO_x targets, LO-SCR deSO_x would need to be conducted at 550°C for long-term sulfur management to be successful. As a result, the LO-SCR deSO_x target was reset to 550°C for the final aging segment to 1000 hours.

It was also noted that the aging cycle, apart from the deSO_x event, includes regular cycling of the LO-SCR to 425°C as part of normal duty cycle operations. Although this represented less than 8% of the total aging cycle operation, it was thought that this temperature would still facilitate some sulfur removal. While the 550°C events appeared to be successful in controlling long-term sulfur storage, there was still a question of whether extended operation on lower temperature duty

cycles could cause short-term buildup of sulfur that could impact performance. A secondary question was whether this sulfur, much which was thought to be more loosely bound, would in fact come off at temperatures between 425°C to 450°C. To examine this question, an experiment was planned to complete the aging at an intermediate point between deSO_x events. It was arranged to halt durability roughly halfway through the time between LO-SCR deSO_x events, and following the end of the lower temperature operating modes without ramping to the 425°C mode. This resulted in the equivalent of 150 hours of potential long term sulfur storage, and the equivalent of 35 hours of operation at temperatures below 350°C (mostly below 260°C). The LO-SCR catalysts would be tested in this state directly following aging with no higher temperature exposure prior to the first FTP cycles.

Those subsequent tests indicated that there was a performance impact from this condition, with hot-FTP emissions at 0.024, due in part to LO-SCR performance. A short deSO_x experiment was conducted to examine two questions:

- Would shorter more frequent deSO_x events be more effective than the longer 30-min events spaced out every 300 hours?
- Would a significant amount of the sulfur stored at low temperature operation come off by raising the temperature above 425°C ?

Figure 128 shows the result of this experiment. It was noted that a large peak of SO₂ was observed to come off very quickly as soon as LO-SCR inlet temperature reached 450°C, even when the outlet was still at 350°C. This release was over within 120 seconds, indicating significant release of sulfur stored at lower temperatures. It should be noted that dosing was set to an ANR of 1.3 to help facilitate this release. Following that initial release of loosely bound sulfur, the SO₂ showed a pattern of continued slower release as the temperature continued to ramp to 550°C. However, this release also ended following roughly 15 minutes at 550°C, about half the time of the normal 30-minutes deSO_x event. This is consistent with having run this experiment roughly halfway through the usual 300-hr storage period between deSO_x events. Following this shorter deSO_x, the LO-SCR NO_x performance showed a recovery similar to what was observed at the 667-hour point for a longer deSO_x. Overall, this result indicates two important conclusions related to LO-SCR deSO_x:

- Shorter and more frequent deSO_x events are just as effective as longer less frequent events. This may be important to keep even short term impacts at bay, and is also important because shorter duration events are easier to arrange during normal driving.
- If a particular duty cycle has an extended period of operation where temperatures never exceed 425°C, it may be necessary to run a secondary deSO_x mode at 425°C to remove loosely bound sulfur. It appears that this could be as short as 5 minutes if conducted after perhaps 50 hours of low temperature operation. This is much easier to arrange than the higher temperature deSO_x. This mode would only be needed if normal operations did not already include enough time over 425°C, which is a temperature

often observed on highway cruise or motorway operations, or when moving heavy loads.

It is apparent that a robust deSO_x strategy for the LO-SCR would contain both of these modes, and would ideally utilize a relatively simple sulfur storage model to trigger these deSO_x modes. In this case, it might also be possible to opportunistically trigger shorter bursts of deSO_x when conditions are ideal to reach the desired thresholds.

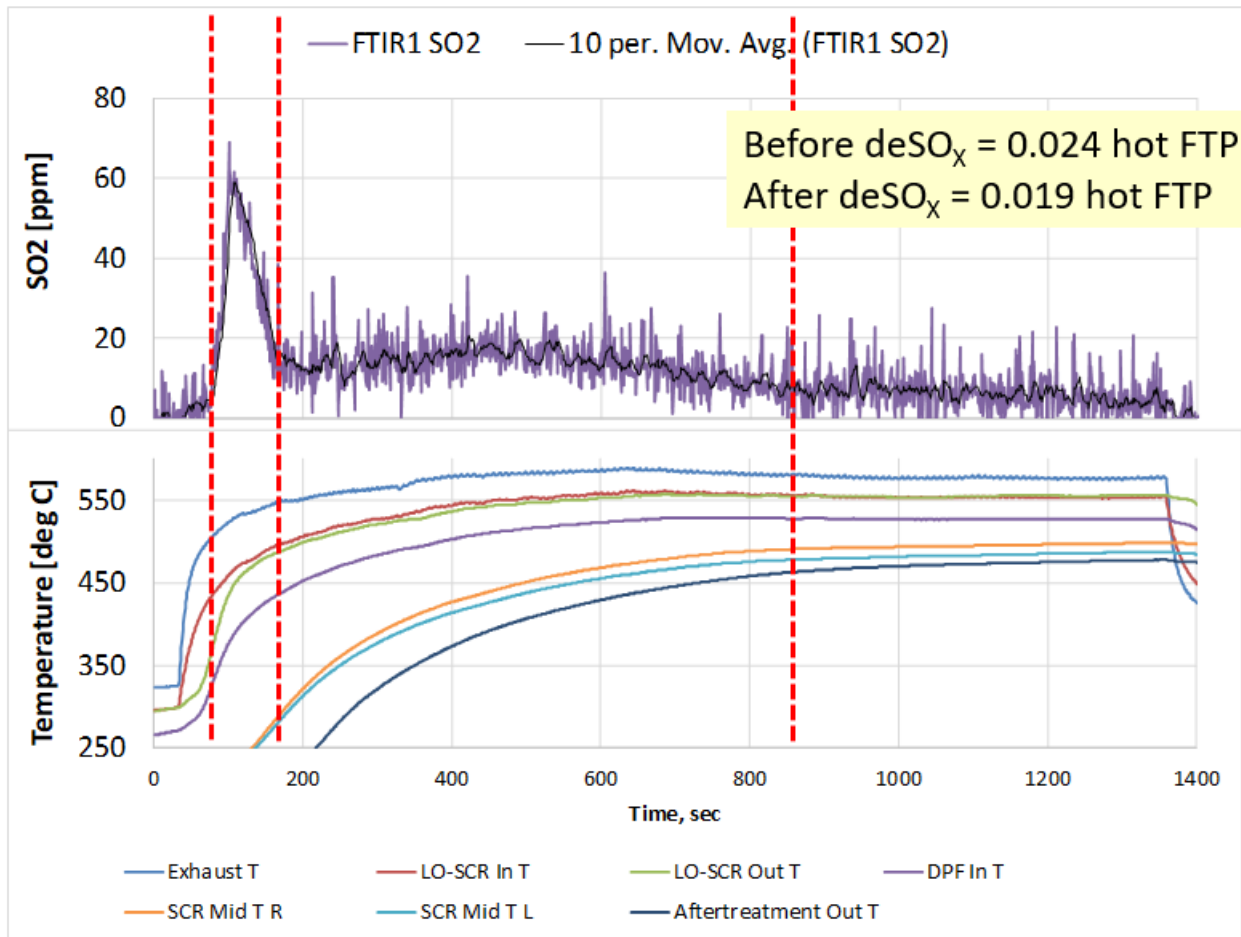


FIGURE 128. SHORT DESO_x EXPERIMENT AT 550°C FOLLOWING 1000-HOUR AGING SEGMENT AND 36-HR EQUIVALENT LOW TEMPERATURE OPERATION

The conclusion from these deSO_x experiments was that management of sulfur on the LO-SCR is feasible, but a robust and flexible strategy will be important to minimize any potential impact to fuel consumption. As noted earlier, CDA can be leveraged to also lower the fuel consumption impact of LO-SCR deSO_x, and to greatly widen the operating range over which deSO_x can be run. In this way, LO-SCR deSO_x can be incorporated in a manner that results in minimal fuel consumption impact, with a small impact potentially observed for very low load duty cycles that do not routinely reach temperatures of 425°C.

3.9 GHG Phase 2 Fuel Mapping Results

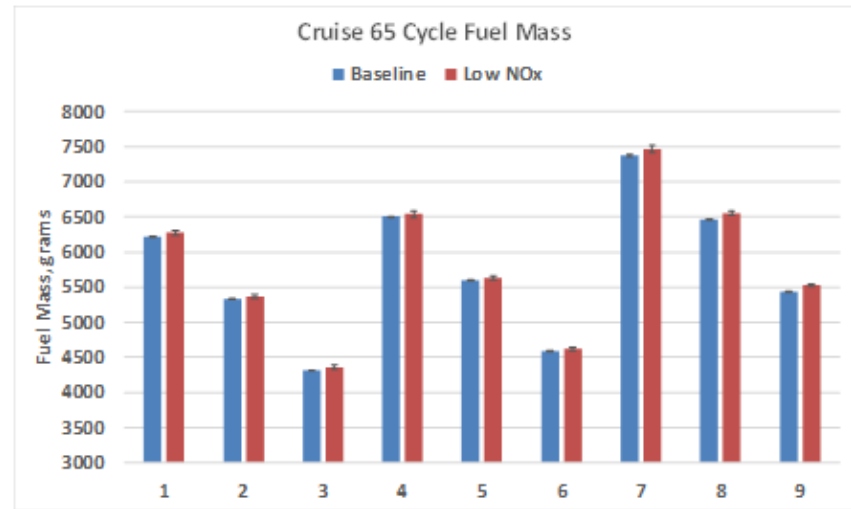
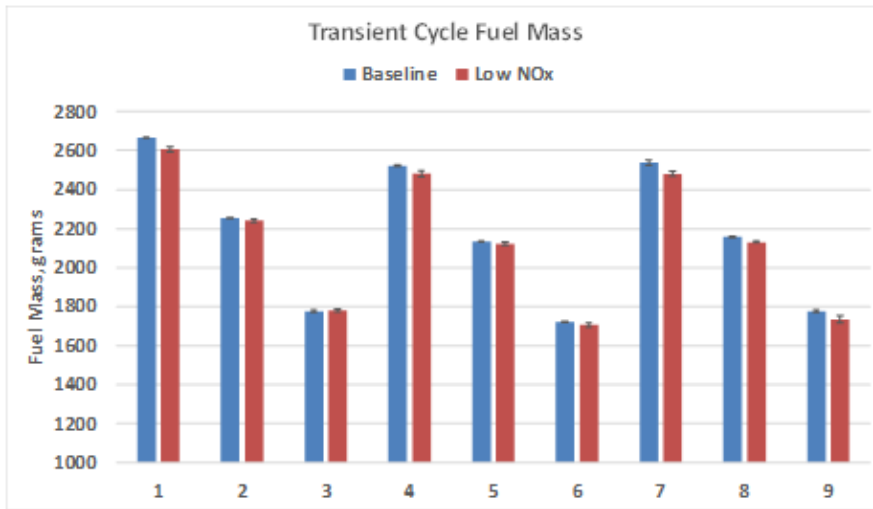
As noted earlier, Phase 2 GHG fuel mapping was run on both the Baseline engine and the Low NO_x engine to help quantify the impact of the Low NO_x configuration on vehicle CO₂ emission results that were generated using the GEM model for vehicle certification. These results also provide some further insight into the potential real-world fuel consumption impact of the Stage 3 Low NO_x configuration. This testing was conducted using the methods given in 40 CFR 1036.535 (for steady-state mapping) and 40 CFR 1036.540 (for cycle average mapping). Results are given for both steady-state mapping and cycle average tests. GEM results are presented using both the default model approach (combining steady-state maps for cruise cycles and cycle average maps for transient cycles), and the cycle average approach (which interpolates cycle average maps for all cycles).

3.9.1. Phase 2 Fuel Mapping Test Results

The complete fuel mapping test sequence consisted of a steady-state fuel map, idle fuel map, and cycle average runs using the 9 default vehicles for the three GEM cycles; the ARB Transient cycle, 55-mph Cruise cycle, and 65-mph Cruise cycle. The test sequence was run in triplicate for both the Baseline engine and the Stage 3 Low NO_x engine. Stage 3 tests were conducted on the Development Aged parts using the final thermal management and engine calibration that was run at the 667-hour and 1000-hour test points. An earlier set of runs was also made after the 333-hour point, but these were repeated after the calibration changes at the 667-hour point as it was expected these would impact the fuel maps (which in fact they did).

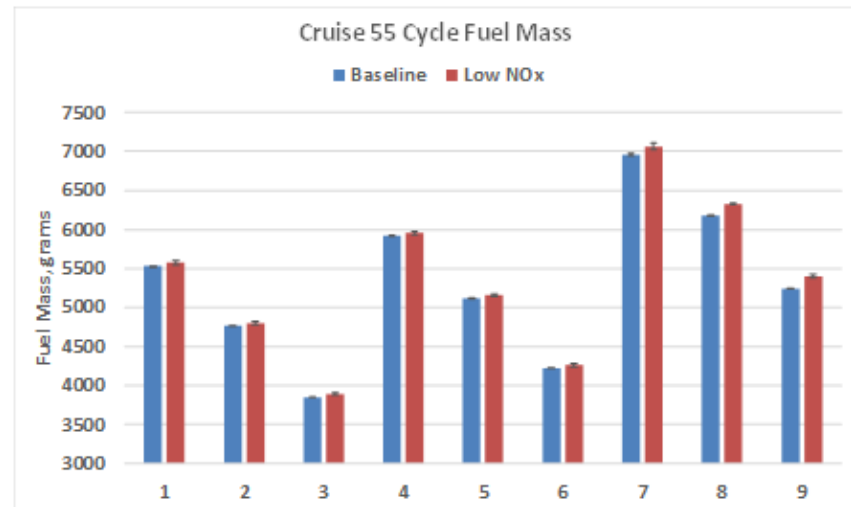
In the interest of protecting confidential information for the program's engine partner (Cummins), fuel map data is not presented directly in this report. Instead, fuel mapping results are presented on the basis of relative change compared to the Baseline engine. In this way, the impact of the Stage 3 Low NO_x engine configuration can be examined without disclosing the Baseline fuel map. The fuel map data is marked as Confidential Business Information and has been submitted under those restrictions to CARB.

A comparison of steady-state fuel map data between the Stage 3 Low NO_x engine and the Baseline engine is given in Figure 129. Each data point is the average of three points, and it should be noted that the three-run COV (one standard deviation over the mean) for each of these data points is on the order of 0.3% (closer to 0.6% at the very light load points), so that any change smaller than 0.5% in most cases (and 1% at very low loads) is not statistically significant. The map data indicates that over most of the map the Stage 3 engine is essentially the same as the Baseline engine, with most changes well under 0.5%. However, at the lightest load points, where CDA is active, the Stage 3 engine shows substantial fuel savings, as much as 45% in some cases, and on the order of 25% at idle. This is not apparent at the highest speed map point due to the 1750 rpm limit of the prototype CDA hardware, a limitation that would not be present in a production system.



Change in Fuel Mass – Low NO_x versus Baseline

Cycle	Transient	Cruise 65	Cruise 55
1	-2.2%	0.8%	0.6%
2	-0.7%	0.6%	0.5%
3	0.1%	1.1%	0.4%
4	-1.6%	0.5%	0.5%
5	-0.6%	0.7%	0.6%
6	-0.9%	0.7%	0.4%
7	-2.2%	1.3%	1.6%
8	-1.2%	1.4%	2.8%
9	-2.2%	1.6%	2.9%
COV on values	0.6%	0.6%	0.5%
Average	-1.3%	1.0%	1.1%
Avg nic (7-9)	n/a	0.7%	0.5%



Note: Vehicle 7-9 cruise cycles target MTS (1800 rpm, above HW limit for prototype CDA hw, production hardware would reduce this delta)

FIGURE 130. COMPARISON OF CYCLE AVERAGE FUEL MAPPING RESULTS BETWEEN STAGE 3 LOW NO_x ENGINE AND BASELINE ENGINE

3.9.2. GEM Vehicle Results

Vehicle modeling was run using GEM version 3.5.1. A variety of different vehicles were examined, but the most relevant ones for the 2027 discussion involve the set of vehicle configurations that were used by EPA for modeling runs that were used in setting the stringency of the 2027 Phase 2 GHG standards. It should be noted in the case of the Vocational vehicles that the original data set did not include vehicles in the HHD-U (Urban) category. Therefore, two of the vehicles were modified to add an evaluation in that category as shown later. MHD and LHD categories were not examined as these were not considered relevant for the X15 engine. It should be noted that some of the lighter Class 7 vehicles may be somewhat small for this 15L engine, especially at the 500 hp rating evaluated. As such these values should be taken as an indication of general trends for those vehicles, rather than looking at the absolute magnitude of the changes. This should be considered in examining these results because of the use of CDA. On the other hand, the fuel maps would not likely have been shaped differently for child ratings, and it is known that this engine is sold at ratings down to 400hp and 2235 Nm (and slightly below 2000 Nm in certain configuration).

Figure 131 shows the results for the Tractor applications, along with vehicle configuration parameters for reference. Again, it should be recalled that the COV on the fuel map results was 0.6% on cycle average mapping and 0.3% for steady-state maps. For the Cycle Average modeling method, a small increase in CO₂ is noted which varies between not significant and as much as 1%, just large enough on some vehicles to be statistically significant. However, it should be noted that the larger increases appear to be on vehicles that may utilize the Cruise cycle results where CDA was not operational, so those would not be expected for a production system. On the other hand, using the Default (hybrid) modeling method, a small decrease in CO₂ is observed, on the order of -0.7%, on the edge of being statistically significant. The Tractor categories in GEM are driven primarily by the Cruise cycles, so the changes observed generally match the results seen on the Cruise cycles. Taken together the overall conclusion is that the Stage 3 engine was essentially fuel consumption neutral as compared to the Baseline engine.

It should be stated that there is a possibility that the hybrid approach using the steady-state maps could slightly over-state the benefit of CDA. This is because the steady-state map will implicitly assume that CDA is on whenever possible as indicated by the map, but in fact there are some cases where the transient controls as implemented in this Stage 3 project will limit this. The extent of this transient CDA limitation can be countered with more advanced control algorithms as has been already reported elsewhere (Tula/Cummins, etc)[9]. This effect of transient vs steady state behavior may be the reason for the difference between the two modeling approaches. More examination of this may be needed, but it does reflect that fact that some technologies can cause modeling to react in unexpected ways.

The GEM results for the Vocational vehicles are given in Figure 132, along with vehicle configuration parameters. The results for these vehicles varied considerably by regulatory

category, and this is generally because the various cycles and idle operations are weighted differently for each category, which results in CDA having a different impact for various vehicles.

For the HHD Rural vehicles, which are most influenced by the Cruise cycles and show less idle, the Stage 3 engine was fuel consumption neutral for Cycle Average model and showed a 1.2% benefit for the Default model approach. For the HHD-Mixed vehicles which is more weighted to the ARB transient and some idle, the Stage 3 engine showed a 1.4% benefit for the Cycle Average model, and a nearly 4% benefit for the Default model approach. For the HHD Urban category that is mostly strongly influenced by idle operations, the Stage 3 engine showed a 2% benefit in Cycle Average modeling and a nearly 5% benefit on the Default mode approach. Taken as a whole these results generally indicated a trend of improved fuel consumption from the Stage 3 engine, although the amount varies greatly by application. Again, it is believed that this is attributed to the impact of CDA, which can be quite large at low load and idle, and has no impact at all at higher loads.

As with the Tractor engines, there is a consistent difference between the two GEM modeling approaches, although this is seen to a lesser extent even on the baseline engine. However, the differing deltas between the Stage 3 engine and the Baseline engines suggest that further examination is important.

The overall result for the Phase 2 GHG mapping was that there were a few cases wherein a small increase was noted for the Stage 3 engine, but the majority of GEM cases shows a fuel consumption and CO₂ improvement compared to the Baseline engine.

It should be noted that with the earlier 333-hour calibration, larger cycle benefits were seen on the ARB transient cycle, averaging a 2.5% improvement, primarily due to less use of thermal management.

Cycle Average approach															Baseline		Low NO _x		Low NO _x GHG Delta
Run ID	Regulatory Subcategory	Configural Ratio	Data	Aerodyna	Rolling Re	Rolling Re	Rolling Re	Loaded Ti	Intelligen	Accessory	Extended	Tire Press	Other	GEM CO2 Emissions	GEM Consumption	GEM CO2 Emissions	GEM Consumption		
Vehicle	(e.g. C8_SC_HR)	(e.g. 6x4) #	File Name	m^2	kg/t	kg/t	kg/t	rev/mi	%	%	%	%	%	g CO2/ton-mile	gal/1000 ton-mile	g CO2/ton-mile	gal/1000 ton-mile		
2027_TRAC1	C8_SC_HR	6X4 3.16	NA	5.26	5.6	5.8	5.8	512	0.8	0.5	3	1.1	5.5	72.77	7.15	73.08	7.18	0.4%	
2027_TRAC2	C8_SC_MR	6X4 3.16	NA	6.21	5.8	6.2	6.2	512	0.8	0.5	3	1.1	5.5	76.94	7.56	77.37	7.60	0.6%	
2027_TRAC3	C8_SC_LR	6X4 3.16	NA	5.08	5.8	6.2	6.2	512	0.8	0.5	3	1.1	5.5	71.02	6.98	71.35	7.01	0.5%	
2027_TRAC4	C8_DC_HR	6X4 3.21	NA	5.67	5.6	5.8	5.8	512	0.8	0.5	0	1.1	5.7	83.75	8.23	84.36	8.29	0.7%	
2027_TRAC5	C8_DC_MR	6X4 3.21	NA	6.21	5.8	6.2	6.2	512	0.8	0.5	0	1.1	5.7	84.82	8.33	85.50	8.40	0.8%	
2027_TRAC6	C8_DC_LR	6X4 3.21	NA	5.12	5.8	6.2	6.2	512	0.8	0.5	0	1.1	5.7	79.93	7.85	80.51	7.91	0.7%	
2027_TRAC7	C7_DC_HR	4X2 3.21	NA	5.67	5.6	5.8	NA	512	0.8	0.5	0	1.1	5.1	109.52	10.76	110.49	10.85	0.9%	
2027_TRAC8	C7_DC_MR	4X2 3.21	NA	6.21	5.8	6.2	NA	512	0.8	0.5	0	1.1	5.1	110.92	10.90	111.90	10.99	0.9%	
2027_TRAC9	C7_DC_LR	4X2 3.21	NA	5.12	5.8	6.2	NA	512	0.8	0.5	0	1.1	5.1	103.12	10.13	104.13	10.23	1.0%	
2027_TRAC10	C8_HH	6X4 3.7	NA	NA	5.8	6.2	6.2	512	0.8	0.5	0	1.1	9.5	48.08	4.72	48.33	4.75	0.5%	

Default (hybrid) approach using SS Maps															Low NO _x GHG Delta			
Run ID	Regulatory S	Configural Ratio	Data	Aerodyna	Rolling Re	Rolling Re	Rolling Re	Loaded Ti	Intelligen	Accessory	Extended	Tire Press	Other	GEM CO2 Emissions		GEM Consumption	GEM CO2 Emissions	GEM Consumption
Vehicle	(e.g. C8_SC_	(e.g. 6x4) #	File Name	m^2	kg/t	kg/t	kg/t	rev/mi	%	%	%	%	%	g CO2/ton-mile	gal/1000 ton-mile	g CO2/ton-mile	gal/1000 ton-mile	
2027_TRAC1	C8_SC_HF	6X4 3.16	NA	5.26	5.6	5.8	5.8	512	0.8	0.5	3	1.1	5.5	71.53	7.03	71.03	6.98	-0.7%
2027_TRAC2	C8_SC_MI	6X4 3.16	NA	6.21	5.8	6.2	6.2	512	0.8	0.5	3	1.1	5.5	75.76	7.44	75.40	7.41	-0.5%
2027_TRAC3	C8_SC_LR	6X4 3.16	NA	5.08	5.8	6.2	6.2	512	0.8	0.5	3	1.1	5.5	69.75	6.85	69.28	6.81	-0.7%
2027_TRAC4	C8_DC_HF	6X4 3.21	NA	5.67	5.6	5.8	5.8	512	0.8	0.5	0	1.1	5.7	82.78	8.13	82.14	8.07	-0.8%
2027_TRAC5	C8_DC_M	6X4 3.21	NA	6.21	5.8	6.2	6.2	512	0.8	0.5	0	1.1	5.7	83.88	8.24	83.32	8.18	-0.7%
2027_TRAC6	C8_DC_LR	6X4 3.21	NA	5.12	5.8	6.2	6.2	512	0.8	0.5	0	1.1	5.7	78.90	7.75	78.25	7.69	-0.8%
2027_TRAC7	C7_DC_HF	4X2 3.21	NA	5.67	5.6	5.8	NA	512	0.8	0.5	0	1.1	5.1	107.95	10.60	107.15	10.53	-0.7%
2027_TRAC8	C7_DC_M	4X2 3.21	NA	6.21	5.8	6.2	NA	512	0.8	0.5	0	1.1	5.1	109.37	10.74	108.62	10.67	-0.7%
2027_TRAC9	C7_DC_LR	4X2 3.21	NA	5.12	5.8	6.2	NA	512	0.8	0.5	0	1.1	5.1	101.59	9.98	100.83	9.91	-0.7%
2027_TRAC1	C8_HH	6X4 3.7	NA	NA	5.8	6.2	6.2	512	0.8	0.5	0	1.1	9.5	47.45	4.66	47.05	4.62	-0.8%

FIGURE 131. 2027 GEM VEHICLE SIMULATION RESULTS FOR TRACTORS

Cycle Average approach														Baseline		Low NO _x		Low NO _x GHG Delta		
Run ID	Regulatory Subc	Drive Axle Configura	Drive Axle Ratio	Drive Axle Data	Drive Axle Aerodyna	Drive Axle Steer	Drive Axle Roll	Drive Axle Roll	Drive Axle Roll	Drive Axle Load	Drive Axle Weight	Technology Improvement	GEM CO2 Emissions	GEM Consumption	GEM CO2 Emissions	GEM Consumption				
Vehicle	(e.g. HDD_R)	(e.g. 6x4)	#	File Name	m^2	kg/t	kg/t	kg/t	rev/mi	lbs		g CO2/ton mile	gal/1000ton mile	g CO2/ton mile	gal/1000ton mile					
cycle average																				
7hrAMTiresweight	HDD_R	6X4	3.76	NA	0	6.2	6.9	6.9	496	125		217.19	21.33	217.56	21.37	0.2%	HDD_R	0.3%		
7hraxle	HDD_R	6X4D	3.76	NA	0	6.2	6.9	6.9	496	125		214.71	21.09	215.07	21.13	0.2%	HDD_M	-1.4%		
7hrNI	HDD_R	6X4	3.76	NA	0	7.7	7.7	7.7	496	0		224.40	22.04	224.80	22.08	0.2%	HDD_U	-1.9%		
7hrSS	HDD_R	6X4	3.76	NA	0	7.7	7.7	7.7	496	0		223.18	21.92	223.79	21.98	0.3%	overall	-0.4%		
7hmAMT350	HDD_M	6X4	4.33	NA	0	6.2	6.9	6.9	496	125		265.64	26.09	261.73	25.71	-1.5%				
7hrengineonly	HDD_R	6X4	3.76	NA	0	7.7	7.7	7.7	496	0		228.71	22.47	229.17	22.51	0.2%				
7hrMTireswt	HDD_R	6X4	3.76	NA	0	6.2	6.9	6.9	496	125		221.36	21.74	221.78	21.79	0.2%				
7hrAES	HDD_R	6X4	3.76	NA	0	7.7	7.7	7.7	496	0		221.78	21.79	223.96	22.00	1.0%				
7hmMT455	HDD_M	6X4	4.33	NA	0	6.2	6.9	6.9	496	125		270.37	26.56	266.51	26.18	-1.4%				
7hmMT455	HDD_U	6X4	4.33	NA	0	6.2	6.9	6.9	496	125		302.17	29.68	296.44	29.12	-1.9%				
7hmMT455	HDD_U	6X4	4.33	NA	0	6.2	6.9	6.9	496	125		302.17	29.68	296.44	29.12	-1.9%				
default using ss maps																				
7hrAMTiresweight	HDD_R	6X4	3.76	NA	0	6.2	6.9	6.9	496	125		213.33	20.96	210.46	20.67	-1.3%	HDD_R	-1.2%		
7hraxle	HDD_R	6X4D	3.76	NA	0	6.2	6.9	6.9	496	125		210.88	20.71	207.98	20.43	-1.4%	HDD_M	-3.8%		
7hrNI	HDD_R	6X4	3.76	NA	0	7.7	7.7	7.7	496	0		220.48	21.66	217.64	21.38	-1.3%	HDD_U	-4.9%		
7hrSS	HDD_R	6X4	3.76	NA	0	7.7	7.7	7.7	496	0		219.27	21.54	216.64	21.28	-1.2%	overall	-2.3%		
7hmAMT350	HDD_M	6X4	4.33	NA	0	6.2	6.9	6.9	496	125		264.08	25.94	253.92	24.94	-3.8%				
7hrengineonly	HDD_R	6X4	3.76	NA	0	7.7	7.7	7.7	496	0		224.72	22.07	221.86	21.79	-1.3%				
7hrMTireswt	HDD_R	6X4	3.76	NA	0	6.2	6.9	6.9	496	125		217.42	21.36	214.54	21.07	-1.3%				
7hrAES	HDD_R	6X4	3.76	NA	0	7.7	7.7	7.7	496	0		217.79	21.39	216.66	21.28	-0.5%				
7hmMT455	HDD_M	6X4	4.33	NA	0	6.2	6.9	6.9	496	125		268.77	26.40	258.54	25.40	-3.8%				
7hmMT455	HDD_U	6X4	4.33	NA	0	6.2	6.9	6.9	496	125		301.73	29.64	287.06	28.20	-4.9%				
7hmMT455	HDD_U	6X4	4.33	NA	0	6.2	6.9	6.9	496	125		301.73	29.64	287.06	28.20	-4.9%				

FIGURE 132. 2027 GEM VEHICLE SIMULATION RESULTS FOR VOCATIONAL VEHICLES

3.10 Estimation of Infrequent Regeneration Adjustment Factors (IRAF)

Another important part of the process that needs to be considered for the final calculation of results is the potential impact of Active Regeneration and LO-SCR deSO_x events on tailpipe emissions. These would generally be considered through the methodology for assessing the impact of Infrequent Regeneration events. During these events, it is possible that emission control could be compromised to some degree, and therefore the impact of these events on overall NO_x emissions must be accounted for, as is required in 40CFR 1065.680. The potential impact of both the Active Regeneration and the LO-SCR deSO_x events is discussed below.

3.10.1. LO-SCR deSO_x

As given in the projections above, the LO-SCR deSO_x event is conducted every 300 hours for a 30-minute duration, and it requires the LO-SCR to be maintained at a temperature of 550°C. It is possible that shorter events could also be conducted more frequently, but it was found during aging that this cumulative amount of high temperature deSO_x is required to maintain the function of the LO-SCR.

The data from deSO_x experiments discussed in Section 3.4.2 and 3.8, indicated that the deSO_x mode could be run with little or no impact on tailpipe NO_x. This is because even in deSO_x mode at temperatures of 550°C, there is still high NO_x conversion over the LO-SCR, in part due to the high dosing rates (ANR 1.3) that are run to facilitate sulfur removal. Given that the downstream SCR will be at temperatures of roughly 450°C, any residual NO_x is easily converted. Measured tailpipe NO_x during these modes was typically in the range of 0.03 g/hp-hr. In addition, the frequency of this mode is roughly 0.2%. As a result, the impact of LO-SCR deSO_x on tailpipe NO_x is negligible at less than 0.0002 g/hp-hr.

With regard to CO₂, as noted in the data in Section 3.4.2 indicated a fuel penalty for CDA-enabled deSO_x on the order of 10% to 15% depending on the load and duty cycle. Even using the highest penalty at 15% with a 0.2% frequency, the net impact on CO₂ is 0.03%.

3.10.1. Active zCSF Regenerations

The assessment of the impact of Active Regeneration on the downstream system was significantly more complicated than the LO-SCR deSO_x. This is because the Active Regeneration frequency was significantly higher, and there was also a real impact from this mode on tailpipe NO_x. IRAF calculations for tailpipe NO_x were carried out for the FTP, the RMC-SET, and the LLC. It should be noted that the base engine regeneration frequency was 0.5%, with a 30 minute regeneration event occurring every 100 hours. This data was supplied by Cummins for this engine, and is assumed to generally reflect the line haul Tractor application for this engine. Data was also monitored during Baseline engine testing to assess the rate of climb differential pressure across the DPF during multiple repeat FTPs, as well as measurement of engine-out PM and soot rates.

This data was used for later comparison with the Stage 3 engine data to help understand the impact of the Low NO_x configuration on passive soot oxidation and regeneration behavior. It was generally noted on all three cycles that the passive soot oxidation behavior on the Stage 3 engine was similar to what had been observed on the Baseline engine. However, it was not clear how to use the baseline regeneration frequency on the different cycles, and therefore other measurements were made to project an Upwards Adjustment Factor (UAF) for each cycle.

For the FTP, it was noted on repeat hot-start FTPs that there was an increase in peak backpressure on the order of 0.1 to 0.15 kPa per FTP cycle, comparable to what was observed on the Baseline engine. The engine-out soot mass was measured at 4.5 grams per FTP cycle, although it should be noted that much of this soot load was offset via passive oxidation in the 600 to 900 second region of the FTP at high NO_x and temperatures in excess of 350°C. Still some residual soot was left after each cycle. From a starting backpressure with a clean filter of 26 kPa it would take roughly 90 FTP cycles to reach a 10 kPa increase in filter differential pressure, at which point a soot load of roughly 6 grams/liter would be expected. This is a fairly typical trigger for soot regeneration. Given the 30-minute regeneration event it is likely that it would take 2 FTP cycles to actually complete a regeneration, which would indicate a regeneration frequency of 2.2%, far higher than the 0.5% given for line haul operation.

Regarding NO_x emissions during a regeneration cycle, this is an area where the dual-SCR dual-dosing AT has an advantage, especially with HC dosing after the LO-SCR. During Active regeneration of the downstream system, the LO-SCR can still remain active, given that it will still be at normal operating temperatures (in fact slightly higher due to the need to maintain zCSF inlet temperatures above 250°C to sustain a HC-based exotherm without the risk of coking). However, the LO-SCR is not large enough to sustain very high NO_x conversion, even when the engine is operating in TM-2 (which is planned for regeneration events). In addition, it was observed during aging that there was essentially no ability to affect further NO_x reduction on the downstream system while an Active regeneration was in progress (the dosing just produced more NO_x via oxidation). Therefore, tailpipe NO_x can be assumed to be equivalent to LO-SCR out NO_x during Active regeneration. Measurements were made of tailpipe NO_x on FTP using only the LO-SCR with downstream dosing disabled and the engine locked in TM-2. This condition simulates a expected operating condition during a downstream regeneration event, and it resulted in a BSNO_x level of roughly 0.12 g/hp-hr, and this was used as the value for regeneration cycles.

There is also a carryover effect on the subsequent cycle because the downstream AT system is completely empty of ammonia and must recover on the next cycle, which compromises NO_x control during this “recovery” cycle. This experiment was also conducted by starting an FTP cycle in a sequence after a previous set of cycles with downstream dosing off to empty the downstream SCR. The resulting BSNO_x level was 0.05 g/hp-hr and this was also considered in the IRAF calculations.

The final calculation of the UAF for the FTP is shown in Figure 133, and the resulting value is 0.002 g/hp-hr which would be added to the final FUL FTP result of 0.023 g/hp-hr, for a final result of 0.025 g/hp-hr.

	cycles	hours	tp bsnox	wtd mass		
FTP	92	30.67	0.017	0.521333	grams	
Regen ftp	2	0.67	0.116	0.077	grams	
next ftp	1	0.33	0.050	0.016667	grams	
total	95	31.7		0.615	grams	
				0.01942	g/hp-hr	
	EFL	0.017	g/hp-hr	0.0024	g/hp-hr	
	EFH	0.094	g/hp-hr			
freq (F)	0.031579		uaf	0.002		

FIGURE 133. NO_x UAF CALCULATION FOR FTP CYCLE

For the RMC-SET it was clear that there was never any soot accumulation on this cycle for the Stage 3 engine, which was again similar to the Baseline engine. As a result, the Active regeneration frequency was driven by the need for periodic deSO_x of the downstream system, and removal of any potential DEF deposits formed during other operations. This frequency was left the same as the Baseline engine frequency of 30 minutes every 100 hours. Test results indicated that this frequency was sufficient for both of those purposes. During regeneration, the engine would be set to the TM-2 mode to control engine-out NO_x within the range of the LO-SCR, and only the LO-SCR would be used, as noted earlier for the FTP. Tailpipe emissions in this mode of operation were 0.286 g/hp-hr, although it should be noted that this could likely have been better except for the maximum dosing rate of the prototype heated doser. This is an overall 89% NO_x conversion efficiency on the regeneration cycle. Regeneration could be completed in a single cycle, and no recovery was needed given the already higher temperatures on the RMC-SET. The UAF calculation for the RMC-SET is shown in Figure 134, and the final value was 0.002 g/hp-hr. This would be added to the FUL RMC-SET result of 0.022 g/hp-hr for a final result of 0.024 g/hp-hr.

	cycles	hours	tp bsnox	wtd mass	
RMC	150	100	0.022	2.2	grams
regen rmc	1	0.67	0.286	0.191938	grams
total	151	100.67		2.391938	grams
				0.02376	g/hp-hr
	EFL	0.0220	g/hp-hr	0.0018	g/hp-hr
	EFH	0.2865	g/hp-hr		
freq (F)	0.006623	0.007	uaf	0.002	

FIGURE 134. NO_x UAF CALCULATION FOR RMC-SET CYCLE

For the LLC, temperatures are so low that it was assumed that no passive soot oxidation was taking place at all, which was generally confirmed by experiment. Engine-out soot rates were measured at 4.4 grams per LLC cycle, and it was assumed that all of this would remain in the filter to be conservative. At this rate of accumulation, the overall soot load in the filter would reach a loading level of 6 grams/liter after 15 LLC cycles. Although backpressure on this cycle was not very high, that level of loading would still trigger the need for an Active regeneration due to concerns about potential exotherms on the zCSF if the soot load got significantly higher. Active regeneration would be completed within 1 LLC given that the cycle has a 90-minute duration, although it should be noted that large segments of the LLC are not really amenable to active regeneration, although CDA could help to raise engine out temperatures to maintain zCSF inlet temperature at levels needed to sustain an exotherm. This would be a regeneration event every 23 hours of LLC operation, which is not surprising given the very light loads and highly transient nature of this cycle. However, the LLC already relies primarily on the LO-SCR for conversion, and the cycle generally already spends most of its time in TM-2. Tailpipe NO_x without the downstream NO_x functioning in this mode would be 0.151 g/hp-hr, which is essentially identical to LO-SCR out NO_x.

The final UAF calculation for the LLC is shown in Figure 135, and the final value was 0.005 g/hp-hr. This is considerably higher than for the other cycles, driven primarily by the projected higher regeneration frequency of nearly 6% on this duty cycle. Unlike the other cycles, this projected regeneration frequency does not have much experimental verification, therefore conservative values with respect to soot loading were chosen. This value would be added to the final FUL result of 0.047 g/hp-hr for a final value of 0.052 g/hp-hr on the LLC.

	cycles	hours	tp bsnox	wtd mass	
LLC	15	22.5	0.047	1.0575	grams
regen llc	1	1.5	0.131	0.197	grams
total	16	24		1.2545	grams
				0.052271	g/hp-hr
	EFL	0.0470	g/hp-hr	0.0053	g/hp-hr
	EFH	0.1313	g/hp-hr		
freq	0.0625	0.063	uaf	0.005	

FIGURE 135. NO_x UAF CALCULATION FOR LLC CYCLE

With regard to CO₂, it is not possible to compare the impact of the Active Regeneration to the Baseline because no baseline UAF is available for CO₂ on any cycles. However, it was noted previously that soot loading and passive soot oxidation behaviors on both the FTP and RMC are similar to those of the baseline engine, therefore regeneration frequency is likely also the same. The same can likely be said for the LLC because temperatures are so low that no passive soot oxidation would be expected for either engine on that cycle. Given comparable engine-out PM rates on other cycles, it is reasonable to assume a similar rate on the LLC. Likewise, regeneration duration was kept similar to that of the Baseline engine. Therefore, it is reasonable to assume that the fuel consumption impact on Active Regeneration is comparable to the Baseline, thus there is no incremental impact for the Stage 3 Low NO_x engine as compared to the Baseline.

3.11 Field Replay Cycle Evaluations

Much of the previous evaluation data presented has focused on the regulatory cycles, the FTP, RMC-SET, and LLC. However, there was a desire on the part of several stakeholders to also examine the Stage 3 engine on off-cycle operations that might represent certain challenging kinds of real-world operations. Given that real world emission control is the ultimate aim of any emission standard, these evaluations were considered important to ensure the flexibility of the emission controls developed for the Stage 3 Low NO_x engine. These results were funded by other parties such as EPA and EMA, but the results are included in this report to provide additional insight into the performance of the Stage 3 system. Taken together these results help demonstrate the flexible and robust nature of the Stage 3 system, and they indicate that the performance observed on laboratory cycles will translate into reliable NO_x control in-use on a variety of duty cycles.

3.11.1. CARB Southern NTE Route (EMA Field Cycle)

One example of a real-world cycle was supplied by EMA, based on data that was collected in actual trucks running in Southern California by West Virginia University (WVU). This particular route was one that is typically utilized by CARB for NTE evaluations on current production trucks, and it is generally considered as a challenging route. This route travels an area

of I-10 and I-15, and includes a particularly challenging segment that travels down through the Cajon Pass and contains long downhill motoring punctuated by grade changes. A 3-hour segment of this route containing some of the more challenging segments was selected for this study. An engine dynamometer cycle was built from recorded vehicle data that could replay this route in the laboratory on the Stage 3 engine. The final cycle is shown Figure 136, with the shaded portion representing an additional 30 minutes of the field run that were included as preconditioning to ensure that the engine entered the route segment of interest in the same conditions as the trucks in the field. Several of the WVU runs on this route had been conducted with a very similar X15 engine to the one used for the Stage 3 program, and SwRI worked with Cummins to evaluate the baseline engine on this route to validate that the laboratory replay cycle translation produced similar performance to the engine in the truck. With that replay cycle validation, the cycle could then be used to evaluate the Stage 3 engine in a realistic simulation of this field route.

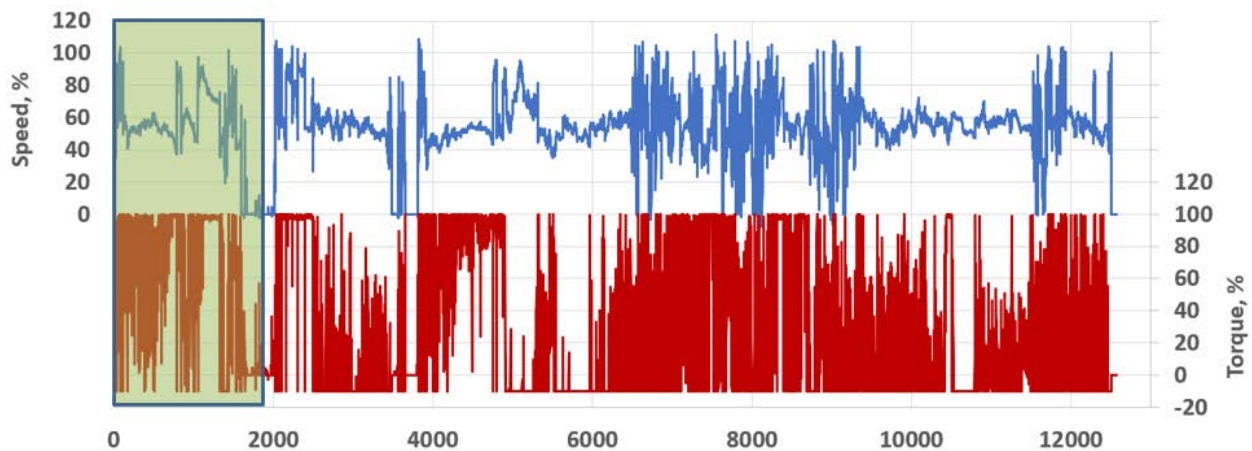


FIGURE 136. NORMALIZED NTE SOUTHERN ROUTE REPLAY CYCLE

Triplicate runs were made over this replay cycle, and example of one of those runs is given in Figure 137, showing resulting temperatures and NO_x performance. It should be noted that these runs were performed using the Development Aged parts while Final Aging was being run. Tailpipe NO_x over the cycle was 0.023 g/hp-hr and fuel consumption compared to the Baseline engine was between 0% to -0.5% different, essentially fuel consumption neutral. It should be noted that this cycle contains several segments that are particularly challenging for current production vehicles. One such segment is in the area from 3000 to 4500 seconds, which simulates the long, downhill motoring segment that is broken by a sudden grade change in the vicinity of Cajon Junction. This long motoring typically causes significant cooling of the today's AT implementations, and the sudden load at the grade change causes a severe demand for high NO_x conversion. This is often a significant challenge for current engines, but the Low NO_x engine demonstrated almost zero tailpipe NO_x breakthrough at this point. Several other segments shown in this cycle show load changes after significant potential cooling segments, and the Low NO_x engine is able to maintain high efficiency NO_x control in all those cases. Overall, tailpipe NO_x is estimated to be in the range of 10X to 20X lower than for the baseline vehicle on this same route. This field route also

gives a good illustration of how the strategy reacts to changing load conditions. Several different areas can be seen where the conversion load shifts between the LO-SCR (outlet in Red) at low temperature and the downstream system at higher temperatures.

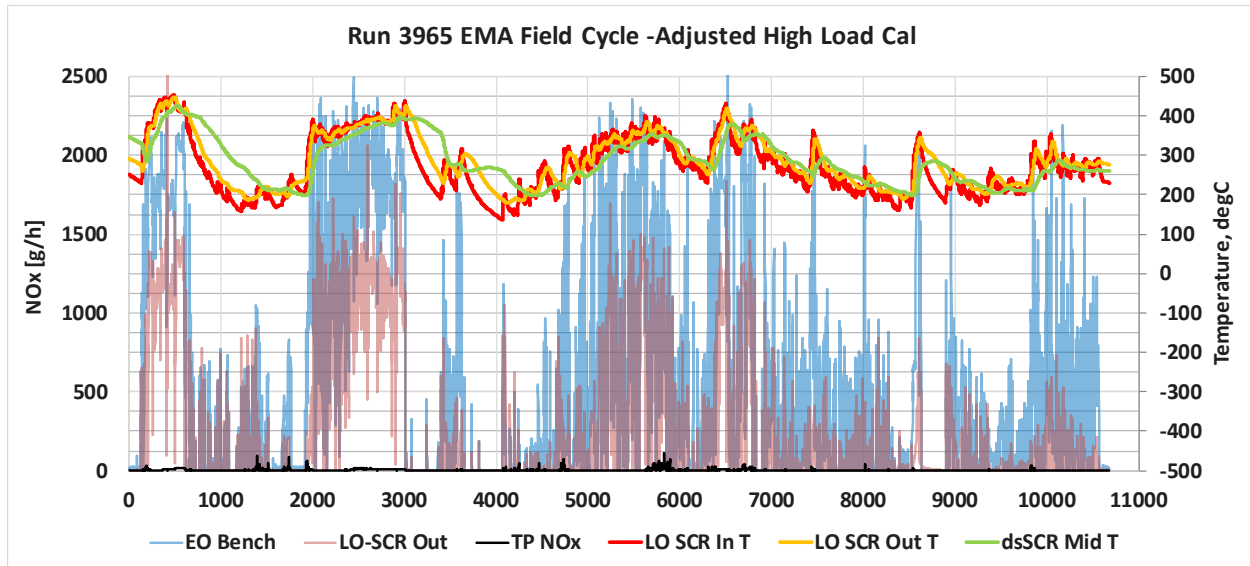


FIGURE 137. EXAMPLE OF STAGE 3 ENGINE TEMPERATURE AND NO_x PERFORMANCE OVER NTE SOUTHERN ROUTE REPLAY CYCLE

However, there is no NO_x standard for this cycle, and instead the proper method for evaluation of this data was to use the new 3-bin Moving Average Window (3B-MAW) method for assessing in-use emissions [14]. This method involves a 300-second fixed time window that is moved through the data set at one-second increments. NO_x and CO₂ mass from each 300-sec window is assigned to a bin based on the ratio of CO₂ to the engine maximum CO₂ rate (as a surrogate for engine load). The three bins are an Idle bin (< 6% max load/CO₂), a Low Load bin (6% to 20% max load/CO₂), and a Mid-High Load bin (> 20% max load/CO₂). Results are then calculated for each bin as a ratio of the sum of total NO_x divided by the sum of total CO₂, multiplied by the FTP BSCO₂, and they are given in g/hp-hr. In the case of the Idle bin, the result is simply given as the average NO_x rate for the bin in g/hr.

The results for this 3B-MAW calculation are shown below in Figure 138, along with the proposed compliance thresholds for the bins. The data indicates that the Stage 3 engine with Development Aged parts was able to meet these in-use thresholds, although it should be noted that the margin to the Mid-High Load bin threshold is relatively small, though the final step down to the 0.030 g/hp-hr threshold isn't scheduled to happen before MY2030. While it is only one field duty cycle, this replay cycle result nevertheless demonstrates the flexibility and capability of the Stage 3 system and control strategy.

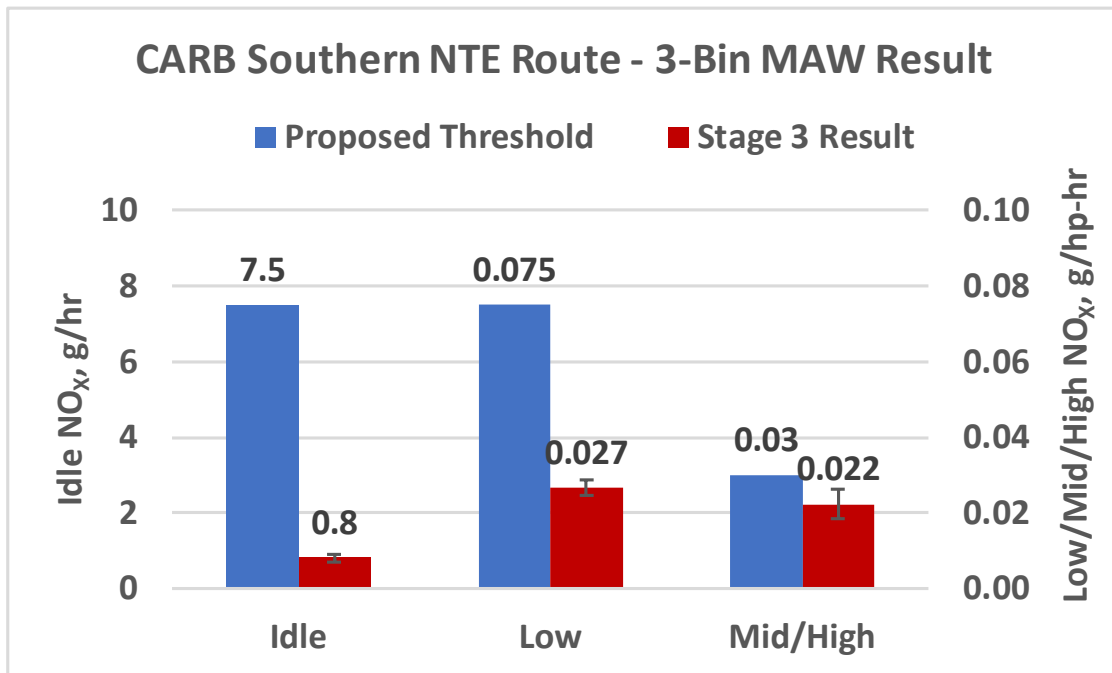


FIGURE 138. 3B-MAW RESULTS FOR NTE SOUTHERN ROUTE REPLAY CYCLE

3.11.2. *Extended Cold-Start Idle*

Another off-cycle case that was examined was a cold-start where the engine is started but then idles for an extended period of time before starting to perform work. This is considered the most challenging case for engine warm-up because there is no load to help warm the engine and AT up quickly. This evaluation was run using a cold-start FTP but with the normal 24-second idle period extended to be 30 minutes in duration. This number was chosen by EPA to represent the high end of cold-start idle periods.

The result of this evaluation is shown in Figure 139 , which shows both system temperatures and NO_x performance. As with the normal cold-start, the engine begins operation at elevated idle speed, and the temperatures show the behavior of the warm-up strategy in response to this condition. The initial high mass flow warm-up mode is switched after roughly 3 minutes to a lower flow higher temperature warmup mode as the engine moves through the transitions discussed earlier in the Methods section based on AT and coolants temperatures. High efficiency tailpipe NO_x control is achieved in roughly 4 minutes, with tailpipe NO_x rates near zero by that time. After 15-minutes the AT system has reached sufficient temperatures that the warm-up modes and elevated idle are disengaged, and the engine moves into a normal idle mode at that point. Mass emissions over the normal cycle segment are comparable to a normal cold-start, and the NO_x rate is below the proposed idle 2027 standard of 5 g/hr 4 minutes after cold-start, and below 1 g/hr 8 minutes after cold-start. The system is also warm enough to achieve maintain substantial NO_x control when the vehicle begins to perform work.

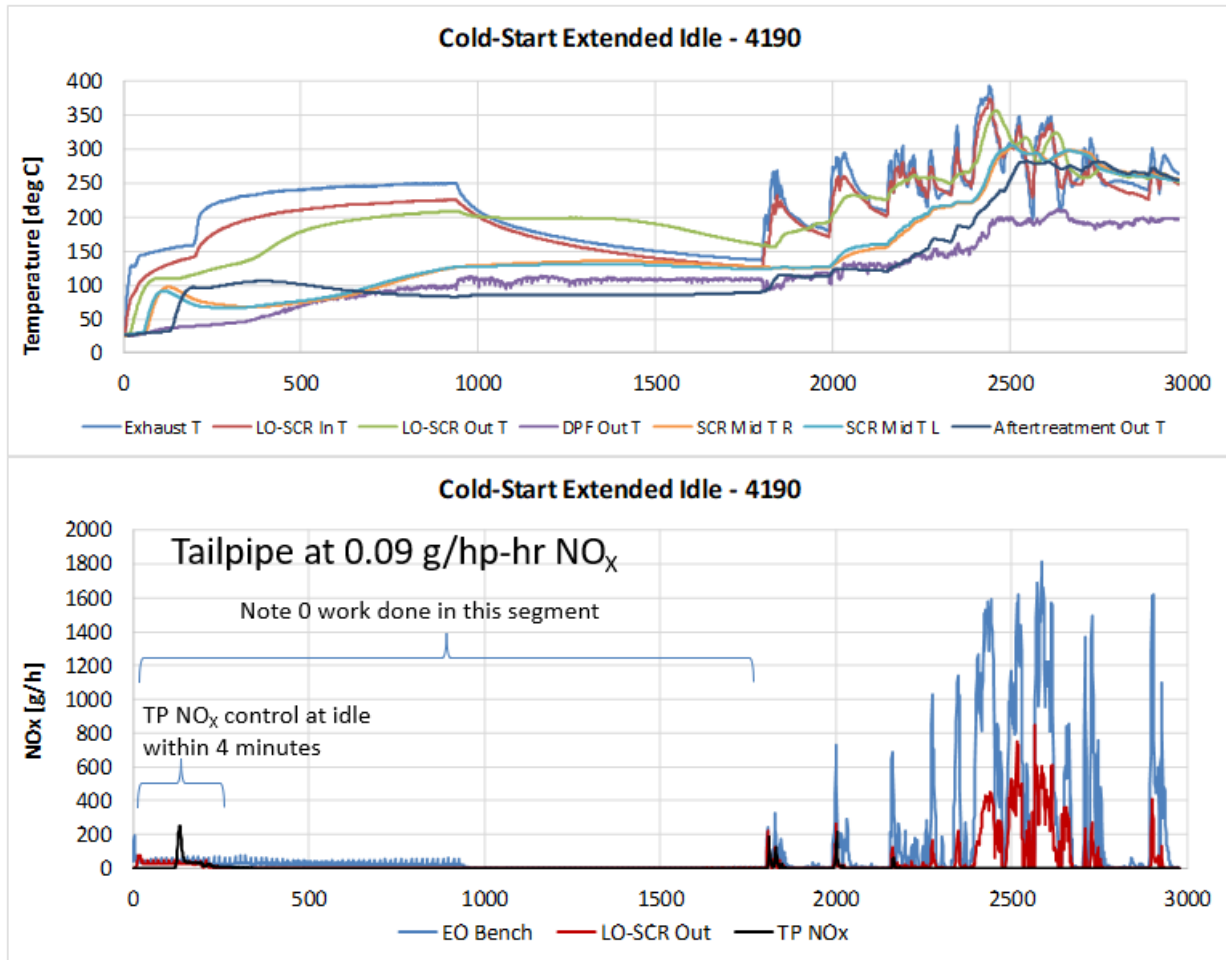


FIGURE 139. STAGE 3 LOW NO_x RESULT FOR COLD-START WITH EXTENDED IDLE PERIOD (30 MINUTES)

3.11.3 Long Idle Periods (hoteling)

Another area of interest for the Stage 3 engine was behavior during very long idle periods, such as what might be performed during what is referred to as “hoteling” on a sleeper cab tractor. This operation was evaluated using a test cycle that was based on the long idle segment at the end of the LLC cycle, except that the idle period was extended from the usual 23 minute duration to an 8-hour duration. This test was run with a 3.5 kw accessory load present at idle. In the LLC this idle segment is entered from a moderate load condition, partway between low load and highway cruise operations. A relatively moderate load “return-to-service” event was placed at the end of this long idle, which consisted of 5 repeats of the first acceleration of and FTP. This relatively light load return-to-service event is somewhat more challenging than the higher load event normally used in the LLC.

The results of this evaluation is shown in Figure 140, which shows temperature and NO_x performance. In the case of the NO_x, the chart is focused on the final 30 minutes of the test so that the final idle after 8 hours and the return-to-service event can be seen clearly. The engine

enters the idle period with the AT at roughly 250°C, and it takes roughly 2.5 hours until all of the AT temperatures to stabilize. This demonstrates the heat retention features of the Low NO_x AT system, as well as the impact of the low exhaust flow rate and higher temperatures at idle due to the combination of CDA and the modified engine calibration. At the same time, the fuel flow rate at idle was 25% to 30% lower than for the baseline engine. The engine-out temperature stabilized at 165°C, with LO-SCR temperature at 145°C. However, despite the low temperatures, the flow rate and associated catalysts space velocity are so low that the LO-SCR is still able to achieve about 66% NO_x conversion long term. There is little requirement for dosing because of the storage capacity of the LO-SCR, with engine-out NO_x at 3 g/hr and tailpipe NO_x at 1 g/hr.

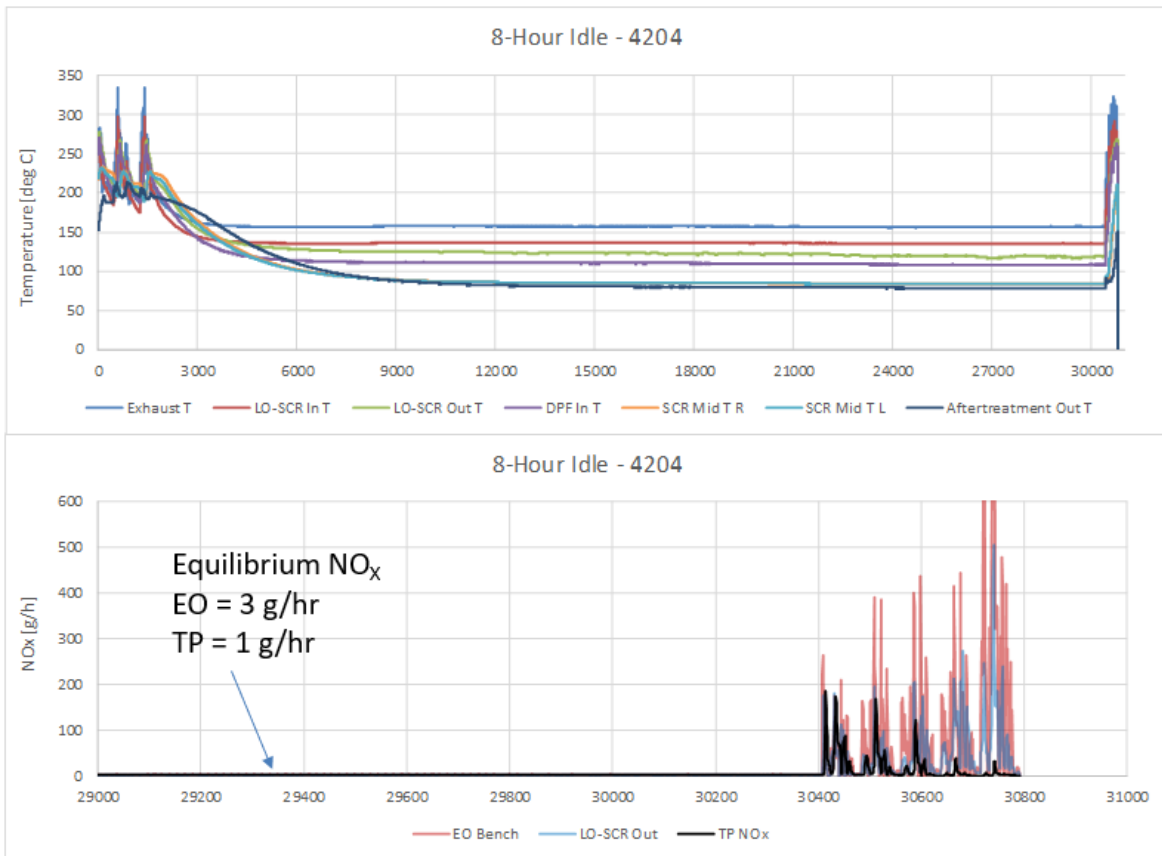


FIGURE 140. STAGE 3 RESULT FOR 8-HOUR IDLE EVALUATION – WITH PART LOAD RETURN-TO-SERVICE

In addition, the heat retention, and the low thermal inertia of the LO-SCR coupled with the stable ammonia coverage, helped the LO-SCR stay ready for an eventual return-to-service event. The LO-SCR begins the light-off within 60 seconds after the load event starts at the end of the cycle, and the downstream system has reached full conversion within 200 seconds. This progression, and the associated mode switching can be seen in the engine-out NO_x behavior over the successive acceleration events. By the 250 second mark, the engine has been released into the most efficient fuel economy mode (FE), with the AT system fully functional. This kind of functionality will enable robust in-use emission controls.

4.0 SUMMARY AND CONCLUSIONS

The objective of this program was to demonstrate the technical feasibility of reaching Low NO_x levels while maintaining a path towards meeting Phase 2 GHG standards. The program goal for Low NO_x was 0.02 g/hp-hr over the FTP and RMC cycles, with LLC and in-use emissions as low as feasible. The goal of maintaining a path towards meeting Phase 2 standards was defined as at least maintaining CO₂ emissions and fuel consumption at a level comparable to the Baseline engine, if not improving them. In both cases, the program intent was to reach these targets with technologies that were feasible for production by the 2027 model year. The results of the program are summarized below, along with conclusions regarding those results with respect to the program targets.

4.1 Demonstration Results

A summary of the final tailpipe NO_x values achieved for the Stage 3 Low NO_x engine is given below in Figure 141. The 1000-hr values in yellow are with the AT aged to 435,000 equivalent miles using the rigorous DAAAC protocol which includes both thermal and chemical aging. These values represent an 85% reduction in tailpipe NO_x from the baseline engine on the FTP and RMC. In addition, the Stage 3 system closes the “low load gap” in tailpipe emissions with a 95% reduction in NO_x over the LLC, which has an average power of only 7% and represents urban and low load operations.

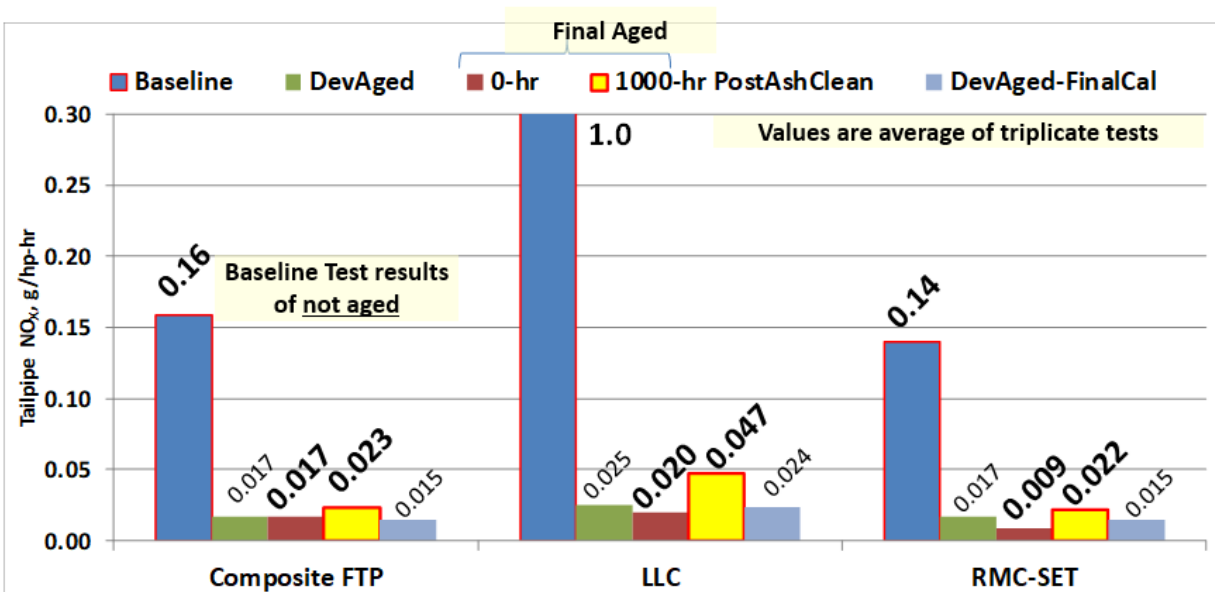


FIGURE 141. FINAL TAILPIPE NO_x VALUES ACHIEVED FOR STAGE 3 DEMONSTRATION (NOT INCLUDING IRAF)

Figure 142 shows the NO_x reduction capability of the AT system at the end of life for both methods of aging used in the program. A comparison between the methods serves to highlight the importance of using a more realistic and rigorous aging methodology that considers both thermal and chemical aspects of aging. At the end of life, the chemical and thermal aged AT was still reducing engine-out NO_x by more than 99% on most cycles, and by 98% even in very light load operations (where the current production system only achieved 67% NO_x reduction). The Stage

3 engine was able to reach high NO_x reduction efficiency less than 4 minutes after cold-start even if the engine was only idling. In addition, the Stage 3 engine demonstrated near-zero emissions at idle, remaining below 1 g/hr of tailpipe NO_x even after 8 hours of idle operation, more than 25X below what most current production engines emit idle. Taken together, these results indicate that Low NO_x levels can be reasonably expected over the full range of field duty cycle operations.

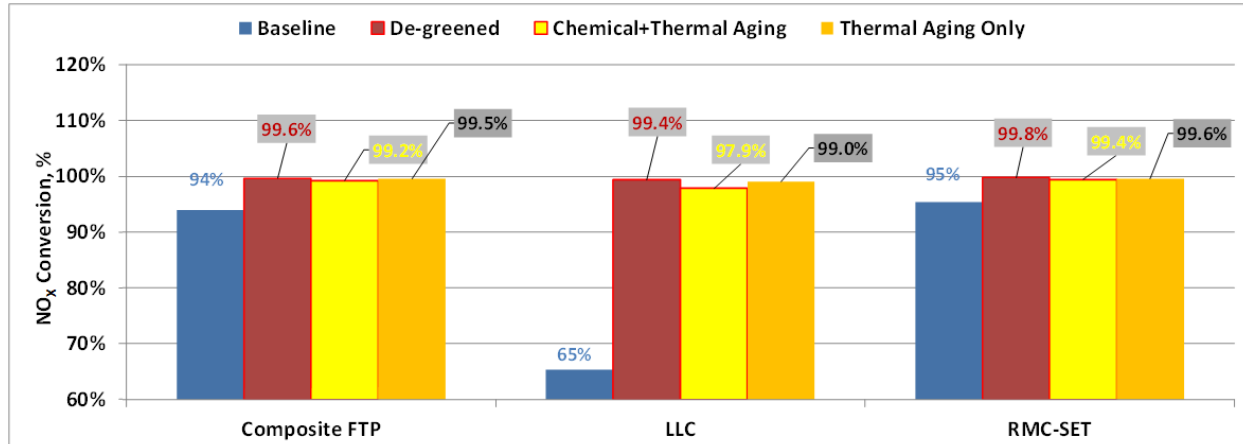


FIGURE 142. CYCLE NO_x CONVERSION EFFICIENCY – COMPARISON OF AGING METHODS

The Stage 3 engine produced these reductions in NO_x while at the same time maintaining GHG emissions at levels that were comparable to the Baseline 2017 engine. CO₂ emissions were the same as the Baseline engine for the FTP and RMC-SET cycle, and showed an increase of roughly 1% on the LLC (which has very low fuel consumption to start with). In addition, on the Phase 2 GHG cycles, the Stage 3 engine produced CO₂ levels either comparable to or lower than the Baseline engine over a wide variety of vehicle configurations and application classes. This was due primarily to the use of CDA, which provided the flexibility needed to both meet Low NO_x and mitigate any negative CO₂ impacts. CDA technology was not widely projected by EPA to be used for meeting Phase 2 GHG standards in 2027, therefore the technology remains available to be used to enable meeting Low NO_x while maintaining a path to meeting Phase 2 GHG standards. It should also be noted that while both the Baseline and Stage 3 engines met the N₂O standard, the Stage 3 engine produced significantly lower N₂O levels, due to the use of LO-SCR, and this is also beneficial from a GHG standpoint.

Although the NO_x emission reductions noted above are impressive and come very close to meeting the program targets, it should be noted that the NO_x levels demonstrated by the Stage 3 engine were not below 0.02 g/hp-hr on the FTP, RMC-SET and LLC. The final emission level demonstrated by the Stage 3 engine at 435,000 miles with IRAF adjustments included was 0.025 g/hp-hr on the FTP, and 0.024 g/hp-hr on the RMC-SET. In this case of the LLC, this number was 0.052 g/hp-hr. For extended idle emissions, the final demonstrated value was 1 g/hr.

As noted earlier, the primary reason that the FUL NO_x emissions were above the 0.02 g/hp-hr target level was the degradation of the AT system. As show above in Figure 142, the AT system went from 99.6% NO_x conversion to 99.2% conversion on the FTP, and from 99.8% to 99.4% on the RMC-SET, a loss of conversion of 0.4%. A significant portion of this loss was due to chemical poisoning due to oil and sulfur exposure. While this loss of conversion is significantly smaller than many current systems in similar situations (which often see a 1% loss of performance), in part

due to more sophisticated controls and feedback algorithms, that is still not small enough to be under 0.02 g/hp-hr at the end of life. The degradation must be reduced to less than 0.25% loss of conversion to be reliably under 0.02 g/hp-hr, therefore improvements must be made to the durability of the AT system if this target is to be reached. Similarly, on the LLC, 1.5% loss of conversion was observed, where a loss of 1% at most is needed to be reliably under 0.05 g/hp-hr.

As this demonstration represents a single attempt with a single system, it is reasonable to consider what improvements could be made to the system to make it more robust against aging. There are several areas wherein the Stage 3 AT system could be improved, including:

- Moving from the zCSF to a traditional DOC+DPF architecture in the downstream system. This would likely improve CO₂ on hot-start and LLC cycles, but it would also result in better and more robust NO-to-NO₂ oxidation behavior ahead of the downstream SCR which could help improve and maintain low temperature performance (EPA is currently testing just such a system).
- Improved DEF mixing on the downstream system.
- Using a slightly larger downstream catalyst volume, by roughly 10% to provide more durability reserve
- Improvement in the LO-SCR formulation to better resist chemical poisoning
- Improvement in the downstream SCR formulation to retain selectivity of the ammonia oxidation function over time
- Calibration of the aging model algorithm in the controller (which was not within the available scope of the current demonstration), which could allow the models to better track storage and performance changes over time.
- Further refinement of long-term trim algorithms

It should be noted that as of the writing of this report, several of these areas are being actively investigated as part of work being conducted in support of the EPA Cleaner Trucks Initiative demonstrating further improvements in NO_x emission control at 433,000 miles of aging.

Although CARB has adopted longer useful life periods beyond 435,000, it is not yet clear what the impact of further aging would be on this Stage 3 system. It should be noted that the system components were designed with a 435,000 mile FUL in mind. It is reasonable to project that, based on the Stage 3 results at 435,000, maintaining 0.020 g/hp-hr levels through significantly longer FUL periods beyond 435,000 miles will require significant continued development effort. Currently, longer aging periods are being investigated in support of the United States Environmental Protection Agency's (U.S. EPA) Cleaner Trucks Initiative.

4.2 Technology Feasibility

With regard to the feasibility of the technology used in the Stage 3 engine, it should be noted that much of the hardware used for the Stage 3 engine is commercially available technology that is either already in serial production or is in a pre-production stage. Based on feedback from suppliers and program partners, it is expected that the technologies utilized can be practically implemented for production by the 2027 model year. Dual SCR bed, dual dosing architectures are already being released in Europe in light-duty applications, and as of the writing of this report, commercial announcements have been made for this kind of architecture in heavy-duty

applications. Similar announcements of valve deactivation hardware in heavy duty diesel applications have been made. However, significant engineering and development effort will be needed to fully implement these technologies in production.

CDA is not yet commercially available in the heavy-duty market, but it has been in production on a variety of light-duty engines for many years. In addition, multiple potential suppliers are already in vehicle demonstration stages, and as of the writing of this report at least one is preparing to move to serial production for the heavy-duty market. The NVH challenges of CDA require significant engineering effort to be expanded in adapting the CDA strategy to match different vehicle and engine combinations, and there are some MHD and LHD applications that may prove more challenging, but the technology is broadly feasible for heavy-duty applications. That said, as with other core engine valvetrain technologies (such as variable valve actuation), significant effort, time, and validation hours on many trucks will be needed to ensure a robust deployment of CDA. There will also be some changes to vehicle integration requirements (engine mount re-design, etc.) and processes to do the necessary engineering to prevent NVH issues. Accomplishing this should be feasible for 2027 model year engines, but may be difficult before that model year.

The catalysts for LO-SCR are not new technology per se, and there have been other applications in production which featured SCR upstream of filters. The Stage 3 demonstration has indicated that LO-SCR can remain efficient and durable over FUL upstream of the rest of the AT system. Implementation of a long-term sulfur management strategy that can work under normal operation will require significant development effort, but the Stage 3 efforts indicate a feasible path to doing this, especially when leveraging CDA to enable deSO_x over a wide operating range. The Stage 3 system uses a design that, while perhaps not strictly “close-coupled” (being roughly 24 inches downstream of the turbine outlet) would nonetheless feature an under-hood mounting location, and this does present a packaging challenge. While SwRI has seen several innovative approaches regarding inlet and outlet cone design for this application, it should be acknowledged that significant engineering effort would be needed to shift and relocate under-hood components to accommodate the LO-SCR. While this will be difficult, it is likely feasible. A fallback approach would be to shift some or all of the LO-SCR to a location further downstream (still upstream of the DOC and DPF), although this will require careful engineering to avoid negative CO₂ impact for the potential need of additional thermal management. Overall, LO-SCR is considered feasible for 2027 and possibly earlier.

The zone coated CSF is a technology which has not yet been demonstrated to be durable in heavy-duty applications. However, as noted earlier, CSF technology is not considered essential to achieving the Stage 3 performance goals, and in fact moving to a more traditional DOC+DPF arrangement may actually be more beneficial in terms of system performance and durability. The lower thermal inertia of the CSF did not prove essential to meeting the cold-start demands of Low NO_x, and a little more thermal inertia would actually be beneficial under hot-start, LLC, and many in-use duty cycles. Therefore, durability concerns around CSF should not be considered an impediment to achieving Low NO_x performance.

The heated doser technology used in the Stage 3 system is currently a late stage prototype system. As of the writing of this report, the technology is moving into vehicle demonstrations and trials on the path towards being ready for 2027 model year introduction. It should also be noted

that there are many other options for low temperature dosing that are actively being pursued, and are in various stages of development.

It should also be noted that although an EGR cooler bypass was not utilized in the Stage 3 demonstration, such a bypass is likely a necessary element for a robust production implementation of the Stage 3 approach. There are concerns related to long-term EGR cooler fouling, and condensation potential at low ambient temperatures, and these would be effectively mitigated by an EGR cooler bypass. EGR cooler bypass systems have been implemented on production light-duty diesel engines for some time, and have proven to be a relatively simple and durable technology.

4.3 Implications for Onboard Diagnostics (OBD)

Heavy-duty engines are subject to strict OBD requirements that require the engine to detect emission related failures, and to provide diagnostic information to a service technician to enable repairs. Therefore, it is important to consider the interaction between new NO_x control technologies and OBD requirements.

Currently, OBD thresholds are often set as a multiple of the applicable emission standard. In the case of some monitors, the thresholds involve an additive factor. For NO_x many of these thresholds are currently at the standard plus 0.2 g/hp-hr, or an OBD threshold of 0.4 g/hp-hr. For a Low NO_x standard of 0.02 g/hp-hr, continuing to scale NO_x thresholds in this manner would prove to be a significant technical barrier at the present time. Many of the current approaches to NO_x monitoring involve the in-use measurement of NO_x reduction across the system using NO_x sensors. As noted earlier, for Low NO_x this would require the detection of very small changes on NO_x conversion, which would be infeasible at very low thresholds with current sensor technology. Therefore, it is recommended that the NO_x OBD thresholds should be maintained at present levels for the near term to allow time for new technology introduction, and to allow time for further development of sensor technologies to improve accuracy. In addition, maintaining the OBD thresholds at their current levels will also mitigate some of the burden of new monitor development for several new technologies used in the Stage 3 system. It should be noted that testing at SwRI has indicated that in the Stage 3 system even a complete loss of conversion on the LO-SCR would not result in tailpipe emissions levels above 0.4 g/hp-hr.

There are several new systems and technologies utilized in the Stage 3 system that will likely require monitoring to be developed. These would include the LO-SCR, dual dosing, the heated doser, and CDA. In addition to these, a third NO_x sensors at the LO-SCR outlet would be added to the system, as well as the mid-bed NH₃ sensor used for feedback control, and two additional temperature sensors in the AT system. An EGR cooler bypass valve would also require monitoring. As noted above a number of these are already in Light Duty production or gasoline applications.

CDA OBD monitoring could potentially be accomplished using the same monitoring algorithms that are used for misfire, except that in this case the system would effectively be looking for an expected “misfire” event. Given that fueling in firing cylinders is actually increased, the waveforms that are being detected at a given speed will have longer periods and higher amplitudes, which may help detection of “missing” cylinders. It should be noted that there is no failure of CDA that would result in NO_x exceeding 0.4 g/hp-hr NO_x OBD threshold, and in fact the most

likely symptom is increased fuel consumption. On the other hand, a mechanical failure of CDA that would result in a cylinder being unable to fire is immediately apparent under even moderate load as vibration. In a hydraulically actuated system, oil pressure would likely need to be monitored via pressure sensors at the system feed for safety and diagnostic purposes, so a pressure related failure should be detectable in a straightforward manner.

The mid-bed NH₃ sensor represents an interesting case for OBD, however, two key points must be made regarding this sensor. The first is that even if the NH₃ sensor was non-operational, tailpipe NO_x emissions would not exceed the OBD threshold of 0.4 g/hp-hr. The second point is that within the Stage 3 control system, the absolute accuracy of the NH₃ sensor is not as important as the ability to see (or not see) a large “wave” of ammonia. Therefore, this function could be examined at high temperature through the intrusive injection of a short pulse of additional ammonia to trigger a visible response under a condition where the storage model indicates that the downstream catalyst beds are already relatively empty. This could be done without a significant tailpipe NO_x or NH₃ impact at higher temperatures, and the monitor would be looking for both a response and an appropriate response duration.

As NO_x sensor technology develops, and as these other technologies mature over time, it is assumed that these OBD thresholds will be re-examined periodically, but it is suggested that this be evaluated carefully only after the rollout of these new technologies is completed sometime after 2027 the model year.

5.0 RECOMMENDATIONS

Given the program results and conclusions presented earlier, a number of recommendations can be made regarding areas for further research and development.

It is clear from the results that the primary challenge with respect to Low NO_x emissions is AT durability. This is relevant within the 435,000 mile useful life demonstrated in this program, and it is even more important when considering longer FUL periods. A number of potential areas of improvement in AT durability were highlighted in the Conclusions section, and it is recommended that this be an area of further development. In addition, examination of system performance over longer FUL periods is another key recommendation for future effort. As of the writing of this report, further examination of both of these areas is being conducted by U.S. EPA under the development of the CTL.

Another area related to AT durability that was outside the scope of this investigation is the potential impact of engine failures on AT, especially those that might be small enough to escape detection for a period of time (such as a small EGR cooler leak). Understanding the “dose response” curve for coolant and oil exposure and the deposition rate thresholds for onset of new deterioration mechanisms could inform how acutely critical these types of failures are to long-term health of the AT system. This program, and in fact all laboratory demonstrations (including deterioration factor testing) focus on “normal” AT degradation, which is generally associated with proper operation over the useful life period. The potential impact of “abnormal” degradation modes, such as could be caused by small engine-related failures, is difficult to assess. Because they are “abnormal”, such failures would only impact a relatively small portion of the fleet, but they could still represent a compliance risk during in-use testing. It should be noted that if such failure impacted a significant portion of the fleet, it should not be considered abnormal and would instead need to be considered as part of a robust AT design.. A better understanding of these “abnormal” modes of degradation would require significant research. Such effort would need to be guided by a clear understanding of current failure mechanisms and frequencies. The results of such efforts could also provide guidance to manufacturers about which of these modes should be prioritized to address in future development of more robust upstream and aftertreatment parts as well as more targeted diagnostics to recognize these repairable defects before they incur expensive cascading damage under warranty. The potential excess emissions, cost and downtime impacts of allowing such failure modes to proliferate highlight the importance of detailed failure mode pinpointing during vehicle operation as the failures are developing.

Several key technologies have been demonstrated in this program on the Stage 3 engine platform in a dynamometer test cell, and that is a very important accomplishment. However, implementation of these technologies on vehicle remains to be completed, and a vehicle-level demonstration would help to further strengthen and expand the program results. Such a demonstration would provide more robust information regarding issues such as packaging, vibration mitigation, the impact of ambient conditions (such as cold temperatures), and in-use compliance.

With regard to in-use compliance, although an initial demonstration was run in an industry developed real-world route, running additional field duty cycles, which could be also done in the laboratory using the Stage 3 engine, would provide more information with regard to in-use compliance. Such efforts could also be used to examine both portable emission measurement

systems and sensor-based measurement at these low levels of NO_x. Indeed initial efforts along these lines are underway with industry and EPA support. A vehicle demonstration platform would also be of great use in further validating these measurement assessments. Achates will have a Low NO_x vehicle on the road summer 2021 that may afford measurement validation opportunities.

6.0 REFERENCES

1. Sharp, C., Webb, C., Neely, G., Carter, M. et al., "Achieving Ultra Low NO_x Emissions Levels with a 2017 Heavy-Duty On-Highway TC Diesel Engine and an Advanced Technology Emissions System - Thermal Management Strategies," SAE Int. J. Engines 10(4):1697-1712, 2017.
2. Sharp, C., Webb, C., Yoon, S., Carter, M. et al., "Achieving Ultra Low NO_x Emissions Levels with a 2017 Heavy-Duty On-Highway TC Diesel Engine - Comparison of Advanced Technology Approaches," SAE Int. J. Engines 10(4):1722-1735, 2017.
3. Sharp, C., Webb, C., Neely, G., Sarlashkar, J. et al., "Achieving Ultra Low NO_x Emissions Levels with a 2017 Heavy-Duty On-Highway TC Diesel Engine and an Advanced Technology Emissions System - NO_x Management Strategies," SAE Int. J. Engines 10(4):1736-1748, 2017. U.S. Department of Transportation, "Summary of Fuel Economy Performance," NHTSA, NVS-220, Apr. 28, 2011.
4. Sharp, C., et.al., "Low NO_x Demonstration - Stage 2 Final Report," www.arb.ca.gov/lists/com-attach/1-hdomnibus2020-VDdXMFhU2IAWQIw.pdf
5. Roberts, L., Magee, M., Fain, D., Shaver, G., et al., "Impact of Cylinder Deactivation at Idle on Thermal Management and Efficiency," SAE CV-0336, SAE Commercial Vehicle Congress, Oct., 2014, Rosemount, IL.
6. McCarthy, J., Jr., "Enabled Improved Vehicle Fuel Economy and Emissions," 2017 Symposium – Engine Research Center, University of Wisconsin-Madison, June 14, 2017.
7. Neely, G., Sharp, C., Pieczko, M., and McCarthy, J., "Simultaneous NO_x and CO₂ Reduction for Meeting Future CARB Standards Using a Heavy-Duty Diesel CDA-NVH Strategy," SAE Int. J. Engines 13(2):2020, doi:10.4271/03-13-02-0014.
8. Archer, A and McCarthy Jr., J., "Quantification of Diesel Engine Vibration Using Cylinder Deactivation for Exhaust Temperature Management and Recipe Implementation in Commercial Vehicles," SAE Technical Paper 2018-01-1284, 2018, doi:10.4271/2018-01-1284
9. Farrell, L., Frazier, T., Younkins, M, et al., 2020. "Diesel Dynamic Skip Fire (dDSFTM): Simultaneous CO₂ and NO_x Reduction", Proceedings of the 41st International Vienna Motor Symposium, Vienna, Austria, 22-24 April 2020
10. Rao, S., Sarlashkar, J., Rengarajan, S., Sharp, C. et al., "A Controls Overview on Achieving Ultra-Low NO_x," SAE Technical Paper 2020-01-1404, 2020, <https://doi.org/10.4271/2020-01-1404>.
11. Zavala, B., Vats, S., and Eakle, S., "The Diesel Aftertreatment Accelerated Aging Cycle Protocol: An Advanced Aftertreatment Case Study," SAE Technical Paper 2020-01-2210, 2020, <https://doi.org/10.4271/2020-01-2210>.
12. Eakle, S.; Bartley, G. In The DAAAC Protocol™ for Diesel Aftertreatment System Accelerated Aging, Emissions 2014: Proceedings of the 2014 Emissions Conference, Troy, MI, June 11-12, 2014, 2014; Troy, MI, 2014.
13. California fuel sampling data submitted to EPA CTI ANRPM docket, https://downloads.regulations.gov/EPA-HQ-OAR-2019-0055-0471/attachment_3.pdf
14. California Exhaust Emission Standards and Test Procedures for 2004 and Subsequent Model Heavy-Duty Diesel Engines and Vehicles, released June 23, 2020, <https://ww3.arb.ca.gov/regact/2020/hdomnibuslownox/appb1.pdf>, 86.1370.B.6.

APPENDIX - EMISSION DATA SUMMARIES FOR ALL TEST POINTS

ZERO-HOUR DATA FOR FINAL AGED PARTS

0-HOUR TAILPIPE EMISSIONS - INDIVIDUAL TEST RUNS

Tailpipe		Cold	Hot 1	Hot 2	Hot 3	Composite	Hot-Avg	RMC1	LLC
		Set 1							
Run No		3663	3664	3665	3666	n/a	n/a	3660	3678
THC	g/hp-hr	0.014	0.001	0.002	0.001	0.003	0.001	0.001	0.022
NMHC	g/hp-hr	0.012	0.001	0.002	0.001	0.003	0.001	0.001	0.015
CO	g/hp-hr	0.118	0.011	0.011	0.012	0.026	0.011	0.007	0.076
NOx	g/hp-hr	0.054	0.012	0.011	0.011	0.018	0.011	0.009	0.017
PM	g/hp-hr	0.0016	0.0015	0.0013	0.0016	0.0015	0.0015	0.0009	0.0040
CO2	g/hp-hr	537.4	498.6	498.0	497.5	504.1	498.0	455.8	598.1
N2O	g/hp-hr	0.040	0.048	0.047	0.047	0.046	0.047	0.054	0.039
Work	hp-hr	34.50	34.12	34.13	34.12	34.17	34.12	173.11	50.06
CH4	g/hp-hr	0.002	0.000	0.000	0.000	0.000	0.000	0.000	0.007
		Set 2							
Run No		3688	3689	3690	3691	n/a	n/a	3668	3685
THC	g/hp-hr	0.009	0.000	0.000	0.001	0.001	0.000	0.001	0.004
NMHC	g/hp-hr	0.008	0.000	0.000	0.001	0.001	0.000	0.001	0.000
CO	g/hp-hr	0.091	0.012	0.011	0.013	0.024	0.012	0.008	0.038
NOx	g/hp-hr	0.055	0.010	0.011	0.010	0.017	0.011	0.009	0.020
PM	g/hp-hr	0.0014	0.0014	0.0014	0.0016	0.0014	0.0015	0.0010	0.0037
CO2	g/hp-hr	540.1	498.8	497.8	498.1	504.7	498.2	453.1	601.3
N2O	g/hp-hr	0.039	0.048	0.046	0.047	0.046	0.047	0.056	0.045
Work	hp-hr	34.58	34.27	34.31	34.17	34.31	34.25	173.07	50.01
CH4	g/hp-hr	0.001	0.000	0.000	0.000	0.000	0.000	0.000	0.003
		Set 3							
Run No		3698	3699	3700	3701	n/a	n/a	3695	3702
THC	g/hp-hr	0.050	0.036	0.035	0.035	0.038	0.036	0.000	0.130
NMHC	g/hp-hr	0.049	0.036	0.034	0.035	0.037	0.035	0.000	0.126
CO	g/hp-hr	0.122	0.013	0.014	0.026	0.028	0.017	0.007	0.072
NOx	g/hp-hr	0.055	0.011	0.011	0.011	0.018	0.011	0.009	0.024
PM	g/hp-hr	0.0025	0.0014	0.0015	0.0016	0.0016	0.0015	0.0008	0.0043
CO2	g/hp-hr	540.0	499.7	497.9	499.3	505.4	498.9	454.2	600.7
N2O	g/hp-hr	0.037	0.047	0.045	0.045	0.045	0.045	0.049	0.045
Work	hp-hr	34.44	34.15	34.26	34.22	34.20	34.21	173.14	50.48
CH4	g/hp-hr	0.001	0.000	0.000	0.000	0.000	0.000	0.000	0.004

0-HOUR TAILPIPE EMISSIONS – AVERAGE DATA

Average		Cold	Hot 1	Hot 2	Hot 3	Composite	Hot-Avg	RMC1	LLC
THC	g/hp-hr	0.024	0.012	0.012	0.012	0.014	0.012	0.001	0.052
NMHC	g/hp-hr	0.023	0.012	0.012	0.012	0.014	0.012	0.001	0.047
CO	g/hp-hr	0.110	0.012	0.012	0.017	0.026	0.013	0.007	0.062
NOx	g/hp-hr	0.055	0.011	0.011	0.011	0.017	0.011	0.009	0.020
PM	g/hp-hr	0.002	0.001	0.001	0.002	0.001	0.001	0.001	0.004
CO2	g/hp-hr	539.1	499.0	497.9	498.3	504.8	498.4	454.4	600.0
N2O	g/hp-hr	0.039	0.047	0.046	0.046	0.046	0.046	0.053	0.043
Work	hp-hr	34.505	34.180	34.234	34.168	34.227	34.194	173.108	50.185
CH4	g/hp-hr	0.002	0.000	0.000	0.000	0.000	0.000	0.000	0.005
Standard Deviation		Cold	Hot 1	Hot 2	Hot 3	Composite	Hot-Avg	RMC1	LLC
THC	g/hp-hr	0.0224	0.0207	0.0198	0.0199	0.0209	0.0201	0.0006	0.0682
NMHC	g/hp-hr	0.0224	0.0203	0.0194	0.0195	0.0206	0.0197	0.0006	0.0687
CO	g/hp-hr	0.0166	0.0010	0.0016	0.0077	0.0024	0.0034	0.0005	0.0206
NOx	g/hp-hr	0.0003	0.0006	0.0004	0.0004	0.0005	0.0002	0.0003	0.0033
PM	g/hp-hr	0.0006	0.0001	0.0001	0.0000	0.0001	0.0000	0.0001	0.0003
CO2	g/hp-hr	1.55	0.57	0.10	0.89	0.65	0.48	1.36	1.67
N2O	g/hp-hr	0.0010	0.0006	0.0010	0.0012	0.0006	0.0009	0.0037	0.0035
Work	hp-hr	0.0721	0.0771	0.0919	0.0496	0.0745	0.0644	0.0337	0.2577
CH4	g/hp-hr	0.0008	0.0000	0.0000	0.0000	0.0000	0.0000	0.0000	0.0019
COV		Cold	Hot 1	Hot 2	Hot 3	Composite	Hot-Avg	RMC1	LLC
THC	g/hp-hr	92%	167%	162%	161%	148%	163%	66%	132%
NMHC	g/hp-hr	98%	167%	162%	161%	150%	163%	66%	145%
CO	g/hp-hr	15%	9%	14%	46%	9%	25%	7%	33%
NOx	g/hp-hr	0.6%	5.5%	4.0%	3.9%	3.1%	1.9%	3.7%	16%
PM	g/hp-hr	32%	4.0%	7.1%	0.0%	5.5%	1.3%	11%	7.5%
CO2	g/hp-hr	0.29%	0.11%	0.02%	0.18%	0.13%	0.10%	0.30%	0.28%
N2O	g/hp-hr	2.6%	1.2%	2.2%	2.5%	1.4%	1.9%	6.9%	8.2%
Work	hp-hr	0.2%	0.2%	0.3%	0.1%	0.2%	0.2%	0.0%	0.5%

0-HOUR ENGINE-OUT DATA – INDIVIDUAL TEST RUNS

Engine-Out		Cold	Hot 1	Hot 2	Hot 3	Composite	Hot-Avg	RMC1	LLC
		Set 1							
Run No		3663	3664	3665	3666	n/a	n/a	3660	3678
THC	g/hp-hr	0.19	0.12	0.12	0.12	0.13	0.12	0.04	0.29
NMHC	g/hp-hr	0.19	0.12	0.12	0.11	0.13	0.12	0.04	0.28
CO	g/hp-hr	0.9	0.6	0.7	0.7	0.7	0.7	0.1	1.6
NOx	g/hp-hr	2.9	3.5	3.5	3.5	3.4	3.5	3.7	3.1
		Set 2							
Run No		3688	3689	3690	3691	n/a	n/a	3685	0
THC	g/hp-hr	0.17	0.11	0.12	0.12	0.12	0.12	0.04	0.29
NMHC	g/hp-hr	0.17	0.11	0.11	0.11	0.12	0.11	0.04	0.28
CO	g/hp-hr	0.8	0.6	0.6	0.7	0.7	0.7	0.1	1.5
NOx	g/hp-hr	2.9	3.4	3.4	3.3	3.3	3.4	3.7	2.9
		Set 3							
Run No		3698	3699	3700	3701	n/a	n/a	3695	3702
THC	g/hp-hr	0.17	0.12	0.11	0.11	0.13	0.11	0.04	0.28
NMHC	g/hp-hr	0.17	0.12	0.11	0.11	0.12	0.11	0.04	0.28
CO	g/hp-hr	0.9	0.7	0.6	0.7	0.7	0.7	0.1	1.5
NOx	g/hp-hr	2.9	3.5	3.6	3.5	3.4	3.5	3.6	3.2

333-HOUR DATA FOR FINAL AGED PARTS

333-HOUR TAILPIPE EMISSIONS - INDIVIDUAL TEST RUNS

Tailpipe		Cold	Hot 1	Hot 2	Hot 3	Composite	Hot-Avg	RMC1	LLC
		Set 1							
Run No		3866	3867	3868	3869	n/a	n/a	3898	3860
THC	g/hp-hr	0.023	0.009	0.008	0.008	0.011	0.008	0.014	0.022
NMHC	g/hp-hr	0.021	0.009	0.008	0.007	0.010	0.008	0.013	0.015
CO	g/hp-hr	0.161	0.021	0.019	0.016	0.041	0.019	0.007	0.083
NOx	g/hp-hr	0.057	0.011	0.013	0.012	0.018	0.012	0.015	0.027
PM	g/hp-hr	0.0013	0.0018	0.0023	0.0015	0.0017	0.0019	0.0007	0.0044
CO2	g/hp-hr	544.2	504.1	503.5	503.9	509.8	503.8	453.2	575.5
N2O	g/hp-hr	0.031	0.039	0.043	0.044	0.038	0.042	0.035	0.033
Work	hp-hr	34.17	33.80	33.69	33.74	33.85	33.74	173.14	49.61
CH4	g/hp-hr	0.002	0.000	0.000	0.000	0.000	0.000	0.000	0.000
		Set 2							
Run No		3884	3885	3886	3887	n/a	n/a	3899	3870
THC	g/hp-hr	0.021	0.008	0.008	0.008	0.010	0.008	0.014	0.027
NMHC	g/hp-hr	0.018	0.008	0.008	0.008	0.010	0.008	0.014	0.015
CO	g/hp-hr	0.169	0.025	0.020	0.025	0.046	0.023	0.008	0.117
NOx	g/hp-hr	0.053	0.012	0.011	0.012	0.018	0.012	0.016	0.021
PM	g/hp-hr	0.0012	0.0017	0.0018	0.0017	0.0016	0.0017	0.0007	0.0034
CO2	g/hp-hr	547.7	507.9	508.0	508.3	513.6	508.1	453.3	576.2
N2O	g/hp-hr	0.034	0.039	0.044	0.045	0.038	0.043	0.036	0.039
Work	hp-hr	34.12	33.75	33.70	33.63	33.80	33.69	173.10	49.34
CH4	g/hp-hr	0.002	0.000	0.000	0.001	0.001	0.000	0.000	0.000
		Set 3							
Run No		3894	3895	3896	3897	n/a	n/a	3904	3881
THC	g/hp-hr	0.063	0.039	0.039	0.039	0.042	0.039	0.003	0.037
NMHC	g/hp-hr	0.060	0.038	0.039	0.038	0.041	0.038	0.003	0.028
CO	g/hp-hr	0.230	0.029	0.031	0.027	0.058	0.029	0.008	0.111
NOx	g/hp-hr	0.057	0.013	0.012	0.010	0.019	0.012	0.015	0.019
PM	g/hp-hr	0.0014	0.0014	0.0011	0.0011	0.0014	0.0012	0.0007	0.0000
CO2	g/hp-hr	545.8	505.9	505.0	505.5	511.6	505.5	454.3	577.1
N2O	g/hp-hr	0.032	0.036	0.035	0.037	0.035	0.036	0.034	0.025
Work	hp-hr	34.17	33.85	33.72	33.80	33.90	33.79	173.25	49.28
CH4	g/hp-hr	0.004	0.000	0.001	0.000	0.001	0.000	0.000	0.000

333-HOUR TAILPIPE EMISSIONS – AVERAGE DATA

Average		Cold	Hot 1	Hot 2	Hot 3	Composite	Hot-Avg	RMC1	LLC
THC	g/hp-hr	0.036	0.019	0.019	0.018	0.021	0.018	0.010	0.029
NMHC	g/hp-hr	0.033	0.018	0.018	0.018	0.020	0.018	0.010	0.019
CO	g/hp-hr	0.186	0.025	0.023	0.023	0.048	0.024	0.007	0.104
NOx	g/hp-hr	0.056	0.012	0.012	0.011	0.018	0.012	0.015	0.022
PM	g/hp-hr	0.001	0.002	0.002	0.001	0.002	0.002	0.001	0.003
CO2	g/hp-hr	545.9	505.9	505.5	505.9	511.7	505.8	453.6	576.3
N2O	g/hp-hr	0.032	0.038	0.041	0.042	0.037	0.040	0.035	0.032
Work	hp-hr	34.151	33.801	33.707	33.722	33.851	33.743	173.162	49.411
CH4	g/hp-hr	0.003	0.000	0.000	0.000	0.000	0.000	0.000	0.000
Standard Deviation		Cold	Hot 1	Hot 2	Hot 3	Composite	Hot-Avg	RMC1	LLC
THC	g/hp-hr	0.0241	0.0172	0.0181	0.0180	0.0182	0.0178	0.0062	0.0078
NMHC	g/hp-hr	0.0232	0.0169	0.0178	0.0178	0.0178	0.0175	0.0061	0.0073
CO	g/hp-hr	0.0378	0.0042	0.0068	0.0056	0.0088	0.0053	0.0005	0.0180
NOx	g/hp-hr	0.0021	0.0007	0.0012	0.0009	0.0007	0.0004	0.0009	0.0037
PM	g/hp-hr	0.0001	0.0002	0.0006	0.0003	0.0002	0.0004	0.0000	0.0023
CO2	g/hp-hr	1.77	1.91	2.31	2.20	1.89	2.13	0.60	0.83
N2O	g/hp-hr	0.0016	0.0018	0.0051	0.0045	0.0016	0.0038	0.0010	0.0070
Work	hp-hr	0.0271	0.0503	0.0145	0.0841	0.0463	0.0478	0.0763	0.1744
CH4	g/hp-hr	0.0009	0.0001	0.0004	0.0003	0.0002	0.0002	0.0000	0.0000
COV		Cold	Hot 1	Hot 2	Hot 3	Composite	Hot-Avg	RMC1	LLC
THC	g/hp-hr	68%	93%	98%	99%	87%	96%	60%	27%
NMHC	g/hp-hr	71%	93%	98%	100%	88%	97%	60%	38%
CO	g/hp-hr	20%	17%	29%	25%	18%	22%	7%	17%
NOx	g/hp-hr	3.8%	5.9%	9.6%	8.2%	3.9%	3.4%	6.0%	17%
PM	g/hp-hr	8%	12.7%	34.8%	21.3%	10.6%	22.0%	0%	88.7%
CO2	g/hp-hr	0.32%	0.38%	0.46%	0.43%	0.37%	0.42%	0.13%	0.14%
N2O	g/hp-hr	4.9%	4.7%	12.4%	10.6%	4.3%	9.4%	2.9%	21.7%
Work	hp-hr	0.1%	0.1%	0.0%	0.2%	0.1%	0.1%	0.0%	0.4%

333-HOUR ENGINE-OUT DATA – INDIVIDUAL TEST RUNS

Engine-Out		Cold	Hot 1	Hot 2	Hot 3	Composite	Hot-Avg	RMC1	LLC
		Set 1							
Run No		3866	3867	3868	3869	n/a	n/a	3898	3860
THC	g/hp-hr	0.18	0.13	0.13	0.13	0.14	0.13	0.05	0.29
NMHC	g/hp-hr	0.18	0.13	0.13	0.13	0.14	0.13	0.05	0.28
CO	g/hp-hr	0.8	0.6	0.6	0.6	0.7	0.6	0.1	1.6
NOx	g/hp-hr	2.8	3.2	3.0	3.1	3.1	3.1	4.0	2.4
		Set 2							
Run No		3884	3885	3886	3887	n/a	n/a	3870	0
THC	g/hp-hr	0.18	0.14	0.13	0.13	0.15	0.13	0.05	0.28
NMHC	g/hp-hr	0.18	0.14	0.13	0.13	0.14	0.13	0.05	0.28
CO	g/hp-hr	0.8	0.6	0.7	0.7	0.7	0.7	0.1	1.8
NOx	g/hp-hr	2.8	3.3	3.1	3.1	3.2	3.2	4.1	2.4
		Set 3							
Run No		3894	3895	3896	3897	n/a	n/a	3904	3881
THC	g/hp-hr	0.22	0.14	0.17	0.15	0.15	0.15	0.04	0.27
NMHC	g/hp-hr	0.21	0.14	0.16	0.14	0.15	0.15	0.04	0.27
CO	g/hp-hr	0.9	0.6	0.7	0.7	0.7	0.7	0.1	1.7
NOx	g/hp-hr	2.9	3.3	3.0	3.2	3.3	3.2	4.0	2.7

667-HOUR DATA FOR FINAL AGED PARTS

667-HOUR TAILPIPE EMISSIONS - INDIVIDUAL TEST RUNS

Tailpipe		Cold	Hot 1	Hot 2	Hot 3	Composite	Hot-Avg	RMC1	LLC
		Set 1							
Run No		4151	4152	4153	4154	n/a	n/a	4156	4133
THC	g/hp-hr	0.037	0.011	0.013	0.014	0.015	0.013	0.003	0.052
NMHC	g/hp-hr	0.034	0.010	0.012	0.013	0.014	0.012	0.003	0.043
CO	g/hp-hr	0.241	0.137	0.153	0.134	0.152	0.142	0.009	0.311
NOx	g/hp-hr	0.063	0.014	0.015	0.015	0.021	0.015	0.019	0.047
PM	g/hp-hr	0.0019	0.0017	0.0023	0.0017	0.0017	0.0019	0.0000	0.0047
CO2	g/hp-hr	543.5	511.4	511.3	510.6	516.0	511.1	460.5	594.5
N2O	g/hp-hr	0.026	0.030	0.030	0.033	0.030	0.031	0.023	0.024
Work	hp-hr	34.58	33.85	33.68	33.69	33.95	33.74	173.14	49.27
CH4	g/hp-hr	0.003	0.001	0.001	0.001	0.001	0.001	0.000	0.000
		Set 2							
Run No		4138	4139	4140	4141	n/a	n/a	4148	4155
THC	g/hp-hr	0.028	0.015	0.014	0.014	0.017	0.014	0.004	0.049
NMHC	g/hp-hr	0.027	0.014	0.014	0.013	0.016	0.013	0.004	0.040
CO	g/hp-hr	0.209	0.149	0.129	0.136	0.158	0.138	0.010	0.286
NOx	g/hp-hr	0.066	0.016	0.017	0.016	0.023	0.017	0.020	0.051
PM	g/hp-hr	0.0016	0.0026	0.0015	0.0014	0.0025	0.0018	0.0012	0.0046
CO2	g/hp-hr	543.0	512.6	511.0	511.7	517.0	511.8	461.9	593.7
N2O	g/hp-hr	0.033	0.035	0.036	0.036	0.035	0.036	0.023	0.021
Work	hp-hr	34.59	33.83	33.76	33.77	33.94	33.79	173.05	49.39
CH4	g/hp-hr	0.001	0.001	0.001	0.001	0.001	0.001	0.000	0.000
		Set 3							
Run No		4159	4160	4161	4162	n/a	n/a	4164	4163
THC	g/hp-hr	0.027	0.013	0.013	0.013	0.015	0.013	0.002	0.053
NMHC	g/hp-hr	0.025	0.012	0.012	0.013	0.014	0.012	0.002	0.045
CO	g/hp-hr	0.230	0.129	0.100	0.123	0.144	0.117	0.011	0.318
NOx	g/hp-hr	0.061	0.015	0.015	0.016	0.022	0.015	0.018	0.052
PM	g/hp-hr	0.0019	0.0017	0.0016	0.0017	0.0017	0.0017	0.0016	0.0043
CO2	g/hp-hr	542.4	510.7	510.5	510.2	515.2	510.5	461.1	594.1
N2O	g/hp-hr	0.026	0.031	0.033	0.033	0.031	0.033	0.025	0.019
Work	hp-hr	34.67	33.91	33.88	33.84	34.02	33.88	173.21	49.39
CH4	g/hp-hr	0.002	0.001	0.000	0.001	0.001	0.001	0.000	0.000

667-HOUR TAILPIPE EMISSIONS – AVERAGE DATA

Average		Cold	Hot 1	Hot 2	Hot 3	Composite	Hot-Avg	RMC1	LLC
THC	g/hp-hr	0.031	0.013	0.013	0.014	0.015	0.013	0.003	0.051
NMHC	g/hp-hr	0.029	0.012	0.013	0.013	0.014	0.012	0.003	0.043
CO	g/hp-hr	0.227	0.139	0.128	0.131	0.151	0.132	0.010	0.305
NOx	g/hp-hr	0.063	0.015	0.016	0.016	0.022	0.016	0.019	0.050
PM	g/hp-hr	0.002	0.002	0.002	0.002	0.002	0.002	0.001	0.005
CO2	g/hp-hr	543.0	511.6	510.9	510.8	516.1	511.1	461.2	594.1
N2O	g/hp-hr	0.029	0.032	0.033	0.034	0.032	0.033	0.023	0.021
Work	hp-hr	34.615	33.861	33.772	33.770	33.971	33.801	173.130	49.348
CH4	g/hp-hr	0.002	0.001	0.001	0.001	0.001	0.001	0.000	0.000
Standard Deviation		Cold	Hot 1	Hot 2	Hot 3	Composite	Hot-Avg	RMC1	LLC
THC	g/hp-hr	0.0053	0.0019	0.0009	0.0003	0.0011	0.0008	0.0009	0.0020
NMHC	g/hp-hr	0.0048	0.0019	0.0009	0.0002	0.0012	0.0009	0.0009	0.0022
CO	g/hp-hr	0.0163	0.0100	0.0263	0.0073	0.0070	0.0130	0.0007	0.0168
NOx	g/hp-hr	0.0025	0.0009	0.0014	0.0006	0.0011	0.0009	0.0009	0.0022
PM	g/hp-hr	0.0002	0.0005	0.0004	0.0002	0.0004	0.0001	0.0008	0.0002
CO2	g/hp-hr	0.55	0.98	0.40	0.76	0.88	0.64	0.68	0.38
N2O	g/hp-hr	0.0035	0.0027	0.0030	0.0018	0.0028	0.0024	0.0012	0.0025
Work	hp-hr	0.0481	0.0413	0.0982	0.0758	0.0421	0.0689	0.0808	0.0674
CH4	g/hp-hr	0.0008	0.0001	0.0005	0.0002	0.0001	0.0003	0.0000	0.0000
COV		Cold	Hot 1	Hot 2	Hot 3	Composite	Hot-Avg	RMC1	LLC
THC	g/hp-hr	17%	15%	6%	3%	7%	6%	31%	4%
NMHC	g/hp-hr	17%	16%	7%	2%	8%	8%	31%	5%
CO	g/hp-hr	7%	7%	21%	6%	5%	10%	7%	5%
NOx	g/hp-hr	4.0%	6.1%	8.6%	3.6%	5.1%	5.7%	5.0%	4%
PM	g/hp-hr	10%	26.0%	24.2%	10.8%	21.2%	6.7%	89%	4.6%
CO2	g/hp-hr	0.10%	0.19%	0.08%	0.15%	0.17%	0.13%	0.15%	0.06%
N2O	g/hp-hr	12.4%	8.3%	9.1%	5.1%	8.8%	7.3%	5.1%	11.8%
Work	hp-hr	0.1%	0.1%	0.3%	0.2%	0.1%	0.2%	0.0%	0.1%

667-HOUR ENGINE-OUT DATA – INDIVIDUAL TEST RUNS

Engine-Out		Cold	Hot 1	Hot 2	Hot 3	Composite	Hot-Avg	RMC1	LLC
		Set 1							
Run No		4151	4152	4153	4154	n/a	n/a	4156	4133
THC	g/hp-hr	0.18	0.13	0.13	0.14	0.14	0.13	0.04	0.28
NMHC	g/hp-hr	0.17	0.13	0.13	0.14	0.14	0.13	0.04	0.28
CO	g/hp-hr	0.8	0.7	0.8	0.7	0.7	0.7	0.1	1.6
NOx	g/hp-hr	2.6	3.0	3.0	3.0	3.0	3.0	3.6	2.2
		Set 2							
Run No		4138	4139	4140	4141	n/a	n/a	4155	0
THC	g/hp-hr	0.19	0.14	0.15	0.14	0.15	0.14	0.05	0.25
NMHC	g/hp-hr	0.18	0.14	0.15	0.13	0.15	0.14	0.05	0.25
CO	g/hp-hr	0.8	0.7	0.7	0.7	0.7	0.7	0.1	1.5
NOx	g/hp-hr	2.6	3.0	3.1	3.0	3.0	3.0	3.7	2.2
		Set 3							
Run No		4159	4160	4161	4162	n/a	n/a	4164	4163
THC	g/hp-hr	0.17	0.13	0.13	0.13	0.14	0.13	0.04	0.26
NMHC	g/hp-hr	0.17	0.13	0.13	0.12	0.14	0.13	0.04	0.25
CO	g/hp-hr	0.8	0.7	0.6	0.7	0.7	0.7	0.1	1.5
NOx	g/hp-hr	2.6	3.0	3.0	3.0	3.0	3.0	3.8	2.2

1000-HOUR DATA FOR FINAL AGED PARTS – BEFORE ASH CLEANING

1000-HOUR TAILPIPE EMISSIONS BEFORE ASH CLEANING - INDIVIDUAL TEST RUNS

Tailpipe		Cold	Hot 1	Hot 2	Hot 3	Composite	Hot-Avg	RMC1	LLC
		Set 1							
Run No		4372	4373	4374	4375	n/a	n/a	4377	4376
THC	g/hp-hr	0.036	0.017	0.018	0.018	0.020	0.018	0.002	0.075
NMHC	g/hp-hr	0.035	0.017	0.018	0.018	0.020	0.018	0.002	0.067
CO	g/hp-hr	0.249	0.138	0.136	0.109	0.154	0.128	0.010	0.316
NOx	g/hp-hr	0.061	0.019	0.020	0.019	0.025	0.019	0.022	0.047
PM	g/hp-hr	0.0028	0.0020	0.0021	0.0030	0.0021	0.0024	0.0018	0.0059
CO2	g/hp-hr	540.1	509.8	510.1	510.6	514.1	510.2	463.2	597.6
N2O	g/hp-hr	0.029	0.032	0.034	0.032	0.032	0.033	0.022	0.029
Work	hp-hr	34.41	33.81	33.74	33.74	33.90	33.77	173.25	48.91
CH4	g/hp-hr	0.001	0.000	0.000	0.000	0.000	0.000	0.000	0.000
		Set 2							
Run No		4381	4382	4383	4384	n/a	n/a	4386	4385
THC	g/hp-hr	0.036	0.019	0.019	0.020	0.021	0.019	0.003	0.053
NMHC	g/hp-hr	0.035	0.018	0.018	0.020	0.021	0.019	0.002	0.046
CO	g/hp-hr	0.234	0.146	0.125	0.153	0.158	0.141	0.011	0.370
NOx	g/hp-hr	0.065	0.018	0.019	0.018	0.025	0.019	0.022	0.051
PM	g/hp-hr	0.0017	0.0015	0.0017	0.0019	0.0015	0.0017	0.0020	0.0052
CO2	g/hp-hr	538.6	509.1	509.0	510.0	513.3	509.4	462.1	596.9
N2O	g/hp-hr	0.003	0.034	0.033	0.032	0.030	0.033	0.022	0.021
Work	hp-hr	34.45	33.83	33.82	33.70	33.92	33.78	173.23	49.05
CH4	g/hp-hr	0.001	0.000	0.000	0.001	0.000	0.000	0.000	0.000
		Set 3							
Run No		4389	4390	4391	4392	n/a	n/a	4397	4393
THC	g/hp-hr	0.034	0.018	0.018	0.018	0.020	0.018	0.003	0.070
NMHC	g/hp-hr	0.033	0.018	0.017	0.018	0.020	0.018	0.003	0.063
CO	g/hp-hr	0.235	0.161	0.125	0.137	0.172	0.141	0.010	0.319
NOx	g/hp-hr	0.068	0.018	0.020	0.019	0.026	0.019	0.022	0.053
PM	g/hp-hr	0.0015	0.0019	0.0018	0.0021	0.0018	0.0019	0.0019	0.0053
CO2	g/hp-hr	538.2	509.4	509.3	509.6	513.5	509.4	459.9	594.9
N2O	g/hp-hr	0.033	0.035	0.034	0.033	0.035	0.034	0.023	0.021
Work	hp-hr	34.46	33.74	33.76	33.66	33.84	33.72	173.27	48.87
CH4	g/hp-hr	0.000	0.000	0.000	0.000	0.000	0.000	0.000	0.000

1000-HOUR TAILPIPE EMISSIONS BEFORE ASH CLEANING – AVERAGE DATA

Average		Cold	Hot 1	Hot 2	Hot 3	Composite	Hot-Avg	RMC1	LLC
THC	g/hp-hr	0.035	0.018	0.018	0.019	0.020	0.018	0.003	0.066
NMHC	g/hp-hr	0.034	0.018	0.018	0.018	0.020	0.018	0.003	0.059
CO	g/hp-hr	0.239	0.148	0.129	0.133	0.161	0.136	0.010	0.335
NOx	g/hp-hr	0.065	0.019	0.020	0.019	0.025	0.019	0.022	0.050
PM	g/hp-hr	0.002	0.002	0.002	0.002	0.002	0.002	0.002	0.005
CO2	g/hp-hr	539.0	509.4	509.5	510.0	513.7	509.7	461.7	596.5
N2O	g/hp-hr	0.022	0.034	0.034	0.033	0.032	0.034	0.023	0.023
Work	hp-hr	34.441	33.794	33.774	33.699	33.888	33.755	173.251	48.942
CH4	g/hp-hr	0.001	0.000	0.000	0.000	0.000	0.000	0.000	0.000
Standard Deviation		Cold	Hot 1	Hot 2	Hot 3	Composite	Hot-Avg	RMC1	LLC
THC	g/hp-hr	0.0013	0.0006	0.0005	0.0013	0.0005	0.0008	0.0006	0.0116
NMHC	g/hp-hr	0.0012	0.0005	0.0005	0.0011	0.0005	0.0007	0.0006	0.0114
CO	g/hp-hr	0.0081	0.0117	0.0068	0.0220	0.0092	0.0075	0.0004	0.0303
NOx	g/hp-hr	0.0034	0.0006	0.0006	0.0005	0.0003	0.0005	0.0004	0.0028
PM	g/hp-hr	0.0007	0.0003	0.0002	0.0006	0.0003	0.0003	0.0001	0.0004
CO2	g/hp-hr	0.99	0.35	0.55	0.48	0.43	0.44	1.69	1.43
N2O	g/hp-hr	0.0165	0.0015	0.0006	0.0006	0.0026	0.0007	0.0006	0.0046
Work	hp-hr	0.0242	0.0487	0.0390	0.0416	0.0400	0.0332	0.0205	0.0907
CH4	g/hp-hr	0.0003	0.0001	0.0001	0.0004	0.0001	0.0001	0.0000	0.0000
COV		Cold	Hot 1	Hot 2	Hot 3	Composite	Hot-Avg	RMC1	LLC
THC	g/hp-hr	4%	3%	3%	7%	2%	4%	21%	17%
NMHC	g/hp-hr	3%	3%	3%	6%	2%	4%	21%	20%
CO	g/hp-hr	3%	8%	5%	17%	6%	6%	4%	9%
NOx	g/hp-hr	5.2%	3.3%	3.0%	2.9%	1.3%	2.6%	1.8%	6%
PM	g/hp-hr	35%	14.7%	11.2%	25.1%	16.1%	16.9%	5%	6.9%
CO2	g/hp-hr	0.18%	0.07%	0.11%	0.09%	0.08%	0.09%	0.37%	0.24%
N2O	g/hp-hr	75.2%	4.5%	1.7%	1.8%	8.1%	2.1%	2.6%	19.5%
Work	hp-hr	0.1%	0.1%	0.1%	0.1%	0.1%	0.1%	0.0%	0.2%

1000-HOUR ENGINE-OUT DATA BEFORE ASH CLEANING – INDIVIDUAL TEST RUNS

Engine-Out		Cold	Hot 1	Hot 2	Hot 3	Composite	Hot-Avg	RMC1	LLC
		Set 1							
Run No		4372	4373	4374	4375	n/a	n/a	4377	4376
THC	g/hp-hr	0.18	0.14	0.14	0.14	0.15	0.14	0.05	0.29
NMHC	g/hp-hr	0.18	0.14	0.14	0.13	0.14	0.14	0.04	0.28
CO	g/hp-hr	0.7	0.6	0.6	0.6	0.6	0.6	0.1	1.5
NOx	g/hp-hr	2.8	3.3	2.9	2.8	3.2	3.0	4.4	2.1
Engine-Out		Set 2							
		Run No		4381	4382	4383	4384	n/a	n/a
THC	g/hp-hr	0.20	0.13	0.13	0.14	0.14	0.14	0.04	0.28
NMHC	g/hp-hr	0.20	0.13	0.13	0.14	0.14	0.13	0.04	0.27
CO	g/hp-hr	0.7	0.6	0.6	0.6	0.6	0.6	0.1	1.5
NOx	g/hp-hr	3.1	3.4	3.5	3.4	3.4	3.4	4.7	2.5
Engine-Out		Set 3							
		Run No		4389	4390	4391	4392	n/a	n/a
THC	g/hp-hr	0.18	0.15	0.14	0.14	0.16	0.14	0.04	0.29
NMHC	g/hp-hr	0.17	0.15	0.14	0.13	0.15	0.14	0.04	0.28
CO	g/hp-hr	0.7	0.6	0.5	0.6	0.6	0.6	0.1	1.4
NOx	g/hp-hr	3.1	3.0	3.3	2.9	3.0	3.1	4.5	2.7

1000-HOUR DATA FOR FINAL AGED PARTS – AFTER ASH CLEANING (FINAL DATA)

1000-HOUR TAILPIPE EMISSIONS BEFORE ASH CLEANING - INDIVIDUAL TEST RUNS

Tailpipe		Cold	Hot 1	Hot 2	Hot 3	Composite	Hot-Avg	RMC1	LLC
		Set 1							
Run No		4401	4402	4403	4404	n/a	n/a	4405	4413
THC	g/hp-hr	0.047	0.030	0.029	0.026	0.033	0.029	0.008	0.070
NMHC	g/hp-hr	0.046	0.030	0.028	0.026	0.032	0.028	0.008	0.062
CO	g/hp-hr	0.238	0.186	0.171	0.126	0.194	0.161	0.012	0.366
NOx	g/hp-hr	0.059	0.017	0.018	0.019	0.023	0.018	0.020	0.049
PM	g/hp-hr	0.0018	0.0020	0.0020	0.0020	0.0020	0.0020	0.0017	0.0062
CO2	g/hp-hr	536.1	511.3	505.4	505.9	514.8	507.5	458.2	590.2
N2O	g/hp-hr	0.040	0.040	0.036	0.035	0.040	0.037	0.024	0.020
Work	hp-hr	34.46	33.83	33.71	33.80	33.92	33.78	173.11	49.26
CH4	g/hp-hr	0.001	0.001	0.001	0.000	0.001	0.001	0.000	0.000
		Set 2							
Run No		4409	4410	4411	4412	n/a	n/a	4422	4421
THC	g/hp-hr	0.041	0.022	0.024	0.024	0.025	0.023	0.004	0.000
NMHC	g/hp-hr	0.041	0.022	0.023	0.024	0.024	0.023	0.004	0.000
CO	g/hp-hr	0.260	0.167	0.148	0.179	0.181	0.165	0.012	0.405
NOx	g/hp-hr	0.064	0.018	0.018	0.018	0.024	0.018	0.022	0.046
PM	g/hp-hr	0.0019	0.0025	0.0023	0.0023	0.0024	0.0024	0.0019	0.0059
CO2	g/hp-hr	543.0	511.7	511.9	512.0	516.2	511.9	462.7	590.7
N2O	g/hp-hr	0.035	0.036	0.037	0.035	0.036	0.036	0.023	0.021
Work	hp-hr	34.38	33.83	33.80	33.75	33.91	33.79	173.33	49.24
CH4	g/hp-hr	0.001	0.001	0.001	0.001	0.001	0.001	0.000	0.000
		Set 3							
Run No		4425	4426	4427	4428	n/a	n/a	4435	4438
THC	g/hp-hr	0.039	0.021	0.021	0.022	0.024	0.021	0.004	0.030
NMHC	g/hp-hr	0.038	0.020	0.020	0.021	0.023	0.021	0.004	0.023
CO	g/hp-hr	0.272	0.198	0.126	0.161	0.208	0.161	0.012	0.341
NOx	g/hp-hr	0.060	0.016	0.016	0.016	0.022	0.016	0.023	0.047
PM	g/hp-hr	0.0021	0.0025	0.0024	0.0024	0.0024	0.0024	0.0019	0.0058
CO2	g/hp-hr	541.1	512.2	512.0	512.0	516.3	512.1	462.6	591.0
N2O	g/hp-hr	0.040	0.052	0.048	0.050	0.050	0.050	0.025	0.012
Work	hp-hr	34.45	33.73	33.75	33.86	33.83	33.78	173.30	49.14
CH4	g/hp-hr	0.002	0.001	0.000	0.000	0.001	0.000	0.000	0.000

1000-HOUR TAILPIPE EMISSIONS BEFORE ASH CLEANING – AVERAGE DATA

Average		Cold	Hot 1	Hot 2	Hot 3	Composite	Hot-Avg	RMC1	LLC
THC	g/hp-hr	0.043	0.024	0.025	0.024	0.027	0.024	0.005	0.033
NMHC	g/hp-hr	0.041	0.024	0.024	0.024	0.026	0.024	0.005	0.028
CO	g/hp-hr	0.257	0.184	0.148	0.155	0.194	0.162	0.012	0.371
NOx	g/hp-hr	0.061	0.017	0.017	0.018	0.023	0.017	0.022	0.047
PM	g/hp-hr	0.002	0.002	0.002	0.002	0.002	0.002	0.002	0.006
CO2	g/hp-hr	540.1	511.7	509.8	510.0	515.8	510.5	461.2	590.6
N2O	g/hp-hr	0.038	0.043	0.040	0.040	0.042	0.041	0.024	0.017
Work	hp-hr	34.431	33.796	33.754	33.802	33.888	33.784	173.247	49.213
CH4	g/hp-hr	0.001	0.001	0.001	0.000	0.001	0.000	0.000	0.000
Standard Deviation		Cold	Hot 1	Hot 2	Hot 3	Composite	Hot-Avg	RMC1	LLC
THC	g/hp-hr	0.0038	0.0051	0.0042	0.0023	0.0049	0.0038	0.0021	0.0351
NMHC	g/hp-hr	0.0041	0.0051	0.0040	0.0022	0.0049	0.0037	0.0021	0.0312
CO	g/hp-hr	0.0175	0.0153	0.0224	0.0271	0.0139	0.0021	0.0002	0.0319
NOx	g/hp-hr	0.0030	0.0011	0.0013	0.0018	0.0011	0.0013	0.0016	0.0015
PM	g/hp-hr	0.0002	0.0003	0.0002	0.0002	0.0003	0.0002	0.0001	0.0002
CO2	g/hp-hr	3.59	0.46	3.77	3.52	0.83	2.56	2.56	0.42
N2O	g/hp-hr	0.0030	0.0085	0.0068	0.0089	0.0076	0.0080	0.0010	0.0049
Work	hp-hr	0.0432	0.0598	0.0443	0.0538	0.0491	0.0066	0.1169	0.0642
CH4	g/hp-hr	0.0005	0.0000	0.0005	0.0004	0.0001	0.0002	0.0000	0.0000
COV		Cold	Hot 1	Hot 2	Hot 3	Composite	Hot-Avg	RMC1	LLC
THC	g/hp-hr	9%	21%	17%	9%	18%	15%	41%	105%
NMHC	g/hp-hr	10%	21%	17%	9%	19%	16%	41%	110%
CO	g/hp-hr	7%	8%	15%	17%	7%	1%	2%	9%
NOx	g/hp-hr	5.0%	6.3%	7.5%	10.1%	4.9%	7.7%	7.1%	3%
PM	g/hp-hr	8%	12.4%	9.3%	9.3%	11.6%	10.3%	6%	3.5%
CO2	g/hp-hr	0.67%	0.09%	0.74%	0.69%	0.16%	0.50%	0.55%	0.07%
N2O	g/hp-hr	7.7%	20.0%	16.9%	22.2%	18.1%	19.5%	4.3%	27.9%
Work	hp-hr	0.1%	0.2%	0.1%	0.2%	0.1%	0.0%	0.1%	0.1%

1000-HOUR ENGINE-OUT DATA BEFORE ASH CLEANING – INDIVIDUAL TEST RUNS

Engine-Out		Cold	Hot 1	Hot 2	Hot 3	Composite	Hot-Avg	RMC1	LLC
		Set 1							
Run No		4401	4402	4403	4404	n/a	n/a	4405	4413
THC	g/hp-hr	0.19	0.15	0.15	0.15	0.16	0.15	0.05	0.28
NMHC	g/hp-hr	0.19	0.15	0.14	0.14	0.16	0.15	0.05	0.28
CO	g/hp-hr	0.7	0.7	0.7	0.6	0.7	0.6	0.1	1.5
NOx	g/hp-hr	2.9	3.1	3.2	3.2	3.0	3.2	4.1	2.5
Engine-Out		Set 2							
		Run No		4409	4410	4411	4412	n/a	n/a
THC	g/hp-hr	0.18	0.15	0.14	0.14	0.15	0.14	0.05	0.30
NMHC	g/hp-hr	0.18	0.14	0.14	0.14	0.15	0.14	0.05	0.29
CO	g/hp-hr	0.7	0.6	0.6	0.6	0.6	0.6	0.1	1.5
NOx	g/hp-hr	3.0	3.2	3.1	3.1	3.2	3.1	4.4	2.4
Engine-Out		Set 3							
		Run No		4425	4426	4427	4428	n/a	n/a
THC	g/hp-hr	0.20	0.14	0.14	0.14	0.15	0.14	0.04	0.29
NMHC	g/hp-hr	0.19	0.14	0.14	0.14	0.15	0.14	0.04	0.28
CO	g/hp-hr	0.7	0.6	0.6	0.6	0.6	0.6	0.1	1.5
NOx	g/hp-hr	2.9	3.0	3.2	3.1	3.0	3.1	4.3	2.8

